



**Università
degli Studi
di Ferrara**

**DOCTORAL COURSE IN
BIOMEDICAL SCIENCES AND BIOTECHNOLOGY
CYCLE XXXII**

DIRECTOR: Prof. Paolo Pinton

**THE DETECTION OF AMBIGUOUS LESIONS IN
BIOLOGICAL ANTHROPOLOGY:
INVESTIGATIVE STRATEGIES FOR HUMAN
SKELETAL REMAINS**

Scientific/Disciplinary Sector (SDS) **BIO/08**

Candidate

Dott. Filippo Scianò

(signature)

Supervisors

Prof. Barbara Bramanti

(signature)

Prof. Emanuela Gualdi

(signature)

TABLE OF CONTENTS

CHAPTER 1 - INTRODUCTION	pag. 1
1.1 – Ambiguous lesions in biological anthropology	pag. 1
1.2 – Paleo-pathologic evidence of difficult diagnosis	pag. 2
1.2.1 – The difficulty to assess β -thalassemia on ancient human remains	pag. 5
1.2.2 – The difficulty to assess tumours in ancient time	pag. 6
1.3 – Evidence of trauma with uncertain diagnosis	pag. 7
1.3.1 – The difficulty to assess the timing of traumatic lesions on human bones	pag. 8
1.4 – Pseudo-pathology and diagenetic changes	pag. 10
1.5 – Methodologic approaches for the lesion's detection in anthropology	pag. 11
1.6 – References	pag. 14
CHAPTER 2 - BONE LESIONS IN THALASSEMIA SYNDROME: A CHALLENGING' IDENTIFICATION IN PALEOPATHOLOGY	pag. 21
2.1 – Introduction	pag. 22
2.2 – Materials and Methods	pag. 26
2.2.1 - Differential diagnosis from published data	pag. 26
2.2.2 - Archaeological samples	pag. 27
2.2.3 – Macroscopic analyses	pag. 29
2.2.4 – Endoscopic and Radiologic analyses	pag. 29
2.2.5 – Microscopic analyses	pag. 30
2.3 – Results	pag. 31
2.3.1 – Evaluation form	pag. 33
2.3.2 – Application of the Evaluation Form	pag. 35
2.4 – Discussion and conclusions	pag. 44
2.5 – References	pag. 48
2.6 – Supplementary	pag. 57

CHAPTER 3 - HIDDEN FROM VIEW: THE SINGULAR DISCOVERY OF TWO HEAD TUMOURS IN SKELETAL HUMAN REMAINS	pag. 101
3.1 – Introduction	pag. 102
3.2 - Materials	pag. 102
3.3 - Methods	pag. 104
3.4 - Results	pag. 105
3.4.1 – SSM 81	pag. 105
3.4.2 – SSM 92	pag. 108
3.5 – Differential Diagnosis	pag. 112
3.6 – Discussion and Conclusion	pag. 116
3.7 - References	pag. 119
CHAPTER 4 - HOW TO ASSESS INJURIES IN BIOLOGICAL ANTHROPOLOGY: A NEW INVESTIGATIVE STRATEGY FOR THE ANALYSIS OF TRAUMATIC LESIONS	pag. 125
4.1 – Introduction	pag. 126
4.2 – Timing and interpretation of skeletal injuries	pag. 127
4.3 – Materials and Methods	pag. 130
4.4 – Results	pag. 132
4.5 – Discussion and Conclusion	pag. 136
4.6 – References	pag. 138
CHAPTER 5 - COLD CASES IN ANCIENT TIME: INVESTIGATION OF CRANIAL LESIONS OF EARLY BRONZE AGE AND RENAISSANCE	pag. 143
5.1 – Introduction	pag. 144
5.2 – Materials and Methods	pag. 145
5.3 – Results	pag. 149
5.3.1 - Ind. D from Ballabio (Early Bronze Age).	pag. 149
5.3.2 - Individual US 217 from Ravenna (17 th - 18 th century).	pag. 153

5.4 – Discussion and Conclusion	pag. 161
5.4.1 – Ind. D from Ballabio (Early Bronze Age)	pag. 161
5.4.2 - Individual US 217 from Ravenna (17 th - 18 th century).	pag. 163
5.5 – References	pag. 167
CHAPTER 6 - CONCLUSION	pag. 177
LIST OF TABLES	pag. 179
LIST OF FIGURES	pag. 183

CHAPTER 1

INTRODUCTION

1.1 – Ambiguous lesions in biological anthropology

In the past decades, a considerable amount of studies has focused on ancient human remains and, in particular, on the topic of the bone lesions, how they can be distinguished and classified.

Over time, the study of bone lesions has embraced innovation, and the progress in technology has led scholars to use a variety of new methods and instruments: radiographic (e.g. X-RAY, TC, CBTC), microscopic (e.g. TGS), and molecular analysis (e.g. aDNA), as well as the search for trace elements (e.g. ESEM, XRF, RAMAN), all these techniques can provide an additional advantage to the accuracy of the results.

From human skeletal remains, both from archaeological or forensic contexts, we can obtain valuable information concerning the biological profile (sex, age at death and stature in life), the diet (via isotopic analysis of carbon (^{13}C) and nitrogen (^{15}N) and paleo-protein analysis; pathologic and traumatic lesions (paleopathological investigation), genetic and genomic traits (disorders and ancestry). The presence of pathogens along with microbiomes can also be defined, mostly with ancient DNA analyses (aDNA).

This information is relevant on an individual level, though it can also provide indications of the population to which the person belonged, an aspect which can be relevant in particular for ancient populations, for which we have otherwise no knowledge. In the eyes of an anthropologist, ancient human remains are real biological archives, precious containers that enhance and enrich the archaeological and historiographic data (Tosi et al., 2017). Skeletal lesions do not escape this rule.

The macroscopic analysis of human remains represents the primary mean by which researchers begin to evaluate the skeletal lesions in detail, as acknowledged by Lovell N. (2000, p. 219):

«Visual observation is generally the first method employed when examining archaeological remains for pathological lesions. In many cases, it may be the only method required, while in some circumstances it may be the only method available».

And:

«[The] first step is to describe what is observed, before attempting a diagnosis. Bony reactions to trauma and disease often can be noted and described relatively easily, but determining what caused the reaction (i.e., making a diagnosis) may not be possible. Although a basic classification, such as “trauma”, “arthritis” or “infection” can usually be attempted, with more than 200 different types of arthritis and a similar variety of nonspecific and specific infections recognized by clinicians it is clear that a more definitive diagnosis is often impossible».

Hence, a precise and complete description of bone lesions, which should include photographic documentation along with a historical and archaeological contextualisation, constitutes the essential starting point for each diagnosis, and this even more in case of lesions of difficult or ambiguous interpretation, which may be the result of different biological processes (Larsen, 1999; Lovell, 2000; Buikstra and Roberts, 2012). Yet, besides the macroscopic investigation, other analyses may be required to disentangle the cause of a lesion.

The goal of this study was to investigate skeletal lesions often identified in human archaeological remains, which may be attributed to a broader spectrum of diseases (e.g. porotic lesions), and provide new tools and strategies for a more accurate identification of their nature and aetiology. Besides considering pathological lesions, we aimed to provide new tools and strategies also for the analysis of other kinds of skeletal lesions, like traumas, to appropriately identify the kind of injury, the conditions in which it occurred, and the timing of infliction *intra-vitam*.

1.2 – Paleo-pathologic evidence of difficult diagnosis

Paleo-pathology is the discipline that studies pathological manifestations on ancient human remains, whether skeletonized or mummified. The term ‘Paleo-pathology’ was coined by R. W. Shufeldt in 1892 from three words in ancient Greek: *πάλιος* (ancient), *πάθος* (pain, emotion) and *λόγος* (analysis). The term was adopted by M. A. Ruffer at the beginning of the last century (Fornaciari, 2013), to define a scientific interest aimed at studying and researching the diseases of the past (Aufderheide and Rodríguez, 2000; Fornaciari G. and Giuffra V., 2009).

In fact, this discipline already existed and began to spread into Europe from 1700, thanks to the German naturalist J. F. Esper, who initially turned his interests towards animal bone samples, before moving onto the study of human remains, in a period of new

archaeological excavations. J. F. Esper's research focused mainly on measuring the proportions of the human skulls. Yet, this kind of study acted as a starting point that inspired the curiosity of many scientists towards the research of the origins of skeletal anomalies and lesions, both of pathological and traumatic origin (Fornaciari G. and Giuffra V., 2009).

Even today, the principal interest of the paleo-pathologic research concerns an essential topic, as pinpointed by Anne Lee Grauer (2012):

«the field of paleopathology, quite simply, entails the study of ancient disease», and, the “paleopathological focus might begin with recognition of bony changes that are quantified and qualified: that is, recognition of “consistent anatomical alterations”; but continues with the exploration of singular or multifactorial causes of these alterations and the ramifications of the conditions on our understanding of human life. It is with these broad perspectives and goals that paleopathologists view the past».

We can share this perspective; however, it seems rather optimistic. More often, our view of the past depends from the type and condition of the ancient human remains retrieved.

Usually, the material which allows the collection of information on past human diseases can be divided into "Direct" and "Indirect" (Moodie, 1923; Capasso, 2002; Buikstra and Roberts, 2012). The first category is mostly constituted by archaeological bone material, mummified soft tissues and preparations. Yet, it can also include pathological materials which can be preserved during long periods of burial (e.g., calculi, ossified haematomas, etc.). The second category (indirect material) is represented by historical information on diseases, which may include clinical documentation, as well as artistic and literary sources. Mainly, for the diagnosis of pathological lesions, physical anthropologists rely on the direct evidence that is found on ancient human bones - given that it exists and is preserved enough to permit a diagnosis.

Pathological findings on the skeleton can be generated by various kinds of disease, divided by categories: arthropathies, congenital diseases, acquired diseases, infections, metabolic disorders, circulatory and haematopoietic disorders, endocrine disorders and neoplasms. Chronic pathologies, which afflict the living individual for a long time, may be more easily diagnosed on ancient human bones, if they are affected. A considerable part of diseases - unfortunately for paleopathologists - leaves no signs on human bones. This category includes some infectious diseases that cause high mortality and have a rapid course (e.g. plague), and diseases that affect soft tissues such as cardiovascular diseases with fatal consequences (e.g. heart attacks, ischemia, apoplexy, embolisms, etc.).

Other pathologies (e.g. hematopoietic disorders, metabolic disorders, neoplasms) are more complex to detect and identify due to several factors including the non-specificity of the bone lesions, the low level of coverage in comparison material (e.g. sporadic tumour lesions or syndromes) or even, the skeletal incompleteness that could mislead the diagnosis.

Thus, many of the pathologies found in ancient human remains could be difficult to determine. Among these, the diseases that affect the blood flow, and consequently, the bone marrow, are particularly challenging to identify. These disorders cause different damages to the bones of the skull, and only in severe cases, we can find evidence on post cranial skeleton (Aufderheide and Rodríguez, 2000; Ortner, 2003; Pinhasi and Mays, 2008; Buikstra and Roberts, 2012; Grauer, 2012).

Among the most discussed and controversial non-specific indicators of bone marrow disorders, we have 'porotic hyperostosis' and 'cribra orbitalia' (Figure 1.1). Both kind of lesion are recognized by the presence of porosity of variable density, more or less visible according to the gravity. Apparently, the only visual distinction between the two lesions is represented by their localisation: 'porotic hyperostosis' can be found on the cranial vault, while 'cribra orbitalia' is located on one or both orbital surfaces (Wapler et al., 2004; Walker et al., 2009; Rivera and Mirazón Lahr, 2017; Rinaldo et al., 2019). Both lesions are due to hypertrophy of the hematopoietic marrow and, consequently, to the thinning of the cortical surface of the bone. In severe cases (Figure. 1.1), the underlying trabecular tissue may remain exposed (Ortner, 2003; Walker et al., 2009; Fredrick Oxenham and Cavill, 2010; Kumar et al., 2011; Rothschild, 2012; Mcilvaine, 2015; Minozzi and Canci, 2015).

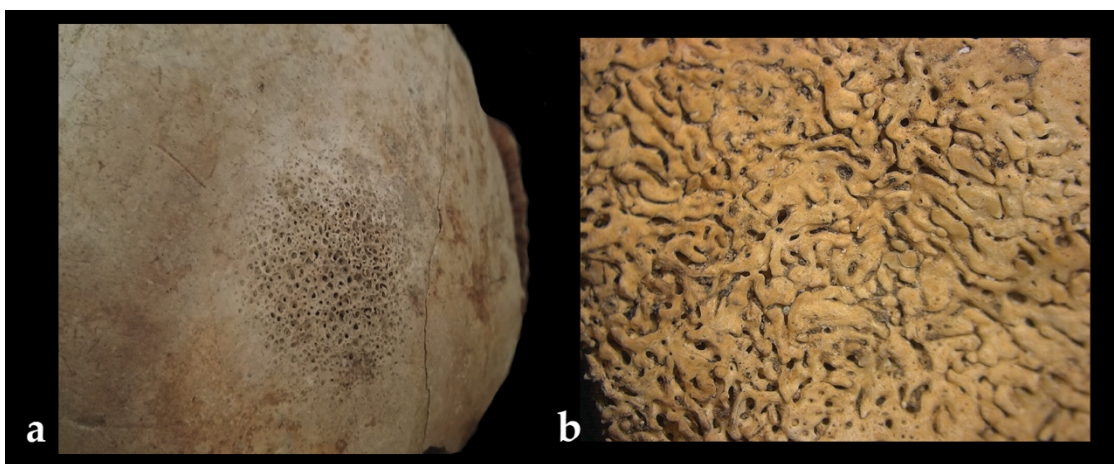


Figure 1.1 – Example of **a)** severe porotic hyperostosis on the right parietal and **b)** severe cribra orbitalia on the orbital roof (Photo: Filippo Scianò).

1.2.1 – The difficulty to assess β -thalassemia on ancient human remains

Among the diseases, which are of difficult identification from ancient human remains, we can count β -thalassemia, a hematopoietic disorder.

Thalassemia was first clinically described nearly a century ago by Thomas Benton Cooley when, in 1925, he presented his new finding with the name of "erythroblasts anaemia" to the American Pediatric Society; today this hereditary blood disease is also known with other different names such as ‘Cooley's disease’, ‘Mediterranean anaemia’ and ‘ β -thalassemia’. The knowledge of this widespread disease has greatly advanced in the last century, mainly thanks to DNA-based diagnoses that elucidated the molecular basis of the disease (Figure 1.2), and clarified the variable clinical picture (Rund and Rachmilewitz, 2005; Rund, 2016). Several scholars (Galanello and Origa, 2010; Wong et al., 2016; Origa, 2017) claim in their researches, that the difficulty to assess a diagnosis of β -thalassemia, especially in ancient skeletons, depends on the large β -thalassemias heterogeneousness at the molecular level, with more than 200 mutations reported to date¹, which may affect bones with great variability.

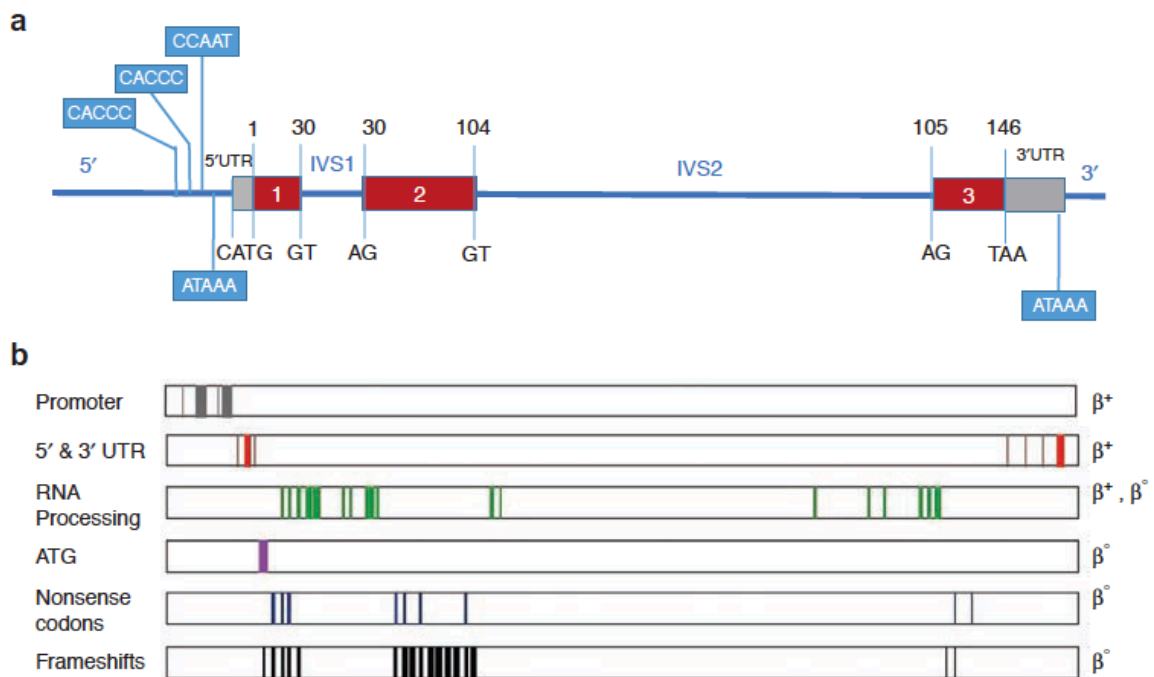


Figure 1.2 – The Molecular basis of β -thalassemia. **a)** Human β -globin gene in chromosome 11. The grey areas are that region transcribed but not translated. The red areas are the exons. The numbers represent the β -globin amino-acids residues encoded by the three exons. **b)** Type and distribution of the mutations in the β -thalassaemia syndrome (Original picture taken from Origa, 2017)[©].

¹ A complete, current list is available at the Globin Gene Server (<http://globin.cse.psu.edu/>).

As a consequence, a precise diagnosis of this disease in human remains is difficult and requires a confirmation from aDNA analyses. However, we tried to outline a new methodological approach for a more accurate diagnosis of this ancient syndrome from dry bones (chapter 2). We benefitted of the indications gained in medical literature about various skeletal markers to develop an evaluation form for a preliminary diagnosis of the thalassemia syndrome.

We deal with the identification of β -thalassemia in ancient times primarily because: **a)** β -thalassemia is the most commonly inherited single-gene disorder and its pathogenesis is well understood in clinical patients (Marengo-Rowe, 2007; De Sanctis et al., 2018; El-Beshlawy and El-Ghamrawy, 2019); **b)** the skeletonized individuals we considered in this study - San Mamiliano, Sovana (GR) - might have suffered of thalassemia based on preliminary morphological observations (abnormal thickening of the diploe); **c)** the same human remains were found in a typical malaria environment (Sovana is placed in the Maremma region, in Tuscany, Italy), and the emergence of thalassemia has been attributed to the prevalence of malaria (Angel, 1966; Flint et al., 1993; Weatherall, 1997; Bianucci et al., 2015; Smith-Guzmán, 2015; Marciniak et al., 2018); **d)** the study of ancient thalassemia and its relationship with malaria can help us to better understand the effects of natural selection on human populations.

1.2.2 – The difficulty to assess tumours in ancient time

Neoplastic lesions, better known as tumors, are due to «an abnormal mass of tissue that grows uncontrolled compared to normal tissues, and that condition persists after the stop of the stimuli that have induced the process» (Kumar et al., 2011).

It is commonly accepted that the neoplastic disease is a prerogative of the post-industrial era, also because the majority of people not reached advanced age in the past. Though, as underlined by several authors, cancer was present also in previous times (Capasso, 2005; David and Zimmerman, 2010), even if during prehistory and protohistoric time it might have been much rarer than nowadays (Aufderheide and Rodríguez, 2000; Buikstra and Roberts, 2012; Binder et al., 2014).

As underlined by Halperin (2004), the discovery of neoplasia in ancient populations can provide particular information on the possible influences of morphological and functional evolution, diet, lifestyle and other environmental factors. The first hominids and non-human primates of the Palaeolithic will most likely have been in contact with different carcinogens than today. They have certainly not been exposed to tobacco, fine particulates

and other carcinogenic chemicals known today. However, they may have been exposed to natural environmental carcinogens (combustion fumes, natural carbon, local outcrops of asbestos, sulphur or other carcinogenic minerals). Domestic occupation of caves may have caused exposure to naturally trapped radon gases, uranium or heavy metal minerals.

Another aspect that mainly does not concern the current west-world, is skin exposure to ultraviolet light, because we use clothing. In prehistoric times, we have no information whether the exposure was the same as nowadays or higher than the recommended maximum limit for humans (Aufderheide and Rodríguez, 2000).

We can also take a position considering that malignant tumours in the past were almost certainly incurable. However, we have no mean to attest this opinion with certainty.

The main concerns for detecting the incidence of neoplastic lesions in past populations are two: **a)** several events, which may be quickly fatal (e.g. secondary bleeding, secondary soft tissue infections, etc.), may have accompanied the pathological occurrence and have not allowed the tumour lesion to affect the bones; **b)** many tumours that affect the soft tissues, and that have a rapid course, do not leave visible signs on the skeleton. As a consequence, the incidence of cancer in the past may be underestimated and it remains also often hidden if the tumour lesions were not specific of the bone, or were not metastasized to the skeleton (Ortner, 2003).

By all means, every reported case, better if carefully diagnosed, helps not only to a better knowledge of the history, of the epidemiology and of the possible concurrent causes in the past, but may significantly contribute to the understanding of the underlying mechanisms leading to cancer nowadays.

We aimed to contribute to the cancer casuistry by reporting about two rarer lesions of the sinus frontalis detected in ancient skulls by visual inspection, and analysed in deep with endoscopic, radiological, and microscopic techniques (chapter 3).

1.2 – Evidences of trauma with uncertain diagnosis

In physical anthropology, the lesions observed during a palaeopathological investigation may have a traumatic origin, considering that in the concept of trauma, we summarize the idea of a quick and unexpected damaging action.

In the last decades, the focus on the traumatic lesion has shifted from the pure description of their morphological features to a more specific interest for the episodes of violence,

which have determined them. Further, many systematic studies on trauma focused on specific populations: Roberts and collaborators have studied trauma in British paleopopulations (Roberts, 1991, 2002; Robb, 2000; Roberts and Cox, 2003), while Webb (1995) included trauma analysis in his study on the skeletons of Australian Aboriginal. Studies on traumatic injuries in ancient North American populations, have been carried out by several scholars (Walker, 1989; Kilgore, Jurmain and Van Gerven, 1997; Lovell, 1997; Jurmain, 2001; Smith, 2003). Anthropological studies of traumas in Europe covering a range of different periods have been carried out as well (Martin and Frayer, 1997; Parker Pearson and Thorpe, 2005; Šlaus, 2008; Turner and Lee, 2018).

Traumatic lesions, along with arthropathies, are among the most frequent changes found in ancient human skeletal remains (Borgognini Tarli and Pacciani, 1993). However, in contrast to arthropathies, traumas show a more considerable diagnostic variability, and may include external factors that complicate the accuracy of the diagnosis.

The mechanisms that determine a fracture or an injury are multiple and different, yet they can be grossly divided into “direct”, “indirect”, “determined by a stress” and “consequent to a pathology”. Each mechanism generates a different type of lesion on the bone. Moreover, each of these evidences depends directly on how the lesion was produced and on the damaging action. In case of an act of interpersonal violence, the variability of the bone injury mostly depends from the weapon used to inflict the lesion.

1.2.3 – The difficulty to assess the timing of traumatic lesions on dry human bones

A considerable amount of literature, in particular in the field of forensic anthropology, has been dedicated to traumatic lesions on dry human bones (Lovell, 1997; Reichs and Bass, 1998; Sauer, 1998; Dirkmaat et al., 2008; Facchini et al., 2008; Kimmerle and Baraybar, 2008; Maat, 2008; Pickering and Bachman, 2009; Black and Ferguson, 2011; Fleming-Farrell et al., 2013; Gualdi-Russo and Fonti, 2013; Wedel and Galloway, 2014; Martin and Harrod, 2015; Jerković et al., 2016; Blau, 2017; Pasini et al., 2019; Scianò et al., 2020). Indeed, a significant contribution to the understanding of traumas comes from the study of forensic cases; this helps us to understand the mechanisms and patterns of trauma caused by different weapons and various types of accidents. Yet, in past populations, the analysis of injuries and their contextualization allows us to increase our knowledge of both interpersonal conflicts and dynamics of violence (Blau and Ubelaker, 2016).

Extensive studies have shown that the shape of the lesion, as well as the thickness and plasticity of the bone are related to the pattern of fractures. Macroscopic and microscopic

studies on healing processes (Barber, 1930; Barbian and Sledzik, 2008; Kranioti et al., 2019), and those on bone tissue degradation (Corron et al., 2017) have provided us with information on the characteristics the bone presents if the lesion has been inflicted around the death.

The interpretation of a violent cause of death may be relatively simple for a trained forensic anthropologist (Sauer, 1998), if traces are left on the skeleton. Nevertheless, in the most difficult cases, the contextual information on the events that lead to the death of an individual may be limited to the wide-view. Interpretations may include the category of trauma, the type of force that caused the injury, the weapon that caused the injury, and, lastly, the possible timing of infliction and, in case of multiple injuries, their timeline of occurrence. Also in this case, without preserved soft tissues, much of the information on the causes of death may be lost (Borgognini Tarli and Pacciani, 1993).

Notwithstanding, the interest in the diagnosis of injuries specifically related to interpersonal violence is growing in bioarchaeological research, as evidenced by the increasing amount of literature on this topic (Keeley, 1996; Walker, 2001; Larsen, 2002; Mielke, 2002; Parker Pearson and Thorpe, 2005b; Otto et al., 2006; Black and Ferguson, 2011; Jerković et al., 2016; Pasini et al., 2019; Scianò et al., 2020).

In this regard, Pia Bennike observed (in Pinhasi and Mays, 2008; pag. 325):

«In spite of new technologies and interdisciplinary collaboration, there are still many problems to be resolved when studying trauma in the past. For one thing, distinguishing between *ante-*, *peri-* and *post-mortem* injuries, violence or accident, treatment or lack of treatment, sacrifice or punishment may still present major challenges in palaeopathology».

Indeed, to date, there is much confusion in the terminology and the methodological approaches to be employed in the study of traumatic lesions. A few years ago, Anne W. Bunch (2014) tried to shed some light on the foggy terminology used for the definition of timing of traumatic lesion in forensic anthropology.

With our work, we tried to determine a methodological approach, even if preliminary, for the timing assessment of traumatic lesions on dry bones (chapter 4). We aim to continue in this direction, to find an increasingly in-depth, standardized way, to clarify and simplify the mechanism of the assessment of lesion timing in anthropology.

1.4 – Pseudo-pathology and diagenetic changes

When approaching the study of a lesion on skeletal bone remains, the first, and most important question to be addressed is the following: Is the lesion occurred *intra-vitam* or is it the result of *post mortem* diagenetic processes? (Brothwell and Sandison, 1967; Aufderheide and Rodríguez, 2000; Ortner, 2003; Schultz, 2003). The term ‘pseudo-pathology’ is used to indicate a structural change in healthy bone or soft tissue that resembles a pathological lesion, but is, in fact, the product of a diagenetic process (Halperin, 2004; Minozzi and Canci, 2015). The morphological similarity between diagenetic changes and different kinds of pathological lesions on bones (Maat, 1993; Corron et al., 2017) is the main reason for calling them ‘pseudo-pathologies’, as it was proposed in the past century (Lortet and Gaillard, 1905; Smith, 1907), as well as in more recent times (Aubry et al., 2003; Wapler et al., 2004).

Indeed, soil and water, with their chemical composition, can modify the bones both macroscopically and microscopically. Bones consist of an inorganic chemical component (hydroxyapatite) and an organic chemical part (collagen, proteins and glycoproteins). Both components may be altered by soil and water.

Macroscopically, the pressure exerted by soil and water can produce severe bone deformation, discolouration, and erosion of the cortical tissue. Microscopically, the changes are mainly influenced by the chemical nature of the soil (Minozzi and Canci, 2015). The degree of acidity or basicity of the soil heavily affects the good preservation of the distinct bone districts. An acidic soil ($\text{pH} < 6$) dissolves the hydroxyapatite, modifying the bone tissue irreparably or destroying it (Mays, 1998).

Bacteria and fungi present in the soil commonly access the Haversian canals, and, producing acids that dissolve the bone’s minerals, promote changes that are easily recognizable histologically to a focused and trained observer (Schultz, 2001, 2003). Animals that have access to the skeleton, especially rodents but also carnivores, as well as insects, can produce pseudopathological lesions (e.g. gnawing marks, scratches, puncture marks, micro-holes and breakage). Plants can cause pseudo-pathological lesions as well. Plant roots can intrude the long bone marrow cavities through a foramen (tunnelling), producing fractures. Rootlets can wrap the long bones trapping groundwater on the bone cortex; the subsequent lithic action of groundwater and/or of plant secretions can create superficial channels in the bones, and give rise to pseudo-pathologies (e.g. blood vessel impressions). In some cases, also extreme climatic conditions may yield pseudo-pathological changes. Alternate phases of frost and defrost can crush the buried bones,

while wind and rain can cause damage or *post mortem* disturbance in exposed skeletons (Maijanen et al., 2016; Corron et al., 2017).

Diagenetic changes can be easily identified with microscopic investigation by a trained observer, who knows each phase of the bone's development, including histogenesis, bone growth, decomposition and the potential effects of diagenetic factors (Schultz, 1997, 1999a; Grauer, 2012). A careful sectioning of the bones for histological inspection, for example, could reveal no pathological changes in the bone structure, thus enabling to discriminate among different kinds of lesions (Schultz, 2001; Van der Merwe et al., 2009).

1.5 – Methodologic approaches for lesion's detection in anthropology

In essence, the most significant challenge for anthropologists is to define criteria for identifying changes that appear to produce similar bone lesions. The introduction of laboratory methodologies in physical anthropology may be of great help to accurately classify each lesion. Following a work-flow, from the preliminary macroscopic observation, through the use of different techniques, it should be possible to carry out an accurate differential diagnosis and understand the actual cause of a lesion.

With these premises, we have carried out differential diagnoses on the lesions of 72 skeletonized individuals from different epochs and proveniences. Sixty-eight individuals came from the necropolis of Sovana San Mamiliano (15th - 16th centuries) - in collaboration with the Soprintendenza Archeologia, Belle Arti e Paesaggio, Firenze, Pistoia e Prato -, whereas the others belonged to the archaeological collection of the Laboratory of Arceo-Anthropology and Forensic Anthropology of the University of Ferrara. In particular, three individuals came from the necropolis of Spina Valle Pega (3rd – 6th centuries BCE) - in collaboration with the National Archaeological Museum of Ferrara -, while one individual was from the archaeological site of Ballabio (Prato della Chiesa, Early Bronze Age) - in collaboration with the Soprintendenza Archeologia, Belle Arti e Paesaggio per le Province Di Como, Lecco, Monza-Brianza, Pavia, Sondrio e Varese.

For the whole study, we used a strict methodological approach constituted by progressive analyses (Figure 1.3).

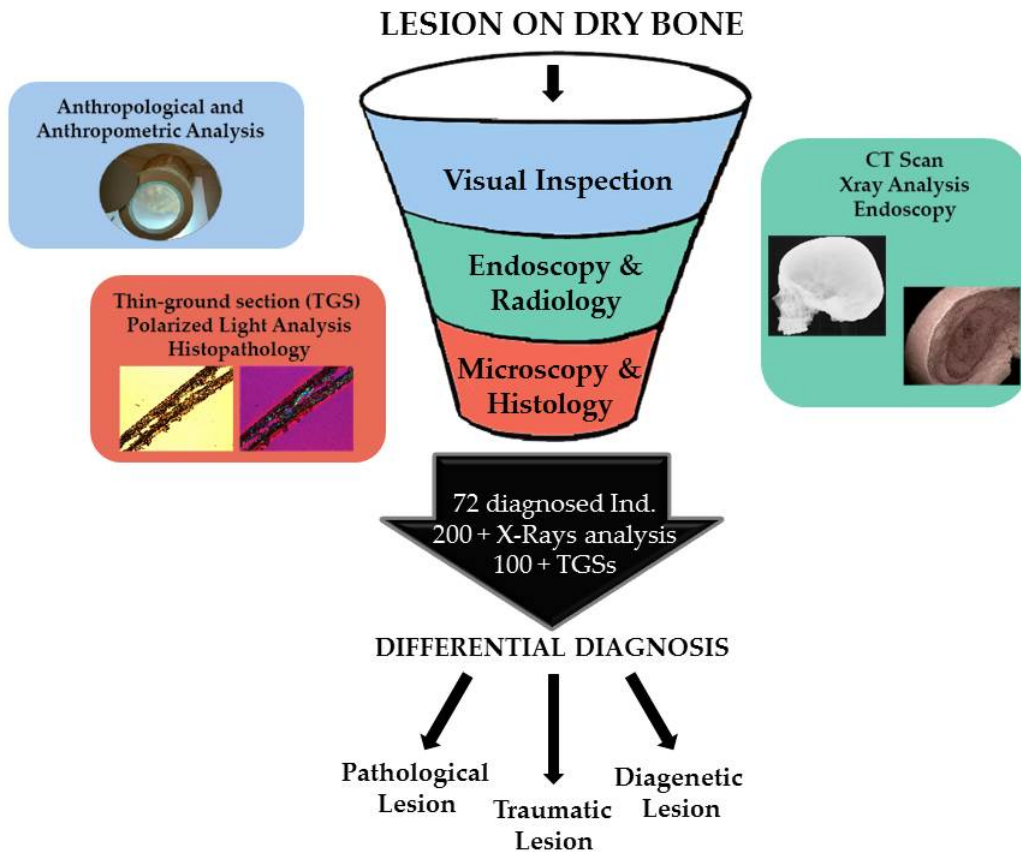


Figure 1.3 – Methodological approach and progressive analysis carried out in our study (Picture: Filippo Scianò).

The workflow included, at the first stage, a macroscopic investigation, at the second stage, endoscopic/radiological examinations, and, at the third stage, microscopic and histological analyses.

- **First stage – Visual inspection:** while determining the biological profile of the individual through macroscopic inspection and anthropometric measures, we examined the bones for possible lesions. We filled in the anthropological forms with the gained data and we took pictures of the lesions. In this phase, we started also the acquisition of contextual data, such as historical and archaeological information.
- **Second stage – Endoscopic/Radiological analyses:** This second part of the research was carried out taking into account the information obtained in the previous step. Specific analyses were carried out using technical instruments (i.e. endoscope, borescope, X-ray machine, CT Scan, CBCT Scan) according to the type, position and nature of the bone lesion observed.

- **Third stage – Microscopic/ Histologic analyses:** taking into account the outcomes of the previous analyses, we deepened the investigation through the use of microscopic examination. We took advantage from the knowledge that I have acquired at the University of Göttingen (Germany) under the supervision of Prof. M. Schultz. On this occasion, I have learnt all the procedures developed by Schultz for preparing osteological material (Schultz, 1993, 1999b, 2001), in particular the so called Thin-Ground Section (TGS), a method for obtaining histological preparations from bones. This technique represents the gold standard for microscopic analysis of dry human bones and may greatly contribute to an accurate differential diagnosis of diseases and other kinds of lesions.

The details of the studies carried out and the results gained constitute the body of this doctoral thesis, which is subdivided into two parts: the first part consists of two chapters in which we describe some pathological lesions diagnosed, while the two chapters of the second part deal with the identification of traumatic lesions. As a by-product of the work, we could propose two preliminary evaluation forms, one for the diagnosis of β -thalassemia and one for the identification of the timing of injuries.

1.6 – References

- Angel JL. 1966. Porotic Hyperostosis, Anemias, Malaras, and Marshes in the Prehistoric Eastern Mediterranean. *Science* (80-) 153:760–763.
- Aubry M, Mafart B, Donat B, Brau JJ. 2003. Brief communication: Study of noncarious cervical tooth lesions in samples of prehistoric, historic, and modern populations from the south of France. *Am J Phys Anthropol* 121:10–14.
- Aufderheide AC, Rodríguez. 2000. *The Cambridge encyclopedia of human paleopathology*.
- Barber CG. 1930. The detailed changes characteristic of healing bone in amputation. *J Bone Jt Surg* 12:353–359.
- Barbian LT, Sledzik PS. 2008. Healing following cranial trauma. *J Forensic Sci* 53:263–268.
- Bianucci R, Araujo A, Pusch CM, Nerlich AG. 2015. The identification of malaria in paleopathology-An in-depth assessment of the strategies to detect malaria in ancient remains. *Acta Trop* 152.
- Binder M, Roberts C, Spencer N, Antoine D, Cartwright C. 2014. On the antiquity of cancer: Evidence for metastatic carcinoma in a young man from ancient Nubia (c. 1200bc). *PLoS One* 9:1–11.
- Black SM, Ferguson E. 2011. *Forensic anthropology : 2000 to 2010*. CRC Press.
- Blau S. 2017. How traumatic: a review of the role of the forensic anthropologist in the examination and interpretation of skeletal trauma. *Aust J Forensic Sci* 49:261–280.
- Blau S, Ubelaker DH. 2016. *Handbook of Forensic Anthropology and Archaeology*. (Blau S, Ubelaker DH, editors.). Routledge.
- Borgognini Tarli S, Pacciani E. 1993. *I resti umani nello scavo archeologico: metodiche di recupero e studio /*. Bulzoni.
- Brothwell DR, Sandison AT. 1967. *Diseases in antiquity; a survey of the diseases, injuries, and surgery of early populations,*. C.C. Thomas.
- Buikstra JE, Roberts CA. 2012. *The global history of paleopathology : pioneers and prospects*. Oxford University Press.
- Capasso L. 2002. *Principi di storia della patologia umana : corso di storia della medicina*

per gli studenti della Facoltà di Medicina e chirurgia e della facoltà di Scienze infermieristiche. Società editrice universo.

Capasso L. 2005. Antiquity of cancer. *Int J Cancer* 113:2–13.

Corron L, Huchet JB, Santos F, Dutour O. 2017. Identification d'agents pathologiques et taphonomiques à l'origine de modifications osseuses à l'aide de classifications : existe-t-il des critères dits « taphognomoniques »? *Bull Mem Soc Anthropol Paris* 29.

David AR, Zimmerman MR. 2010. Cancer: an old disease, a new disease or something in between? *Nat Rev Cancer* 10:728–733.

Dirkmaat DC, Cabo LL, Ousley SD, Symes SA. 2008. New perspectives in forensic anthropology. *Am J Phys Anthropol* 137:33–52.

El-Beshlawy A, El-Ghamrawy M. 2019. Recent trends in treatment of thalassemia. *Blood Cells, Mol Dis* 76:53–58.

Facchini F, Rastelli E, Belcastro MG. 2008. Peri mortem cranial injuries from a medieval grave in Saint Peter's Cathedral, Bologna, Italy. *Int J Osteoarchaeol* 18:421–430.

Fleming-Farrell D, Michailidis K, Karantanas A, Roberts N, Kranioti EF. 2013. Virtual assessment of perimortem and postmortem blunt force cranial trauma. *Forensic Sci Int*.

Flint J, Harding RM, Boyce AJ, Clegg JB. 1993. The population genetics of the haemoglobinopathies. *Baillieres Clin Haematol* 6:215–62.

Fornaciari G. 2013. Cenni di storia della Paleopatologia in Italia.

Fornaciari G., Giuffra V. 2009. *Lezioni di paleopatologia*. (Ecig, editor.).

Fredrick Oxenham M, Cavill I. 2010. Porotic hyperostosis and cribra orbitalia: the erythropoietic response to iron-deficiency anaemia. *Anthropol Sci* 118.

Galanello R, Origa R. 2010. Beta-thalassemia. *Galanello Origa Orphanet J Rare Dis* 5:1–15.

Grauer AL. 2012. *A companion to paleopathology*. Wiley-Blackwell.

Gualdi-Russo E, Fonti G. 2013. Recent trend and perspectives in forensic anthropology: a bibliometric analysis. *Coll Antropol* 37:595–9.

Halperin EC. 2004. *Paleo-Oncology: The Role of Ancient Remains in the Study of*

- Cancer. *Perspect Biol Med* 47:1–14.
- Jerković I, Bašić Ž, Bečić K, Jambrešić G, Grujić I, Alujević A, Kružić I. 2016. Anthropological analysis of the Second World War skeletal remains from three karst sinkholes located in southern Croatia. *J Forensic Leg Med* 44:63–67.
- Jurmain R. 2001. Paleoepidemiological patterns of trauma in a prehistoric population from Central California. *Am J Phys Anthropol* 115:13–23.
- Keeley LH. 1996. *War Before Civilization*. Oxford Oxford Univ Press Kekes, J 106pp:834–44.
- Kilgore L, Jurmain R, Van gerven D. 1997. Palaeoepidemiological Patterns of Trauma in a Medieval Nubian Skeletal Population. *Int J Osteoarchaeol* 7:103–114.
- Kimmerle EH, Baraybar JP. 2008. *Skeletal Trauma: Identification of Injuries Resulting from Human Rights Abuse and Armed Conflict*. CRC Press.
- Kranioti EF, Grigorescu D, Id KH. 2019. State of the art forensic techniques reveal evidence of interpersonal violence ca. 30,000 years ago.
- Kumar V, Abbas AK, Fausto N, Aster JC. 2011. *Robbins e Cotran - Le basi patologiche delle malattie: Vol. 1 Patologia generale - Vol. 2 Malattie degli organi e degli apparati*. Elsevier Health Sciences Italy.
- Larsen CS. 1999. *Bioarchaeology: interpreting behavior from the human skeleton*. Cambridge University Press.
- Larsen CS. 2002. *Bioarchaeology: The Lives and Lifestyles of Past People*.
- Lortet L (1836-1909). *A du texte*, Gaillard C (1861-1945). *A du texte*. 1905. *La faune momifiée de l'ancienne Égypte. Série 3 / par le Dr Lortet,... M.-C. Gaillard,... ; préface de M. V. Loret,...*
- Lovell NC. 1997. Trauma Analysis in Paleopathology. *Yrbk Phys Anthr* 40:139–170.
- Lovell NC. 2000. Paleopathological description and diagnosis. In: Katzenberg M, Saunders S, editors. *Biological Anthropology of Human Skeleton*. New York: Wiley-Liss. p 217–248.
- Maat GJR. 1993. Bone preservation, decay and its related conditions in ancient human bones from Kuwait. *Int J Osteoarchaeol* 3:77–86.
- Maat GJR (George. 2008. Case Study 5.3: Dating of fractures in human dry bone tissue - the Berisha case. In: Erin H. Kimmerle JPB, editor. *Skeletal Trauma Identification of*

- Injuries Resulting from Human Rights Abuse and Armed Conflict. . p 245–254.
- Maijanen H, Wilson-Taylor RJ, Jantz LM. 2016. Storm-Related Postmortem Damage to Skeletal Remains. *J Forensic Sci* 61:823–827.
- Marciniak S, Herring DA, Sperduti A, Poinar HN, Prowse TL. 2018. A multi-faceted anthropological and genomic approach to framing *Plasmodium falciparum* malaria in Imperial period central-southern Italy (1st–4th c. CE). *J Anthropol Archaeol* 49:210–224.
- Marengo-Rowe AJ. 2007. The thalasseмии and related disorders. *Proc (Bayl Univ Med Cent)* 20:27–31.
- Martin DL, Frayer DW eds. 1997. *Troubled times: Evidence for violence and warfare in the past*. Gordon and Breach.
- Martin DL, Harrod RP. 2015. Bioarchaeological contributions to the study of violence. *Am J Phys Anthropol* 156:116–145.
- Mays SA. 1998. Mays - The Archaeology of Human Bones.pdf. *Am Antiq* 65:582.
- Mcilvaine BK. 2015. Implications of Reappraising the Iron-Deficiency Anemia Hypothesis. *Int J Osteoarchaeol*.
- Van der Merwe AE, Maat GJR, Steyn M. 2009. Ossified haematomas and infectious bone changes on the anterior tibia: histomorphological features as an aid for accurate diagnosis. *Int J Osteoarchaeol*:n/a-n/a.
- Mielke JH. 2002. Warfare and population structure. In: Smith M, editor. *Human Biology and History*. . p 98–111.
- Minozzi S, Canci A. 2015. *Archeologia dei resti umani: dallo scavo al laboratorio*. Carocci.
- Moodie R. 1923. *Paleopathology, an introduction to the study of ancient evidence of disease*. Urbana Ill.: University of Illinois Press.
- Origa R. 2017. β -Thalassemia. *Genet Med* 19:609–619.
- Ortner DJ. 2003. *Identification of pathological conditions in human skeletal remains*.
- Otto T, Thrane H, Vandkilde H. 2006. *Warfare and society: archaeological and social anthropological perspectives*. Aarhus University Press.
- Parker Pearson M, Thorpe IJ. 2005a. *Warfare, violence and slavery in prehistory:*

- proceedings of a Prehistoric Society conference at Sheffield University. London: Archaeopress.
- Parker Pearson M, Thorpe IJ. 2005b. Warfare, violence and slavery in prehistory: proceedings of a Prehistoric Society conference at Sheffield University. Archaeopress.
- Pasini A, Gualdi-Russo E, Scianò F, Thun Hohenstein U. 2019. Violence in the Early Bronze Age. Diagnosis of skull lesions using anthropological, taphonomic and scanning electron microscopy techniques. *Forensic Sci Med Pathol* 15:324–328.
- Pickering RB, Bachman DC (David C. 2009. *The use of forensic anthropology*. CRC Press.
- Pinhasi R, Mays S. 2008. *Advances in Human Palaeopathology*.
- Reichs K, Bass WM. 1998. *Forensic osteology: advances in the identification of human remains*. Charles C Thomas.
- Rinaldo N, Zedda N, Bramanti B, Rosa I, Gualdi-Russo E. 2019. How reliable is the assessment of Porotic Hyperostosis and Cribra Orbitalia in skeletal human remains? A methodological approach for quantitative verification by means of a new evaluation form. *Archaeol Anthropol Sci*.
- Rivera F, Mirazón Lahr M. 2017. New evidence suggesting a dissociated etiology for cribra orbitalia and porotic hyperostosis. *Am J Phys Anthropol* 164:76–96.
- Robb J. 2000. Analyzing human skeletal data. In: Cox M, Mays S, editors. *Human Osteology in Archaeology and Forensic Science*. . p 475–490.
- Roberts C. 1991. Trauma and treatment in the British Isles in the Historic Period: A design for multidisciplinary research. In: *Human Paleopathology: Current Synthesis and Future Options*. . p 225–240.
- Roberts C. 2002. Palaeopathology and archaeology: the current state of play. In: Arnott R, editor. *The Archaeology of Medicine*. . p 1–20.
- Roberts CA, Cox M. 2003. *Health and disease in Britain: from prehistory to the present day*. Gloucester Sutt Publ.
- Rothschild B. 2012. Extirpation of the Mythology That Porotic Hyperostosis Is Caused by Iron Deficiency Secondary to Dietary Shift to Maize. *Adv Anthropol* 2:157–160.
- Rund D. 2016. *Thalassemia 2016: Modern medicine battles an ancient disease*. Am J

Hematol 91:15–21.

Rund D, Rachmilewitz E. 2005. β -Thalassemia. *N Engl J Med* 353:1135–1146.

De Sanctis V, Soliman AT, Elsefdy H, Soliman N, Bedair E, Fiscina B, Kattamis C. 2018. Bone disease in β thalassemia patients: past, present and future perspectives. *Metabolism* 80:66–79.

Sauer N. 1998. The timing of injuries and manner of death: distinguishing among antemortem, perimortem and postmortem trauma. In: Reichs K, editor. *Forensic osteology: advances in the identification of human remains*. Springfield: Charles C Thomas Publisher. p 321–32.

Schultz M. 1993. Light Microscopic Analysis of Macerated Pathologically Changed Bones. :253–296.

Schultz M. 1997. Microscopic investigation of excavated skeletal remains A contribution to paleopathology and forensic medicine. In: Haglund W, Sorg M, editors. *Forensic taphonomy. The postmortem fate of human remains*. Boca Raton, FL: CRC Press. p 201–222.

Schultz M. 1999a. Microscopic Investigation in Fossil Hominoidea : A Clue to Taxonomy , Functional Anatomy , and the History of Diseases. :225–232.

Schultz M. 1999b. Light Microscopic Analysis in Skeletal Paleopathology.

Schultz M. 2001. Paleohistopathology of bone: A new approach to the study of ancient diseases. *Am J Phys Anthropol* 116:106–147.

Schultz M. 2003. Light microscopic analysis in skeletal paleopathology. In: Ortner DJ, editor. *Identification of pathological conditions in human skeletal remains*. Amsterdam: Academic Press/Elsevier Science. p 73–108.

Scianò F, Bramanti B, Manzon VS, Gualdi-Russo E. 2020. An investigative strategy for assessment of injuries in forensic anthropology. *Leg Med* 42:101632.

Šlaus M. 2008. Osteological and dental markers of health in the transition from the Late Antique to the Early Medieval period in Croatia. *Am J Phys Anthropol* 136:455–469.

Smith-Guzmán NE. 2015. The skeletal manifestation of malaria: An epidemiological approach using documented skeletal collections. *Am J Phys Anthropol*.

Smith GE. 1907. The Alleged Discovery Of Syphilis In Prehistoric Egyptians. *Lancet* 170:1788–1789.

- Smith MO. 2003. Beyond palisades: The nature and frequency of late prehistoric deliberate violent trauma in the Chickamauga Reservoir of East Tennessee. *Am J Phys Anthropol* 121:303–318.
- Tosi A, Badino P, Pezzoni B. 2017. Medical conditions observed in osteoarchaeological remains: Arthropathies, traumatic lesions, tumours, metabolic diseases and dental pathologies. *Med Hist* 1:29–34.
- Turner WJ, Lee C. 2018. *Trauma in Medieval Society*. (Turner WJ, Lee C, editors.). BRILL.
- Walker PL. 1989. Cranial injuries as evidence of violence in prehistoric southern California. *Am J Phys Anthropol* 80:313–23.
- Walker PL. 2001. a B Ioarchaeological P Eerspective.
- Walker PL, Bathurst RR, Richman R, Gjerdrum T, Andrushko VA. 2009. The causes of porotic hyperostosis and cribra orbitalia: A reappraisal of the iron-deficiency-anemia hypothesis. *Am J Phys Anthropol* 139:109–125.
- Wapler U, Crube E, Schultz M. 2004. Is Cribra Orbitalia Synonymous With Anemia? Analysis and Interpretation of Cranial Pathology in Sudan. 339:333–339.
- Weatherall DJ. 1997. Thalassaemia and malaria, revisited. *Ann Trop Med Parasitol* 91:885–890.
- Webb S. 1995. *Palaeopathology of aboriginal Australians: health and disease across a hunter-gatherer continent*. Cambridge University Press.
- Wedel VL, Galloway A. 2014. Broken bones: anthropological analysis of blunt force trauma.
- Wong P, Fuller PJ, Gillespie MT, Milat F. 2016. Bone Disease in Thalassemia: A Molecular and Clinical Overview. *Endocr Rev* 37:320–346.

CHAPTER 2

BONE LESIONS IN THALASSEMIA SYNDROME: A CHALLENGING' IDENTIFICATION IN PALEOPATHOLOGY

The study of thalassaemia syndromes in archaeological human remains is of growing interest in the field of paleopathology. However, a certain diagnosis of this disease in human skeletons remains difficult.

Depending on the globin strain damaged, the thalassemic syndromes are classified as α -thalassaemia or β -thalassaemia. Each of these two categories includes different forms of the disease related to the homozygous, heterozygous or compound heterozygous status of the person affected.

In archaeological samples, several non-specific lesions were suggested as the most probably evidence of β -thalassaemia syndrome. In particular, lesions of the skull have been considered as the most indicative of this haematopoietic disorder, whereas other authors identified in post cranial lesions the best evidence for β -thalassaemia.

Diagnostic features were determined thanks to an extensive bibliographic research of clinical cases, radiological and microscopic analyses. This study aims to identify those skeletal lesions as “diagnostic” or “indicative not-diagnostic” of β -thalassaemia syndrome. We applied this method to some individuals from the necropolis of San Mamiliano (SSM), a hamlet of Sovana (Grosseto, Italy), dated to the 15th - 16th centuries. The area was endemic for malaria at that time, a condition which let presume the presence of individuals with β -thalassaemia. Another interesting archeological site under investigation was the Etruscan port of Spina on the Po Delta, whereas the cemetery of St. Biagio in Ravenna (17th-19th centuries) was used as a negative control.

2.1 – Introduction

Thalassemias are the most common hemoglobinopathies worldwide. The name ‘thalassemia’, used for one of the most widespread hereditary form of anemia, derived from ‘thalatta’ or ‘thalassa’, which in ancient Greek means ‘sea’, and the word “haema” indicating a blood disorder. In this sense, “thalassic” anemia (Whipple, 1932) sounds such as “sea” anemia, although a better term would be ‘Mediterranean anemia’ since it was first observed and reported in patients from the Mediterranean areas (Frassetto, 1918; Chini et al., 1939; Gatto, 1942; Silvestroni and Gentili, 1946; Martuzzi Veronesi and Zanotti, 1973; Zanotti et al., 1973; Silvestroni and Bianco, 1975; Martuzzi Veronesi and Gualdi-Russo, 1976; Dacie, 1988).

The WHO estimates that almost 270 million of people are nowadays carriers of the syndrome, of which 70 millions are carriers of β -thalassemia (De Sanctis et al., 2017). Thalassemic individuals arwidespread not only in the Mediterranean basin, but also in Africa, India, south-eastern Asia, Melanesia, and the Pacific Islands (Kountouris et al., 2014), on the so-called thalassemia belt (Figure 2.1)

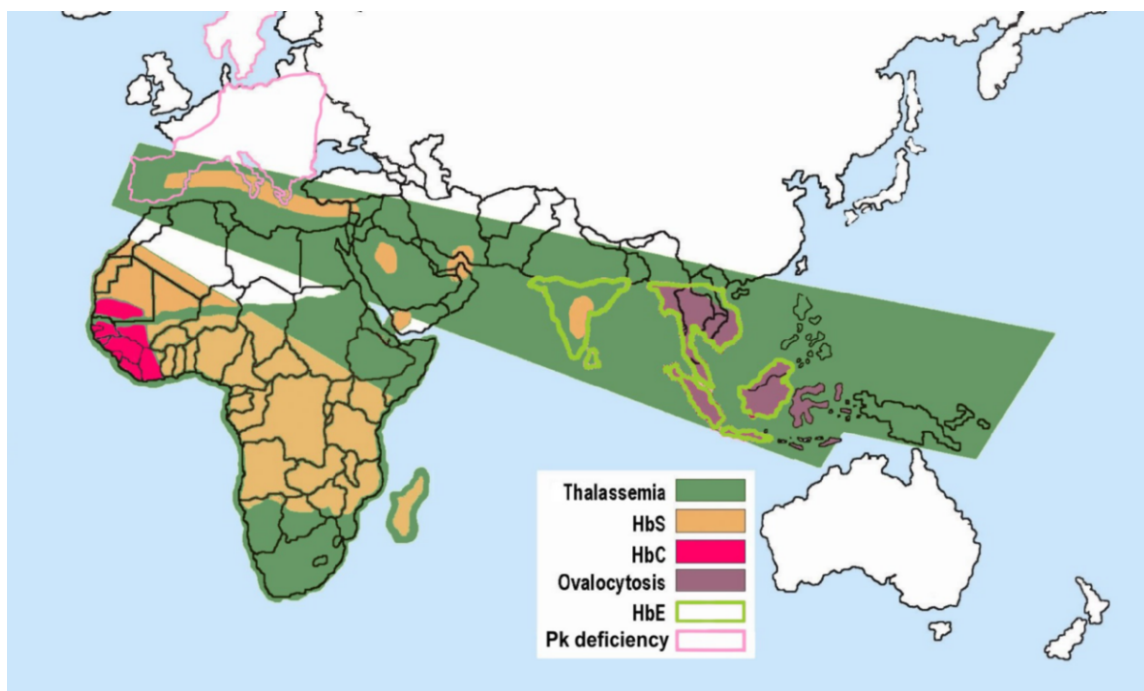


Figure 2.1 – Red Blood Cell abnormalities in Eurasia¹

¹ Available free at: https://it.wikipedia.org/wiki/File:Red_Blood_Cell_abnormalities.png original work of Armando Moreno Vranich.

Thalassemia is a genetic anemia characterized by reduced or absent synthesis of the globin chains in the hemoglobin (Hb) molecule due to genetic mutations, which afflict with different degrees of severity the patients (Weatherall, 1997).

With particular attention to the β -thalassemia, three main forms have been described (resumed in Table 2.1):

1 - *β -thalassemia major* (β -TM also called “*Cooley’s disease*”), which is the most serious form and requires nowadays regular RBCs (Red Blood Cells)-transfusions to survive. For this reason, in the past, before transfusion therapy became a routine therapy, children should not have survived the first few years of life (Rund and Rachmilewitz, 2005; De Sanctis et al., 2018);

2 - *β -thalassemia intermedia* (β -TI) with a mild RBCs deficiency. Individuals with β -TI show no significant deficiency and clinically are between the two other forms. The term ‘thalassemia intermedia’ (TI) was proposed to describe those affected with manifestations too mild to be considered TM and too severe to be considered thalassemia minor. The clinical phenotype of patients with β -TI varies greatly: from the severe, needing transfusions after the age of 6 years, to the mild, who in adulthood remains in the non-transfusion-dependent thalassemias group (De Sanctis et al., 2018). If patients possess both, a defective β -globin gene and a defective alpha globin gene, this trait decreases the imbalance of the α - and β -globin-chains resulting in mild to moderate severity (Wainscoat et al., 1983; Thein, 2013; Inati et al., 2015).

3 - *β -thalassemia minor* (β -Tm), with a low RBCs deficiency. Individuals are heterozygous for mutations that disrupt the globin chain, thus produce microcytic RBCs. These individuals need no medical treatment; they only are potential candidate parent of children with β -TM or with a combination of sickle cell anemia and β -Tm (Hilliard and Berkow, 1996).

Table 2.1 - Characteristics of β -Thalassemia Syndromes (from Kumar et al. 2011, modified)

Syndrome	Alleles	Laboratory details	Clinical features
<i>β-thalassemia major (Cooley's Disease)</i>	β^0/β^0	High anemia, microcytosis. RBCs fragments and striking morphologic abnormalities.	Patients need chronic transfusion, iron overload resulting in endocrine abnormalities and chronic organ damage.
<i>β-thalassemia intermedia</i>	β^+/β^+ or β^0/β^+	Medium anemia, microcytosis. RBCs morphologic abnormalities.	Clinical phenotype between β -Tm and β -TM
<i>β-thalassemia minor</i>	β^+/β or β^0/β	Low anemia, microcytosis. RBCs morphologic abnormalities.	Asymptomatic in life

β -Tm: β -thalassemia minor; β -TM: β -thalassemia major; RBCs: Red Blood Cells.
 β^+ Defective HB ; β^0 Absent Hb

Gene sequencing has identified more than 100 different mutations involved, which consist mostly of point mutations of the HBB gene, which is placed on chromosome 11 and is coding for hemoglobin (Kumar et al., 2011; Thein, 2013; Wong et al., 2016)².

Mutations can be classified in (Vuch et al., 2013; Galliera and Romanelli, 2017; Gupta et al., 2018):

(i) - *Splice site mutations*: They are the most frequent causes of β -thalassemia. They occur mostly in introns, while the others mutations are located in exons. Some of these mutations destroy normal RNA splicing junctions and block the production of normal mRNA for β -globin, causing β -thalassemia.

(ii) - *Mutations in the promoter region*: They reduce the transcriptional function of 75-80%. Since normal β -globin can also be synthesized, these mutations are associated with the milder forms of β -thalassemia (**β -Tm** and **β -TI**).

(iii) - *Premature termination codons mutations*: They represent the most frequent cause of β^0 -thalassemia. We distinguish two different mutations; 1) the most common one creates a stop codon into an exon; 2) the other mutation produces changes in the reading frame by insertion or deletion of a single to a few nucleotides and cause an alteration of the mRNA frameshift. Both mutations block the translation and inhibit the synthesis of β -globin.

As a rule, the reduced synthesis of β -globin chains causes anemia because the subsistence of RBCs and of their pre-cursors is lowered due to an imbalance in the synthesis of the β -globin chains. Many RBCs precursors have a damaged membrane and die by apoptosis.

² See also <http://globin.cse.psu.edu/globin/hbvar/> for an updated list of thalassemia variants, available through the Globin Gene Server Web Site.

This is a consequence of the deficient synthesis of Hb, which produces RBCs with not sufficient hemoglobin, (i.e. hypochromic, microcytic RBCs) and with a lower oxygen transport capacity.

In the most severe cases of β -thalassemia, it is estimated that 70-85% of the RBCs undergo apoptosis. Since erythropoiesis is ineffective in these patients, it causes a massive erythroid hyperplasia of the bone marrow, which results in an expanded mass of the RBCs precursors, which erode the cortical bone, compromise bone growth and cause skeletal abnormalities (Myers et al., 1986; Kumar et al., 2011; Vuch et al., 2013). In the skull, this process causes porotic hyperostosis.

In the last century the high incidence of HBB-mutations (De Sanctis et al., 2017, 2018) was recognized as a consequence of the positive selection of the heterozygotes in environments of endemic malaria, as highlighted since the end of the 40's (Haldane, 1949).

It has been proposed that common thalassemic mutations have occurred in Neolithic or Late Palaeolithic populations (Weatherall, 1997), consistent with the time frame suggested for the onset of malaria (De Sanctis et al., 2018). The persistence of these mutations until present day on the thalassemic belt (Filon et al., 1995; Kumar et al., 2015) could indicate that malaria was likely endemic earlier than 6000 years ago as well, as historical and scientific sources suggest (Thomas, 2016; Viganó et al., 2017).

Retrospective diagnosis of thalassemia should thus be possible on Mediterranean skeletons from the Late Paleolithic period onwards and would reveal important insights in the environmental history of human populations from this area. Considering the knowledge acquired on β -thalassemia syndrome, its pathological features should be easily detectable on human skeletal remains. Unfortunately, most lesions associated with β -thalassemia are not specific, but can be found in association with other forms of anemia, as well as in rickets, scurvy, chronic infections and parasitosis.

Few studies based on aDNA (ancient DNA) analyses have allowed identifying β -thalassemia's mutations in human skeletons from the thalassemic belt from up to 12.000 years ago (e.g. Béraud-Colomb *et al.*, 1995; Filon *et al.*, 1995; Viganó *et al.*, 2017), whereas an aDNA study carried out on 4,000 human remains from Crete (Hughey et al., 2012), did not yielded any pathological variation in the PCR-investigated regions. Yet, the molecular investigation was not preceded by any osteometric work that could have restricted the number of samples to be submitted to genetic investigation. hence, to carry

out further and wider molecular investigations, it remains of importance to define detectable characters through traditional anthropological methods in the skeletons for selecting potential candidates for the aDNA analyses. Thus, we propose a new evaluation form and a flowchart to make a preliminary diagnosis of β -thalassaemia on osteological material, observing that the form might be the only possible tool in the analyses of all ancient human remains which do not have preserved DNA. This may be of major importance since malaria's areas can offers difficulties (temperature, humidity) to aDNA preservation.

We applied the work-flow to published data which gave information about the features they used for the diagnosis of β -thalassemia. We used all the data retrieved from the literature to fill-in the evaluation form implemented in the work-flow and get a score of probability. In addition, we tested this new methodologic approach on 28 medieval individuals, who were only represented by their skull in a mixed burial context.

2.2 – Materials and Methods

The preliminary step for the study of thalassemia syndrome in a skeletal human population requires the splitting of the sample in two age classes, *subadults* and *adults*. This distinction is necessary because during the past, the life expectation of children with Cooley's disease did usually not exceed the 8 years of age (Ortner 2003). In other words, adolescent and adult individuals with pathognomonic traits should be carriers.

For the successive steps, the work-flow makes use of an evaluation form which provides scores of probability. In turn, the evaluation form makes use of different investigation methods (macroscopic, microscopic and radiographic analyses). We describe in detail the evaluation forms and the investigation methods in the following paragraphs.

Depending on the score of probability obtained for an individual, and considering the environmental conditions during his/her life-time, we obtain a differential diagnosis.

2.2.1 - Differential diagnosis from published data

We screened the scientific peer reviewed literature for skeletal markers of the β -thalassemia syndrome published in the last decades (June 1996 – December 2018) with the generic engine 'Google'. Then, we resort to other more specialized web search engines; in particular, we used "J-Stor", "WorldCat", "Firstsearch", "Pub-Med", "Google Scholar", "Research-Gate", "Elsevier Journal" and "Wiley Online". We carried out a first

screening of the retrieved publications by excluding all those publications that strictly regarded the pathological conditions of soft tissues; doing so, we selected 104 articles. After duplicates removal, we selected only those papers, which have considered macroscopic and microscopic skeletal markers in human bone. In total, 46 full-text papers were assessed for eligibility. As further criteria for selection, we included only papers in English, which had undergone to peer review process. As a result, 8 publications were used for the application of the evaluation form. This careful is considered essential to identify the most frequent traits that are considered bone markers of thalassemia.

2.2.2 - Archaeological samples

We analyzed the skulls of 71 individuals and employed distinct analytical methods on 31 skulls which have shown morphological and pathological traits found in the literature.

Three skulls belonged to the necropolis of Spina, the most renowned Etruscan settlement of Norhen Italy during the 6th - 3rd centuries BCE. The skulls were chosen on the basis of previous studies (Benassi and Toti, 1957; Manzon and Gualdi-Russo, 2016) which had proposed that these individuals were affected by β -thalassemia syndrome. The other twenty-eight skulls, come from a secondary deposition at the Church of San Mamiliano, Sovana (Grosseto, Italy) and date back to the 15th-16th century. They were found mixed together with other human skeletal remains. The skulls showed recurrent pathological features that could be associated with β -thalassemia. The bones were melted in a single layer of reddish-brown filling earth, a circumstance which suggests a re-burial following an elder exhumation (Tondo et al., 2004; Tuci, 2008). The region where Sovana is placed is called Maremma (Tuscany), and was hit by malaria by human memory (Figure 2.2). Only in July 1950, started the final swamp remediation works on the area, and March 1964, with the "structuring of the sanitary facilities", malaria was eradicated from the region (Partempi, 1989). An historical study (Snowden, 2006) recorded that in 1333 the regional government established that the mayor in charge of the city of Grosseto could abandon the Maremma during the summer period. This is the beginning of the so-called "estatura" a migration process to higher altitudes to escape malaria swampy areas. This information is of considerable importance, since it shows that malaria was widespread already in medieval times in Maremma.



Figure 2.2 – Distribution of Malaria in Italy, Distribution of Malaria in Italy, illustrated by Luigi Torelli - Firenze: G. Pellas, 1882, Firenze³

³ Available via free license: [CC BY 2.0](https://creativecommons.org/licenses/by/2.0/): (<https://creativecommons.org/licenses/by/2.0/>.)

2.2.3 – Macroscopic analyses

The macroscopic analyses included: **a)** the reconstruction of the biological profile through the classic anthropologic methods, such as sex-determination (Acsadi and Nemeskeri, 1970; Workshop of European Anthropologists, 1980; Jane E. Buikstra and Douglas H. Ubelaker, 1994; Gualdi-Russo, 2007), and age-at-death estimation (Brothwell, 1981; Meindl and Lovejoy, 1985; Işcan and Loth, 1986; Brooks and Suchey, 1990; Albert and Maples, 1995); **b)** osteometric measurements of the skull (Mallegni and Lippi, 2009; Minozzi and Canci, 2015) and **c)** palaeopathological diagnosis with particular consideration to the diagnostic features of β -thalassemia in the skeletons (Zimmerman and M. A. Kelley, 1983; Ascenzi et al., 1991; Aufderheide and Rodríguez, 2000; Ortner, 2003; Belcastro et al., 2007; Pinhasi and Mays, 2008; Fornaciari G. and Giuffra V., 2009; Baggieri G. and Mallegni, 2011; Perisano et al., 2012; Galliera and Romanelli, 2017; El-Beshlawy and El-Ghamrawy, 2019; Rinaldo et al., 2019). The macroscopic analyses were carried out in the laboratory of Archaeo-Anthropology and Forensic Anthropology of the Department of Biomedical and Specialty Surgical Sciences, University of Ferrara, Italy.

2.2.4 – Endoscopic and Radiologic analyses

Endoscopic examinations are particularly useful for a more accurate diagnosis and mainly for the investigation of those areas difficult to reach with other means (e.g. medullary cavity, paranasal sinuses, endocranial surface). We carried out the endoscopic investigation by using a rigid light borescope with Canon 28 mm 1:1 conversion lens and processed by IntraVison Capture Version.1.8©.

In addition, we used the radiological analysis, an essential tool for the investigation of beta-thalassemia in skeletons since it enables the examination of the bone internal structure and its matrix, adding more details for the interpretation of pathological traits. Radiologic analyses can be carried out with several tools, which include X-Ray, Computed Tomography (CB) and Computed Tomography Cone Beam (CTCB) scans to investigate at the deep level the lesions found with the macroscopic investigation. For our investigation, we used a conventional X-Ray static machine for planar scans 24” SFD, (Hp Cabinet 43805n Faxitron System). The scan parameters of the X-ray beams were 90 kVp with a variable time of scanning, due to the samples sizes. Images data were transferred to ix-Pect EZ Software© to perform the radiological analyses. All the endoscopic and radiological analyses were carried out in the laboratory of, and in collaboration with the

“Zentrum Anatomie, AG-Paläopathologie, of the Georg-August-Universität, Göttingen, Germany”.

2.2.5 – Microscopic analyses

Microscopic analysis, with optical microscope and especially with polarized light, allows paleopathologists to make very accurate differential diagnosis on dry bones thanks to its high diagnostic value (Schultz and Drommer, 1983; Schultz, 1988). Evaluation through the use of microscopy produces more reliable results than the use of radiological investigation (Rühli et al., 2002, 2007), and the combined use of both methods greatly increases the possibility of achieving reliable postumous diagnosis.

We applied the microscopic analyses on “Thin Ground Sections” (TGS) from macerated bone tissue using the procedures developed by M. Schultz in his studies (Schultz and Drommer, 1983; Schultz and Brandt, 1987; Schultz, 1988, 1993, 1994, 1997a; b, 2001, 2003; Wapler and Schultz, 1996; Schmidt-Schultz and Schultz, 2004, 2015) in order to investigate the histological structure of the bone lesion via light microscopy.

Although this is an invasive technique and we need to damage the bones to obtain samples, this technique allow us to compare the microstructure of archaeological specimens with the microstructure of recent tissue samples with certain diagnosis (Crowder and Stout, 2012). The procedure requires that the samples are collected from the area with the most characteristic morphological changes and should include: (1) a healthy, non-affected area, (2) an area with modestly developed changes, and (3) an area with severely pronounced changes (Schultz, 2001; Ortner, 2003; Crowder and Stout, 2012).

Deeper and more accurate analyses were carried out by polarized light microscopy (Leica DMRX Compound Polarised Light Microscope Image with Leica DFC 500 digital camera) for the identification of the bone structure on 50µm and 70µm TGSs. The microscopic analyses were carried out in the laboratory of, and in collaboration with the “Zentrum Anatomie, AG-Paläopathologie, of the Georg-August-Universität, Göttingen, Germany”.

2.3 – Results

To identify probable β -thalassemic individuals in skeletal populations, we developed a strategy resumed in a work-flow (Figure 2.3) based on the application of a new evaluation form.

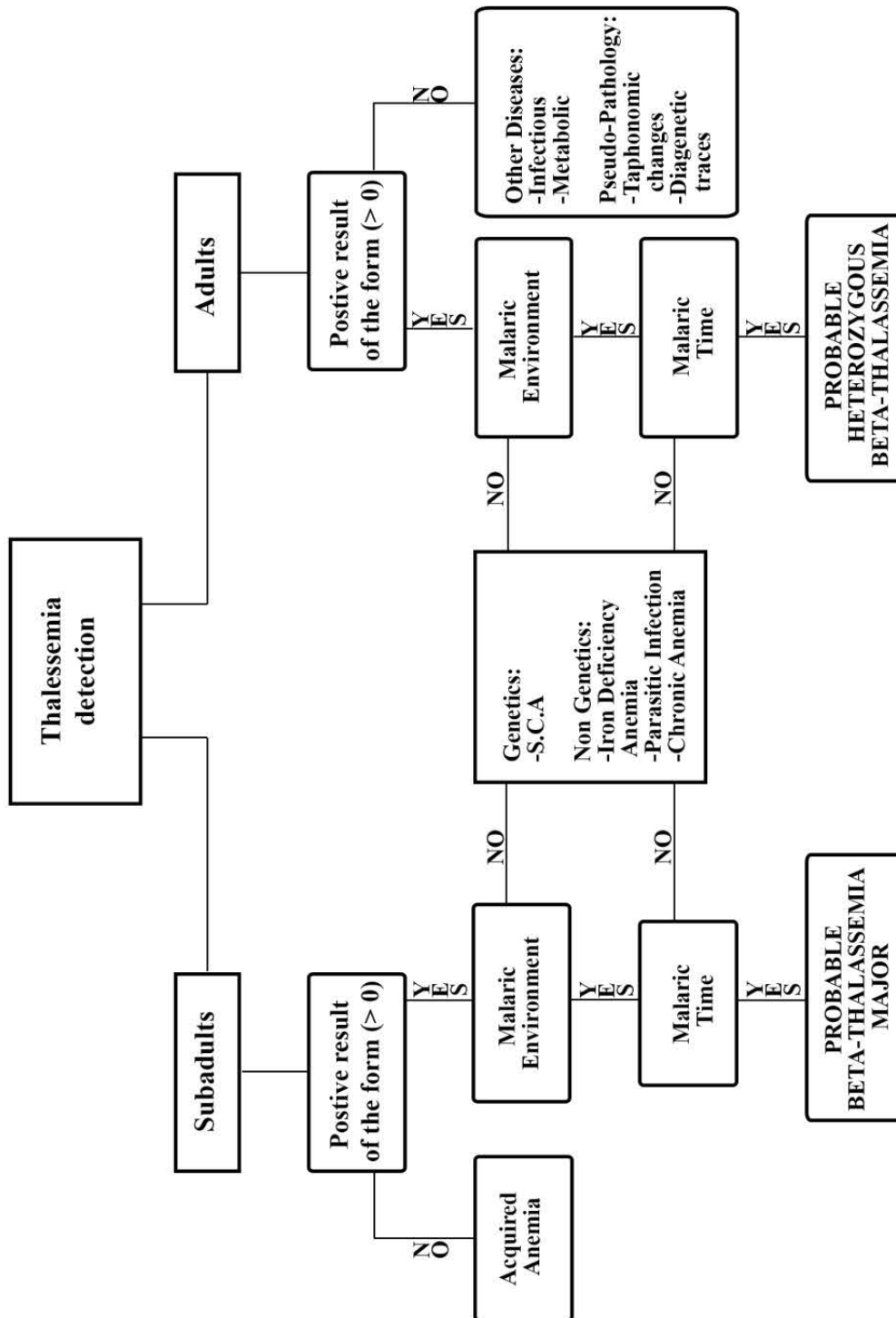


Figure 2.3 – Work-flow for the detection of probable β -thalassemia individuals in skeletal populations

To arrive at its formulation, we started from the delineation of **11 indicators** for the thalassaemia syndrome (Table 2.2) following indications retrieved in the literature (Lagia et al., 2007; Lewis, 2010; Baggieri G. and Mallegni, 2011; Perisano et al., 2012; Wong et al., 2014; De Sanctis et al., 2018) and classified them as **Non-specific, Indicative/non-diagnostic and Diagnostic**, also after the indication obtained from clinical cases (Aksoy, M; Camli, N; Dincol, K; Erdem, 1973; Moseley, 1974; Martuzzi Veronesi and Gualdi-Russo, 1976; Lehmann, 1982; Lawson et al., 1983; Kalef-Ezra et al., 1995; Wonke, 1998; Dresner Pollack et al., 2000; De Roeck et al., 2003; Voskaridou and Terpos, 2004; Azam and Bhatti, 2006; Tyler et al., 2006; Galanello and Origa, 2010; Haidar et al., 2010; Lewis, 2010; Haidar et al., 2012; Perisano et al., 2012; Jha and Jha, 2014; Wong et al., 2016; Rivera and Mirazón Lahr, 2017; Risoluti et al., 2018).

Table 2.2 - Lesions of β -thalassaemia syndrome on archaeological human remains

Cranium	Porotic Hyperostosis*
	Cribriform Orbitalia*
	Hair on end [‡]
Postcranial skeleton	Growth arrest lines*
	Marrow hyperplasia [†]
	Porosity of long bones [†]
	Rib within a rib [‡]
	Maxillary Hypertrophy*
	Premature fusion of epiphyses of humerus [†]
	Spine deformity (vertebral body) [†]
	Enlarged foramina of Metacarpals
*: Non-specific indicator present also in β -thalassaemia syndrome	
†: Complementary indicator suggesting β -thalassaemia (Indicative/non-diagnostic)	
‡: β -thalassaemia syndrome prevalent indicator (Diagnostic)	

The presence or absence of the indicators, and their mutual association, allowed us to develop the evaluation form for the preliminary detection of β -thalassaemia syndrome on archaeological remains.

2.3.1 – Evaluation form

Our main result was the development of a new evaluation form to be implemented in the work-flow (Figure 2.3). In the evaluation form (Figure 2.4)., we reported the most relevant bone lesions associated with β -thalassemia.

The form is subdivided in two sections with reference to cranial and post cranial lesions. This permit to perform the analysis even in presence of partial human remains. For each lesion, we assigned a different value based on its pathognomonic impact. We evaluated the pathognomonic impact (*Degree of importance*) for each indicator on the basis of multiple parameters, as revealed by the scientific literature, such as: the high frequency of the lesion in patients or carriers, the lower recurrence of the lesion in patients or carriers, the severity of the lesion and the exclusivity of the lesion for this pathology. We have, therefore, attributed a weight to each indicator: **higher values (3)** for those relevant lesions that are exclusively indicative of β -thalassemia syndrome; **intermediate values (2)** for those lesions that are associated with other indicators and could indicate the presence of β -thalassemia syndrome; **lower values (1)** for those lesions that are present in a wide spectrum of disease, but are associated with anaemia and could also be found complementarily in β -thalassemia syndrome. Missing data are indicated with a **neutral value (empty field)**.

As long as the *evaluation form* is functional, a minimum number of 4 evaluable markers are required; or, at least, 2 evaluable markers plus an optional specific analysis (X-ray investigation - Microscopy -TGS) are necessary.

After filling, the *evaluation form* will provide a probability score with a cutoff of 0 (Table 2.3). Scores >0 indicate that a putative β -thalassemic individual has been identified.

Table 2.3 – Evaluation Form Score Results (Accuracy Range)

Range	Diagnosis
0	Not Evaluable
From 0 to 0,5	Suggestive of β -thalassemia syndrome
From 0,51 to 1	Compatible with β -thalassemia syndrome
From 1,1 to 2	High probability of β -thalassemia syndrome
>2	Presence of β -thalassemia syndrome

**Negative results suggest the absence of β -thalassemia syndrome*

Figure 2.4 – Evaluation Form for the investigation of β -thalassemia in skeletons.

Indicators of β -thalassemia syndrome on skull	Degree of importance (X)	Assigned value (Y)	Results (X * Y)
Porotic Hyperostosis † ‡	1		
Cribræ Orbitalia ‡	1		
Hair on end*	3		
Maxillary Hypertrophy	2		
	n° X¹ (max 4 values)=	-----	Σ R¹ =

Presence of β - thalassemia on skull	$\frac{\Sigma R^1}{n^{\circ} X^1} =$	Positive Value result: possibly thalassemia syndrome
		Negative Value result: absence of thalassemia syndrome

Indicators of β -thalassemia syndrome on postcranial skeleton	Degree of importance (X)	Assigned value (Y)	Results (X * Y)
Growth arrest lines*	1		
Marrow hyperplasia	2		
Porosity of long bones	1		
Rib within a rib*	3		
Premature fusion of epiphyses of humerus	1		
Spine deformity (vertebral body)	2		
Enlarged foramina of Metacarpals	3		
	n° X² (max 7 values)=	-----	Σ R² =

Presence of β -thalassemia on postcranial skeleton	$\frac{R^2 \Sigma}{n^{\circ} X^2} =$	Positive Value result: possibly thalassemia syndrome
		Negative Value result: absence of thalassemia syndrome

Presence of β - thalassemia on skeleton		
Σ total	$\frac{\Sigma R^1 + \Sigma R^2}{n^{\circ} X^1 + n^{\circ} X^2} =$	Positive Value result: possibly thalassemia syndrome
		Negative Value result: absence of thalassemia syndrome

Legenda:

Degree of importance (X):
1 = Nonspecific indicator present also in β -thalassemia syndrome
2 = Complementary indicator suggesting β thalassemia/ not-diagnostic
3 = β -thalassaemia syndrome prevalent indicator/ Diagnostic

Value of interest (Y):
‡-3 = If the histologic analysis doesn't show lateralization of trabeculae (for Porotic Hyperostosis and Cribræ Orbitalia)
†-2 = If the radiological analysis denies skull vault thickness with destruction of external lamina and trabecular outgrowth (for Porotic Hyperostosis and Cribræ Orbitalia)
-1= Not present
0= Not detectable because the bone district is present but disturbances compromise its diagnosis or if the bone district is missing
+1 = Present
†+2 = If the radiological analysis confirms skull vault thickness with destruction of external lamina and trabecular outgrowth (for Porotic Hyperostosis and Cribræ Orbitalia)
‡+3 = If the histologic analysis shows lateralization of trabeculae (for Porotic Hyperostosis and Cribræ Orbitalia)

* X-ray analysis required

2.3.2 – Application of the Evaluation Form

We employed the new evaluation form on a selection of relevant historical and pre-historical archaeological putative β -thalassemia cases taken from the scientific literature (Table 2.4; see also SI for the forms generated for any single case). Mainly, the Authors have formulated their diagnoses using morphological analyses, and only occasionally they have used radiological methods, while none of the examined Scholars resorted previously to microscopic techniques.

From the **17** archaeological cases, we have found **2** individual with evidences suggestive of β -thalassemia major and **3**, who may potentially be cases of intermedia or minor β -thalassemic. For **5** individuals we confirm the probable diagnosis of β -thalassemia; whilst **4** specimens were not compatible/not suggestive with the diagnosis of β -thalassemia and **3** specimens were not evaluable/diagnosable because of the lack of minimum number of detectable indicators.

Table 2.4 – Application of the Evaluation Form on specimens from published studies.

Archeological Site / Reference	Country	Period	Ind no / Burial no	Individual age	Morphologic analysis	Radiologic analyses	Score and diagnosis
Herskovitz, I., / Edelson, G. (1991)	Israel	VI mill. BCE	Homo 25	About 16-17 years	Skull fragment, postcranial skeleton complete.	Humerus	Not Evaluable (no min number of indicators available).
Khuk Phanon Di / Tayles N. (1996)	Thailand	II sec CE	21	About 8 years	Skull, upper and lower limbs and extremities.	Metatarsal	+ 0.2 suggestive of β -thalassemia syndrome.
		II sec CE	24	About 25 years	Skull and upper limb	Humerus	- 0.83 not Suggestive of β -thalassemia syndrome.
		II sec CE	56	About 45 years	Skull (fragmented)		Not Evaluable (no min number of indicators available)
		II sec CE	88	About 9 months	Skull, Lower limbs (fragmented)	Tibia and fibula	- 0.75 not compatible with β -thalassemia syndrome.
		II sec CE	101	About 15 months	Skull (fragmented)		Not Evaluable (no min number of indicators available)
		II sec CE	121	About 15 months	Skull (fragmented), humerus	Humerus	+ 0.66 compatible with β -thalassemia syndrome.
		II sec CE	150	About 30 months	Skull (fragmented), Femura	Femur	+ 0.6 compatible with β -thalassemia syndrome.
Lagia A. et al. (2007)	Greece	XVI - XX sec CE	ABH-76	About 14 years	Skull, vertebrae, ribs, scapulae, coxae, long bones	Skull, ribs, coxae, long bones	+ 1.54 high probability of β -thalassemia syndrome.
Poundbury Camp / Lewis M. E. (2010)	UK	I - V sec CE	PC525	About 1 years	Parietal bones, thoracic vertebrae, ribs, left humerus, radius and ulna and the left femoral shaft.	Parietal bones, Ribs	+2 high probability of β -thalassemia syndrome.

Continues from: Table 2.4 – Application of the Evaluation Form on specimens from published studies.

			PC1083	About 6 months	Skull (fragmented), Ribs (fragmented), Vertebral column, Femora (fragmented), left ilium, phalanges (indet)	Ribs	- 1 not compatible with β -thalassemia syndrome.
			PC920b	About 9 months	Skull and ribs (fragmented)		- 0.1 not suggestive of β -thalassemia syndrome.
San Giovenale / Fornaciari G. (2015)	Italy	III sec BCE	Tomb III	About 4-5 years	Skull, long bones (fragmented)	Skull, left femur	+ 1.66 high probability of β -thalassemia syndrome.
		III sec BCE	Tomb V	About 16-17 years	Skull, long bones and vertebral column (fragmented)	Skull, vertebrae, humerus	+ 1.5 high probability of β -thalassemia syndrome.
Colchester / Rohnberg A. (2016)	UK	IV-V sec BCE	G145	About 1-2 years	Skull (fragmented), Ribs, Upper limbs (right hand excluded), Left ilium, Vertebral column	Ribs	+ 1 compatible with β -thalassemia syndrome
Windover / Thomas G. 2016	USA	VI sec CE	76	20-25 years	Skull, ribs, long bones	Skull, ribs, long bones	+ 0.42 suggestive β -thalassemia syndrome
Tell Masaik / J. Tomczyk et al. (2016)	Syria	II - IV sec CE	MK11G107	About 30 years	Skull, Ribs, scapulae, Left arm, right and, right femora and fibula	Skull, ribs	+ 2 high probability of β -thalassemia syndrome.

After checking the method on the data from literature, we have applied the same workflow on our skeletal populations, respectively from the Necropolis of Spina Valle Pega (Spina VP) (Table 2.5; see also SI for the forms generated for any single case) and Church of San Mamiliano (SSM), (Table 2.6; see also SI for the forms generated for any single case). For the secondary deposition of Sovana, each individual is represented only by his/her skull.

Table 2.5 – Kind of analyses performed and results obtained with the application of the Evaluation Form on Spina Valle Pega human remains

Ind. no	Age Class	Macroscopic analysis	Radiologic analysis	Microscopic analysis	Score and diagnosis
125A - Ind A	Old Adult	✓	✓	✓	- 0.5 not compatible with β -thalassemia syndrome
126D	Young Adult	✓	✓	✓	- 0.44 not suggestive of β -thalassemia syndrome
2E	Middle Adult	✓	✓	✓	- 1.55 high probability of absence of β -thalassemia syndrome.

By using the new evaluation form on the individuals from the necropolis of Spina, none of the three specimens resulted probably affected by *β -thalassemia*. However, interesting features of other disease, previously discovered (Manzon and Gualdi-Russo, 2016), were confirmed (e. g. Hyperostosis frontalis interna)⁴.

Table 2.6 – Kind of analyses performed and Results obtained with the application of the Evaluation Form on the Sovana, Chiesa di San Mamiliano human remains.

Ind. no	Age Class	Macroscopic analysis	Radiologic analysis	Microscopic analysis	Score and diagnosis
1	Young Adult	✓	✓	✓	- 1.25 high probability of absence of β -thalassemia syndrome.
2	Middle Adult	✓	✓	✓	- 2,5 absence of β -thalassemia syndrome.
4IIa	Child	✓	✓	✓	+ 3 presence of β -thalassemia syndrome.
6	Middle Adult	✓	✓		- 1.5 absence of β -thalassemia syndrome.
15	Old Adult	✓	✓	✓	- 0.33 not suggestive with β -thalassemia syndrome.
22	ND	✓		✓	Not evaluable (no min number of indicators available).
25	ND	✓	✓	✓	- 0.33 not suggestive with β -thalassemia syndrome.

⁴ For more information about Hyperostosis Frontalis interna see: Rühli, Böni and Henneberg, 2004; Belcastro, Facchini and Rastelli, 2006; Cvetković *et al.*, 2019)

Continues from: Table 2.6 – Kind of analyses performed and Results obtained with the application of the Evaluation Form on the Sovana, Chiesa di San Mamiliano human remains.

26	Young Adult	✓	✓	✓	- 2 high probability of absence of β -thalassemia syndrome.
30	Young Adult	✓	✓	✓	- 0.66 not compatible with β -thalassemia syndrome.
40	Young Adult	✓	✓		- 2 high probability of absence of β -thalassemia syndrome.
42	Young Adult	✓	✓	✓	+ 0.25 suggestive of β -thalassemia syndrome.
51	Middle Adult	✓	✓		- 0.25 not suggestive of β -thalassemia syndrome.
56	ND	✓	✓	✓	Not evaluable (no min number of indicators available).
57	Young Adult	✓	✓		- 0.5 not suggestive of β -thalassemia syndrome.
58	Old Adult	✓	✓	✓	- 0.66 not compatible with β -thalassemia syndrome.
68	Middle Adult	✓	✓		- 0.66 not compatible with β -thalassemia syndrome.
70	Middle Adult	✓	✓	✓	- 0.33 not suggestive of β -thalassemia syndrome.
75	ND	✓		✓	+ 0.66 compatible with β -thalassemia syndrome.
76	ND	✓	✓	✓	0 Not evaluable.
77	Old Adult	✓	✓	✓	- 0.66 not compatible with β -thalassemia syndrome
79	Middle Adult	✓	✓		- 0.5 not suggestive of β -thalassemia syndrome.
80	Young Adult	✓	✓		- 0.5 not suggestive of β -thalassemia syndrome.
81	Middle Adult	✓	✓	✓	0.33 suggestive of β -thalassemia syndrome.
82	ND	✓	✓		- 0.75 not compatible with β -thalassemia syndrome.
84	ND	✓	✓		- 0.66 not compatible with β -thalassemia syndrome.
86	ND	✓		✓	Not evaluable (no min number of indicators available).
92	ND	✓	✓	✓	0.33 suggestive of β -thalassemia syndrome.
94	ND	✓			Not evaluable (no min number of indicators available).

Macroscopic analyses were performed on the totality of the SSM specimens, radiographic investigation were performed in the 90% of all cases and microscopic analyses and TGS on 64% of all cases.

By using the new evaluation form on the SSM necropolis, on a total of **28** cases - distributed in four main individual age classes (Figure 2.5) we have diagnosed **1** individuals with the evidence of presence of β -thalassemia major, **1** with evidences compatible with the diagnosis of β -thalassemia intermedia or minor and **3** with evidences wich would suggest the presence of a mild form of β -thalassemia; whilst the absence/high probability of absence of β -thalassemia was diagnosed for **5** specimens and the probable absence was diagnosed in **13** specimens; **5** specimens were not evaluable because of the lack of the minimum number of detectable indicators.

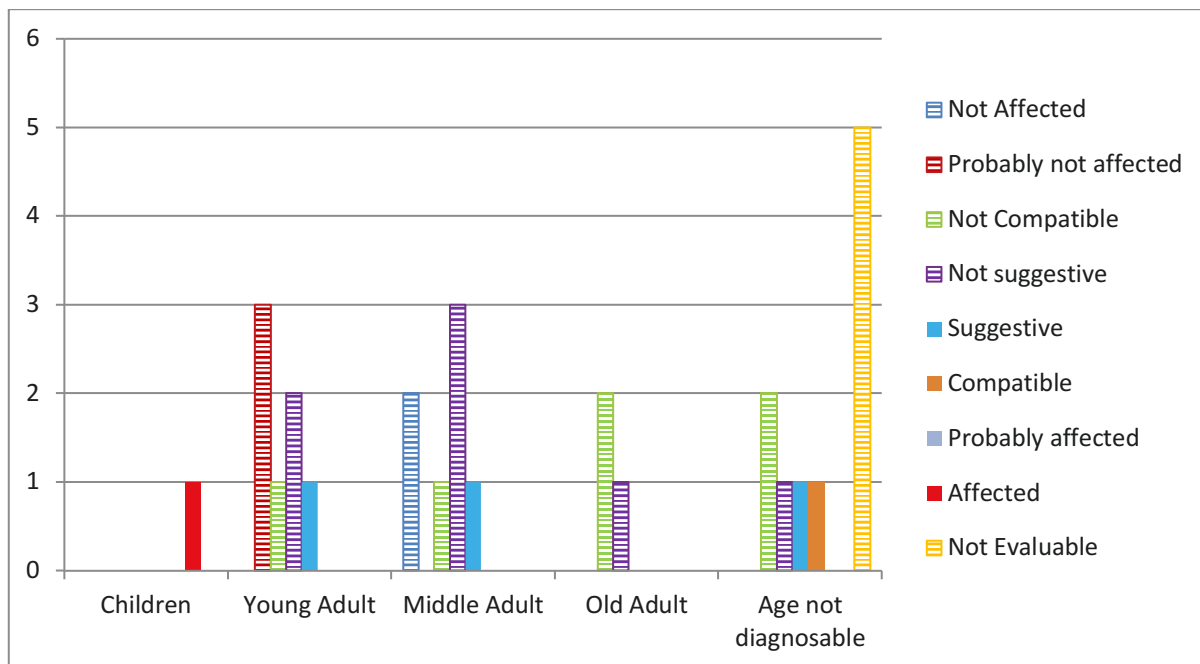


Figure 2.5 – Distribution of presence/absence of β -thalassemia syndrome in the Sovana San Mamiliano specimens.

Of particular interest is the diagnosis of a 2-4 years old child, individual 4IIa (Figure 2.6). – highlited in Table 2.4.-Macroscopic and osteometric observations of the frontal bone have shown the presence of serious Cribra orbitalia with a *degree of severity* of **4** and a *degree of healing* of **1**, as determined with a quantitative method developed in our group (Rinaldo et al., 2019), and several blood vessel impressions on the entire surface of the external lamina.



Figure 2.6 – Frontal, superior and basal view of the neurocranium of Individual 4IIa (Photo: Filippo Scianò).

In this regard, the radiological investigations (Figure 2.7) have shown the presence of critical cribrotic formation of the orbital roofs, loss of cortical morphology and swelling with trabecular expansion. Brush-like trabecular structure compatible with hair-on-end appearance were observed in both orbital roofs. The frontal bone has shown areas of lower density in correspondence of vascular impressions indicative of a haemorrhagic process. The diploe appears rarefied and the surface is affected by an inflammatory process active at the time of death, which occurred presumably 3/4 weeks after the haemorrhagic episode.

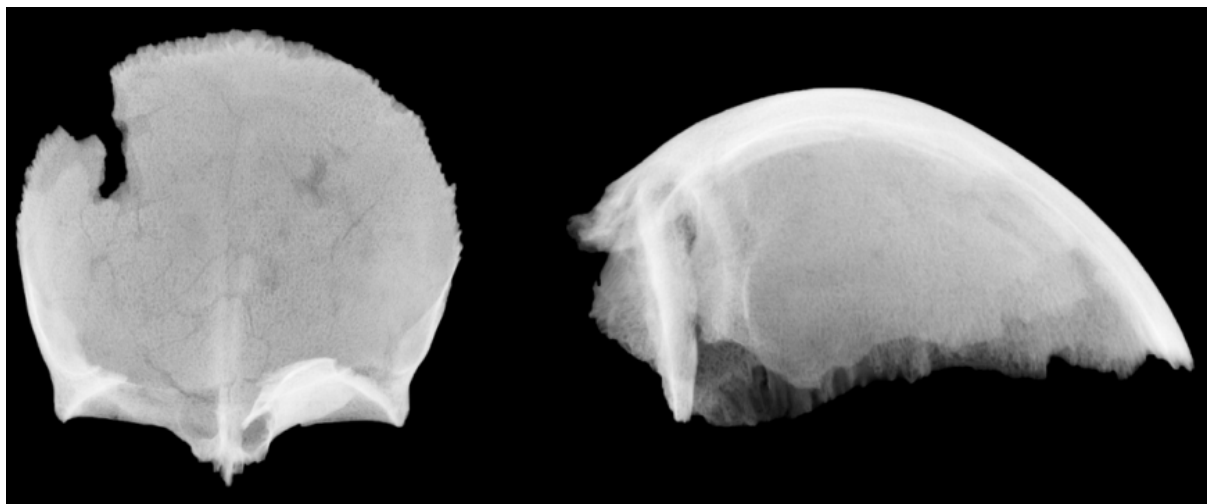


Figure 2.7 – X-ray view of the frontal bone of Individual 4IIa (Photo: Filippo Scianò).

Microscopic and histological analyses confirmed the information obtained by macroscopic and radiologic methods. The TGS of the calvaria (Figure 2.8) confirmed that the bone was interested by a hemolytic process. In addition, the TGS of the orbital roofs (Figure 2.9) have shown lateralization of the trabeculae, a condition which is suggestive of an expansion of the bone marrow due to a pathological enlargement of the cancellous bone by radial growth of the bone trabeculae. The external lamina appears restricted by the

active remodeling stimulated by the hematopoietic marrow hyperplasia and by the atrophy due to pressure, an evidence compatible with hair-on-end phenomena.

By using the evaluation form, the obtained score suggests that the individual could have been affected by Cooley's disease or another severe form of anemia. Further, aDNA analyses could help refining the diagnosis.

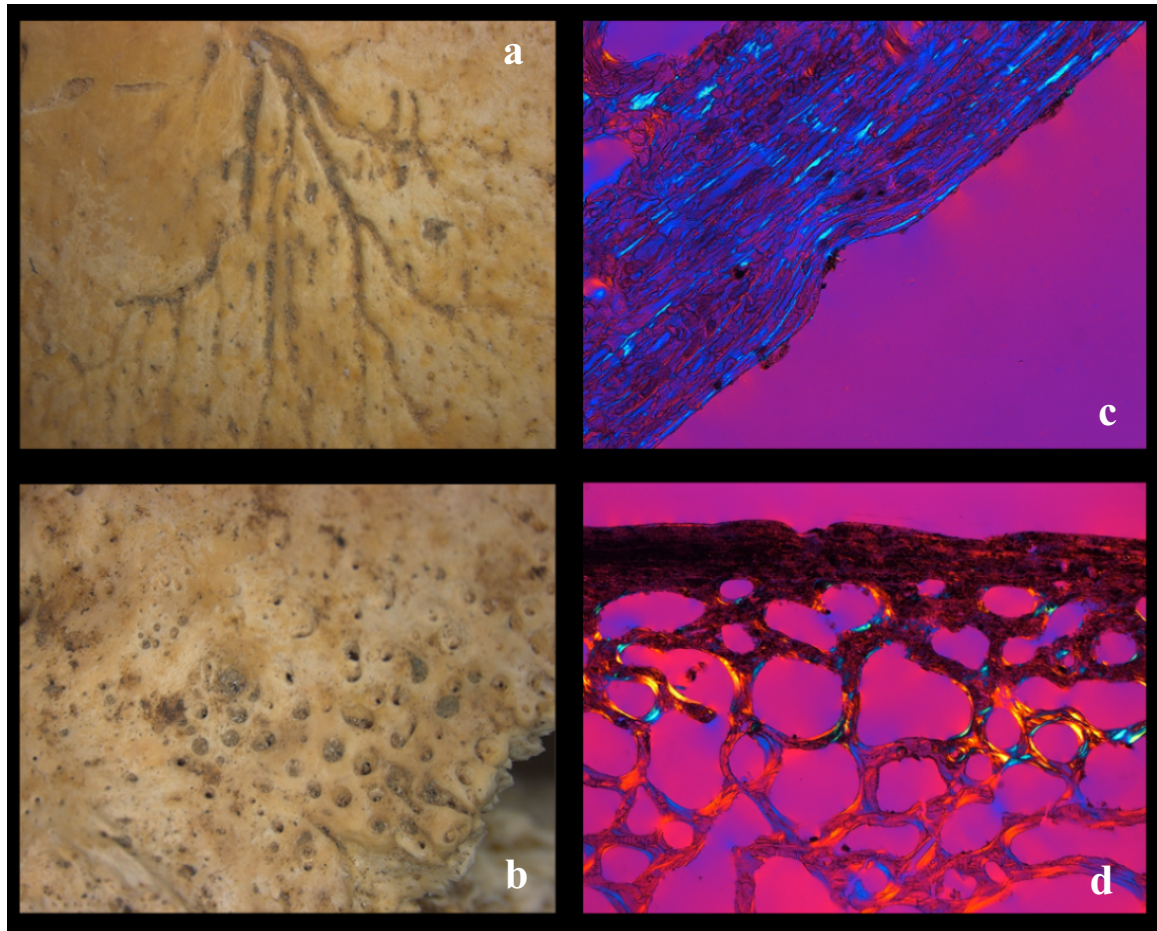


Figure 2.8 – Endoscopic views of: **a)** vascular impression due to an emorragic process and **b)** Porotic Hyperostosis of the frontal bone; The TGSs show: **c)** compression of the cortical bone tissue by blood vessels (70 μ , polarized light microscope with quartz as compensator, 100x magnification); **d)** sclerosis of the diploë which appears irregular and enlarged (70 μ , polarized light microscope with quartz as compensator, 25x magnification) (Photo: Filippo Scianò).

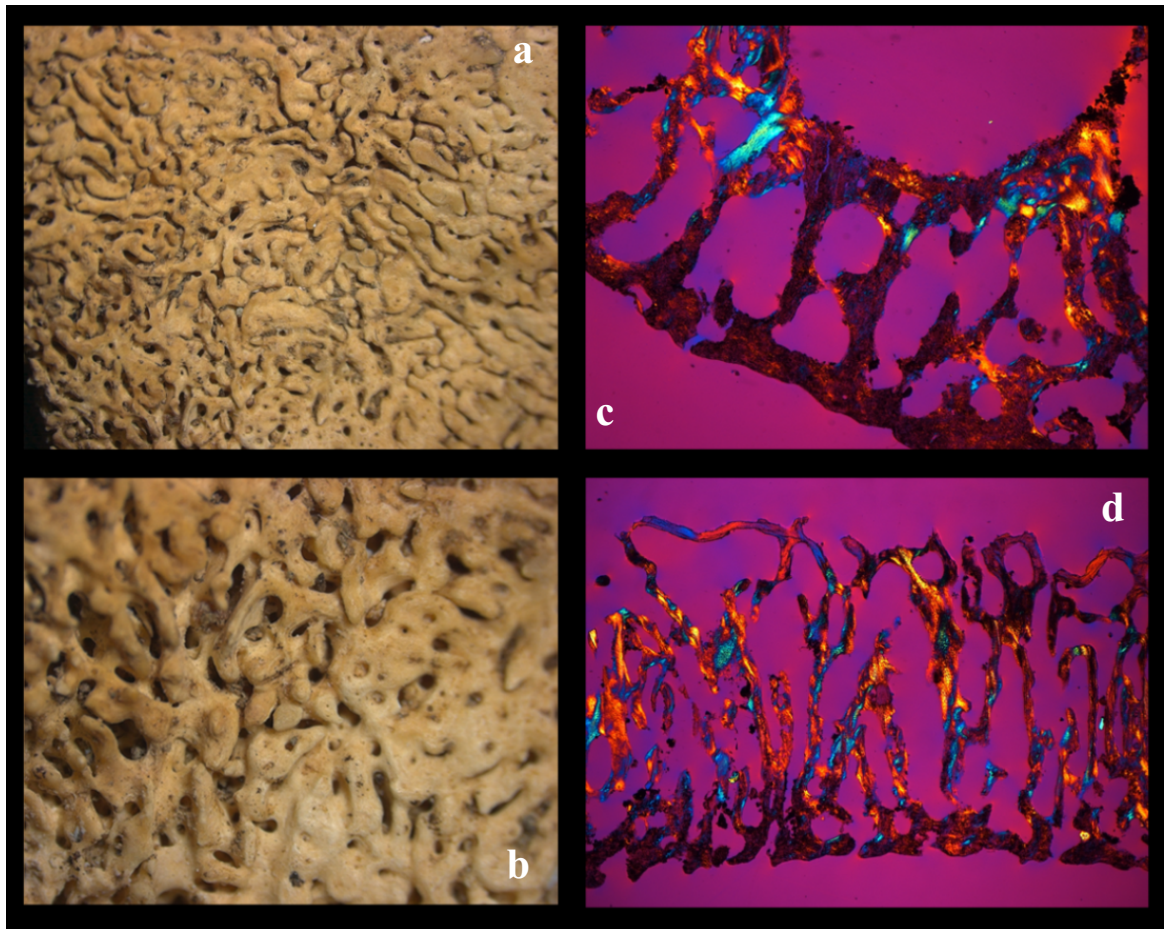


Figure 2.9 – Endoscopic **(a)** and microscopic **(b)** view of the severe Cribria Orbitalia of the right orbital roof. The TGSs show: **(c)** sclerotic changes with a lateralization of the trabeculae (70 μ , polarized light microscope with quartz as compensator, 25x magnification), and **(d)** a severe brush-like trabeculae with thinning process of the external lamina (50 μ , polarized light microscope with quartz as compensator, 16x magnification) (Photo: Filippo Scianò).

2.4 – Discussion and conclusions

The recognition of the pathognomonic characteristics of β -thalassemia major in an ancient population is relatively simple due to bone changes caused by the severity of the syndrome in absence of transfusion treatment. As a rule, pathologic bone changes in addition to other macroscopic features of the Cooley's disease occur prevalently in the neurocranium (e.g. Hair-on-end), and in the splanchnocranium, due to enlargement of the bone marrow. These evidences are sufficient for a preliminary diagnosis of β -thalassemia major, if the individual is less than 10 years old.

More problematic is the diagnosis of heterozygous thalassemia syndrome in archaeological populations since several lesions are non-specific for β -thalassemia but are the expression of a wide range of haematological disorders, including hypovitaminoses such as scurvy and rickets, as well as chronic hemorrhagic diseases caused by fragile vessels and hypervascularization (Ortner, 2003; Schultz, 2003; Zuckerman et al., 2014).

Starting from the morphological analysis of human dry bones, a confident diagnosis is difficult due to the lack of exclusive lesions connected to the diseases. Even though, the same facial characteristics of the thalassemia major observed in living patients might be present also in the mild form of this disorder (Martuzzi Veronesi and Gualdi-Russo, 1976).

The first important indicator of β -thalassemia syndrome in human dry bones is the presence of marrow hyperplasia (Tunaci et al., 1999; Haidar et al., 2010), which is considered a very good distinguishing element for thalassemia/genetic anemia since it is almost never seen in iron deficiency anemia and is very rare in sickle cell anemia (Lagia et al., 2007; Tomczyk et al., 2016). In addition, marrow hyperplasia (and consequently the evidences of Porotic Hyperostosis and Cribra Orbitalia) are unusual for scurvy and are considered suggestive of a comorbidity with a form of anaemia, including β -thalassemia (Walker et al., 2009; Tomczyk et al., 2016).

Bone marrow with marked erythroid hyperplasia and high levels of serum ferritin is more present in thalassemia major than in any other form of anemia. Conversion and re-conversion of the red marrow is a crucial aspect in the pathogenesis of the bone (Lagia, Eliopoulos and Manolis, 2007). In cases of severe anaemia, such as in β -thalassemia, in fact, the increasing of the erythropoietin' production causes the expansion of the bone marrow up to 15-30 times its initial volume (Wonke, 1998).

Marrow expansion causes mechanical interruption of bone formation, leading to cortical thinning, and increased distortion and fragility of the bones (Haidar et al., 2012).

Thus, bone modifications in individuals, who have suffered of β -thalassemia during their life, are mostly the result of marrow hyperplasia in reaction to the process generated by the anemia (Schultz, 2003).

Despite the outcome is known, the exact mechanism/s of reduction of the bone mass in thalassaemic patients is still unclarified. Increased bone resorption can also result from marrow hyperplasia with the release of cytokines, which stimulate osteoclast activity along with increasing oxidative stress (Dede et al., 2016). In this connection, some interesting findings regards the origin of the porotic lesions. As reported by Polo et al, (1999), porotic lesions can be caused not only by lack of iron, but also by magnesium deficiency (due to low intake, malabsorption or high loss).

A possible explanation could be the role of magnesium as a cofactor in the process of mineralisation (Ravaglioli et al., 1996; Djuric et al., 2008). Low level of magnesium promotes osteoporosis (Rude et al., 2009; Castiglioni et al., 2013) and induces a negative effect on the cortical thickness resulting in fragile bones (Rude and Gruber, 2004).

All these features together confer a loss of bone density (Tunaci et al., 1999; Ortner, 2003) and the expression of the classical porotic features, such as Porotic Hyperostosis and Cribra Orbitalia. The precise understanding of the interaction between iron/magnesium and thalassaemia could be a crucial challenge in the study of the bone lesions in β -thalassaemia syndrome.

Assuming this, the indicators that were developed for the evaluation form were mostly observed in patients affected by the Cooley's disease. Thus, the appearance of these markers in skeletons of sub-adults under 10 age at death can be attributed with confidence to β -TM individuals, as it is the case of individual ABH-76 (Lagia et al., 2007) and SSM 4IIa.

Whilst, adult individuals with a compatible scores obtained with the form would be excellent candidates for heterozygous thalassaemia. The condition of β -thalassaemia's carrier is generally asymptomatic during life, though, in some cases, also heterozygous individuals show symptoms of anemia due to a combination of ineffective erythropoiesis, peripheral red blood cell hemolysis, progressive splenomegaly (Marengo-Rowe, 2007), and microcytic red cells (mean corpuscular volume <70 fL) with anisochromasia. Signals of bone expansions in the skull can therefore be attributed to this genetic condition, if

found in adults. This is, in particular, the case of individual SSM 75 which reports a probabilist score compatible with the diagnosis of thalassemia (Evaluation form value of +0.66).

Considering the results obtained with the evaluation form on the cases indicated in literature, most of the information used for a preliminary identification of putative β -thalassemic individuals comes from the analysis of the skull. Among all the analyzed specimens, 47.1% showed porotic hyperostosis, 41.2 % cribra orbitalia, 29.4% Hair-on-end and 35.29% Maxillar Hypertrophy.

Further indicators compatible with the diagnosis of thalassaemia can also be found in the axile and appendicular postcranial skeleton, in the long bones, ribs and vertebral column. The radiological and microscopic investigations carried out in this study confirmed that the cortical porosity of long bones is present mainly in subadults as a result of marrow expansion. These changes are more commonly observed in the humerus and femur, while short tubular bones are more commonly affected in children than in adults (Aufderheide and Rodríguez, 2000; Tyler et al., 2006; Buikstra and Roberts, 2012). We observed these changes in the 35.3% of the reviewed individuals and in particular on the Ind. No. 21 (Khuk Phanon Di) together with the enlarged foramina of the metacarpals (Tayles, 1996).

X-ray and CT examination detected another important feature which suggests the presence of a β -thalassemia syndrome, since it was often observed in living patients. The *rib-within-a-rib* appearance displays a build-up of secondary bone growth formation. It is the most striking rib change present in patients with thalassemia who were never transfused (Aksoy, M; Camli, N; Dincol, K; Erdem, 1973; Lawson et al., 1981; Tunaci et al., 1999; Mohamed et al., 2008). This indicator has been observed in five of the reconsidered studies (see also SI for detailed information). These subject who were subadults in the 90% of cases.

The spine is also a relevant part for the diagnosis, in particular the vertebral bodies (Lagia et al., 2007), which show vertical striation due to thickened vertical trabeculae in individuals affected. In severely affected patients, biconcavity of the superior and inferior margins of the vertebral bodies or fractures may occur by compression (Wonke, 1998; Aufderheide and Rodríguez, 2000; Ortner, 2003; Haidar et al., 2012). This characteristic was observed only in three cases in literature of archaeological remains. Yer, we should consider that in the other fourteen cases the spine was not present. Unfortunately, none of the indicators of the postcranial skeleton was detectable in the individuals of the Sovana's

Church San Mamiliano' because of the lack of the postcranial skeleton due to their condition of secondary burial (mixed bones).

In general, we were not surprised to find several potentially (homozygote or heterozygote) beta-thalassemic individuals at Sovana. For many centuries, the presence of large marshlands in Maremma, in the South of Tuscany, in fact, has been an ideal boost for the development of malaria and, consequently, a favorable condition for the presence of thalassaemia in the genetic pool of the population of this region. We expected to find more clear indication for Spina, which was retrieved in a similar environment. Yet, with three skulls, the investigation was a preliminary recognition and much more individuals need to be analyzed before concluding that β -thalassemia was absent from the region in Etruscan times.

In conclusion, it is hard to distinguish between bone lesions due to thalassemic syndrome and chronic anemias such as dietary iron-deficiency (Steinbock, 1976; Ascenzi et al., 1991; Ortner, 2003). Therefore we think that our work-flow, which takes in account biological, but also historical and environmental information, provides important insights for the differential diagnosis of β -thalassemia syndrome in archaeological remains, even in the absence of detectable ancient DNA. At the current stage of knowledge, macroscopical and microscopical evidence for the homozygous status (affected patient) as well as for the heterozygous status are so strong that we cannot other than a confirmation by ancient DNA analysis.

2.5 – References

- Acsadi G, Nemeskeri J. 1970. History of Human Life Span and Mortality. Budapest: Akadémiai Kiadó.
- Aksoy, M; Camli, N; Dincol, K; Erdem S. 1973. On the problem of rib-within-a-rib appearance in thalassemia intermedia. *Ultraschall Der Medizin* 42:126–33.
- Albert AM, Maples WR. 1995. Stages of epiphyseal union for thoracic and lumbar vertebral centra as a method of age determination for teenage and young adult skeletons. *J Forensic Sci* 40:623–33.
- Ascenzi A, Bellelli A, Brunori M, Citro G, Ippoliti R, Lendaro E, Zito R. 1991. Diagnosis of thalassemia in ancient bones: problems and prospects in pathology. In: Ortner DJ AA, editor. *Human paleopathology current synthesis and future options*. Washington, DC and London. p 73–75.
- Aufderheide AC, Rodríguez. 2000. *The Cambridge encyclopedia of human paleopathology*.
- Azam M, Bhatti N. 2006. Hair-on-end appearance. *Arch Dis Child* 91:735.
- Baggieri G., Mallegni F. 2011. Morphopathology of some osseous alterations of thalassic nature. *Ultraschall Der Medizin* 40:154–157.
- Belcastro G, Rastelli E, Mariotti V, Consiglio C, Facchini F, Bonfiglioli B. 2007. Continuity or discontinuity of the life-style in central Italy during the Roman Imperial Age-Early Middle Ages transition: diet, health, and behavior. *Am J Phys Anthropol* 132:381–94.
- Belcastro MG, Facchini F, Rastelli E. 2006. Hyperostosis Frontalis Interna and sex identification of two skeletons from the Early Middle Ages necropolis of Vicenne-Campochiaro (Molise, Italy). *Int J Osteoarchaeol* 16:506–516.
- Benassi E, Toti A. 1957. [Observations on bone found in excavations of the necropolis of Spina; confirmation of the Greek racial origin of thalassemia]. *Minerva Fisioter Radiobiol* 2:215–23.
- Béraud-Colomb E, Roubin R, Martin J, Maroc N, Gardeisen A, Trabuchet G, Goossens M. 1995. Human beta-globin gene polymorphisms characterized in dna extracted from ancient bones 12,000 years old. *Am J Hum Genet* 57:1267–1274.
- Brooks S, Suchey JM. 1990. Skeletal age determination based on the os pubis: A

comparison of the Acsádi-Nemeskéri and Suchey-Brooks methods. *Hum Evol* 5:227–238.

Brothwell DR. 1981. *Digging up bones : the excavation, treatment, and study of human skeletal remains*. Cornell University Press.

Buikstra JE, Roberts CA. 2012. *The global history of paleopathology : pioneers and prospects*. Oxford University Press.

Castiglioni S, Cazzaniga A, Albisetti W, Maier JAM. 2013. Magnesium and osteoporosis: current state of knowledge and future research directions. *Nutrients* 5:3022–33.

Chini V, Ferrarini A, Pona G. 1939. Indagini sulla familiarità della “anemia mediterranea” o morbo di Cooley. *Minerva Med*:377–386.

Crowder C, Stout S. 2012. *Bone Histology: An Anthropological Perspective*. CRC Press.

Cvetković D, Nikolić S, Brković V, Živković V. 2019. Hyperostosis frontalis interna as an age-related phenomenon - Differences between males and females and possible use in identification. *Sci Justice* 59:172–176.

Dacie J. 1988. *The Haemolytic Anaemias Vol. 2. The Hereditary Haemolytic Anaemias Part 2*. (Churchill Livingstone. Edinburgh., editor.).

Dede AD, Trovas G, Chronopoulos E, Triantafyllopoulos IK, Dontas I, Papaioannou N, Tournis S. 2016. Thalassaemia-associated osteoporosis: a systematic review on treatment and brief overview of the disease. *Osteoporos Int* 27:3409–3425.

Djuric M, Milovanovic P, Janovic A, Draskovic M, Djukic K, Milenkovic P. 2008. Porotic lesions in immature skeletons from Stara Torina, late medieval Serbia. *Int J Osteoarchaeol* 18:458–475.

Dresner Pollack R, Rachmilewitz E, Blumenfeld A, Idelson M, Goldfarb AW. 2000. Bone mineral metabolism in adults with beta-thalassaemia major and intermedia. *Br J Haematol* 111:902–907.

El-Beshlawy A, El-Ghamrawy M. 2019. Recent trends in treatment of thalassaemia. *Blood Cells, Mol Dis* 76:53–58.

Filon D, Faerman M, Smith P, Oppenheim A. 1995. Sequence analysis reveals a beta-thalassaemia mutation in the DNA of skeletal remains from the archaeological site of Akhziv, Israel. *Nat Genet* 9:365–368.

Fornaciari G., Giuffra V. 2009. *Lezioni di paleopatologia*. (Ecig, editor.).

- Frassetto F. 1918. *Lezioni di Antropologia*. Milano: Hoepli U.
- Galanello R, Origa R. 2010. Beta-thalassemia. *Galanello Origa Orphanet J Rare Dis* 5:1–15.
- Galliera E, Romanelli MMC. 2017. Molecular basis of bone diseases. *Mol Pathol Mol Basis Hum Dis*:627–649.
- Gatto I. 1942. Ricerche sui familiari di bambini affetti da malattia di Cooley. *Arch It Pediatr e Pueric* 9:128–168.
- Gualdi-Russo E. 2007. Sex determination from the talus and calcaneus measurements. *Forensic Sci Int* 171:151–156.
- Gupta R, Musallam KM, Taher AT, Rivella S. 2018. Ineffective Erythropoiesis: Anemia and Iron Overload. *Hematol Oncol Clin North Am* 32:213–221.
- Haidar R, Mhaidli H, Musallam KM, Taher AT. 2012. The Spine in beta thalassemia Syndrome.
- Haidar R, Musallam KM, Taher AT. 2010. Bone disease and skeletal complications in patients with beta thalassemia major. *Bone* 48:425–432.
- Haldane J. 1949. Disease and evolution. *Ric Sci* 19:68–76.
- Hilliard LM, Berkow RL. 1996. The thalassemia syndromes. *Prim Care Update Ob Gyns* 3:157–162.
- Hughey JR, Du M, Li Q, Michalodimitrakis M, Stamatoyannopoulos G. 2012. A search for β thalassemia mutations in 4000year old ancient DNAs of Minoan Cretans. *Blood Cells, Mol Dis* 48:7–10.
- Inati A, Noureldine MA, Mansour A, Abbas HA. 2015. Endocrine and bone complications in β -thalassemia intermedia: Current understanding and treatment. *Biomed Res Int* 2015.
- Işcan MY, Loth SR. 1986. Determination of age from the sternal rib in white males: a test of the phase method. *J Forensic Sci* 31:122–32.
- Jane E. Buikstra and Douglas H. Ubelaker. 1994. Standards for data collection from human skeletal remains. *Archeol Surv Res Ser n° 44* 7:672.
- Jha R, Jha S. 2014. Beta thalassemia - a review. *J Pathol Nepal* 4:663–671.
- Kalef-Ezra J, Challa A, Chaliasos N, Hatzikonstantinou I, Papaefstathiou I, Cholevas V,

- Glaros D, Lapatsanis P. 1995. Bone minerals in β -thalassemia minor. *Bone* 16:651–655.
- Kountouris P, Lederer CW, Fanis P, Feleki X, Old J, Kleanthous M. 2014. IthaGenes: An interactive database for haemoglobin variations and epidemiology. *PLoS One* 9.
- Kumar R, Sagar C, Sharma D, Kishor P. 2015. β -Globin Genes: Mutation Hot-Spots in the Global Thalassemia Belt. *Hemoglobin* 39:1–8.
- Kumar V, Abbas AK, Fausto N, Aster JC. 2011. Robbins e Cotran - Le basi patologiche delle malattie : Vol. 1 Patologia generale - Vol. 2 Malattie degli organi e degli apparati. Elsevier Health Sciences Italy.
- Lagia A, Eliopoulos C, Manolis S. 2007. Thalassemia: macroscopic and radiological study of a case. *Int J Osteoarchaeol* 17:269–285.
- Lawson JP, Ablow RC, Pearson HA. 1981. The ribs in thalassemia. I. The relationship to therapy. *Radiology* 140:663–672.
- Lawson JP, Ablow RC, Pearson HA. 1983. Premature fusion of the proximal humeral epiphyses in thalassemia. *Am J Roentgenol* 140:239–244.
- Lehmann H. 1982. The history of thalassemia. *Birth Defects Orig Artic Ser* 18:1–11.
- Lewis ME. 2010. Thalassaemia: Its diagnosis and interpretation in past skeletal populations. *Int J Osteoarchaeol* 22:685–693.
- Mallegni F, Lippi B. 2009. Non omnis moriar : manuale di antropologia : dar voce ai resti umani del passato. CISU.
- Manzon VS, Gualdi-Russo E. 2016. Health Patterns of the Etruscan Population (6th-3rd Centuries bc) in Northern Italy: The Case of Spina. *Int J Osteoarchaeol* 26:490–501.
- Marengo-Rowe AJ. 2007. The thalassemiias and related disorders. *Proc (Bayl Univ Med Cent)* 20:27–31.
- Martuzzi Veronesi F, Gualdi-Russo E. 1976. Studio dei caratteri morfometrici in adolescenti microcitemici. :151–165.
- Martuzzi Veronesi F, Zanotti M. 1973. Indagine sulla frequenza degli eterozigoti beta talassemici nel comune di Bologna - Nota I. *Tec Sanit* 5:581–583.
- Meindl RS, Lovejoy CO. 1985. Ectocranial suture closure: A revised method for the determination of skeletal age at death based on the lateral-anterior sutures. *Am J Phys Anthropol* 68:57–66.

- Minozzi S, Canci A. 2015. Archeologia dei resti umani: dallo scavo al laboratorio. Carocci.
- Mohamed E, Bedair A, Medical H, Hamad S, Corporation M. 2008. Review of radiologic skeletal changes in Review of Radiologic Skeletal Changes in Thalassemia By Elsaid M Aziz Bedair , Abbas N E Helmy *, Khaled And University of ElMenia *, Egypt Corresponding Author : Elsaid M Aziz Bedair Professor of Radiology and Sen.
- Moseley JE. 1974. Skeletal changes in the anemias. *Semin Roentgenol* 9:169–184.
- Myers RM, Tilly K, Maniatis T. 1986. Fine structure genetic analysis of a beta-globin promoter. *Science* (80-) 232:613–618.
- Ortner DJ. 2003. Identification of pathological conditions in human skeletal remains.
- Partempi S. 1989. Miseria, malaria, malattia mentale nella Maremma ottocentesca. Il ruolo delle istituzioni. In: *La maremma Grossetana tra il '700 e il '900. Trasformazioni economiche e mutamenti sociali*. Città di Castello: Labirinto Editrice.
- Perisano C, Marzetti E, Spinelli MS, Callà CAM, Graci C, MacCauro G. 2012. Physiopathology of bone modifications in β -Thalassemia. *Anemia* 2012:1–6.
- Pinhasi R, Mays S. 2008. *Advances in Human Palaeopathology*.
- Polo M, Miquel-Feucht MJ, Villalaín JD. 1999. Un modelo experimental de cribra orbitalia: estudio preliminar. *Actas del V Congr Nac Paleopatol (Alcalá la Real, 1999)*.
- Ravaglioli A, Krajewski A, Celotti GC, Piancastelli A, Bacchini B, Montanari L, Zama G, Piombi L. 1996. Mineral evolution of bone. *Biomaterials* 17:617–622.
- Rinaldo N, Zedda N, Bramanti B, Rosa I, Gualdi-Russo E. 2019. How reliable is the assessment of Porotic Hyperostosis and Cribra Orbitalia in skeletal human remains? A methodological approach for quantitative verification by means of a new evaluation form. *Archaeol Anthropol Sci*.
- Risoluti R, Materazzi S, Sorrentino F, Bozzi C, Caprari P. 2018. Update on thalassemia diagnosis: New insights and methods. *Talanta* 183:216–222.
- Rivera F, Mirazón Lahr M. 2017. New evidence suggesting a dissociated etiology for cribra orbitalia and porotic hyperostosis. *Am J Phys Anthropol* 164:76–96.
- De Roeck J, Vanhoenacker F, Gielen J, De Schepper A. 2003. Bilateral humeral changes in thalassemia major. *J Belge Radiol* 86:154–155.

- Rude RK, Gruber HE. 2004. Magnesium deficiency and osteoporosis: animal and human observations. *J Nutr Biochem* 15:710–716.
- Rude RK, Singer FR, Gruber HE. 2009. Skeletal and hormonal effects of magnesium deficiency. *J Am Coll Nutr* 28:131–41.
- Rühli FJ, Böni T, Henneberg M. 2004. Hyperostosis frontalis interna: Archaeological evidence of possible microevolution of human sex steroids? *HOMO- J Comp Hum Biol* 55:91–99.
- Rühli FJ, Kuhn G, Evison R, Müller R, Schultz M. 2007. Diagnostic value of micro-CT in comparison with histology in the qualitative assessment of historical human skull bone pathologies. *Am J Phys Anthropol* 133:1099–1111.
- Rühli FJ, Lanz C, Ulrich-Bochsler S, Alt KW. 2002. State-of-the-art imaging in palaeopathology: The value of multislice computed tomography in visualizing doubtful cranial lesions. *Int J Osteoarchaeol* 12:372–379.
- Rund D, Rachmilewitz E. 2005. β -Thalassemia. *N Engl J Med* 353:1135–1146.
- De Sanctis V, Kattamis C, Canatan D, Soliman AT, Elsedfy H, Karimi M, Daar S, Wali Y, Yassin M, Soliman N, Sobti P, Jaouni S Al, Kholy M El, Fiscina B, Angastiniotis M. 2017. β -thalassemia distribution in the old world: An ancient disease seen from a historical standpoint. *Mediterr J Hematol Infect Dis* 9:1–14.
- De Sanctis V, Soliman AT, Elsedfy H, Soliman N, Bedair E, Fiscina B, Kattamis C. 2018. Bone disease in β thalassemia patients: past, present and future perspectives. *Metabolism* 80:66–79.
- Schmidt-Schultz TH, Schultz M. 2004. Bone Protects Proteins over Thousands of Years: Extraction, Analysis, and Interpretation of Extracellular Matrix Proteins in Archeological Skeletal Remains. *Am J Phys Anthropol* 123:30–39.
- Schmidt-Schultz TH, Schultz M. 2015. *Handbook of Paleoanthropology*. (Henke W, Tattersall I, editors.). Berlin, Heidelberg: Springer Berlin Heidelberg.
- Schultz M. 1988. Paläopathologische Diagnostik. In: Knußmann R, editor. *Anthropologie. Handbuch der vergleichenden Biologie des Menschen I*, 1. Stuttgart. p 480–496.
- Schultz M. 1993. Light Microscopic Analysis of Macerated Pathologically Changed Bones. :253–296.
- Schultz M. 1994. Krankheit und Tod im Kindesalter bei bronzezeitlichen Populationen

Disease and death in infancy in Bronze Age populations.

- Schultz M. 1997a. Microscopic structure of bone. In: Haglund W, Sorg M, editors. Forensic taphonomy. The postmortem fate of human remains. Boca Raton, FL: CRC Press. p 187–199.
- Schultz M. 1997b. Microscopic investigation of excavated skeletal remains A contribution to paleopathology and forensic medicine. In: Haglund W, Sorg M, editors. Forensic taphonomy. The postmortem fate of human remains. Boca Raton, FL: CRC Press. p 201–222.
- Schultz M. 2001. Paleohistopathology of bone: A new approach to the study of ancient diseases. *Am J Phys Anthropol* 116:106–147.
- Schultz M. 2003. Light microscopic analysis in skeletal paleopathology. In: Ortner DJ, editor. Identification of pathological conditions in human skeletal remains. Amsterdam: Academic Press/Elsevier Science. p 73–108.
- Schultz M, Brandt M. 1987. Neue Methoden zur Einbettung von Knochengewebe und zur Herstellung von Knochendünnschliffen. In: Kußmann R, editor. Anthropologie. Handbuch der vergleichenden Biologie des Menschen I. Stuttgart: Stuttgart: G. Fischer. p 698–730.
- Schultz M, Drommer R. 1983. Möglichkeiten der Präparateherstellung aus dem Gesichtsschädelbereich für die makroskopische und mikroskopische Untersuchung unter Verwendung neuer Kunststofftechniken. In: Hoppe W, editor. Experimentelle Mund-Kiefer-Gesichts-Chirurgie. Mikrochirurgische Eingriffe. Stuttgart: G. Thieme. p 95–97.
- Silvestroni E, Bianco I. 1975. Screening for microcytemia in Italy: analysis of data collected in the past 30 years. *Am J Hum Genet* 27:198–212.
- Silvestroni E, Gentili M. 1946. Qualche osservazione antropologica sui portatori di microcitemia. *Riv Ric di Morfol* 22.
- Snowden FM. 2006. The conquest of malaria in Italy. Yale: University Press.
- Steinbock RT. 1976. Paleopathological diagnosis and interpretation: bone diseases in ancient human populations. Thomas.
- Tayles N. 1996. Anemia, genetic diseases, and malaria in prehistoric Mainland Southeast Asia. *Am J Phys Anthropol* 101:11–27.

- Thein SL. 2013. The Molecular Basis of β -thalassemia. *Cold Spring Harb Perspect Med* 3:a011700–a011700.
- Thomas GP. 2016. An 8000-year-old case of thalassemia from the Windover, Florida skeletal population. *Int J Paleopathol* 14:81–90.
- Tomczyk J, Palczewski P, Mańkowska-Pliszka H, Płoszaj T, Jedrychowska-Dańska K, Witas HW. 2016. A Probable Case of Thalassemia Intermedia from Tell Masaikh, Syria. *Int J Osteoarchaeol* 26:549–554.
- Tondo L, Pellegrini E, Nanni M, Rafanelli S, Benicchi S. 2004. Indagini archeologiche a Sovana nel biennio 1998-1999. In: *Archeologica Pisana. Scritti per Orlanda Pancrazzi*.
- Tuci DBGMG. 2008. Scavi nella chiesa di San Mamiliano a Sovana. *Scavi nella chiesa di San Mamiliano a Sovana*:9–42.
- Tunaci M, Tunaci A, Engin G, Özkorkmaz B, Dinçol G, Acunaş G, Acunaş B. 1999. Imaging features of thalassemia. *Eur Radiol* 9:1804–1809.
- Tyler PA, Madani G, Chaudhuri R, Wilson LF, Dick EA. 2006. The radiological appearances of thalassaemia. *Clin Radiol* 61:40–52.
- Viganó C, Haas C, Rühli FJ, Bouwman A. 2017. 2,000 Year old β -thalassemia case in Sardinia suggests malaria was endemic by the Roman period. *Am J Phys Anthropol*:1–9.
- Voskaridou E, Terpos E. 2004. New insights into the pathophysiology and management of osteoporosis in patients with beta thalassaemia. *Br J Haematol* 127:127–139.
- Vuch J, Siori MS, Bigatti MP, Segat L, De Fabrizio G, Crovella S. 2013. Analysis of the beta-globin gene in DNA of suspected thalassaemic great apes. *Genet Mol Res* 12:1731–1739.
- Wainscoat JS, Kanavakis E, Wood WG, Letsky EA, Huehns ER, Marsh GW, Higgs DR, Clegg JB, Weatherall DJ. 1983. Thalassaemia intermedia in Cyprus: the interaction of α and β thalassaemia. *Br J Haematol* 53:411–416.
- Walker PL, Bathurst RR, Richman R, Gjerdrum T, Andrushko VA. 2009. The causes of porotic hyperostosis and cribra orbitalia: A reappraisal of the iron-deficiency-anemia hypothesis. *Am J Phys Anthropol* 139:109–125.
- Wapler U, Schultz M. 1996. Une méthode de recherche histologique appliquée au matériel

- osseux archéologique : l'exemple des cribra orbitalia. *Bull Mem Soc Anthropol Paris* 8:421–431.
- Weatherall DJ. 1997. The thalassaemias. *BMJ* 314:1675–8.
- Whipple GH. 1932. Racial or Familiar Anemia of Children. *Am J Dis Child* 44:336.
- Wong P, Fuller PJ, Gillespie MT, Kartsogiannis V, Kerr PG, Doery JCG, Paul E, Bowden DK, Strauss BJ, Milat F. 2014. Thalassaemia bone disease: A 19-year longitudinal analysis. *J Bone Miner Res*.
- Wong P, Fuller PJ, Gillespie MT, Milat F. 2016. Bone Disease in Thalassaemia: A Molecular and Clinical Overview. *Endocr Rev* 37:320–346.
- Wonke B. 1998. Bone disease in beta-thalassaemia major. *Br J Haematol* 103:897–901.
- Workshop of European Anthropologists. 1980. Recommendations for Age and Sex Diagnosis of Skeletons. *J Hum Evol* 9:517–549.
- Zanotti M, Martuzzi Veronesi F, Faggioli A, Favero A. 1973. Indagine sulla frequenza degli eterozigoti beta talassemici nel comune di Bologna - Nota II. *Tec Sanit* 5:585–588.
- Zimmerman and M. A. Kelley. 1983. *Atlas of human paleopathology*.
- Zuckerman MK, Garofalo EM, Frohlich B, Ortner DJ. 2014. Anemia or scurvy: A pilot study on differential diagnosis of porous and hyperostotic lesions using differential cranial vault thickness in subadult humans. *Int J Paleopathol* 5:27–33.

SUPPLEMENTARY

Method for a preliminary diagnosis of β -thalassemia syndrome on archaeological human remains Tayles N. (1996) Ind. no 21

Indicators of β -thalassemia syndrome on skull	Degree of importance (X)	Assigned value (Y)	Results (X * Y)
Porotic Hyperostosis † ‡	1	-1	-1
Cribræ Orbitalia ‡	1	1	1
Hair on end*	3	-1	-3
Maxillary Hypertrophy	2		
	n° X¹ (max 4 values) = 3	-----	Σ R¹ = -3

Presence of β -thalassemia on skull	$\frac{\Sigma R^1}{n^{\circ} X^1} = -3:3 = -1$	Positive Value result: possibly thalassemia syndrome
		Negative Value result: absence of thalassemia syndrome

Indicators of β -thalassemia syndrome on postcranial skeleton	Degree of importance (X)	Assigned value (Y)	Results (X * Y)
Growth arrest lines*	1		
Marrow hyperplasia	2		
Porosity of long bones	1	1	1
Rib within a rib*	3		
Premature fusion of epiphyses of humerus	1		
Spine deformity (vertebral body)	2		
Enlarged foramina of Metacarpals	3	1	3
	n° X² (max 7 values) = 2	-----	Σ R² = 4

Presence of β -thalassemia on postcranial skeleton	$\frac{\Sigma R^2}{n^{\circ} X^2} = 4:2 = 2$	Positive Value result: possibly thalassemia syndrome
		Negative Value result: absence of thalassemia syndrome

Presence of β -thalassemia on skeleton		
Σ total	$\frac{\Sigma R^1 + \Sigma R^2}{n^{\circ} X^1 + n^{\circ} X^2} = 1:5 = 0,2$	Positive Value result: possibly thalassemia syndrome
		Negative Value result: absence of thalassemia syndrome

Legenda:

Degree of importance (X):
1 = Nonspecific indicator present also in β -thalassemia syndrome
2 = Complementary indicator suggesting β -thalassemia/ not-diagnostic
3 = β -thalassaemia syndrome prevalent indicator/ Diagnostic

Value of interest (Y):
‡-3 = If the histologic analysis doesn't show lateralization of trabeculae (for Porotic Hyperostosis and Cribræ Orbitalia)
†-2 = If the radiological analysis denies skull vault thickness with destruction of external lamina and trabecular outgrowth (for Porotic Hyperostosis and Cribræ Orbitalia)
-1 = Not present
"empty field" = Not detectable because the bone district is present but disturbances compromise its diagnosis or if the bone district is missing
+1 = Present
†+2 = If the radiological analysis confirms skull vault thickness with destruction of external lamina and trabecular outgrowth (for Porotic Hyperostosis and Cribræ Orbitalia)
‡+3 = If the histologic analysis shows lateralization of trabeculae (for Porotic Hyperostosis and Cribræ Orbitalia)

* X-ray analysis required

Method for a preliminary diagnosis of β -thalassemia syndrome on archaeological human remains Tayles N. (1996) Ind. No 24

Indicators of β -thalassemia syndrome on skull	Degree of importance (X)	Assigned value (Y)	Results (X * Y)
Porotic Hyperostosis † ‡	1	-1	-1
Cribræ Orbitalia ‡	1	-1	-1
Hair on end*	3	-1	-3
Maxillary Hypertrophy	2	-1	-2
	n° X¹ (max 4 values) = 4	-----	$\Sigma R^1 = -7$

Presence of β - thalassaemia on skull	$\frac{\Sigma R^1}{n^{\circ} X^1} = -7:4 = -1,75$	Positive Value result: possibly thalassaemia syndrome Negative Value result: absence of thalassaemia syndrome

Indicators of β -thalassemia syndrome on postcranial skeleton	Degree of importance (X)	Assigned value (Y)	Results (X * Y)
Growth arrest lines*	1		
Marrow hyperplasia	2		
Porosity of long bones	1	1	1
Rib within a rib*	3		
Premature fusion of epiphyses of humerus	1	1	1
Spine deformity (vertebral body)	2		
Enlarged foramina of Metacarpals	3		
	n° X² (max 7 values) = 2	-----	$\Sigma R^2 = 2$

Presence of β -thalassaemia on post cranial skeleton	$\frac{\Sigma R^2}{n^{\circ} X^2} = 2:2 = 1$	Positive Value result: possibly thalassaemia syndrome Negative Value result: absence of thalassaemia syndrome

Presence of β - thalassaemia on skeleton		
Σ total	$\frac{\Sigma R^1 + \Sigma R^2}{n^{\circ} X^1 + n^{\circ} X^2} = -5:6 = -0,83$	Positive Value result: possibly thalassaemia syndrome Negative Value result: absence of thalassaemia syndrome

Legenda:

Degree of importance (X):
1 = Nonspecific indicator present also in β - thalassaemia syndrome
2 = Complementary indicator suggesting β - thalassaemia/ not-diagnostic
3 = β - thalassaemia syndrome prevalent indicator/ Diagnostic

Value of interest (Y):
‡-3 = If the histologic analysis doesn't show lateralization of trabeculae (for Porotic Hyperostosis and Cribræ Orbitalia)
†-2 = If the radiological analysis denies skull vault thickness with destruction of external lamina and trabecular outgrowth (for Porotic Hyperostosis and Cribræ Orbitalia)
-1 = Not present
“empty field” = Not detectable because the bone district is present but disturbances compromise its diagnosis or if the bone district is missing
+1 = Present
†+2 = If the radiological analysis confirms skull vault thickness with destruction of external lamina and trabecular outgrowth (for Porotic Hyperostosis and Cribræ Orbitalia)
‡+3 = If the histologic analysis shows lateralization of trabeculae (for Porotic Hyperostosis and Cribræ Orbitalia)
*X-ray analysis required

Method for a preliminary diagnosis of β -thalassemia syndrome on archaeological human remains Tayles N. (1996) Ind. No 88

Indicators of β -thalassemia syndrome on skull	Degree of importance (X)	Assigned value (Y)	Results (X * Y)
Porotic Hyperostosis † ‡	1	-1	-1
Cribræ Orbitalia ‡	1	-1	-1
Hair on end*	3		
Maxillary Hypertrophy	2	-1	-2
	n° X¹ (max 4 values) = 3	-----	$\Sigma R^1 = -4$

Presence of β - thalassemia on skull	ΣR^1	Positive Value result: possibly thalassemia syndrome Negative Value result: absence of thalassemia syndrome
	$n^\circ X^1$ = -4:3 = - 1,33	

Indicators of β - thalassemia syndrome on postcranial skeleton	Degree of importance (X)	Assigned value (Y)	Results (X * Y)
Growth arrest lines*	1		
Marrow hyperplasia	2		
Porosity of long bones	1	1	1
Rib within a rib*	3		
Premature fusion of epiphyses of humerus	1		
Spine deformity (vertebral body)	2		
Enlarged foramina of Metacarpals	3		
	n° X² (max 7 values) = 1	-----	$\Sigma R^2 = 1$

Presence of β - thalassemia on postcranial skeleton	ΣR^2	Positive Value result: possibly thalassemia syndrome Negative Value result: absence of thalassemia syndrome
	$n^\circ X^2$ = -1:1 = 1	

Presence of β - thalassemia on skeleton		
Σ total	$R^1 \Sigma + R^2 \Sigma$	Positive Value result: possibly thalassemia syndrome Negative Value result: absence of thalassemia syndrome
	$n^\circ X^1 + n^\circ X^2$ = -3:4 = -0,75	

Legenda:

Degree of importance (X):
1 = Nonspecific indicator present also in β -thalassemia syndrome
2 = Complementary indicator suggesting β -thalassemia/ not-diagnostic
3 = β -thalassaemia syndrome prevalent indicator/ Diagnostic

Value of interest (Y):
‡-3 = If the histologic analysis doesn't show lateralization of trabeculae (for Porotic Hyperostosis and Cribræ Orbitalia)
†-2 = If the radiological analysis denies skull vault thickness with destruction of external lamina and trabecular outgrowth (for Porotic Hyperostosis and Cribræ Orbitalia)
-1 = Not present
“empty field” = Not detectable because the bone district is present but disturbances compromise its diagnosis or if the bone district is missing
+1 = Present
†+2 = If the radiological analysis confirms skull vault thickness with destruction of external lamina and trabecular outgrowth (for Porotic Hyperostosis and Cribræ Orbitalia)
‡+3 = If the histologic analysis shows lateralization of trabeculae (for Porotic Hyperostosis and Cribræ Orbitalia)

*X-ray analysis required

Method for a preliminary diagnosis of β -thalassemia syndrome on archaeological human remains Tayles N. (1996) Ind. no 121

Indicators of β -thalassemia syndrome on skull	Degree of importance (X)	Assigned value (Y)	Results (X * Y)
Porotic Hyperostosis † ‡	1	1	1
Cribræ Orbitalia ‡	1	1	1
Hair on end*	3	-1	-3
Maxillary Hypertrophy	2	1	2
	n° X¹ (max 4 values)= 4	-----	Σ R¹=1

Presence of β -thalassemia on skull	$\frac{\Sigma R^1}{n^{\circ} X^1} = 1:4 = 0,25$	Positive Value result: possibly thalassaemia syndrome
		Negative Value result: absence of thalassaemia syndrome

Indicators of β -thalassemia syndrome on postcranial skeleton	Degree of importance (X)	Assigned value (Y)	Results (X * Y)
Growth arrest lines*	1	1	1
Marrow hyperplasia	2	1	2
Porosity of long bones	1		
Rib within a rib*	3		
Premature fusion of epiphyses of humerus	1		
Spine deformity (vertebral body)	2		
Enlarged foramina of Metacarpals	3		
	n° X² (max 7 values)= 2	-----	Σ R²= 3

Presence of β -thalassemia on postcranial skeleton	$\frac{\Sigma R^2}{n^{\circ} X^2} = 3:2 = 1,5$	Positive Value result: possibly thalassaemia syndrome
		Negative Value result: absence of thalassaemia syndrome

Presence of β -thalassemia on skeleton		
Σ total	$\frac{\Sigma R^1 + \Sigma R^2}{n^{\circ} X^1 + n^{\circ} X^2} = 4:6 = 0,66$	Positive Value result: possibly thalassaemia syndrome
		Negative Value result: absence of thalassaemia syndrome

Legenda:

Degree of importance (X):
1 = Nonspecific indicator present also in β -thalassaemia syndrome
2 = Complementary indicator suggesting β -thalassaemia/ not-diagnostic
3 = β - thalassaemia syndrome prevalent indicator/ Diagnostic

Value of interest (Y):
‡-3 = If the histologic analysis doesn't show lateralization of trabeculae (for Porotic Hyperostosis and Cribræ Orbitalia)
†-2 = If the radiological analysis denies skull vault thickness with destruction of external lamina and trabecular outgrowth (for Porotic Hyperostosis and Cribræ Orbitalia)
-1 = Not present
"empty field" = Not detectable because the bone district is present but disturbances compromise its diagnosis or if the bone district is missing
+1 = Present
†+2 = If the radiological analysis confirms skull vault thickness with destruction of external lamina and trabecular outgrowth (for Porotic Hyperostosis and Cribræ Orbitalia)
‡+3 = If the histologic analysis shows lateralization of trabeculae (for Porotic Hyperostosis and Cribræ Orbitalia)

*X-ray analysis required

Method for a preliminary diagnosis of β -thalassemia syndrome on archaeological human remains Tayles N. (1996) Ind. no 150

Indicators of β -thalassemia syndrome on skull	Degree of importance (X)	Assigned value (Y)	Results (X * Y)
Porotic Hyperostosis † ‡	1		
Cribræ Orbitalia ‡	1	1	1
Hair on end*	3	-1	-3
Maxillary Hypertrophy	2	1	2
	n° X¹ (max 4 values)= 3	-----	Σ R¹ = 0

Presence of β - thalassemia on skull	$\frac{\Sigma R^1}{n^\circ X^1} = 0$	Positive Value result: possibly thalassemia syndrome
		Negative Value result: absence of thalassemia syndrome

Indicators of β -thalassemia syndrome on postcranial skeleton	Degree of importance (X)	Assigned value (Y)	Results (X * Y)
Growth arrest lines*	1	1	1
Marrow hyperplasia	2	1	2
Porosity of long bones	1		
Rib within a rib*	3		
Premature fusion of epiphyses of humerus	1		
Spine deformity (vertebral body)	2		
Enlarged foramina of Metacarpals	3		
	n° X² (max 7 values)= 2	-----	Σ R² = 3

Presence of β -thalassemia on postcranial skeleton	$\frac{\Sigma R^2}{n^\circ X^2} = 3:2 = 1,5$	Positive Value result: possibly thalassemia syndrome
		Negative Value result: absence of thalassemia syndrome

Presence of β -thalassemia on skeleton		
Σ total	$\frac{\Sigma R^1 + \Sigma R^2}{n^\circ X^1 + n^\circ X^2} = 3:5 = 0.6$	Positive Value result: possibly thalassemia syndrome
		Negative Value result: absence of thalassemia syndrome

Legenda:

Degree of importance (X):
1 = Nonspecific indicator present also in β - thalassemia syndrome
2 = Complementary indicator suggesting β - thalassemia/ not-diagnostic
3 = β - thalassaemia syndrome prevalent indicator/ Diagnostic

Value of interest (Y):
‡-3 = If the histologic analysis doesn't show lateralization of trabeculae (for Porotic Hyperostosis and Cribræ Orbitalia)
†-2 = If the radiological analysis denies skull vault thickness with destruction of external lamina and trabecular outgrowth (for Porotic Hyperostosis and Cribræ Orbitalia)
-1= Not present
"empty field"= Not detectable because the bone district is present but disturbances compromise its diagnosis or if the bone district is missing
+1 = Present
†+2 = If the radiological analysis confirms skull vault thickness with destruction of external lamina and trabecular outgrowth (for Porotic Hyperostosis and Cribræ Orbitalia)
‡+3 = If the histologic analysis shows lateralization of trabeculae (for Porotic Hyperostosis and Cribræ Orbitalia)

*X-ray analysis required

Method for a preliminary diagnosis of β -thalassemia syndrome on archaeological human remains (Lagia et al 2006)

Indicators of β -thalassemia syndrome on skull	Degree of importance (X)	Assigned value (Y)	Results (X * Y)
Porotic Hyperostosis † ‡	1	2	2
Cribræ Orbitalia ‡	1	1	1
Hair on end*	3	1	3
Maxillary Hypertrophy	2	1	2
	n° X¹ (max 4 values)= 4	-----	Σ R¹ = 8

Presence of β - thalassaemia on skull	$\frac{R^1 \Sigma}{n^o X^1} = 8:4 = 2$	Positive Value result: possibly thalassaemia syndrome Negative Value result: absence of thalassaemia syndrome
---------------------------------------------	----------------------------------------	------------------------------------------------------------------------------------------------------------------

Indicators of β -thalassemia syndrome on postcranial skeleton	Degree of importance (X)	Assigned value (Y)	Results (X * Y)
Growth arrest lines*	1	1	1
Marrow hyperplasia	2	1	2
Porosity of long bones	1	-1	-1
Rib within a rib*	3	1	3
Premature fusion of epiphyses of humerus	1	-1	-1
Spine deformity (vertebral body)	2	1	2
Enlarged foramina of Metacarpals	3	1	3
	n° X² (max 7 values) = 7	-----	Σ R² = 9

Presence of β - thalassaemia on postcranial skeleton	$\frac{R^2 \Sigma}{n^o X^2} = 9:7 = 1,21$	Positive Value result: possibly thalassaemia syndrome Negative Value result: absence of thalassaemia syndrome
------------------------------------------------------------	-------------------------------------------	------------------------------------------------------------------------------------------------------------------

Presence of β - thalassaemia on skeleton		
Σ total	$\frac{R^1 \Sigma + R^2 \Sigma}{n^o X^1 + n^o X^2} = 17:11 = 1,54$	Positive Value result: possibly thalassaemia syndrome Negative Value result: absence of thalassaemia syndrome

Legenda:

Degree of importance (X):
1 = Nonspecific indicator present also in β - thalassaemia syndrome
2 = Complementary indicator suggesting β - thalassaemia/ not-diagnostic
3 = β - thalassaemia syndrome prevalent indicator/ Diagnostic

Value of interest (Y):
‡-3 = If the histologic analysis doesn't show lateralization of trabeculae (for Porotic Hyperostosis and Cribræ Orbitalia)
†-2 = If the radiological analysis denies skull vault thickness with destruction of external lamina and trabecular outgrowth (for Porotic Hyperostosis and Cribræ Orbitalia)
-1= Not present
"empty field"= Not detectable because the bone district is present but disturbances compromise its diagnosis or if the bone district is missing
+1 = Present
†+2 = If the radiological analysis confirms skull vault thickness with destruction of external lamina and trabecular outgrowth (for Porotic Hyperostosis and Cribræ Orbitalia)
‡+3 = If the histologic analysis shows lateralization of trabeculae (for Porotic Hyperostosis and Cribræ Orbitalia)

* X-ray analysis required

Method for a preliminary diagnosis of β -thalassemia syndrome on archaeological human remains Lewis M. E. 2010 Ind no. PC525

Indicators of β -thalassemia syndrome on skull	Degree of importance (X)	Assigned value (Y)	Results (X * Y)
Porotic Hyperostosis † ‡	1	2	2
Cribræ Orbitalia ‡	1		
Hair on end*	3	1	3
Maxillary Hypertrophy	2		
	$n^{\circ} X^1$ (max 4 values) = 2	-----	$\Sigma R^1 = 5$

Presence of β -thalassemia on skull	$\frac{\Sigma R^1}{n^{\circ} X^1} = 5:2 = 2,5$	Positive Value result: possibly thalassemia syndrome
		Negative Value result: absence of thalassemia syndrome

Indicators of β -thalassemia syndrome on postcranial skeleton	Degree of importance (X)	Assigned value (Y)	Results (X * Y)
Growth arrest lines*	1		
Marrow hyperplasia	2		
Porosity of long bones	1		
Rib within a rib*	3	1	3
Premature fusion of epiphyses of humerus	1		
Spine deformity (vertebral body)	2	1	2
Enlarged foramina of Metacarpals	3		
	$n^{\circ} X^2$ (max 7 values) = 2	-----	$\Sigma R^2 = 5$

Presence of β -thalassemia on postcranial skeleton	$\frac{R^2 \Sigma}{n^{\circ} X^2} = 5:2 = 2,5$	Positive Value result: possibly thalassemia syndrome
		Negative Value result: absence of thalassemia syndrome

Presence of β thalassemia on skeleton		
Σ total	$\frac{\Sigma R^1 + \Sigma R^2}{n^{\circ} X^1 + n^{\circ} X^2} = 10:4 = 2$	Positive Value result: possibly thalassemia syndrome
		Negative Value result: absence of thalassemia syndrome

Legenda:

Degree of importance (X):
1 = Nonspecific indicator present also in β thalassemia syndrome
2 = Complementary indicator suggesting β thalassemia/ not-diagnostic
3 = β -thalassaemia syndrome prevalent indicator/ Diagnostic

Value of interest (Y):
‡-3 = If the histologic analysis doesn't show lateralization of trabeculae (for Porotic Hyperostosis and Cribræ Orbitalia)
†-2 = If the radiological analysis denies skull vault thickness with destruction of external lamina and trabecular outgrowth (for Porotic Hyperostosis and Cribræ Orbitalia)
-1 = Not present
"empty field" = Not detectable because the bone district is present but disturbances compromise its diagnosis or if the bone district is missing
+1 = Present
†+2 = If the radiological analysis confirms skull vault thickness with destruction of external lamina and trabecular outgrowth (for Porotic Hyperostosis and Cribræ Orbitalia)
‡+3 = If the histologic analysis shows lateralization of trabeculae (for Porotic Hyperostosis and Cribræ Orbitalia)

* X-ray analysis required

Method for a preliminary diagnosis of β -thalassemia syndrome on archaeological human remains Lewis M. E. 2010 Ind no. PC1083

Indicators of β -thalassemia syndrome on skull	Degree of importance (X)	Assigned value (Y)	Results (X * Y)
Porotic Hyperostosis † ‡	1	1	1
Cribræ Orbitalia ‡	1		
Hair on end*	3	-1	-3
Maxillary Hypertrophy	2		
	n° X¹ (max 4 values)= 2	-----	Σ R¹ = -2

Presence of β -thalassemia on skull	$\frac{R^1 \Sigma}{n^o X^1} = -2:2 = -1$	Positive Value result: possibly thalassaemia syndrome
		Negative Value result: absence of thalassaemia syndrome

Indicators of β -thalassemia syndrome on postcranial skeleton	Degree of importance (X)	Assigned value (Y)	Results (X * Y)
Growth arrest lines*	1		
Marrow hyperplasia	2		
Porosity of long bones	1	1	1
Rib within a rib*	3	-1	-3
Premature fusion of epiphyses of humerus	1		
Spine deformity (vertebral body)	2		
Enlarged foramina of Metacarpals	3		
	n° X² (max 7 values)= 2	-----	Σ R² = -2

Presence of β -thalassemia on postcranial skeleton	$\frac{R^2 \Sigma}{n^o X^2} = -2:2 = -1$	Positive Value result: possibly thalassaemia syndrome
		Negative Value result: absence of thalassaemia syndrome

Presence of β -thalassemia on skeleton		
Σ total	$\frac{\Sigma R^1 + \Sigma R^2}{n^o X^1 + n^o X^2} = -4:4 = -1$	Positive Value result: possibly thalassaemia syndrome
		Negative Value result: absence of thalassaemia syndrome

Legenda:

Degree of importance (X):

- 1 = Nonspecific indicator present also in β -thalassaemia syndrome
- 2 = Complementary indicator suggesting β -thalassaemia/ not-diagnostic
- 3 = β -thalassaemia syndrome prevalent indicator/ Diagnostic

Value of interest (Y):

- ‡-3 = If the histologic analysis doesn't show lateralization of trabeculae (for Porotic Hyperostosis and Cribræ Orbitalia)
- †-2 = If the radiological analysis denies skull vault thickness with destruction of external lamina and trabecular outgrowth (for Porotic Hyperostosis and Cribræ Orbitalia)
- 1 = Not present
- “empty field” = Not detectable because the bone district is present but disturbances compromise its diagnosis or if the bone district is missing
- +1 = Present
- †+2 = If the radiological analysis confirms skull vault thickness with destruction of external lamina and trabecular outgrowth (for Porotic Hyperostosis and Cribræ Orbitalia)
- ‡+3 = If the histologic analysis shows lateralization of trabeculae (for Porotic Hyperostosis and Cribræ Orbitalia)

* X-ray analysis required

Method for a preliminary diagnosis of β -thalassemia syndrome on archaeological human remains Lewis M. E. 2010 Ind no. PC920b

Indicators of β -thalassemia syndrome on skull	Degree of importance (X)	Assigned value (Y)	Results (X * Y)
Porotic Hyperostosis † ‡	1	1	1
Cribræ Orbitalia ‡	1		
Hair on end*	3	-1	-3
Maxillary Hypertrophy	2	1	1
	n° X¹ (max 4 values)= 3	-----	Σ R¹=-1

Presence of β -thalassemia on skull	$\frac{\Sigma R^1}{n^\circ X^1} = -1:3 = -0,3$	Positive Value result: possibly thalassaemia syndrome
		Negative Value result: absence of thalassaemia syndrome

Indicators of β -thalassemia syndrome on postcranial skeleton	Degree of importance (X)	Assigned value (Y)	Results (X * Y)
Growth arrest lines*	1		
Marrow hyperplasia	2	1	2
Porosity of long bones	1		
Rib within a rib*	3	1	3
Premature fusion of epiphyses of humerus	1		
Spine deformity (vertebral body)	2		
Enlarged foramina of Metacarpals	3		
	n° X² (max 7 values)= 2	-----	Σ R²= 5

Presence of β -thalassemia on postcranial skeleton	$\frac{\Sigma R^2}{n^\circ X^2} = 5:2 = 2,5$	Positive Value result: possibly thalassaemia syndrome
		Negative Value result: absence of thalassaemia syndrome

Presence of β - thalassaemia on skeleton		
Σ total	$\frac{\Sigma R^1 + \Sigma R^2}{n^\circ X^1 + n^\circ X^2} = 4:5 = 0,8$	Positive Value result: possibly thalassaemia syndrome
		Negative Value result: absence of thalassaemia syndrome

Legenda:

Degree of importance (X):
1 = Nonspecific indicator present also in β - thalassaemia syndrome
2 = Complementary indicator suggesting β - thalassaemia/ not-diagnostic
3 = β -thalassaemia syndrome prevalent indicator/ Diagnostic

Value of interest (Y):
‡-3 = If the histologic analysis doesn't show lateralization of trabeculae (for Porotic Hyperostosis and Cribræ Orbitalia)
†-2 = If the radiological analysis denies skull vault thickness with destruction of external lamina and trabecular outgrowth (for Porotic Hyperostosis and Cribræ Orbitalia)
-1 = Not present
"empty field" = Not detectable because the bone district is present but disturbances compromise its diagnosis or if the bone district is missing
+1 = Present
†+2 = If the radiological analysis confirms skull vault thickness with destruction of external lamina and trabecular outgrowth (for Porotic Hyperostosis and Cribræ Orbitalia)
‡+3 = If the histologic analysis shows lateralization of trabeculae (for Porotic Hyperostosis and Cribræ Orbitalia)

* X-ray analysis required

Method for a preliminary diagnosis of β -thalassemia syndrome on archaeological human remains Fornaciari (2015) Tomb. III

Indicators of β -thalassemia syndrome on skull	Degree of importance (X)	Assigned value (Y)	Results (X * Y)
Porotic Hyperostosis † ‡	1	2	2
Cribræ Orbitalia ‡	1	1	1
Hair on end*	3	1	3
Maxillary Hypertrophy	2	-1	-2
	n° X¹ (max 4 values) = 4	-----	$\Sigma R^1 = 4$

Presence of β - thalassemia on skull	$\frac{\Sigma R^1}{n^{\circ} X^1} = 7:4 = 1,75$	Positive Value result: possibly thalassemia syndrome Negative Value result: absence of thalassemia syndrome
--------------------------------------------	-------------------------------------------------	----------------------------------------------------------------------------------------------------------------

Indicators of β -thalassemia syndrome on postcranial skeleton	Degree of importance (X)	Assigned value (Y)	Results (X * Y)
Growth arrest lines*	1		
Marrow hyperplasia	2	1	2
Porosity of long bones	1	1	1
Rib within a rib*	3		
Premature fusion of epiphyses of humerus	1		
Spine deformity (vertebral body)	2		
Enlarged foramina of Metacarpals	3		
	n° X² (max 7 values)= 2	-----	$\Sigma R^2 = 3$

Presence of β -thalassemia on postcranial skeleton	$\frac{\Sigma R^2}{n^{\circ} X^2} = 3:2 = 1,5$	Positive Value result: possibly thalassemia syndrome Negative Value result: absence of thalassemia syndrome
----------------------------------------------------------	------------------------------------------------	----------------------------------------------------------------------------------------------------------------

Presence of β - thalassemia on skeleton		
Σ total	$\frac{\Sigma R^1 + \Sigma R^2}{n^{\circ} X^1 + n^{\circ} X^2} = 10:6 = 1,66$	Positive Value result: possibly thalassemia syndrome Negative Value result: absence of thalassemia syndrome

Legenda:

Degree of importance (X):
1 = Nonspecific indicator present also in β - thalassemia syndrome
2 = Complementary indicator suggesting β - thalassemia/ not-diagnostic
3 = β - thalassaemia syndrome prevalent indicator/ Diagnostic

Value of interest (Y):
‡-3 = If the histologic analysis doesn't show lateralization of trabeculae (for Porotic Hyperostosis and Cribræ Orbitalia)
†-2 = If the radiological analysis denies skull vault thickness with destruction of external lamina and trabecular outgrowth (for Porotic Hyperostosis and Cribræ Orbitalia)
-1 = Not present
“empty field”= Not detectable because the bone district is present but disturbances compromise its diagnosis or if the bone district is missing
+1 = Present
†+2 = If the radiological analysis confirms skull vault thickness with destruction of external lamina and trabecular outgrowth (for Porotic Hyperostosis and Cribræ Orbitalia)
‡+3 = If the histologic analysis shows lateralization of trabeculae (for Porotic Hyperostosis and Cribræ Orbitalia)

*X-ray analysis required

Method for a preliminary diagnosis of β -thalassemia syndrome on archaeological human remains Fornaciari (2015) Tomb. V

Indicators of β -thalassemia syndrome on skull	Degree of importance (X)	Assigned value (Y)	Results (X * Y)
Porotic Hyperostosis † ‡	1	2	2
Cribræ Orbitalia ‡	1	1	1
Hair on end*	3	1	3
Maxillary Hypertrophy	2	1	2
	n° X¹ (max 4 values) = 4	-----	Σ R¹ = 8

Presence of β -thalassemia on skull	$\frac{\Sigma R^1}{n^{\circ} X^1} = 8:4 = 2$	Positive Value result: possibly thalassaemia syndrome
		Negative Value result: absence of thalassaemia syndrome

Indicators of β -thalassemia syndrome on postcranial skeleton	Degree of importance (X)	Assigned value (Y)	Results (X * Y)
Growth arrest lines*	1	-1	-1
Marrow hyperplasia	2	1	2
Porosity of long bones	1	1	1
Rib within a rib*	3		
Premature fusion of epiphyses of humerus	1		
Spine deformity (vertebral body)	2	1	2
Enlarged foramina of Metacarpals	3		
	n° X² (max 7 values) = 4	-----	Σ R² = 4

Presence of β -thalassemia on postcranial skeleton	$\frac{\Sigma R^2}{n^{\circ} X^2} = 4:4 = 1$	Positive Value result: possibly thalassaemia syndrome
		Negative Value result: absence of thalassaemia syndrome

Presence of β -thalassemia on skeleton		
Σ total	$\frac{\Sigma R^1 + \Sigma R^2}{n^{\circ} X^1 + n^{\circ} X^2} = 12: 8 = 1,5$	Positive Value result: possibly thalassaemia syndrome
		Negative Value result: absence of thalassaemia syndrome

Legenda:

Degree of importance (X):
1 = Nonspecific indicator present also in β -thalassaemia syndrome
2 = Complementary indicator suggesting β -thalassaemia/ not-diagnostic
3 = β -thalassaemia syndrome prevalent indicator/ Diagnostic

Value of interest (Y):
‡-3 = If the histologic analysis doesn't show lateralization of trabeculae (for Porotic Hyperostosis and Cribræ Orbitalia)
†-2 = If the radiological analysis denies skull vault thickness with destruction of external lamina and trabecular outgrowth (for Porotic Hyperostosis and Cribræ Orbitalia)
-1 = Not present
"empty field" = Not detectable because the bone district is present but disturbances compromise its diagnosis or if the bone district is missing
+1 = Present
†+2 = If the radiological analysis confirms skull vault thickness with destruction of external lamina and trabecular outgrowth (for Porotic Hyperostosis and Cribræ Orbitalia)
‡+3 = If the histologic analysis shows lateralization of trabeculae (for Porotic Hyperostosis and Cribræ Orbitalia)

* X-ray analysis required

Method for a preliminary diagnosis of β -thalassemia syndrome on archaeological human remains Rohnberg A. (2016)

Indicators of β -thalassemia syndrome on skull	Degree of importance (X)	Assigned value (Y)	Results (X * Y)
Porotic Hyperostosis † ‡	1		
Cribræ Orbitalia ‡	1		
Hair on end*	3		
Maxillary Hypertrophy	2	-1	-2
	n° X¹ (max 4 values)= 1	-----	$\Sigma R^1 = -2$

Presence of β - thalassaemia on skull	$\frac{\Sigma R^1}{n^{\circ} X^1} = -2:1 = -2$	Positive Value result: possibly thalassaemia syndrome Negative Value result: absence of thalassaemia syndrome
---------------------------------------------	------------------------------------------------	------------------------------------------------------------------------------------------------------------------

Indicators of β -thalassemia syndrome on postcranial skeleton	Degree of importance (X)	Assigned value (Y)	Results (X * Y)
Growth arrest lines*	1		
Marrow hyperplasia	2	1	2
Porosity of long bones	1	1	1
Rib within a rib*	3	1	3
Premature fusion of epiphyses of humerus	1		
Spine deformity (vertebral body)	2		
Enlarged foramina of Metacarpals	3		
	n° X² (max 7 values)= 3	-----	$\Sigma R^2 = 6$

Presence of β -thalassaemia on postcranial skeleton	$\frac{\Sigma R^2}{n^{\circ} X^2} = 6:3 = 2$	Positive Value result: possibly thalassaemia syndrome Negative Value result: absence of thalassaemia syndrome
-----------------------------------------------------------	----------------------------------------------	------------------------------------------------------------------------------------------------------------------

Presence of β - thalassaemia on skeleton		
Σ total	$\frac{\Sigma R^1 + \Sigma R^2}{n^{\circ} X^1 + n^{\circ} X^2} = 4:4 = 1$	Positive Value result: possibly thalassaemia syndrome Negative Value result: absence of thalassaemia syndrome

Legenda:

Degree of importance (X):
1 = Nonspecific indicator present also in β - thalassaemia syndrome
2 = Complementary indicator suggesting β - thalassaemia/ not-diagnostic
3 = β - thalassaemia syndrome prevalent indicator/ Diagnostic

Value of interest (Y):
‡-3 = If the histologic analysis doesn't show lateralization of trabeculae (for Porotic Hyperostosis and Cribræ Orbitalia)
†-2 = If the radiological analysis denies skull vault thickness with destruction of external lamina and trabecular outgrowth (for Porotic Hyperostosis and Cribræ Orbitalia)
-1 = Not present
“empty field”= Not detectable because the bone district is present but disturbances compromise its diagnosis or if the bone district is missing
+1 = Present
†+2 = If the radiological analysis confirms skull vault thickness with destruction of external lamina and trabecular outgrowth (for Porotic Hyperostosis and Cribræ Orbitalia)
‡+3 = If the histologic analysis shows lateralization of trabeculae (for Porotic Hyperostosis and Cribræ Orbitalia)

*X-ray analysis required

Method for a preliminary diagnosis of β -thalassemia syndrome on archaeological human remains (Thomas et al 2016)

Indicators of β -thalassemia syndrome on skull	Degree of importance (X)	Assigned value (Y)	Results (X * Y)
Porotic Hyperostosis † ‡	1	1	1
Cribræ Orbitalia ‡	1	1	1
Hair on end*	3	1	3
Maxillary Hypertrophy	2		
	n° X¹ (max 4 values) = 3	-----	Σ R¹ = 5

Presence of β -thalassemia on skull	$\frac{\Sigma R^1}{n^\circ X^1} = 5:3 = 1,66$	Positive Value result: possibly thalassemia syndrome Negative Value result: absence of thalassemia syndrome
-------------------------------------------	-----------------------------------------------	----------------------------------------------------------------------------------------------------------------

Indicators of β -thalassemia syndrome on postcranial skeleton	Degree of importance (X)	Assigned value (Y)	Results (X * Y)
Growth arrest lines*	1		
Marrow hyperplasia	2	1	1
Porosity of long bones	1	-1	-1
Rib within a rib*	3	-1	-3
Premature fusion of epiphyses of humerus	1	1	1
Spine deformity (vertebral body)	2		
Enlarged foramina of Metacarpals	3		
	n° X² (max 7 values) = 4	-----	Σ R² = -2

Presence of β -thalassemia on postcranial skeleton	$\frac{\Sigma R^2}{n^\circ X^2} = -2:4 = -0,5$	Positive Value result: possibly thalassemia syndrome Negative Value result: absence of thalassemia syndrome
----------------------------------------------------------	------------------------------------------------	----------------------------------------------------------------------------------------------------------------

Presence of β -thalassemia on skeleton		
Σ total	$\frac{\Sigma R^1 + \Sigma R^2}{n^\circ X^1 + n^\circ X^2} = 3:7 = 0,42$	Positive Value result: possibly thalassemia syndrome Negative Value result: absence of thalassemia syndrome

Legenda:

Degree of importance (X):
1 = Nonspecific indicator present also in β -thalassemia syndrome
2 = Complementary indicator suggesting β -thalassemia/ not-diagnostic
3 = β -thalassaemia syndrome prevalent indicator/ Diagnostic

Value of interest (Y):
‡-3 = If the histologic analysis doesn't show lateralization of trabeculae (for Porotic Hyperostosis and Cribræ Orbitalia)
†-2 = If the radiological analysis denies skull vault thickness with destruction of external lamina and trabecular outgrowth (for Porotic Hyperostosis and Cribræ Orbitalia)
-1 = Not present
"empty field" = Not detectable because the bone district is present but disturbances compromise its diagnosis or if the bone district is missing
+1 = Present
†+2 = If the radiological analysis confirms skull vault thickness with destruction of external lamina and trabecular outgrowth (for Porotic Hyperostosis and Cribræ Orbitalia)
‡+3 = If the histologic analysis shows lateralization of trabeculae (for Porotic Hyperostosis and Cribræ Orbitalia)

* X-ray analysis required

Method for a preliminary diagnosis of β -thalassemia syndrome on archaeological human remains (Tomczyk et al 2016)

Indicators of β -thalassemia syndrome on skull	Degree of importance (X)	Assigned value (Y)	Results (X * Y)
Porotic Hyperostosis † ‡	1	1	1
Cribræ Orbitalia ‡	1	1	1
Hair on end*	3	1	3
Maxillary Hypertrophy	2	1	2
	n° X¹ (max 4 values) = 4	-----	$\Sigma R^1 = 7$

Presence of β - thalassaemia on skull	$\frac{\Sigma R^1}{n^{\circ} X^1} = 7:4 = 1,75$	Positive Value result: possibly thalassaemia syndrome Negative Value result: absence of thalassaemia syndrome

Indicators of β -thalassemia syndrome on postcranial skeleton	Degree of importance (X)	Assigned value (Y)	Results (X * Y)
Growth arrest lines*	1		
Marrow hyperplasia	2		
Porosity of long bones	1		
Rib within a rib*	3	1	3
Premature fusion of epiphyses of humerus	1		
Spine deformity (vertebral body)	2		
Enlarged foramina of Metacarpals	3		
	n° X² (max 7 values) = 1	-----	$\Sigma R^2 = 3$

Presence of β -thalassaemia on postcranial skeleton	$\frac{\Sigma R^2}{n^{\circ} X^2} = 3:1 = 3$	Positive Value result: possibly thalassaemia syndrome Negative Value result: absence of thalassaemia syndrome

Presence of β - thalassaemia on skeleton		
Σ total	$\frac{\Sigma R^1 + \Sigma R^2}{n^{\circ} X^1 + n^{\circ} X^2} = 10:5 = 2$	Positive Value result: possibly thalassaemia syndrome Negative Value result: absence of thalassaemia syndrome

Legenda:

Degree of importance (X):
1 = Nonspecific indicator present also in β - thalassaemia syndrome
2 = Complementary indicator suggesting β - thalassaemia/ not-diagnostic
3 = β - thalassaemia syndrome prevalent indicator/ Diagnostic

Value of interest (Y):
‡-3 = If the histologic analysis doesn't show lateralization of trabeculae (for Porotic Hyperostosis and Cribræ Orbitalia)
†-2 = If the radiological analysis denies skull vault thickness with destruction of external lamina and trabecular outgrowth (for Porotic Hyperostosis and Cribræ Orbitalia)
-1 = Not present
“empty field”= Not detectable because the bone district is present but disturbances compromise its diagnosis or if the bone district is missing
+1 = Present
†+2 = If the radiological analysis confirms skull vault thickness with destruction of external lamina and trabecular outgrowth (for Porotic Hyperostosis and Cribræ Orbitalia)
‡+3 = If the histologic analysis shows lateralization of trabeculae (for Porotic Hyperostosis and Cribræ Orbitalia)

*X-ray analysis required

Method for a preliminary diagnosis of β -thalassemia syndrome on archaeological human remains Spina VP 125A – Ind. A

Indicators of β -thalassemia syndrome on skull	Degree of importance (X)	Assigned value (Y)	Results (X * Y)
Porotic Hyperostosis † ‡	1	3	3
Cribræ Orbitalia ‡	1	3	3
Hair on end*	3	-1	-3
Maxillary Hypertrophy	2	-1	-2
	n° X¹ (max 4 values) = 4	-----	Σ R¹ = 1

Presence of β -thalassemia on skull	$\frac{\Sigma R^1}{n^\circ X^1} = 1:4 = 0,25$	Positive Value result: possibly thalassaemia syndrome
		Negative Value result: absence of thalassaemia syndrome

Indicators of β -thalassemia syndrome on postcranial skeleton	Degree of importance (X)	Assigned value (Y)	Results (X * Y)
Growth arrest lines*	1	-1	-1
Marrow hyperplasia	2	1	2
Porosity of long bones	1	-1	-1
Rib within a rib*	3		
Premature fusion of epiphyses of humerus	1	-1	-1
Spine deformity (vertebral body)	2	-1	-2
Enlarged foramina of Metacarpals	3	-1	-3
	n° X² (max 7 values) = 6	-----	Σ R² = - 6

Presence of β -thalassemia on postcranial skeleton	$\frac{\Sigma R^2}{n^\circ X^2} = -6:6 = -1$	Positive Value result: possibly thalassaemia syndrome
		Negative Value result: absence of thalassaemia syndrome

Presence of β -thalassemia on skeleton		
Σ total	$\frac{\Sigma R^1 + \Sigma R^2}{n^\circ X^1 + n^\circ X^2} = -5:10 = -0,5$	Positive Value result: possibly thalassaemia syndrome Negative Value result: absence of thalassaemia syndrome

Legenda:

Degree of importance (X):
1 = Nonspecific indicator present also in β -thalassaemia syndrome
2 = Complementary indicator suggesting β -thalassaemia/ not-diagnostic
3 = β -thalassaemia syndrome prevalent indicator/ Diagnostic

Value of interest (Y):
‡-3 = If the histologic analysis doesn't show lateralization of trabeculae (for Porotic Hyperostosis and Cribræ Orbitalia)
†-2 = If the radiological analysis denies skull vault thickness with destruction of external lamina and trabecular outgrowth (for Porotic Hyperostosis and Cribræ Orbitalia)
-1 = Not present
"empty field" = Not detectable because the bone district is present but disturbances compromise its diagnosis or if the bone district is missing
+1 = Present
†+2 = If the radiological analysis confirms skull vault thickness with destruction of external lamina and trabecular outgrowth (for Porotic Hyperostosis and Cribræ Orbitalia)
‡+3 = If the histologic analysis shows lateralization of trabeculae (for Porotic Hyperostosis and Cribræ Orbitalia)

* X-ray analysis required

Method for a preliminary diagnosis of β -thalassemia syndrome on archaeological human remains Spina VP 126D

Indicators of β -thalassemia syndrome on skull	Degree of importance (X)	Assigned value (Y)	Results (X * Y)
Porotic Hyperostosis † ‡	1	3	3
Cribræ Orbitalia ‡	1	3	3
Hair on end*	3	-1	-3
Maxillary Hypertrophy	2	-1	-2
	n° X¹ (max 4 values)= 4	-----	$\Sigma R^1 = 1$

Presence of β - thalassaemia on skull	$\frac{\Sigma R^1}{n^{\circ} X^1} = 1:4= 0,25$	Positive Value result: possibly thalassaemia syndrome
		Negative Value result: absence of thalassaemia syndrome

Indicators of β -thalassemia syndrome on postcranial skeleton	Degree of importance (X)	Assigned value (Y)	Results (X * Y)
Growth arrest lines*	1		
Marrow hyperplasia	2	1	2
Porosity of long bones	1	-1	-1
Rib within a rib*	3		
Premature fusion of epiphyses of humerus	1	-1	-1
Spine deformity (vertebral body)	2	-1	-2
Enlarged foramina of Metacarpals	3	-1	-3
	n° X² (max 7 values)= 5	-----	$\Sigma R^2 = -5$

Presence of β -thalassaemia on postcranial skeleton	$\frac{\Sigma R^2}{n^{\circ} X^2} = -5:5= -1$	Positive Value result: possibly thalassaemia syndrome
		Negative Value result: absence of thalassaemia syndrome

Presence of β - thalassaemia on skeleton		
Σ total	$\frac{\Sigma R^1 + \Sigma R^2}{n^{\circ} X^1 + n^{\circ} X^2} = -4:9= -0,44$	Positive Value result: possibly thalassaemia syndrome
		Negative Value result: absence of thalassaemia syndrome

Legenda:

Degree of importance (X):
1 = Nonspecific indicator present also in β - thalassaemia syndrome
2 = Complementary indicator suggesting β - thalassaemia/ not-diagnostic
3 = β - thalassaemia syndrome prevalent indicator/ Diagnostic

Value of interest (Y):
‡-3 = If the histologic analysis doesn't show lateralization of trabeculae (for Porotic Hyperostosis and Cribræ Orbitalia)
†-2 = If the radiological analysis denies skull vault thickness with destruction of external lamina and trabecular outgrowth (for Porotic Hyperostosis and Cribræ Orbitalia)
-1= Not present
“empty field”= Not detectable because the bone district is present but disturbances compromise its diagnosis or if the bone district is missing
+1 = Present
†+2 = If the radiological analysis confirms skull vault thickness with destruction of external lamina and trabecular outgrowth (for Porotic Hyperostosis and Cribræ Orbitalia)
‡+3 = If the histologic analysis shows lateralization of trabeculae (for Porotic Hyperostosis and Cribræ Orbitalia)

*X-ray analysis required

Method for a preliminary diagnosis of β -thalassemia syndrome on archaeological human remains Spina VP 2E

Indicators of β -thalassemia syndrome on skull	Degree of importance (X)	Assigned value (Y)	Results (X * Y)
Porotic Hyperostosis † ‡	1	-3	-3
Cribræ Orbitalia ‡	1	-3	-3
Hair on end*	3	-1	-3
Maxillary Hypertrophy	2	-1	-2
	n° X¹ (max 4 values) = 4	-----	Σ R¹ = -11

Presence of β -thalassemia on skull	$\frac{\Sigma R^1}{n^\circ X^1} = -11:4 = -2,75$	Positive Value result: possibly thalassaemia syndrome
		Negative Value result: absence of thalassaemia syndrome

Indicators of β -thalassemia syndrome on postcranial skeleton	Degree of importance (X)	Assigned value (Y)	Results (X * Y)
Growth arrest lines*	1		
Marrow hyperplasia	2	1	2
Porosity of long bones	1	1	1
Rib within a rib*	3		
Premature fusion of epiphyses of humerus	1	-1	-1
Spine deformity (vertebral body)	2	-1	-2
Enlarged foramina of Metacarpals	3	-1	-3
	n° X² (max 7 values) = 5	-----	Σ R² = -3

Presence of β -thalassemia on postcranial skeleton	$\frac{\Sigma R^2}{n^\circ X^2} = -3:5 = -0,6$	Positive Value result: possibly thalassaemia syndrome
		Negative Value result: absence of thalassaemia syndrome

Presence of β -thalassemia on skeleton		
Σ total	$\frac{\Sigma R^1 + \Sigma R^2}{n^\circ X^1 + n^\circ X^2} = -14:9 = -1,55$	Positive Value result: possibly thalassaemia syndrome Negative Value result: absence of thalassaemia syndrome

Legenda:

Degree of importance (X):
1 = Nonspecific indicator present also in β -thalassaemia syndrome
2 = Complementary indicator suggesting β -thalassaemia/ not-diagnostic
3 = β -thalassaemia syndrome prevalent indicator/ Diagnostic

Value of interest (Y):
‡-3 = If the histologic analysis doesn't show lateralization of trabeculae (for Porotic Hyperostosis and Cribræ Orbitalia)
†-2 = If the radiological analysis denies skull vault thickness with destruction of external lamina and trabecular outgrowth (for Porotic Hyperostosis and Cribræ Orbitalia)
-1 = Not present
"empty field" = Not detectable because the bone district is present but disturbances compromise its diagnosis or if the bone district is missing
+1 = Present
†+2 = If the radiological analysis confirms skull vault thickness with destruction of external lamina and trabecular outgrowth (for Porotic Hyperostosis and Cribræ Orbitalia)
‡+3 = If the histologic analysis shows lateralization of trabeculae (for Porotic Hyperostosis and Cribræ Orbitalia)
* X-ray analysis required

Method for a preliminary diagnosis of β -thalassemia syndrome on archaeological human remains SSM 1

Indicators of β -thalassemia syndrome on skull	Degree of importance (X)	Assigned value (Y)	Results (X * Y)
Porotic Hyperostosis † ‡	1	1	1
Cribræ Orbitalia ‡	1	-1	-1
Hair on end*	3	-1	-3
Maxillary Hypertrophy	2	-1	-2
	n° X¹ (max 4 values) = 4	-----	$\Sigma R^1 = -5$

Presence of β - thalassaemia on skull	$\frac{\Sigma R^1}{n^{\circ} X^1} = -5:4 = -1,25$	Positive Value result: possibly thalassaemia syndrome Negative Value result: absence of thalassaemia syndrome

Indicators of β -thalassemia syndrome on postcranial skeleton	Degree of importance (X)	Assigned value (Y)	Results (X * Y)
Growth arrest lines*	1		
Marrow hyperplasia	2		
Porosity of long bones	1		
Rib within a rib*	3		
Premature fusion of epiphyses of humerus	1		
Spine deformity (vertebral body)	2		
Enlarged foramina of Metacarpals	3		
	n° X² (max 7 values) =	-----	$\Sigma R^2 =$

Presence of β -thalassaemia on postcranial skeleton	$\frac{\Sigma R^2}{n^{\circ} X^2} =$	Positive Value result: possibly thalassaemia syndrome Negative Value result: absence of thalassaemia syndrome

Presence of β - thalassaemia on skeleton		
Σ total	$\frac{\Sigma R^1 + \Sigma R^2}{n^{\circ} X^1 + n^{\circ} X^2} =$	Positive Value result: possibly thalassaemia syndrome Negative Value result: absence of thalassaemia syndrome

Legenda:

Degree of importance (X):
1 = Nonspecific indicator present also in β - thalassaemia syndrome
2 = Complementary indicator suggesting β - thalassaemia/ not-diagnostic
3 = β - thalassaemia syndrome prevalent indicator/ Diagnostic

Value of interest (Y):
‡-3 = If the histologic analysis doesn't show lateralization of trabeculae (for Porotic Hyperostosis and Cribræ Orbitalia)
†-2 = If the radiological analysis denies skull vault thickness with destruction of external lamina and trabecular outgrowth (for Porotic Hyperostosis and Cribræ Orbitalia)
-1 = Not present
“empty field” = Not detectable because the bone district is present but disturbances compromise its diagnosis or if the bone district is missing
+1 = Present
†+2 = If the radiological analysis confirms skull vault thickness with destruction of external lamina and trabecular outgrowth (for Porotic Hyperostosis and Cribræ Orbitalia)
‡+3 = If the histologic analysis shows lateralization of trabeculae (for Porotic Hyperostosis and Cribræ Orbitalia)

*X-ray analysis required

Method for a preliminary diagnosis of β -thalassemia syndrome on archaeological human remains SSM 2

Indicators of β -thalassemia syndrome on skull	Degree of importance (X)	Assigned value (Y)	Results (X * Y)
Porotic Hyperostosis † ‡	1	-2	-2
Cribræ Orbitalia ‡	1	-3	-3
Hair on end*	3	-1	-3
Maxillary Hypertrophy	2	-1	-2
	n° X¹ (max 4 values) = 4	-----	$\Sigma R^1 = -10$

Presence of β -thalassemia on skull	$\frac{\Sigma R^1}{n^{\circ} X^1} = -10:4 = -2,5$	Positive Value result: possibly thalassaemia syndrome
		Negative Value result: absence of thalassaemia syndrome

Indicators of β -thalassemia syndrome on postcranial skeleton	Degree of importance (X)	Assigned value (Y)	Results (X * Y)
Growth arrest lines*	1		
Marrow hyperplasia	2		
Porosity of long bones	1		
Rib within a rib*	3		
Premature fusion of epiphyses of humerus	1		
Spine deformity (vertebral body)	2		
Enlarged foramina of Metacarpals	3		
	n° X² (max 7 values)=	-----	$\Sigma R^2 =$

Presence of β -thalassemia on postcranial skeleton	$\frac{\Sigma R^2}{n^{\circ} X^2} =$	Positive Value result: possibly thalassaemia syndrome
		Negative Value result: absence of thalassaemia syndrome

Presence of β -thalassemia on skeleton		
Σ total	$\frac{\Sigma R^1 + \Sigma R^2}{n^{\circ} X^1 + n^{\circ} X^2} =$	Positive Value result: possibly thalassaemia syndrome Negative Value result: absence of thalassaemia syndrome

Legenda:

Degree of importance (X):
1 = Nonspecific indicator present also in β -thalassaemia syndrome
2 = Complementary indicator suggesting β -thalassaemia/ not-diagnostic
3 = β -thalassaemia syndrome prevalent indicator/ Diagnostic

Value of interest (Y):
‡-3 = If the histologic analysis doesn't show lateralization of trabeculae (for Porotic Hyperostosis and Cribræ Orbitalia)
†-2 = If the radiological analysis denies skull vault thickness with destruction of external lamina and trabecular outgrowth (for Porotic Hyperostosis and Cribræ Orbitalia)
-1 = Not present
"empty field" = Not detectable because the bone district is present but disturbances compromise its diagnosis or if the bone district is missing
+1 = Present
†+2 = If the radiological analysis confirms skull vault thickness with destruction of external lamina and trabecular outgrowth (for Porotic Hyperostosis and Cribræ Orbitalia)
‡+3 = If the histologic analysis shows lateralization of trabeculae (for Porotic Hyperostosis and Cribræ Orbitalia)
* X-ray analysis required

Method for a preliminary diagnosis of β -thalassemia syndrome on archaeological human remains SSM 4IIa

Indicators of β -thalassemia syndrome on skull	Degree of importance (X)	Assigned value (Y)	Results (X * Y)
Porotic Hyperostosis † ‡	1	3	3
Cribræ Orbitalia ‡	1	3	3
Hair on end*	3		
Maxillary Hypertrophy	2		
	n° X¹ (max 4 values) = 2	-----	Σ R¹ = 6

Presence of β - thalassaemia on skull	$\frac{\Sigma R^1}{n^{\circ} X^1} = 6:2 = 3$	Positive Value result: possibly thalassaemia syndrome
		Negative Value result: absence of thalassaemia syndrome

Indicators of β -thalassemia syndrome on postcranial skeleton	Degree of importance (X)	Assigned value (Y)	Results (X * Y)
Growth arrest lines*	1		
Marrow hyperplasia	2		
Porosity of long bones	1		
Rib within a rib*	3		
Premature fusion of epiphyses of humerus	1		
Spine deformity (vertebral body)	2		
Enlarged foramina of Metacarpals	3		
	n° X² (max 7 values)=	-----	Σ R² =

Presence of β -thalassaemia on postcranial skeleton	$\frac{\Sigma R^2}{n^{\circ} X^2} =$	Positive Value result: possibly thalassaemia syndrome
		Negative Value result: absence of thalassaemia syndrome

Presence of β - thalassaemia on skeleton		
Σ total	$\frac{\Sigma R^1 + \Sigma R^2}{n^{\circ} X^1 + n^{\circ} X^2} =$	Positive Value result: possibly thalassaemia syndrome
		Negative Value result: absence of thalassaemia syndrome

Legenda:

Degree of importance (X):
1 = Nonspecific indicator present also in β - thalassaemia syndrome
2 = Complementary indicator suggesting β - thalassaemia/ not-diagnostic
3 = β - thalassaemia syndrome prevalent indicator/ Diagnostic

Value of interest (Y):
‡-3 = If the histologic analysis doesn't show lateralization of trabeculae (for Porotic Hyperostosis and Cribræ Orbitalia)
†-2 = If the radiological analysis denies skull vault thickness with destruction of external lamina and trabecular outgrowth (for Porotic Hyperostosis and Cribræ Orbitalia)
-1 = Not present
“empty field”= Not detectable because the bone district is present but disturbances compromise its diagnosis or if the bone district is missing
+1 = Present
†+2 = If the radiological analysis confirms skull vault thickness with destruction of external lamina and trabecular outgrowth (for Porotic Hyperostosis and Cribræ Orbitalia)
‡+3 = If the histologic analysis shows lateralization of trabeculae (for Porotic Hyperostosis and Cribræ Orbitalia)

*X-ray analysis required

Method for a preliminary diagnosis of β -thalassemia syndrome on archaeological human remains SSM 6

Indicators of β -thalassemia syndrome on skull	Degree of importance (X)	Assigned value (Y)	Results (X * Y)
Porotic Hyperostosis † ‡	1	-2	-2
Cribræ Orbitalia ‡	1	1	1
Hair on end*	3	-1	-3
Maxillary Hypertrophy	2	-1	-2
	n° X¹ (max 4 values) = 4	-----	$\Sigma R^1 = -6$

Presence of β -thalassemia on skull	$\frac{\Sigma R^1}{n^{\circ} X^1} = -6:4 = -1,5$	Positive Value result: possibly thalassaemia syndrome
		Negative Value result: absence of thalassaemia syndrome

Indicators of β -thalassemia syndrome on postcranial skeleton	Degree of importance (X)	Assigned value (Y)	Results (X * Y)
Growth arrest lines*	1		
Marrow hyperplasia	2		
Porosity of long bones	1		
Rib within a rib*	3		
Premature fusion of epiphyses of humerus	1		
Spine deformity (vertebral body)	2		
Enlarged foramina of Metacarpals	3		
	n° X² (max 7 values)=	-----	$\Sigma R^2 =$

Presence of β -thalassemia on postcranial skeleton	$\frac{\Sigma R^2}{n^{\circ} X^2} =$	Positive Value result: possibly thalassaemia syndrome
		Negative Value result: absence of thalassaemia syndrome

Presence of β -thalassemia on skeleton		
Σ total	$\frac{\Sigma R^1 + \Sigma R^2}{n^{\circ} X^1 + n^{\circ} X^2} =$	Positive Value result: possibly thalassaemia syndrome
		Negative Value result: absence of thalassaemia syndrome

Legenda:

Degree of importance (X):
1 = Nonspecific indicator present also in β -thalassaemia syndrome
2 = Complementary indicator suggesting β -thalassaemia/ not-diagnostic
3 = β -thalassaemia syndrome prevalent indicator/ Diagnostic

Value of interest (Y):
‡-3 = If the histologic analysis doesn't show lateralization of trabeculae (for Porotic Hyperostosis and Cribræ Orbitalia)
†-2 = If the radiological analysis denies skull vault thickness with destruction of external lamina and trabecular outgrowth (for Porotic Hyperostosis and Cribræ Orbitalia)
-1 = Not present
"empty field" = Not detectable because the bone district is present but disturbances compromise its diagnosis or if the bone district is missing
+1 = Present
†+2 = If the radiological analysis confirms skull vault thickness with destruction of external lamina and trabecular outgrowth (for Porotic Hyperostosis and Cribræ Orbitalia)
‡+3 = If the histologic analysis shows lateralization of trabeculae (for Porotic Hyperostosis and Cribræ Orbitalia)
* X-ray analysis required

Method for a preliminary diagnosis of β -thalassemia syndrome on archaeological human remains SSM 15

Indicators of β -thalassemia syndrome on skull	Degree of importance (X)	Assigned value (Y)	Results (X * Y)
Porotic Hyperostosis † ‡	1	3	3
Cribræ Orbitalia ‡	1	-1	-1
Hair on end*	3	-1	-3
Maxillary Hypertrophy	2		
	n° X¹ (max 4 values) = 3	-----	$\Sigma R^1 = -1$

Presence of β - thalassaemia on skull	$\frac{\Sigma R^1}{n^{\circ} X^1} = -1: 3 = -0,33$	Positive Value result: possibly thalassaemia syndrome
		Negative Value result: absence of thalassaemia syndrome

Indicators of β -thalassemia syndrome on postcranial skeleton	Degree of importance (X)	Assigned value (Y)	Results (X * Y)
Growth arrest lines*	1		
Marrow hyperplasia	2		
Porosity of long bones	1		
Rib within a rib*	3		
Premature fusion of epiphyses of humerus	1		
Spine deformity (vertebral body)	2		
Enlarged foramina of Metacarpals	3		
	n° X² (max 7 values) =	-----	$\Sigma R^2 =$

Presence of β -thalassaemia on postcranial skeleton	$\frac{\Sigma R^2}{n^{\circ} X^2} =$	Positive Value result: possibly thalassaemia syndrome
		Negative Value result: absence of thalassaemia syndrome

Presence of β - thalassaemia on skeleton		
Σ total	$\frac{\Sigma R^1 + \Sigma R^2}{n^{\circ} X^1 + n^{\circ} X^2} =$	Positive Value result: possibly thalassaemia syndrome
		Negative Value result: absence of thalassaemia syndrome

Legenda:

Degree of importance (X):
1 = Nonspecific indicator present also in β - thalassaemia syndrome
2 = Complementary indicator suggesting β - thalassaemia/ not-diagnostic
3 = β - thalassaemia syndrome prevalent indicator/ Diagnostic

Value of interest (Y):
‡-3 = If the histologic analysis doesn't show lateralization of trabeculae (for Porotic Hyperostosis and Cribræ Orbitalia)
†-2 = If the radiological analysis denies skull vault thickness with destruction of external lamina and trabecular outgrowth (for Porotic Hyperostosis and Cribræ Orbitalia)
-1 = Not present
“empty field”= Not detectable because the bone district is present but disturbances compromise its diagnosis or if the bone district is missing
+1 = Present
†+2 = If the radiological analysis confirms skull vault thickness with destruction of external lamina and trabecular outgrowth (for Porotic Hyperostosis and Cribræ Orbitalia)
‡+3 = If the histologic analysis shows lateralization of trabeculae (for Porotic Hyperostosis and Cribræ Orbitalia)

*X-ray analysis required

Method for a preliminary diagnosis of β -thalassemia syndrome on archaeological human remains SSM 25

Indicators of β -thalassemia syndrome on skull	Degree of importance (X)	Assigned value (Y)	Results (X * Y)
Porotic Hyperostosis † ‡	1	3	3
Cribræ Orbitalia ‡	1	-1	-1
Hair on end*	3	-1	-3
Maxillary Hypertrophy	2		
	n° X¹ (max 4 values) = 3	-----	$\Sigma R^1 = -1$

Presence of β -thalassemia on skull	$\frac{\Sigma R^1}{n^{\circ} X^1} = -1:3 = -0,33$	Positive Value result: possibly thalassaemia syndrome Negative Value result: absence of thalassaemia syndrome

Indicators of β -thalassemia syndrome on postcranial skeleton	Degree of importance (X)	Assigned value (Y)	Results (X * Y)
Growth arrest lines*	1		
Marrow hyperplasia	2		
Porosity of long bones	1		
Rib within a rib*	3		
Premature fusion of epiphyses of humerus	1		
Spine deformity (vertebral body)	2		
Enlarged foramina of Metacarpals	3		
	n° X² (max 7 values)=	-----	$\Sigma R^2 =$

Presence of β -thalassemia on postcranial skeleton	$\frac{\Sigma R^2}{n^{\circ} X^2} =$	Positive Value result: possibly thalassaemia syndrome Negative Value result: absence of thalassaemia syndrome

Presence of β -thalassemia on skeleton		
Σ total	$\frac{\Sigma R^1 + \Sigma R^2}{n^{\circ} X^1 + n^{\circ} X^2} =$	Positive Value result: possibly thalassaemia syndrome Negative Value result: absence of thalassaemia syndrome

Legenda:

Degree of importance (X):
1 = Nonspecific indicator present also in β -thalassaemia syndrome
2 = Complementary indicator suggesting β -thalassaemia/ not-diagnostic
3 = β -thalassaemia syndrome prevalent indicator/ Diagnostic

Value of interest (Y):
‡-3 = If the histologic analysis doesn't show lateralization of trabeculae (for Porotic Hyperostosis and Cribræ Orbitalia)
†-2 = If the radiological analysis denies skull vault thickness with destruction of external lamina and trabecular outgrowth (for Porotic Hyperostosis and Cribræ Orbitalia)
-1 = Not present
"empty field" = Not detectable because the bone district is present but disturbances compromise its diagnosis or if the bone district is missing
+1 = Present
†+2 = If the radiological analysis confirms skull vault thickness with destruction of external lamina and trabecular outgrowth (for Porotic Hyperostosis and Cribræ Orbitalia)
‡+3 = If the histologic analysis shows lateralization of trabeculae (for Porotic Hyperostosis and Cribræ Orbitalia)
* X-ray analysis required

Method for a preliminary diagnosis of β -thalassemia syndrome on archaeological human remains SSM 26

Indicators of β -thalassemia syndrome on skull	Degree of importance (X)	Assigned value (Y)	Results (X * Y)
Porotic Hyperostosis † ‡	1	-2	-2
Cribræ Orbitalia ‡	1	-1	-1
Hair on end*	3	-1	-3
Maxillary Hypertrophy	2		
	n° X¹ (max 4 values) = 3	-----	$\Sigma R^1 = -6$

Presence of β - thalassaemia on skull	$\frac{\Sigma R^1}{n^{\circ} X^1} = -6:3 = -2$	Positive Value result: possibly thalassaemia syndrome Negative Value result: absence of thalassaemia syndrome
---------------------------------------------	------------------------------------------------	------------------------------------------------------------------------------------------------------------------

Indicators of β -thalassemia syndrome on postcranial skeleton	Degree of importance (X)	Assigned value (Y)	Results (X * Y)
Growth arrest lines*	1		
Marrow hyperplasia	2		
Porosity of long bones	1		
Rib within a rib*	3		
Premature fusion of epiphyses of humerus	1		
Spine deformity (vertebral body)	2		
Enlarged foramina of Metacarpals	3		
	n° X² (max 7 values) =	-----	$\Sigma R^2 =$

Presence of β -thalassaemia on postcranial skeleton	$\frac{\Sigma R^2}{n^{\circ} X^2} =$	Positive Value result: possibly thalassaemia syndrome Negative Value result: absence of thalassaemia syndrome
-----------------------------------------------------------	--------------------------------------	------------------------------------------------------------------------------------------------------------------

Presence of β - thalassaemia on skeleton		
Σ total	$\frac{\Sigma R^1 + \Sigma R^2}{n^{\circ} X^1 + n^{\circ} X^2} =$	Positive Value result: possibly thalassaemia syndrome Negative Value result: absence of thalassaemia syndrome

Legenda:

Degree of importance (X):
1 = Nonspecific indicator present also in β - thalassaemia syndrome
2 = Complementary indicator suggesting β - thalassaemia/ not-diagnostic
3 = β - thalassaemia syndrome prevalent indicator/ Diagnostic

Value of interest (Y):
‡-3 = If the histologic analysis doesn't show lateralization of trabeculae (for Porotic Hyperostosis and Cribræ Orbitalia)
†-2 = If the radiological analysis denies skull vault thickness with destruction of external lamina and trabecular outgrowth (for Porotic Hyperostosis and Cribræ Orbitalia)
-1 = Not present
“empty field”= Not detectable because the bone district is present but disturbances compromise its diagnosis or if the bone district is missing
+1 = Present
†+2 = If the radiological analysis confirms skull vault thickness with destruction of external lamina and trabecular outgrowth (for Porotic Hyperostosis and Cribræ Orbitalia)
‡+3 = If the histologic analysis shows lateralization of trabeculae (for Porotic Hyperostosis and Cribræ Orbitalia)

*X-ray analysis required

Method for a preliminary diagnosis of β -thalassemia syndrome on archaeological human remains SSM 30

Indicators of β -thalassemia syndrome on skull	Degree of importance (X)	Assigned value (Y)	Results (X * Y)
Porotic Hyperostosis † ‡	1	2	2
Cribræ Orbitalia ‡	1	-1	-1
Hair on end*	3	-1	-3
Maxillary Hypertrophy	2		
	n° X¹ (max 4 values) = 3	-----	$\Sigma R^1 = -2$

Presence of β -thalassemia on skull	$\frac{\Sigma R^1}{n^{\circ} X^1} = -2:3 = -0,66$	Positive Value result: possibly thalassaemia syndrome Negative Value result: absence of thalassaemia syndrome
-------------------------------------------	---------------------------------------------------	------------------------------------------------------------------------------------------------------------------

Indicators of β -thalassemia syndrome on postcranial skeleton	Degree of importance (X)	Assigned value (Y)	Results (X * Y)
Growth arrest lines*	1		
Marrow hyperplasia	2		
Porosity of long bones	1		
Rib within a rib*	3		
Premature fusion of epiphyses of humerus	1		
Spine deformity (vertebral body)	2		
Enlarged foramina of Metacarpals	3		
	n° X² (max 7 values)=	-----	$\Sigma R^2 =$

Presence of β -thalassemia on postcranial skeleton	$\frac{\Sigma R^2}{n^{\circ} X^2} =$	Positive Value result: possibly thalassaemia syndrome Negative Value result: absence of thalassaemia syndrome
----------------------------------------------------------	--------------------------------------	------------------------------------------------------------------------------------------------------------------

Presence of β -thalassemia on skeleton		
Σ total	$\frac{\Sigma R^1 + \Sigma R^2}{n^{\circ} X^1 + n^{\circ} X^2} =$	Positive Value result: possibly thalassaemia syndrome Negative Value result: absence of thalassaemia syndrome

Legenda:

Degree of importance (X):
1 = Nonspecific indicator present also in β -thalassaemia syndrome
2 = Complementary indicator suggesting β -thalassaemia/ not-diagnostic
3 = β -thalassaemia syndrome prevalent indicator/ Diagnostic

Value of interest (Y):
‡-3 = If the histologic analysis doesn't show lateralization of trabeculae (for Porotic Hyperostosis and Cribræ Orbitalia)
†-2 = If the radiological analysis denies skull vault thickness with destruction of external lamina and trabecular outgrowth (for Porotic Hyperostosis and Cribræ Orbitalia)
-1 = Not present
"empty field" = Not detectable because the bone district is present but disturbances compromise its diagnosis or if the bone district is missing
+1 = Present
†+2 = If the radiological analysis confirms skull vault thickness with destruction of external lamina and trabecular outgrowth (for Porotic Hyperostosis and Cribræ Orbitalia)
‡+3 = If the histologic analysis shows lateralization of trabeculae (for Porotic Hyperostosis and Cribræ Orbitalia)
* X-ray analysis required

Method for a preliminary diagnosis of β -thalassemia syndrome on archaeological human remains SSM 40

Indicators of β -thalassemia syndrome on skull	Degree of importance (X)	Assigned value (Y)	Results (X * Y)
Porotic Hyperostosis † ‡	1	-2	-2
Cribræ Orbitalia ‡	1	-1	-1
Hair on end*	3	-1	-3
Maxillary Hypertrophy	2		
	n° X¹ (max 4 values) = 3	-----	$\Sigma R^1 = -6$

Presence of β - thalassaemia on skull	$\frac{\Sigma R^1}{n^{\circ} X^1} = -6:3 = -2$	Positive Value result: possibly thalassaemia syndrome Negative Value result: absence of thalassaemia syndrome
---------------------------------------------	------------------------------------------------	------------------------------------------------------------------------------------------------------------------

Indicators of β -thalassemia syndrome on postcranial skeleton	Degree of importance (X)	Assigned value (Y)	Results (X * Y)
Growth arrest lines*	1		
Marrow hyperplasia	2		
Porosity of long bones	1		
Rib within a rib*	3		
Premature fusion of epiphyses of humerus	1		
Spine deformity (vertebral body)	2		
Enlarged foramina of Metacarpals	3		
	n° X² (max 7 values) =	-----	$\Sigma R^2 =$

Presence of β -thalassaemia on postcranial skeleton	$\frac{\Sigma R^2}{n^{\circ} X^2} =$	Positive Value result: possibly thalassaemia syndrome Negative Value result: absence of thalassaemia syndrome
-----------------------------------------------------------	--------------------------------------	------------------------------------------------------------------------------------------------------------------

Presence of β - thalassaemia on skeleton		
Σ total	$\frac{\Sigma R^1 + \Sigma R^2}{n^{\circ} X^1 + n^{\circ} X^2} =$	Positive Value result: possibly thalassaemia syndrome Negative Value result: absence of thalassaemia syndrome

Legenda:

Degree of importance (X):
1 = Nonspecific indicator present also in β - thalassaemia syndrome
2 = Complementary indicator suggesting β - thalassaemia/ not-diagnostic
3 = β - thalassaemia syndrome prevalent indicator/ Diagnostic

Value of interest (Y):
‡-3 = If the histologic analysis doesn't show lateralization of trabeculae (for Porotic Hyperostosis and Cribræ Orbitalia)
†-2 = If the radiological analysis denies skull vault thickness with destruction of external lamina and trabecular outgrowth (for Porotic Hyperostosis and Cribræ Orbitalia)
-1 = Not present
“empty field” = Not detectable because the bone district is present but disturbances compromise its diagnosis or if the bone district is missing
+1 = Present
†+2 = If the radiological analysis confirms skull vault thickness with destruction of external lamina and trabecular outgrowth (for Porotic Hyperostosis and Cribræ Orbitalia)
‡+3 = If the histologic analysis shows lateralization of trabeculae (for Porotic Hyperostosis and Cribræ Orbitalia)

*X-ray analysis required

Method for a preliminary diagnosis of β -thalassemia syndrome on archaeological human remains SSM 42

Indicators of β -thalassemia syndrome on skull	Degree of importance (X)	Assigned value (Y)	Results (X * Y)
Porotic Hyperostosis † ‡	1	3	3
Cribræ Orbitalia ‡	1	3	3
Hair on end*	3	-1	-3
Maxillary Hypertrophy	2	-1	-2
	n° X¹ (max 4 values) = 4	-----	$\Sigma R^1 = 1$

Presence of β -thalassemia on skull	$\frac{\Sigma R^1}{n^{\circ} X^1} = 1:4 = 0,25$	Positive Value result: possibly thalassaemia syndrome
		Negative Value result: absence of thalassaemia syndrome

Indicators of β -thalassemia syndrome on postcranial skeleton	Degree of importance (X)	Assigned value (Y)	Results (X * Y)
Growth arrest lines*	1		
Marrow hyperplasia	2		
Porosity of long bones	1		
Rib within a rib*	3		
Premature fusion of epiphyses of humerus	1		
Spine deformity (vertebral body)	2		
Enlarged foramina of Metacarpals	3		
	n° X² (max 7 values)=	-----	$\Sigma R^2 =$

Presence of β -thalassemia on postcranial skeleton	$\frac{\Sigma R^2}{n^{\circ} X^2} =$	Positive Value result: possibly thalassaemia syndrome
		Negative Value result: absence of thalassaemia syndrome

Presence of β -thalassemia on skeleton		
Σ total	$\frac{\Sigma R^1 + \Sigma R^2}{n^{\circ} X^1 + n^{\circ} X^2} =$	Positive Value result: possibly thalassaemia syndrome Negative Value result: absence of thalassaemia syndrome

Legenda:

Degree of importance (X):
1 = Nonspecific indicator present also in β -thalassaemia syndrome
2 = Complementary indicator suggesting β -thalassaemia/ not-diagnostic
3 = β -thalassaemia syndrome prevalent indicator/ Diagnostic

Value of interest (Y):
‡-3 = If the histologic analysis doesn't show lateralization of trabeculae (for Porotic Hyperostosis and Cribræ Orbitalia)
†-2 = If the radiological analysis denies skull vault thickness with destruction of external lamina and trabecular outgrowth (for Porotic Hyperostosis and Cribræ Orbitalia)
-1 = Not present
"empty field" = Not detectable because the bone district is present but disturbances compromise its diagnosis or if the bone district is missing
+1 = Present
†+2 = If the radiological analysis confirms skull vault thickness with destruction of external lamina and trabecular outgrowth (for Porotic Hyperostosis and Cribræ Orbitalia)
‡+3 = If the histologic analysis shows lateralization of trabeculae (for Porotic Hyperostosis and Cribræ Orbitalia)
* X-ray analysis required

Method for a preliminary diagnosis of β -thalassemia syndrome on archaeological human remains SSM 51

Indicators of β -thalassemia syndrome on skull	Degree of importance (X)	Assigned value (Y)	Results (X * Y)
Porotic Hyperostosis † ‡	1	1	1
Cribræ Orbitalia ‡	1	-1	-1
Hair on end*	3	-1	-3
Maxillary Hypertrophy	2	1	2
	n° X¹ (max 4 values) = 4	-----	$\Sigma R^1 = -1$

Presence of β - thalassaemia on skull	$\frac{\Sigma R^1}{n^{\circ} X^1} = -1:4 = -0,25$	Positive Value result: possibly thalassaemia syndrome Negative Value result: absence of thalassaemia syndrome

Indicators of β -thalassemia syndrome on postcranial skeleton	Degree of importance (X)	Assigned value (Y)	Results (X * Y)
Growth arrest lines*	1		
Marrow hyperplasia	2		
Porosity of long bones	1		
Rib within a rib*	3		
Premature fusion of epiphyses of humerus	1		
Spine deformity (vertebral body)	2		
Enlarged foramina of Metacarpals	3		
	n° X² (max 7 values) =	-----	$\Sigma R^2 =$

Presence of β -thalassaemia on postcranial skeleton	$\frac{\Sigma R^2}{n^{\circ} X^2} =$	Positive Value result: possibly thalassaemia syndrome Negative Value result: absence of thalassaemia syndrome

Presence of β - thalassaemia on skeleton		
Σ total	$\frac{\Sigma R^1 + \Sigma R^2}{n^{\circ} X^1 + n^{\circ} X^2} =$	Positive Value result: possibly thalassaemia syndrome Negative Value result: absence of thalassaemia syndrome

Legenda:

Degree of importance (X):
1 = Nonspecific indicator present also in β - thalassaemia syndrome
2 = Complementary indicator suggesting β - thalassaemia/ not-diagnostic
3 = β - thalassaemia syndrome prevalent indicator/ Diagnostic

Value of interest (Y):
‡-3 = If the histologic analysis doesn't show lateralization of trabeculae (for Porotic Hyperostosis and Cribræ Orbitalia)
†-2 = If the radiological analysis denies skull vault thickness with destruction of external lamina and trabecular outgrowth (for Porotic Hyperostosis and Cribræ Orbitalia)
-1 = Not present
“empty field” = Not detectable because the bone district is present but disturbances compromise its diagnosis or if the bone district is missing
+1 = Present
†+2 = If the radiological analysis confirms skull vault thickness with destruction of external lamina and trabecular outgrowth (for Porotic Hyperostosis and Cribræ Orbitalia)
‡+3 = If the histologic analysis shows lateralization of trabeculae (for Porotic Hyperostosis and Cribræ Orbitalia)

*X-ray analysis required

Method for a preliminary diagnosis of β -thalassemia syndrome on archaeological human remains SSM 57

Indicators of β -thalassemia syndrome on skull	Degree of importance (X)	Assigned value (Y)	Results (X * Y)
Porotic Hyperostosis † ‡	1	2	2
Cribræ Orbitalia ‡	1	1	1
Hair on end*	3	-1	-3
Maxillary Hypertrophy	2	1	2
	n° X¹ (max 4 values) = 4	-----	Σ R¹ = 2

Presence of β -thalassemia on skull	$\frac{\Sigma R^1}{n^\circ X^1} = 2:4 = 0,5$	Positive Value result: possibly thalassaemia syndrome
		Negative Value result: absence of thalassaemia syndrome

Indicators of β -thalassemia syndrome on postcranial skeleton	Degree of importance (X)	Assigned value (Y)	Results (X * Y)
Growth arrest lines*	1		
Marrow hyperplasia	2		
Porosity of long bones	1		
Rib within a rib*	3		
Premature fusion of epiphyses of humerus	1		
Spine deformity (vertebral body)	2		
Enlarged foramina of Metacarpals	3		
	n° X² (max 7 values)=	-----	Σ R² =

Presence of β -thalassemia on postcranial skeleton	$\frac{\Sigma R^2}{n^\circ X^2} =$	Positive Value result: possibly thalassaemia syndrome
		Negative Value result: absence of thalassaemia syndrome

Presence of β -thalassemia on skeleton		
Σ total	$\frac{\Sigma R^1 + \Sigma R^2}{n^\circ X^1 + n^\circ X^2} =$	Positive Value result: possibly thalassaemia syndrome Negative Value result: absence of thalassaemia syndrome

Legenda:

Degree of importance (X):
1 = Nonspecific indicator present also in β -thalassaemia syndrome
2 = Complementary indicator suggesting β -thalassaemia/ not-diagnostic
3 = β -thalassaemia syndrome prevalent indicator/ Diagnostic

Value of interest (Y):
‡-3 = If the histologic analysis doesn't show lateralization of trabeculae (for Porotic Hyperostosis and Cribræ Orbitalia)
†-2 = If the radiological analysis denies skull vault thickness with destruction of external lamina and trabecular outgrowth (for Porotic Hyperostosis and Cribræ Orbitalia)
-1 = Not present
"empty field" = Not detectable because the bone district is present but disturbances compromise its diagnosis or if the bone district is missing
+1 = Present
†+2 = If the radiological analysis confirms skull vault thickness with destruction of external lamina and trabecular outgrowth (for Porotic Hyperostosis and Cribræ Orbitalia)
‡+3 = If the histologic analysis shows lateralization of trabeculae (for Porotic Hyperostosis and Cribræ Orbitalia)
* X-ray analysis required

Method for a preliminary diagnosis of β -thalassemia syndrome on archaeological human remains SSM 58

Indicators of β -thalassemia syndrome on skull	Degree of importance (X)	Assigned value (Y)	Results (X * Y)
Porotic Hyperostosis † ‡	1	2	2
Cribræ Orbitalia ‡	1	3	3
Hair on end*	3	-1	-3
Maxillary Hypertrophy	2		
	n° X¹ (max 4 values) = 3	-----	Σ R¹ = 2

Presence of β - thalassaemia on skull	$\frac{\Sigma R^1}{n^{\circ} X^1} = 2:3 = 0,66$	Positive Value result: possibly thalassaemia syndrome
		Negative Value result: absence of thalassaemia syndrome

Indicators of β -thalassemia syndrome on postcranial skeleton	Degree of importance (X)	Assigned value (Y)	Results (X * Y)
Growth arrest lines*	1		
Marrow hyperplasia	2		
Porosity of long bones	1		
Rib within a rib*	3		
Premature fusion of epiphyses of humerus	1		
Spine deformity (vertebral body)	2		
Enlarged foramina of Metacarpals	3		
	n° X² (max 7 values) =	-----	Σ R² =

Presence of β -thalassaemia on postcranial skeleton	$\frac{\Sigma R^2}{n^{\circ} X^2} =$	Positive Value result: possibly thalassaemia syndrome
		Negative Value result: absence of thalassaemia syndrome

Presence of β - thalassaemia on skeleton		
Σ total	$\frac{\Sigma R^1 + \Sigma R^2}{n^{\circ} X^1 + n^{\circ} X^2} =$	Positive Value result: possibly thalassaemia syndrome
		Negative Value result: absence of thalassaemia syndrome

Legenda:

Degree of importance (X):
1 = Nonspecific indicator present also in β - thalassaemia syndrome
2 = Complementary indicator suggesting β - thalassaemia/ not-diagnostic
3 = β - thalassaemia syndrome prevalent indicator/ Diagnostic

Value of interest (Y):
‡-3 = If the histologic analysis doesn't show lateralization of trabeculae (for Porotic Hyperostosis and Cribræ Orbitalia)
†-2 = If the radiological analysis denies skull vault thickness with destruction of external lamina and trabecular outgrowth (for Porotic Hyperostosis and Cribræ Orbitalia)
-1 = Not present
“empty field” = Not detectable because the bone district is present but disturbances compromise its diagnosis or if the bone district is missing
+1 = Present
†+2 = If the radiological analysis confirms skull vault thickness with destruction of external lamina and trabecular outgrowth (for Porotic Hyperostosis and Cribræ Orbitalia)
‡+3 = If the histologic analysis shows lateralization of trabeculae (for Porotic Hyperostosis and Cribræ Orbitalia)

*X-ray analysis required

Method for a preliminary diagnosis of β -thalassemia syndrome on archaeological human remains SSM 68

Indicators of β -thalassemia syndrome on skull	Degree of importance (X)	Assigned value (Y)	Results (X * Y)
Porotic Hyperostosis † ‡	1	2	2
Cribræ Orbitalia ‡	1	3	3
Hair on end*	3	-1	-3
Maxillary Hypertrophy	2		
	$n^{\circ} X^1$ (max 4 values) = 3	-----	$\Sigma R^1 = 2$

Presence of β -thalassemia on skull	$\frac{\Sigma R^1}{n^{\circ} X^1} = 2:3 = 0,66$	Positive Value result: possibly thalassaemia syndrome
		Negative Value result: absence of thalassaemia syndrome

Indicators of β -thalassemia syndrome on postcranial skeleton	Degree of importance (X)	Assigned value (Y)	Results (X * Y)
Growth arrest lines*	1		
Marrow hyperplasia	2		
Porosity of long bones	1		
Rib within a rib*	3		
Premature fusion of epiphyses of humerus	1		
Spine deformity (vertebral body)	2		
Enlarged foramina of Metacarpals	3		
	$n^{\circ} X^2$ (max 7 values)=	-----	$\Sigma R^2 =$

Presence of β -thalassemia on postcranial skeleton	$\frac{\Sigma R^2}{n^{\circ} X^2} =$	Positive Value result: possibly thalassaemia syndrome
		Negative Value result: absence of thalassaemia syndrome

Presence of β -thalassemia on skeleton		
Σ total	$\frac{\Sigma R^1 + \Sigma R^2}{n^{\circ} X^1 + n^{\circ} X^2} =$	Positive Value result: possibly thalassaemia syndrome
		Negative Value result: absence of thalassaemia syndrome

Legenda:

Degree of importance (X):
1 = Nonspecific indicator present also in β -thalassaemia syndrome
2 = Complementary indicator suggesting β -thalassaemia/ not-diagnostic
3 = β -thalassaemia syndrome prevalent indicator/ Diagnostic

Value of interest (Y):
‡-3 = If the histologic analysis doesn't show lateralization of trabeculae (for Porotic Hyperostosis and Cribræ Orbitalia)
†-2 = If the radiological analysis denies skull vault thickness with destruction of external lamina and trabecular outgrowth (for Porotic Hyperostosis and Cribræ Orbitalia)
-1 = Not present
"empty field" = Not detectable because the bone district is present but disturbances compromise its diagnosis or if the bone district is missing
+1 = Present
†+2 = If the radiological analysis confirms skull vault thickness with destruction of external lamina and trabecular outgrowth (for Porotic Hyperostosis and Cribræ Orbitalia)
‡+3 = If the histologic analysis shows lateralization of trabeculae (for Porotic Hyperostosis and Cribræ Orbitalia)
* X-ray analysis required

Method for a preliminary diagnosis of β -thalassemia syndrome on archaeological human remains SSM 70

Indicators of β -thalassemia syndrome on skull	Degree of importance (X)	Assigned value (Y)	Results (X * Y)
Porotic Hyperostosis † ‡	1	3	3
Cribræ Orbitalia ‡	1	-1	-1
Hair on end*	3	-1	-3
Maxillary Hypertrophy	2		
	n° X¹ (max 4 values) = 3	-----	$\Sigma R^1 = -1$

Presence of β - thalassaemia on skull	$\frac{\Sigma R^1}{n^{\circ} X^1} = -1:3 = -0,33$	Positive Value result: possibly thalassaemia syndrome Negative Value result: absence of thalassaemia syndrome

Indicators of β -thalassemia syndrome on postcranial skeleton	Degree of importance (X)	Assigned value (Y)	Results (X * Y)
Growth arrest lines*	1		
Marrow hyperplasia	2		
Porosity of long bones	1		
Rib within a rib*	3		
Premature fusion of epiphyses of humerus	1		
Spine deformity (vertebral body)	2		
Enlarged foramina of Metacarpals	3		
	n° X² (max 7 values) =	-----	$\Sigma R^2 =$

Presence of β -thalassaemia on postcranial skeleton	$\frac{\Sigma R^2}{n^{\circ} X^2} =$	Positive Value result: possibly thalassaemia syndrome Negative Value result: absence of thalassaemia syndrome

Presence of β - thalassaemia on skeleton		
Σ total	$\frac{\Sigma R^1 + \Sigma R^2}{n^{\circ} X^1 + n^{\circ} X^2} =$	Positive Value result: possibly thalassaemia syndrome Negative Value result: absence of thalassaemia syndrome

Legenda:

Degree of importance (X):
1 = Nonspecific indicator present also in β - thalassaemia syndrome
2 = Complementary indicator suggesting β - thalassaemia/ not-diagnostic
3 = β - thalassaemia syndrome prevalent indicator/ Diagnostic

Value of interest (Y):
‡-3 = If the histologic analysis doesn't show lateralization of trabeculae (for Porotic Hyperostosis and Cribræ Orbitalia)
†-2 = If the radiological analysis denies skull vault thickness with destruction of external lamina and trabecular outgrowth (for Porotic Hyperostosis and Cribræ Orbitalia)
-1 = Not present
“empty field” = Not detectable because the bone district is present but disturbances compromise its diagnosis or if the bone district is missing
+1 = Present
†+2 = If the radiological analysis confirms skull vault thickness with destruction of external lamina and trabecular outgrowth (for Porotic Hyperostosis and Cribræ Orbitalia)
‡+3 = If the histologic analysis shows lateralization of trabeculae (for Porotic Hyperostosis and Cribræ Orbitalia)

*X-ray analysis required

Method for a preliminary diagnosis of β -thalassemia syndrome on archaeological human remains SSM75

Indicators of β -thalassemia syndrome on skull	Degree of importance (X)	Assigned value (Y)	Results (X * Y)
Porotic Hyperostosis † ‡	1	2	2
Cribræ Orbitalia ‡	1	2	2
Hair on end*	3		
Maxillary Hypertrophy	2	-1	-2
	n° X¹ (max 4 values) = 3	-----	$\Sigma R^1 = 2$

Presence of β -thalassemia on skull	$\frac{\Sigma R^1}{n^\circ X^1} = 2:3 = 0,66$	Positive Value result: possibly thalassaemia syndrome
		Negative Value result: absence of thalassaemia syndrome

Indicators of β -thalassemia syndrome on postcranial skeleton	Degree of importance (X)	Assigned value (Y)	Results (X * Y)
Growth arrest lines*	1		
Marrow hyperplasia	2		
Porosity of long bones	1		
Rib within a rib*	3		
Premature fusion of epiphyses of humerus	1		
Spine deformity (vertebral body)	2		
Enlarged foramina of Metacarpals	3		
	n° X² (max 7 values)=	-----	$\Sigma R^2 =$

Presence of β -thalassemia on postcranial skeleton	$\frac{\Sigma R^2}{n^\circ X^2} =$	Positive Value result: possibly thalassaemia syndrome
		Negative Value result: absence of thalassaemia syndrome

Presence of β -thalassemia on skeleton		
Σ total	$\frac{\Sigma R^1 + \Sigma R^2}{n^\circ X^1 + n^\circ X^2} =$	Positive Value result: possibly thalassaemia syndrome Negative Value result: absence of thalassaemia syndrome

Legenda:

Degree of importance (X):
1 = Nonspecific indicator present also in β -thalassaemia syndrome
2 = Complementary indicator suggesting β -thalassaemia/ not-diagnostic
3 = β -thalassaemia syndrome prevalent indicator/ Diagnostic

Value of interest (Y):
‡-3 = If the histologic analysis doesn't show lateralization of trabeculae (for Porotic Hyperostosis and Cribræ Orbitalia)
†-2 = If the radiological analysis denies skull vault thickness with destruction of external lamina and trabecular outgrowth (for Porotic Hyperostosis and Cribræ Orbitalia)
-1 = Not present
"empty field" = Not detectable because the bone district is present but disturbances compromise its diagnosis or if the bone district is missing
+1 = Present
†+2 = If the radiological analysis confirms skull vault thickness with destruction of external lamina and trabecular outgrowth (for Porotic Hyperostosis and Cribræ Orbitalia)
‡+3 = If the histologic analysis shows lateralization of trabeculae (for Porotic Hyperostosis and Cribræ Orbitalia)
* X-ray analysis required

Method for a preliminary diagnosis of β -thalassemia syndrome on archaeological human remains SSM 76

Indicators of β -thalassemia syndrome on skull	Degree of importance (X)	Assigned value (Y)	Results (X * Y)
Porotic Hyperostosis † ‡	1	2	2
Cribræ Orbitalia ‡	1	1	1
Hair on end*	3	-1	-3
Maxillary Hypertrophy	2		
	n° X¹ (max 4 values) = 3	-----	$\Sigma R^1 = 0$

Presence of β - thalassaemia on skull	$\frac{\Sigma R^1}{n^{\circ} X^1} = 0$	Positive Value result: possibly thalassaemia syndrome
		Negative Value result: absence of thalassaemia syndrome

Indicators of β -thalassemia syndrome on postcranial skeleton	Degree of importance (X)	Assigned value (Y)	Results (X * Y)
Growth arrest lines*	1		
Marrow hyperplasia	2		
Porosity of long bones	1		
Rib within a rib*	3		
Premature fusion of epiphyses of humerus	1		
Spine deformity (vertebral body)	2		
Enlarged foramina of Metacarpals	3		
	n° X² (max 7 values)=	-----	$\Sigma R^2 =$

Presence of β -thalassaemia on postcranial skeleton	$\frac{\Sigma R^2}{n^{\circ} X^2} =$	Positive Value result: possibly thalassaemia syndrome
		Negative Value result: absence of thalassaemia syndrome

Presence of β -thalassaemia on skeleton		
Σ total	$\frac{\Sigma R^1 + \Sigma R^2}{n^{\circ} X^1 + n^{\circ} X^2} =$	Positive Value result: possibly thalassaemia syndrome
		Negative Value result: absence of thalassaemia syndrome

Legenda:

Degree of importance (X):
1 = Nonspecific indicator present also in β - thalassaemia syndrome
2 = Complementary indicator suggesting β - thalassaemia/ not-diagnostic
3 = β - thalassaemia syndrome prevalent indicator/ Diagnostic

Value of interest (Y):
‡-3 = If the histologic analysis doesn't show lateralization of trabeculae (for Porotic Hyperostosis and Cribræ Orbitalia)
†-2 = If the radiological analysis denies skull vault thickness with destruction of external lamina and trabecular outgrowth (for Porotic Hyperostosis and Cribræ Orbitalia)
-1 = Not present
“empty field”= Not detectable because the bone district is present but disturbances compromise its diagnosis or if the bone district is missing
+1 = Present
†+2 = If the radiological analysis confirms skull vault thickness with destruction of external lamina and trabecular outgrowth (for Porotic Hyperostosis and Cribræ Orbitalia)
‡+3 = If the histologic analysis shows lateralization of trabeculae (for Porotic Hyperostosis and Cribræ Orbitalia)

*X-ray analysis required

Method for a preliminary diagnosis of β -thalassemia syndrome on archaeological human remains SSM 77

Indicators of β -thalassemia syndrome on skull	Degree of importance (X)	Assigned value (Y)	Results (X * Y)
Porotic Hyperostosis † ‡	1	2	2
Cribræ Orbitalia ‡	1	-1	-1
Hair on end*	3	-1	-3
Maxillary Hypertrophy	2		
	n° X¹ (max 4 values) = 3	-----	$\Sigma R^1 = -2$

Presence of β -thalassemia on skull	$\frac{\Sigma R^1}{n^\circ X^1} = -2:3 = -0,66$	Positive Value result: possibly thalassaemia syndrome Negative Value result: absence of thalassaemia syndrome

Indicators of β -thalassemia syndrome on postcranial skeleton	Degree of importance (X)	Assigned value (Y)	Results (X * Y)
Growth arrest lines*	1		
Marrow hyperplasia	2		
Porosity of long bones	1		
Rib within a rib*	3		
Premature fusion of epiphyses of humerus	1		
Spine deformity (vertebral body)	2		
Enlarged foramina of Metacarpals	3		
	n° X² (max 7 values)=	-----	$\Sigma R^2 =$

Presence of β -thalassemia on postcranial skeleton	$\frac{\Sigma R^2}{n^\circ X^2} =$	Positive Value result: possibly thalassaemia syndrome Negative Value result: absence of thalassaemia syndrome

Presence of β -thalassemia on skeleton		
Σ total	$\frac{\Sigma R^1 + \Sigma R^2}{n^\circ X^1 + n^\circ X^2} =$	Positive Value result: possibly thalassaemia syndrome Negative Value result: absence of thalassaemia syndrome

Legenda:

Degree of importance (X):
1 = Nonspecific indicator present also in β -thalassaemia syndrome
2 = Complementary indicator suggesting β -thalassaemia/ not-diagnostic
3 = β -thalassaemia syndrome prevalent indicator/ Diagnostic

Value of interest (Y):
‡-3 = If the histologic analysis doesn't show lateralization of trabeculae (for Porotic Hyperostosis and Cribræ Orbitalia)
†-2 = If the radiological analysis denies skull vault thickness with destruction of external lamina and trabecular outgrowth (for Porotic Hyperostosis and Cribræ Orbitalia)
-1 = Not present
"empty field" = Not detectable because the bone district is present but disturbances compromise its diagnosis or if the bone district is missing
+1 = Present
†+2 = If the radiological analysis confirms skull vault thickness with destruction of external lamina and trabecular outgrowth (for Porotic Hyperostosis and Cribræ Orbitalia)
‡+3 = If the histologic analysis shows lateralization of trabeculae (for Porotic Hyperostosis and Cribræ Orbitalia)
* X-ray analysis required

Method for a preliminary diagnosis of β -thalassemia syndrome on archaeological human remains SSM 79

Indicators of β -thalassemia syndrome on skull	Degree of importance (X)	Assigned value (Y)	Results (X * Y)
Porotic Hyperostosis † ‡	1	2	2
Cribræ Orbitalia ‡	1	1	1
Hair on end*	3	-1	-3
Maxillary Hypertrophy	2	-1	-2
	n° X¹ (max 4 values) = 4	-----	$\Sigma R^1 = -2$

Presence of β - thalassaemia on skull	$\frac{\Sigma R^1}{n^{\circ} X^1} = -2:4 = -0,5$	Positive Value result: possibly thalassaemia syndrome Negative Value result: absence of thalassaemia syndrome

Indicators of β -thalassemia syndrome on postcranial skeleton	Degree of importance (X)	Assigned value (Y)	Results (X * Y)
Growth arrest lines*	1		
Marrow hyperplasia	2		
Porosity of long bones	1		
Rib within a rib*	3		
Premature fusion of epiphyses of humerus	1		
Spine deformity (vertebral body)	2		
Enlarged foramina of Metacarpals	3		
	n° X² (max 7 values)=	-----	$\Sigma R^2 =$

Presence of β -thalassaemia on postcranial skeleton	$\frac{\Sigma R^2}{n^{\circ} X^2} =$	Positive Value result: possibly thalassaemia syndrome Negative Value result: absence of thalassaemia syndrome

Presence of β -thalassaemia on skeleton		
Σ total	$\frac{\Sigma R^1 + \Sigma R^2}{n^{\circ} X^1 + n^{\circ} X^2} =$	Positive Value result: possibly thalassaemia syndrome Negative Value result: absence of thalassaemia syndrome

Legenda:

Degree of importance (X):
1 = Nonspecific indicator present also in β - thalassaemia syndrome
2 = Complementary indicator suggesting β - thalassaemia/ not-diagnostic
3 = β - thalassaemia syndrome prevalent indicator/ Diagnostic

Value of interest (Y):
‡-3 = If the histologic analysis doesn't show lateralization of trabeculae (for Porotic Hyperostosis and Cribræ Orbitalia)
†-2 = If the radiological analysis denies skull vault thickness with destruction of external lamina and trabecular outgrowth (for Porotic Hyperostosis and Cribræ Orbitalia)
-1 = Not present
“empty field”= Not detectable because the bone district is present but disturbances compromise its diagnosis or if the bone district is missing
+1 = Present
†+2 = If the radiological analysis confirms skull vault thickness with destruction of external lamina and trabecular outgrowth (for Porotic Hyperostosis and Cribræ Orbitalia)
‡+3 = If the histologic analysis shows lateralization of trabeculae (for Porotic Hyperostosis and Cribræ Orbitalia)

*X-ray analysis required

Method for a preliminary diagnosis of β -thalassemia syndrome on archaeological human remains SSM 80

Indicators of β -thalassemia syndrome on skull	Degree of importance (X)	Assigned value (Y)	Results (X * Y)
Porotic Hyperostosis † ‡	1	2	2
Cribræ Orbitalia ‡	1	1	1
Hair on end*	3	-1	-3
Maxillary Hypertrophy	2	-1	-2
	n° X¹ (max 4 values) = 4	-----	$\Sigma R^1 = -2$

Presence of β -thalassemia on skull	$\frac{\Sigma R^1}{n^{\circ} X^1} = -2:4 = -0,5$	Positive Value result: possibly thalassemia syndrome
		Negative Value result: absence of thalassemia syndrome

Indicators of β -thalassemia syndrome on postcranial skeleton	Degree of importance (X)	Assigned value (Y)	Results (X * Y)
Growth arrest lines*	1		
Marrow hyperplasia	2		
Porosity of long bones	1		
Rib within a rib*	3		
Premature fusion of epiphyses of humerus	1		
Spine deformity (vertebral body)	2		
Enlarged foramina of Metacarpals	3		
	n° X² (max 7 values)=	-----	$\Sigma R^2 =$

Presence of β -thalassemia on postcranial skeleton	$\frac{\Sigma R^2}{n^{\circ} X^2} =$	Positive Value result: possibly thalassemia syndrome
		Negative Value result: absence of thalassemia syndrome

Presence of β -thalassemia on skeleton		
Σ total	$\frac{\Sigma R^1 + \Sigma R^2}{n^{\circ} X^1 + n^{\circ} X^2} =$	Positive Value result: possibly thalassemia syndrome Negative Value result: absence of thalassemia syndrome

Legenda:

Degree of importance (X):
1 = Nonspecific indicator present also in β -thalassemia syndrome
2 = Complementary indicator suggesting β -thalassemia/ not-diagnostic
3 = β -thalassaemia syndrome prevalent indicator/ Diagnostic

Value of interest (Y):
‡-3 = If the histologic analysis doesn't show lateralization of trabeculae (for Porotic Hyperostosis and Cribræ Orbitalia)
†-2 = If the radiological analysis denies skull vault thickness with destruction of external lamina and trabecular outgrowth (for Porotic Hyperostosis and Cribræ Orbitalia)
-1 = Not present
"empty field" = Not detectable because the bone district is present but disturbances compromise its diagnosis or if the bone district is missing
+1 = Present
†+2 = If the radiological analysis confirms skull vault thickness with destruction of external lamina and trabecular outgrowth (for Porotic Hyperostosis and Cribræ Orbitalia)
‡+3 = If the histologic analysis shows lateralization of trabeculae (for Porotic Hyperostosis and Cribræ Orbitalia)
* X-ray analysis required

Method for a preliminary diagnosis of β -thalassemia syndrome on archaeological human remains SSM 81

Indicators of β -thalassemia syndrome on skull	Degree of importance (X)	Assigned value (Y)	Results (X * Y)
Porotic Hyperostosis † ‡	1	3	3
Cribræ Orbitalia ‡	1	1	1
Hair on end*	3	-1	-3
Maxillary Hypertrophy	2		
	n° X¹ (max 4 values) = 3	-----	Σ R¹ = 1

Presence of β - thalassaemia on skull	$\frac{\Sigma R^1}{n^{\circ} X^1} = 1:3 = 0,33$	Positive Value result: possibly thalassaemia syndrome
		Negative Value result: absence of thalassaemia syndrome

Indicators of β -thalassemia syndrome on postcranial skeleton	Degree of importance (X)	Assigned value (Y)	Results (X * Y)
Growth arrest lines*	1		
Marrow hyperplasia	2		
Porosity of long bones	1		
Rib within a rib*	3		
Premature fusion of epiphyses of humerus	1		
Spine deformity (vertebral body)	2		
Enlarged foramina of Metacarpals	3		
	n° X² (max 7 values) =	-----	Σ R² =

Presence of β -thalassaemia on postcranial skeleton	$\frac{\Sigma R^2}{n^{\circ} X^2} =$	Positive Value result: possibly thalassaemia syndrome
		Negative Value result: absence of thalassaemia syndrome

Presence of β -thalassaemia on skeleton		
Σ total	$\frac{\Sigma R^1 + \Sigma R^2}{n^{\circ} X^1 + n^{\circ} X^2} =$	Positive Value result: possibly thalassaemia syndrome
		Negative Value result: absence of thalassaemia syndrome

Legenda:

Degree of importance (X):
1 = Nonspecific indicator present also in β - thalassaemia syndrome
2 = Complementary indicator suggesting β - thalassaemia/ not-diagnostic
3 = β - thalassaemia syndrome prevalent indicator/ Diagnostic

Value of interest (Y):
‡-3 = If the histologic analysis doesn't show lateralization of trabeculae (for Porotic Hyperostosis and Cribræ Orbitalia)
†-2 = If the radiological analysis denies skull vault thickness with destruction of external lamina and trabecular outgrowth (for Porotic Hyperostosis and Cribræ Orbitalia)
-1 = Not present
“empty field” = Not detectable because the bone district is present but disturbances compromise its diagnosis or if the bone district is missing
+1 = Present
†+2 = If the radiological analysis confirms skull vault thickness with destruction of external lamina and trabecular outgrowth (for Porotic Hyperostosis and Cribræ Orbitalia)
‡+3 = If the histologic analysis shows lateralization of trabeculae (for Porotic Hyperostosis and Cribræ Orbitalia)

*X-ray analysis required

Method for a preliminary diagnosis of β -thalassemia syndrome on archaeological human remains SSM 82

Indicators of β -thalassemia syndrome on skull	Degree of importance (X)	Assigned value (Y)	Results (X * Y)
Porotic Hyperostosis † ‡	1	2	2
Cribræ Orbitalia ‡	1		
Hair on end*	3	-1	-3
Maxillary Hypertrophy	2	-1	-2
	n° X¹ (max 4 values) = 4	-----	$\Sigma R^1 = -3$

Presence of β -thalassemia on skull	$\frac{\Sigma R^1}{n^{\circ} X^1} = -3:4 = -0,75$	Positive Value result: possibly thalassaemia syndrome Negative Value result: absence of thalassaemia syndrome

Indicators of β -thalassemia syndrome on postcranial skeleton	Degree of importance (X)	Assigned value (Y)	Results (X * Y)
Growth arrest lines*	1		
Marrow hyperplasia	2		
Porosity of long bones	1		
Rib within a rib*	3		
Premature fusion of epiphyses of humerus	1		
Spine deformity (vertebral body)	2		
Enlarged foramina of Metacarpals	3		
	n° X² (max 7 values)=	-----	$\Sigma R^2 =$

Presence of β -thalassemia on postcranial skeleton	$\frac{\Sigma R^2}{n^{\circ} X^2} =$	Positive Value result: possibly thalassaemia syndrome Negative Value result: absence of thalassaemia syndrome

Presence of β -thalassemia on skeleton		
Σ total	$\frac{\Sigma R^1 + \Sigma R^2}{n^{\circ} X^1 + n^{\circ} X^2} =$	Positive Value result: possibly thalassaemia syndrome Negative Value result: absence of thalassaemia syndrome

Legenda:

Degree of importance (X):
1 = Nonspecific indicator present also in β -thalassaemia syndrome
2 = Complementary indicator suggesting β -thalassaemia/ not-diagnostic
3 = β -thalassaemia syndrome prevalent indicator/ Diagnostic

Value of interest (Y):
‡-3 = If the histologic analysis doesn't show lateralization of trabeculae (for Porotic Hyperostosis and Cribræ Orbitalia)
†-2 = If the radiological analysis denies skull vault thickness with destruction of external lamina and trabecular outgrowth (for Porotic Hyperostosis and Cribræ Orbitalia)
-1 = Not present
"empty field" = Not detectable because the bone district is present but disturbances compromise its diagnosis or if the bone district is missing
+1 = Present
†+2 = If the radiological analysis confirms skull vault thickness with destruction of external lamina and trabecular outgrowth (for Porotic Hyperostosis and Cribræ Orbitalia)
‡+3 = If the histologic analysis shows lateralization of trabeculae (for Porotic Hyperostosis and Cribræ Orbitalia)
* X-ray analysis required

Method for a preliminary diagnosis of β -thalassemia syndrome on archaeological human remains SSM84

Indicators of β -thalassemia syndrome on skull	Degree of importance (X)	Assigned value (Y)	Results (X * Y)
Porotic Hyperostosis † ‡	1	2	2
Cribræ Orbitalia ‡	1	-1	-1
Hair on end*	3	-1	-3
Maxillary Hypertrophy	2		
	n° X¹ (max 4 values) = 3	-----	$\Sigma R^1 = -2$

Presence of β - thalassaemia on skull	$\frac{\Sigma R^1}{n^{\circ} X^1} = -2:3 = -0,66$	Positive Value result: possibly thalassaemia syndrome Negative Value result: absence of thalassaemia syndrome

Indicators of β -thalassemia syndrome on postcranial skeleton	Degree of importance (X)	Assigned value (Y)	Results (X * Y)
Growth arrest lines*	1		
Marrow hyperplasia	2		
Porosity of long bones	1		
Rib within a rib*	3		
Premature fusion of epiphyses of humerus	1		
Spine deformity (vertebral body)	2		
Enlarged foramina of Metacarpals	3		
	n° X² (max 7 values)=	-----	$\Sigma R^2 =$

Presence of β -thalassaemia on postcranial skeleton	$\frac{\Sigma R^2}{n^{\circ} X^2} =$	Positive Value result: possibly thalassaemia syndrome Negative Value result: absence of thalassaemia syndrome

Presence of β -thalassaemia on skeleton		
Σ total	$\frac{\Sigma R^1 + \Sigma R^2}{n^{\circ} X^1 + n^{\circ} X^2} =$	Positive Value result: possibly thalassaemia syndrome Negative Value result: absence of thalassaemia syndrome

Legenda:

Degree of importance (X):
1 = Nonspecific indicator present also in β - thalassaemia syndrome
2 = Complementary indicator suggesting β - thalassaemia/ not-diagnostic
3 = β - thalassaemia syndrome prevalent indicator/ Diagnostic

Value of interest (Y):
‡-3 = If the histologic analysis doesn't show lateralization of trabeculae (for Porotic Hyperostosis and Cribræ Orbitalia)
†-2 = If the radiological analysis denies skull vault thickness with destruction of external lamina and trabecular outgrowth (for Porotic Hyperostosis and Cribræ Orbitalia)
-1 = Not present
“empty field”= Not detectable because the bone district is present but disturbances compromise its diagnosis or if the bone district is missing
+1 = Present
†+2 = If the radiological analysis confirms skull vault thickness with destruction of external lamina and trabecular outgrowth (for Porotic Hyperostosis and Cribræ Orbitalia)
‡+3 = If the histologic analysis shows lateralization of trabeculae (for Porotic Hyperostosis and Cribræ Orbitalia)

*X-ray analysis required

Method for a preliminary diagnosis of β -thalassemia syndrome on archaeological human remains SSM 92

Indicators of β -thalassemia syndrome on skull	Degree of importance (X)	Assigned value (Y)	Results (X * Y)
Porotic Hyperostosis † ‡	1	3	3
Cribræ Orbitalia ‡	1	-1	-1
Hair on end*	3	-1	-1
Maxillary Hypertrophy	2		
	n° X¹ (max 4 values) = 3	-----	$\Sigma R^1 = 1$

Presence of β -thalassemia on skull	$\frac{\Sigma R^1}{n^{\circ} X^1} = 1:3 = 0,33$	Positive Value result: possibly thalassaemia syndrome
		Negative Value result: absence of thalassaemia syndrome

Indicators of β -thalassemia syndrome on postcranial skeleton	Degree of importance (X)	Assigned value (Y)	Results (X * Y)
Growth arrest lines*	1		
Marrow hyperplasia	2		
Porosity of long bones	1		
Rib within a rib*	3		
Premature fusion of epiphyses of humerus	1		
Spine deformity (vertebral body)	2		
Enlarged foramina of Metacarpals	3		
	n° X² (max 7 values) =	-----	$\Sigma R^2 =$

Presence of β -thalassemia on postcranial skeleton	$\frac{\Sigma R^2}{n^{\circ} X^2} =$	Positive Value result: possibly thalassaemia syndrome
		Negative Value result: absence of thalassaemia syndrome

Presence of β -thalassemia on skeleton		
Σ total	$\frac{\Sigma R^1 + \Sigma R^2}{n^{\circ} X^1 + n^{\circ} X^2} =$	Positive Value result: possibly thalassaemia syndrome Negative Value result: absence of thalassaemia syndrome

Legenda:

Degree of importance (X):
1 = Nonspecific indicator present also in β -thalassaemia syndrome
2 = Complementary indicator suggesting β -thalassaemia/ not-diagnostic
3 = β -thalassaemia syndrome prevalent indicator/ Diagnostic

Value of interest (Y):
‡-3 = If the histologic analysis doesn't show lateralization of trabeculae (for Porotic Hyperostosis and Cribræ Orbitalia)
†-2 = If the radiological analysis denies skull vault thickness with destruction of external lamina and trabecular outgrowth (for Porotic Hyperostosis and Cribræ Orbitalia)
-1 = Not present
"empty field" = Not detectable because the bone district is present but disturbances compromise its diagnosis or if the bone district is missing
+1 = Present
†+2 = If the radiological analysis confirms skull vault thickness with destruction of external lamina and trabecular outgrowth (for Porotic Hyperostosis and Cribræ Orbitalia)
‡+3 = If the histologic analysis shows lateralization of trabeculae (for Porotic Hyperostosis and Cribræ Orbitalia)
* X-ray analysis required

CHAPTER 3

HIDDEN FROM VIEW: THE SINGULAR DISCOVERY OF TWO HEAD TUMORS IN SKELETAL HUMAN REMAINS

Detection of neoplastic formation in human dry bones is quite uncommon. The reason of this rareness is, on one side, that only visible bone lesions can be detected on skeletons, and, on the other side, that the incidence of tumors in ancient populations was lower than nowadays. Possibly, different life habits of people (e.g. food, lifestyle), environmental factors and a shorter lifespan might be responsible for a lower cancer incidence in ancient times.

For all these reasons, the retrieval of two adult individuals (out of 68 from the necropolis of the St. Mamiliano Church, Sovana, Italy), who were affected by different osteolytic lesions, all attributable to neoplasia, represents a singular finding. The first individual showed a single lesion on the right frontal sinus, whereas the second two lesions, respectively on the right frontal sinus and on the internal lamina of the right parietal bone.

A differential retrospective diagnosis carried out with anthropological and histological methods has revealed an osteoma osteomata, a quite common slow-growing benign osteogenic lesion in the first individual, and an osteoblastoma, a rare bone-forming tumor that accounts for less than 14% of all bone tumors, in the second individual.

This evidence has not only a historical interest, it could also be useful in implementing modern oncological research to obtain new and additional information on the occurrence, spread and frequency of specific forms of cancer.

3.1 – Introduction

The development of neoplastic bone tissue is induced by a variety of elements (genetic susceptibility, lifestyle, environmental factors), and manifests as an uncontrolled growth of one of the tissues that makes up the osteogenic mesenchyme (bone, cartilage, fibrous tissue, blood vessels).

We can distinguish two types of tumor: *benign neoplasms*, which consist of well differentiated and localized neoplastic tissue, and *malignant tumors*, made up of poorly differentiated tissue that continues to grow without any control and has the potential to involve other tissues through blood vessels or the lymphatic system (Aufderheide and Rodríguez, 2000; Ortner, 2003).

Notoriously, the detection and identification of frontal sinus cancer in paleopathology occurs only incidentally, when the skull is broken, thus permitting the visual inspection of the internal areas, or when the skull is radiologically examined for other research purposes. In our case, pathological evidence of different etiology suggested an in-depth investigation of the endocranial bones by means of endoscopy and microscopy (Schultz, 1993, 2001; Wapler and Schultz, 1996).

We discovered, in two ancient individuals, tumors similar in appearance but different in their conformation. To correctly diagnose and differentiate them, we needed to take in consideration the type of bone tissue affected, the localization, and, in particular, the contingent connection with other diseases.

In addition to macroscopic observation, the application of additional scientific techniques allowed us to identify with confidence the two lesions and to provide a detailed description of the tumors, which are rarely reported in the paleo-oncologic field.

3.2 – Materials

The skeletons examined were retrieved in the complex of the Church of San Mamiliano (Sovana, Central-West-Italy) (Figure 3.1).

Historically, the Church of San Mamiliano was built on a pre-existing building of the Etruscan-Roman era (Burattini, 1997; Citter, 2002), which may be the most ancient edifice of the settlement Sovana. The complex of San Mamiliano is an archaeological site of great interest because it represents the entire stratigraphic sequence that characterized Sovana,

from prehistory to the Middle Ages and Renaissance (Figure 3.2) (Tondo et al., 2004; Tuci, 2008; Barbieri et al., 2012).



Figure 3.1 – Sovana (GR), Italy, and the complex of the Church of San Mamiliano (Ph®)¹.

During the first excavation, conducted in 1998, the archaeologists brought to light a complex of fifty-seven graves attributable to the 15th - 16th century (Tondo et al., 2004; Tuci, 2008). The human bones, a secondary deposition, were confused and distributed at different levels, embedded in a single layer of reddish-brown filling earth, and suggested a subsequent burial following an elder exhumation (Tondo et al., 2004; Tuci, 2008).



Figure 3.2 – Plan of the Church of San Mamiliano (Sovana, Italy). The floor is entirely occupied by burials. Underneath, the ruins of a Roman building (red) and of late antique structures (green) are visible.¹

¹ Barbieri G., Arcangeli L., Turchetti M. A., 2012, *Il tesoro ritrovato. Sovana: la sezione archeologica nella Chiesa di San Mamiliano*, Laurum Ed.

The two individuals with the neoplastic lesions were respectively represented by a 90% complete skull (inventory number: SSM 81. The splanchnocranium is missed), and a fragmented skull (inventory number: SSM 92).

3.3 – Methods

For both skulls, a careful anthropological analysis was performed using standard methods for the diagnosis of sex (Broca, 1975, Acsadi & Nemeskéri, 1970, WEA, 1980, Buikstra J. E., Ubelaker D. H., 1994), and estimation of age-at-death (Acsadi & Nemeskéri 1970, Meindl & Lovejoy, 1985).

Due to the incompleteness and fragmentary nature of the specimens, it was not possible to estimate with accuracy the biological profile of the two individuals, especially for SSM 92, due to the lack of diagnostic parts. Despite, we carried out an estimation of the possible age-at-death, doing our best according to the cited methods.

The identification of the pathological evidences was performed in accordance with the main literature in the field of paleopathology (Brothwell, 1981; Schajowicz, 1981; Aufderheide and Rodríguez, 2000; Ortner, 2003; Pinhasi and Mays, 2008; Fornaciari G. and Giuffra V., 2009; Kumar et al., 2011; Crowder and Stout, 2012; Mann and Hunt, 2015; Galliera and Romanelli, 2017; Galliera and Corsi Romanelli, 2018; Pilloud, 2018). For the analyses, we used different approaches such as morphology, radiology, endoscopy and microscopy.

Once identified the lesions, we collected samples from both skulls to generate “Thin Ground Sections” (TGSs) from macerated bone tissue, using the procedures proposed by Schultz in his studies (Schultz and Drommer, 1983; Schultz and Brandt, 1987; Schultz, 1988, 1993, 1994, 1997b; a, 2001, 2003; Schultz M, 1993; Wapler and Schultz, 1996; Schmidt-Schultz and Schultz, 2004; Schultz and Schmidt-Schultz, 2015). The goal was to investigate the histological structure of the bone lesions via light microscopy. We took samples in the area with the most characteristic morphological changes to include: (1) a healthy, nonaffected area, (2) an area with modestly developed changes, and (3) an area with severely pronounced changes (Schultz, 2001; Ortner, 2003; Crowder and Stout, 2012). This method is invasive and damage irreversibly the bone sample. Therefore, we carried out a restoration of the skulls at the end of the work. Microscopic analyses for the identification of the bone structure on 50µm and 70µm TGSs were carried out employing a microscopy with transmitted and polarized light (Leica DMRX Compound Polarised Light Microscope Image with Leica DFC 500 digital camera).

Radiological analyses of the skulls were carried out using a conventional X-Ray static machine for planar scans 24" SFD, (Hp Cabinet 43805n Faxitron System). The scan parameters of the X-ray beams were 70-130 kVp with a time of scanning of 5-7 minutes. Images data were transferred to ix-Pect EZ Software[©] for visual inspection.

Endoscopic examinations of the skulls were performed with a rigid light borescope with Canon 28 mm 1:1 conversion lens. The images were processed with IntraVison Capture Version.1.8[©].

All the analyses were carried out in the laboratory of, and in collaboration with, the Zentrum Anatomie, AG-Paläopathologie, of the Georg-August-Universität (Göttingen, Germany).

3.4 – Results

Both individuals examined were represented only by their skull, as their postcranial skeletons could not be identified in the context of the secondary deposition.

3.4.1 – SSM 81

The skull was in good condition (Figure 3.3), well-preserved with no deep diagenetic changes on the *lamina externa* except for a rounded *post mortem* abrasion on the right parietal (Figure 3.3 c red arrow). On the *lamina interna*, several traces due to the action of roots, and discoloration caused by a mixture of soil and water were observed. The splanocranium and the mandibula were missed.

The anthropological features of the skull let us argue that the individual was a male. The age-at-death was estimated to be 35-50 years, considering the obliteration status of the ectocranial sutures. From the anthropological analysis, several lesions of undetermined nature (e. g. inflammation of the cortical bone), were identified on both the parietal bones and on the frontal bone (Figure 3.3a), in particular on the glabella. Thus, we decided to perform radiological (Figure 3.4) and microscopic (TGS) (Figure 3.5) analyses for a more accurate diagnosis.

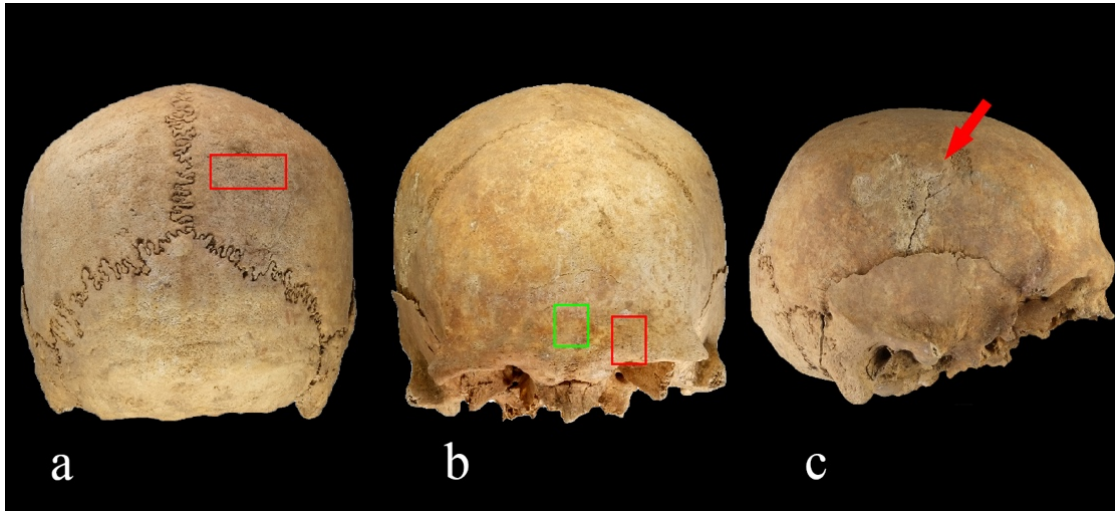


Figure 3.3 – Skull of Individual SSM 81: a) Posterior view: signs of inflammation of the cortical bone are present on both parietals. The red square shows the area where a sample was taken; b) Frontal view: the red square shows the area where the first sample was taken, the green one shows the place where the second sample was taken; c) Right lateral view: *post mortem* abrasion on the right parietal (red arrow) (Photo: Filippo Scianò).

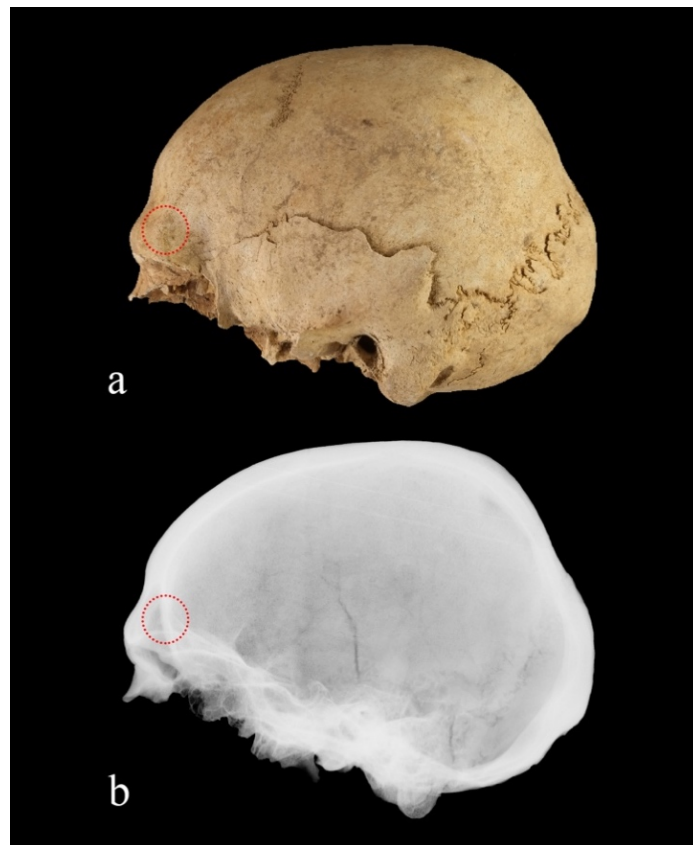


Figure 3.4 - Skull of Individual SSM 81: The Radiography (b) in left lateral view (a), shows the presence of the small teardrop-shaped new bone formation on the edge of the left frontal sinus (red circle) (Photo: Filippo Scianò).

Samples for the analyses were taken on the right parietal (39 x 17 mm) (Figure 3.3a red square) and on the frontal bone (19 x 16 mm) (Figure 3.3b red square) in the area of the lesions. After removing the sample from the frontal bone, we observed a small teardrop-shaped new bone formation on the edge of the left frontal sinus. Thus, we decided to collect a second sample from this area (15 x 12 mm) (Figure 3.3b green square). The samples were used to generate TGSs for the histologic analyses.

The radiological scanning confirms the presence of a small bone formation (6.4 mm in length and 2.7 mm in width) inside of the frontal sinus (Figure 3.4b red circle). The scan showed no other similar lesion on the calvaria.

From the microscopic perspective, the histology of the TGSs of the right parietal (Figure 3.5) confirmed the thickened and discontinuous shape of the *lamina externa*. Traces of inflammation of the periosteum were clearly recognizable. The cause may have been a localized and reabsorbed blunt force trauma or scalp inflammation. The diploe did not appear to be affected by any disease.

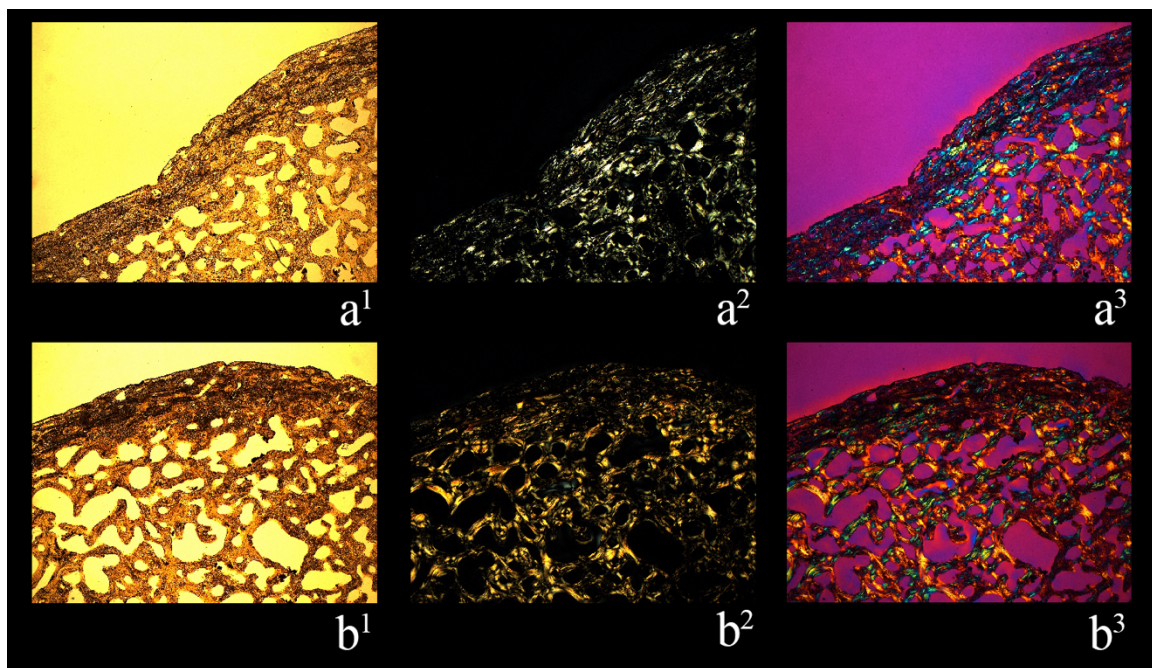


Figure 3.5 –TGSs of the right parietal from the skull of Individual SSM 81: **a¹**) microscopy of the cortical bone, which appears enlarged and irregular, and shows presence of periosteal inflammation (16x Magnification, 50µm and 70µm, transmitted light); **a²**) vision in polarized light; **a³**) vision in transmitted light and polarizing filter with quartz as compensator; **b¹**) microscopy of the cortical and trabecular bone. The external lamina appears thick with traces of blood vessel canals. The trabeculae are irregular but normal for the range of age-at-death of the individual; **b²**) vision in polarized light; **b³**) vision in transmitted light and polarizing filter with quartz as compensator (16x Magnification, 50µm and 70µm, transmitted light and polarizing filter with quartz as compensator) (Photo: Filippo Scianò).

The rarefaction of the trabecular tissue (Figure 3.6b¹) indicated that the individual was actually over 45 years of age. The *internal lamina* presented postmortal variations of diagenetic origin, primarily traces of roots and abrasion, which were not related with the frontal sinus lesion.

The TGS-histology of the frontal bone presented slight signs of taphonomic nature. Moreover, the surface of the *external lamina* was affected by an osteolytic reaction due to nonspecific chronic inflammatory processes, and appeared irregular and thickened with presence of blood vessel canals (Figure 3.6). The *internal lamina* presented normal signs of vascularization as well as diagenetic changes (e.g. exfoliation of the lamellar bone).

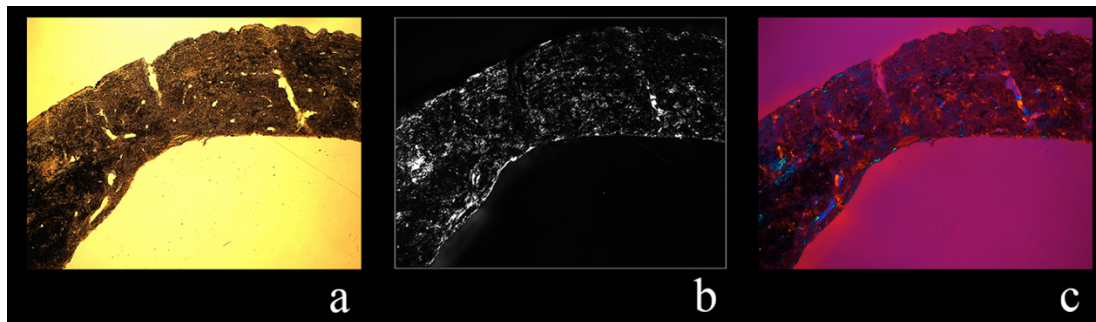


Figure 3.6 –TGS of the frontal bone from the skull of Individual SSM 81: **a)** microscopy of the cortical bone, which appears thickened due an osteolytic reaction of the bone. Some traces of diagenetic changes are present; **b)** vision in polarized light, post production in B&W; **c)** vision in transmitted light and polarizing filter with quartz as compensator (16x Magnification, 70 μ m) (Photo: Filippo Scianò).

At the deeper level, the examination of the TGS in the area of the tumor-like lesion is in progress.

3.4.2 – SSM 92

The skull of Individual 92 was fragmented and poor-preserved: only the frontal bone and a small part of the parietal bones were present (Figure 3.7). Diagenetic changes are visible on both surfaces of the internal and external lamina, represented by discoloration, exfoliation and porosity. Traces of pathological evidence were visible primarily on the frontal bone, where the *post mortem* fracture let us observe a small, globular new bone formation in the right frontal sinus (Figure 3.7a, white circle).

Another circumscribed pathological evidence was visible on the right parietal bone on both, the external and the internal lamina. From the outer surface, the lesion appeared irregular, rough and cribrotic. From the inner surface, instead, it appeared smooth and showed both, osteoblastic and osteolytic bone reaction (Figure 3.7b).

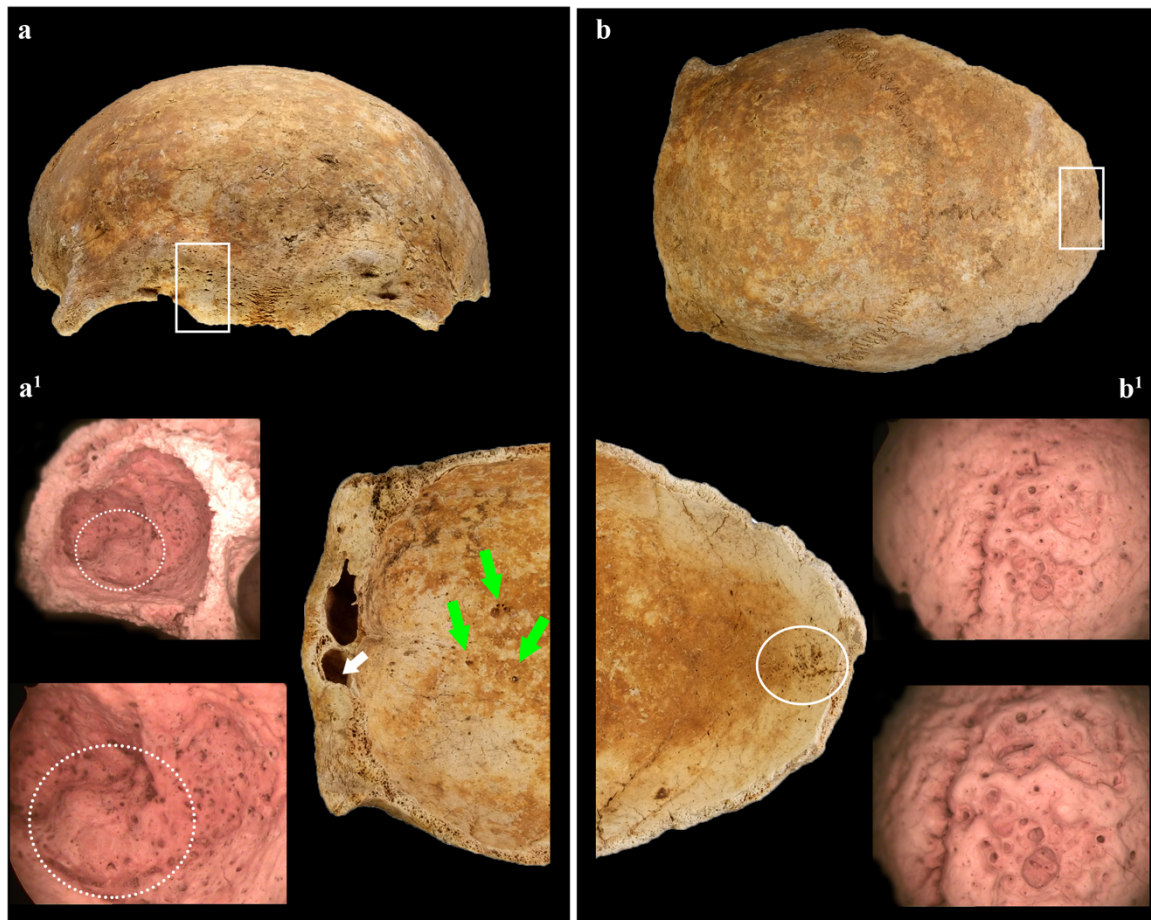


Figure 3.7 - Skull vault of Individual SSM 92: **a**) Area (white square), where a sample of the frontal bone was taken from; **a¹**) endoscopy of the frontal right sinus with the neoplastic lesion on the internal surface of the bone. Two level of magnification (10x & 20x) (white circles). Green arrows show the *fovea granulares*; The white narrow indicates the localization of the lesion in the frontal sinus; **b**) Norma superioris of the right parietal with the lesioned area, where the sample was taken (white square); **b¹**) magnified view (10x & 20x) of the area with the lesion which affects the lamina interna (white circle) (Photo: Filippo Scianò).

Moreover, multiple osteolytic lesions recognized as *fovea granulares*², interested the surface of the *lamina interna* along with the *sinus sagittalis superior*.

The poor conservation of the skull did not allow us to estimate the sex of the individual with confidence. On the other hand, the age-at-death of 35-50 years was approximated on the basis of the obliteration status of the ectocranial and endocranial sutures even if only the coronal, medio-coronal and the sagittal sutures were present.

² The *fovea granulares*, also called Pacchionian pits or arachnoid granulation are herniations of the thin, arachnoid membrane and are often located at the end of meningeal artery. They push through the inner table of the skull, and may appear as single pit, or as a cluster resembling grapes. This non pathological condition increases in size and number with age and it is often present in osteoarcheological sample (Aufderheide and Rodríguez, 2000; Ortner, 2003; Mann and Hunt, 2015).

As well as for the other individual, two cranial samples were taken, the first on the frontal bone (30 x 14 mm) and the second on the right parietal bone (41 x 14 mm).

From both perspective, macroscopic and microscopic, we could observe pathological changes. The microscopic structures of the TGS of the frontal bone (Figure 3.8a) showed a lamina externa thickened, compact and irregular, with a porous structure. Traces of periostosis were visible, while numerous blood vessel canals suggested a high vascularization of the area. The presence of vascularization and the rarefaction of the cortical bone also suggested the presence of a chronic inflammatory/infectious process, which involved the frontal sinus. The aspect of the bone was compatible with an untreated sinusitis. In connection, the structure of the diploe was affected by a slow-growing and repeated bone neoformation that compromised the normal conformation of the area (Figure 3.8b). The lesion, presumably a bone tumor, was highly developed (12.3 mm in length and 6.1 mm in width) and affected approximately 30% of the left frontal sinus.

The tumor-like lesion was well defined; it presented an external thin calcified layer, with well-defined wavy borders and a disorganized internal structure. However, the internal matrix showed absence of wide vascular spaces with lack of mature lamellar bone and poorly mineralized woven-bone trabeculae.

The lesion of the right parietal bone showed an organized structure (Figure 3.8c); it revealed relatively slight osteolytic processes with new built bone formations on the endocranial surface; a secondary remodeling of the diploe with new bone formations on the internal lamina with osteolytic lesions was visible along the side of the sagittal suture. Traces of inflammation of the endosteum were present. The lamina interna on the lesion's area was completely affected by a slow growing polster-like formation with multiple layers of young bone apposition, already developed in mature bone (Haversian systems are clearly visible). This condition may suggest a proliferative bone or a proliferative bone reaction due to a meningioma or a tumorous process, or due to the healing phase of a pathological condition (Schultz, 2001). As a rule, the vestiges of inflammatory process of the skull are more frequent in adult than in subadult individuals because of the higher competence of the immune system. The presence of the newly bone formation is characteristic of infectious diseases of the skull vault such as osteomyelitis or meningitis. Unfortunately, the severe taphonomic changes erased completely the external lamina of the bone, thus irreversibly compromising a differential diagnosis of this lesion.

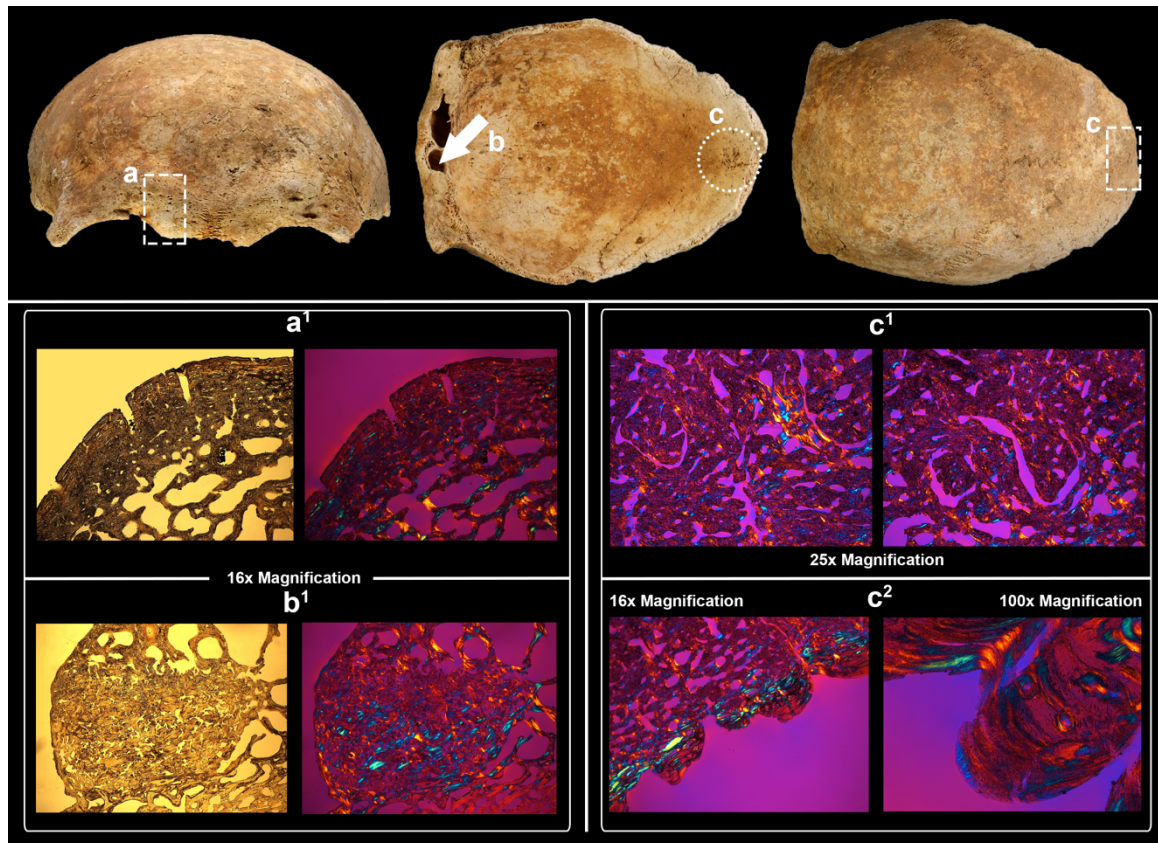


Figure 3.8 - Skull vault of Individual SSM 92: **a**) Sampling area of the right supraorbital margin taken for TGSs preparation (white square); **a¹**) microscopy of the cortical bone, which appears enlarged, sclerotic and ipervascularized (50 μ m, transmitted light and polarizing filter with quartz as compensator); **b**) TGS of the neoplastic lesion (white arrow); **b¹**) Partially globular new bone formation which involved the diploe (70 μ m, transmitted light and polarizing filter with quartz as compensator); **c**) TGS of the right parietal bone (white circle & white square); **c¹**) irregular and confused trabecular growth; **c²**) Slight osteolytic slow-growing lesion with multiple layers of new bone apposition which became mature bone (Haversian systems are present) (50 μ m and 70 μ m, polarizing filter with quartz as compensator) (Photo: Filippo Scianò).

3.5 – Differential diagnosis of the skull lesions found in the two individuals

The lesions of the frontal sinus described in this study displayed the characteristic of neoplastic bone formation. Both pathological evidences of the frontal bone had in common the manifestation of bone hypertrophy as a consequence of a chronic infection or of inflammation of the surrounding tissues (Alexander et al., 2007; Menezes & Davidson, 1994). From a microscopic perspective, the presence of vascularization and the enlargement of the cortical bone suggested a co-morbidity process which involved the frontal sinus, an untreated sinusitis or a non-specific osteitis in addition to the tumors. This condition could have been the outlier that caused the neoplastic onset. However, the two tumorous lesions showed a different histological structure.

A careful differential diagnosis of the most probable bone neo-formation affecting the skull, and especially the frontal sinus, was carried out (Table 3.1). For each pathology, several factors were taken into consideration for the diagnosis: tissue type affected, position in the skeleton, sex predilection and age-range of occurrence.

Table 3.1: Differential diagnosis carried out considering the most probable tumors affecting the skull

Tumor lesion	Arising location	Sex & Age of insurgence	Morphological features	SSM 81	SSM 92
Osteoma Benign Tumor	Skull: Frontal sinus	Prevalent in males (ratio 2.5:1)	Slow growth	✓	✓
			Dense immature bone structure	✓	x
	Long bones Spine	Age: 10-25 years (70%)	Expansive lesions with peripheral ossification	✓	✓
			Regular borders	✓	x
			Smooth surface	✓	x
			Globular shape	✓	✓
Osteoblastoma Benign Tumor	Long bones Spine	Prevalent in males (ratio 3:1)	Slow growth	✓	✓
			Poor mineralized woven bone structure	x	✓
	Skull: Frontal sinus (Rare)	Age: < 30 years	Expansive lesions with peripheral ossification	✓	✓
			Lysis and/or sclerosis	x	✓
			Wavy calcified borders	x	✓
			Globular shape	✓	✓
Cemento- Ossifying Fibroma (COF) Benign Tumor	Splanocranium	Prevalent in females (2.5:1)	Slow growth	✓	✓
			Haphazardly distributed lamellated bony spicules	x	x
		Age: < 25 years (in long bones); 30-40 years (splanocranium)	Fibrous tissue	x	x
			Calcified tissue resembling bone and/or cementum	x	✓
			Expansive lesions with peripheral ossification	✓	✓
			Central lucency	x	x

Continues from: Table 3.1: Differential diagnosis carried out considering the most probable tumors affecting the skull

Hemangioma	Skull Spine	Predominant in females	Thinning and expansion of the cortex	x	x
Benign Tumor	Chest Long bones (rare)	Age: >40 years	Sunburst like periosteal reaction	x	x
			Destruction and substitution of trabecular tissue	x	x
			“Sunburst” appearance	x	x
			Rounded shape	✓	✓
Osteosarcoma	Long bones Skull: Frontal sinus (Rare)	Prevalent in males (ratio 2:1)	Rapid growth	x	x
Malign Tumor		Age: 12-35 years	Aggressive infiltration	x	x
			Mixed of lytic and/or sclerotic tissue	x	✓
			“Sunburst” appearance	x	x
			Irregular and chaotic borders (different degree of density)	x	x
			Cloudy appearance	x	x
Metastatic Carcinoma	All skeleton	No sex predilection	High metastatic activity	x	x
		Age: >30 years old	Osteoblastic activity	x	x
Malign Tumor			Destructive margin	x	x

x= absence; ✓= presence

According to the morphological, radiographic and histologic features, and the biological profile presented in Table 3.1, the frontal lesion of Individual SSM 81 was compatible with the diagnosis of *osteoma*. This tumor is represented by a benign outgrowth of membranous dense, sclerotic, homogenous bone that mostly occurs in the skull. It is called homoplastic when it grows on bone, and heteroplastic when it grows on other tissues and is formed by osseous tissue with well-defined border (Pinhasi & Mays, 2008; Zileli et al., 2003). Histologically, the osteoid component and woven bone are connected to each other by trabeculae, while the bone that covers the lesion is dense and consists of a mix of woven and lamellar bone (Zileli et al., 2003; Galliera et al. 2018). The anatomical region of insurgence was compatible with the suggested diagnosis as well: in fact, clinical data confirm that the frontal sinus is the most affected of the paranasal sinuses (between 71.8% and 80% of cases) (Lehmer et al., 2012; Rokade and Sama, 2012; Sanchez Burgos et al., 2013; Riccomi et al., 2018b).

The others benign neoplasms were quite unlikely candidates, except for the osteoblastoma which share with the osteoma some morphological features. No other osteoma was present on both, the internal and the external surfaces of the skull, or in the cerebral and paranasal

sinuses. This condition allowed us to exclude the Gardner's Syndrome as a possible cause of the osteoma's onset (Alexander et al., 2007; Weidner, 2009; Lehmer et al., 2012).

On the other side, the malignant cancers considered would only be compatible with the estimated age, the sex of individual SSM 81 and the localization in the skeletal district. Yet, no other traces of metastatic focuses were present on the skull, and the lesion located on the lamina externa of the right parietal bone seemed to have a different etiology, distinct from a malign neoplastic lesion (Ragsdale et al., 2018). This lesion appeared porous with a morphology similar to that of a healed Porotic hyperostosis (Stuart-Macadam, 1987; Stuart-Macadam, 1987; Schultz, 2001; Ortner, 2003; Walker et al., 2009; Rinaldo et al., 2019), but differed from this for radiographical and histological features (Crowder and Stout, 2012; De Boer et al., 2013; de Boer and Maat, 2018). Traces of inflammation of the periosteum were present, possibly caused by non-specific and specific periostitis, osteitis, hematogenous osteomyelitis or osteomyelitis. Similar changes could have been caused by hemorrhagic reaction to a subperiosteal hematoma due to a traumatic event (Schultz, 1986, 1987a; b, 2003; Schultz M, 1993). Hemorrhagic modifications, in contrast to inflammatory processes, were only found external to the original bone surface. According to these observations, the most likely diagnosis suggested an healed process in consequence of a blunt force trauma occurred *intra-vitam*.

On the other hand, the characteristics of the frontal sinus lesions of Individual SSM 92 were compatible with an osteoma with osteoblastoma-like histology (Lehmer et al., 2012) or with an osteoblastoma. Osteoblastoma is a benign bone tumor accounting for 3.5% of all benign bone tumors and 1% of all bone neoplasms (Riccomi et al., 2018a). For its clinical and pathological manifestation, it is similar to an osteoid osteoma and it occurs usually in the second and third decade of life. Its preferential arising location is the axial skeleton and the vertebral column. Rarely, but it occurs also in the skull and especially in the frontal and ethmoid sinuses. At the growing site, osteoblastoma forms a well vascularized nidus composed by dense sclerotic woven bone trabeculae with an osteolytic, sclerotic and disorganized structure in connection with the surrounding bone (Weidner, 2009). The tumor has irregular borders forming a highly dense calcified tissue, as a shell. As resumed in Table 3.1, all these features were compatible with the observations carried out on Individual SSM 92. The uncommon arising location, the age of occurrence and all the morphological and histological recognized features confirmed the diagnosis of a rare example of osteoblastoma of the frontal sinus.

Other forms of benign tumors were screened for differential diagnosis, such as Osteoma, Cemento-Ossifying Fibroma (COF) and Hemangioma. Features of osteoma, as described for the previous case, are similar to the cited tumor form, but differ for the poorly mineralized woven bone and for the sclerosis of the structure (Premužić et al., 2013).

COF affects the splanchnocranium, primarily the mandible and rarely the paranasal sinuses; it consists of fibrous tissue which is less dense than the resembling multilayered bone structure found here. Hemangioma of the frontal sinus is an extremely rare tumor, which is composed of large, endothelium-lined vascular spaces (Raboso et al., 1997; Kanazawa et al., 2009); macroscopically, the changes are very similar to the changes found in hemorrhagic processes (e.g. subdural hematoma) (Schultz, 2001, 2003). These lesions are usually round, measure several centimeters in diameter, and usually destroy the inner and outer table. None of compatible features were present here; moreover, no destructive bone process was observed.

Osteosarcoma and Metastatic Carcinoma are aggressive, fast growing malignant tumor primarily affecting long bones, and reach the skull with metastatic focuses. Osteosarcoma produces an irregular mass characterized by a mixture of lytic and sclerotic changes with irregular and chaotic lamellar borders (*sunburst appearance*) (Suzuki, 1987; Premužić et al., 2013). Metastatic carcinoma, on the other hand, displays multiple lesions and destructive activity due to a highly invasive metastatic process (Lieverse et al., 2014).

None of these features were present in the skull here reported.

For Individual SSM 81, the lesion on the right parietal did not share similar traits with the frontal sinus tumor (osteoma). Both macroscopic and microscopic analyses showed osteoclastic and osteoblastic activities limited to the small area of the lesion. The already described features are products of a meningeal reaction due to an inflammatory process, to a chronic infection (e.g. *leptomeningitis tuberculosa*), or to a meningioma.

3.6 - Discussion and Conclusion

As emphasized by several scholars, it is commonly acknowledged that cancer is not a pathological prerogative of modern times (Aufderheide and Rodríguez, 2000; Ortner, 2003; Capasso, 2005; David and Zimmerman, 2010a; Buikstra and Roberts, 2012; Binder et al., 2014; Seiler et al., 2019). Yet, the infrequency of the findings of cancer among ancient humans could support current epidemiological evidences suggesting that modern habits have greatly influenced the incidence of tumors in modern populations. As a rule, the prolonged lifespan and changes in the diet, along with the consumption of tobacco, alcohol, and additional environmental factors play a major role in the etiology of cancer in current populations (Halperin, 2005).

One should anyway observe that the most investigated bone neoplasms, paleo-oncologists are mostly interested in, are primary malignant and metastatic cancers, such as carcinoma, sarcoma and osteosarcoma that have high mortality indexes. Despite the fact that the lesions in our study are benign neo-formations, both tumors could have compromised the life quality of the two individuals due to the compression exerted on the surrounding healthy bone tissue, a condition which may have caused pain and skeletal dysfunction (Hakim et al., 2015). Once the osteoblastic lesion reaches a considerable size (diameter greater than 30 mm or weighing >110 mg), it should be considered “large” or “giant” (Cheng et al., 2013; Sanchez Burgos et al., 2013). In this case, the compression of soft tissues and the internal organs (e.g. the brain) would certainly lead to important consequences and, in the most serious cases, to the individuals’ death. In our two individuals, the dimensions of the tumors did not exceed the given measures, nevertheless they may have implied an impairment of their life quality, causing for instance headache, dizziness and located pain.

In our study, we have defined the retrieved tumors as rare, both because they are difficult to detect and there are rarely reported in paleopathological literature (Table 3.2). In general, paleopathological literature accounts for a very limited number of cases of tumorous lesions affecting the paranasal and frontal sinus; most of these concern osteomas, while only one reports on an osteoblastoma (Riccomi et al., 2018a).

Table 3.2: Paleopathological scientific literature reporting cases of osteoma and osteoblastomas in ancient human remains

Specimen	Lesion	Localization	Sex	Age	Country	Period	References
Mummy	Osteoma	Lt Frontal sinus	Male	30 + years	Egypt	664–332 BCE	(Seiler et al., 2019)
Skeleton	Osteoblastoma	Rt Frontal sinus	Male	20-25 years	Italy	10 th -12 th centuries CE	(Riccomi et al., 2018a)
Skeleton	Osteoma	Rt frontal sinus	Male	40-50 years	Italy	1 st – 3 rd centuries CE	(Riccomi et al., 2018b)
Skeleton	Osteoma	Rt Frontal sinus	Male	40-50 years	Italy	1 st – 3 rd centuries CE	
Skeleton	Osteoma	Lt Frontal sinus	Female	35-50 years	Croatia	16 th century CE	(Premužić et al., 2013)
Skeleton	Osteoma	Frontal sinus	Male	30+ years	Switzerland	150 – 80 BCE	(Rühli et al., 2004)
Skeleton	Osteoma	Lt Paranasal sinus	NA	NA	Egypt	15 th century BCE	(Hagedorn et al., 2002)
Skeleton	Osteoma	Frontal sinus	NA	NA	Germany	Paleolithic	(Kindler, W., 1972)
Skeleton	Osteoma	Lt Frontal sinus	Male	35-50 years	Italy	15th – 16th centuries CE	Our sample (SSM 81)
Skeleton	Osteoblastoma	Rt Frontal sinus + Rt parietal	NA	30 + years	Italy	15th – 16th centuries CE	Our sample (SSM 92)

According to Marques et al. (2018), Faltas (2011) and Halperin (2005), the principal cause that inhibits the evaluation of oncological disorders in ancient populations is the limitation of the investigative methods. Several studies (Rothschild and Rothschild, 1995; Hershkovitz et al., 1997; Halperin, 2005; David and Zimmerman, 2010b; Marques et al., 2018) indicate that the limitation to macroscopic examination might constrain cancer detection in human skeletal remains.

Yet, in many cases, benign tumors are not adequately examined also because they are not considered worth of attention. Possibly this situation has led to underestimating the actual percentage of some benign neoplasms in the past, which are therefore considered rarer. The

lack of more in-depth systematic investigations of the skeletons as well as the absence of paleoepidemiological approaches are two of the main challenges to the real assessment of cancer in the past.

A better understanding of the incidence of tumors in the past may significantly contribute to further investigation into the underlying mechanisms leading to cancer nowadays, although it must be acknowledged that it is not possible to obtain reliable cancer estimates through the analysis of ancient human remains (Riccomi et al., 2018a), due to the limited findings. Anyway, in the paleopathological context, more cases should be reported, since their number is currently too low. We will never know if this is part of the “osteological paradox” (Wood et al., 2002; Wright and Yoder, 2003), but we expect more reliable results to be obtained using more insightful procedures during the anthropological examinations, such as endoscopic or radiological analyses, in particular for those regions usually hidden by intact surrounding bones

3.7 – References

- Alexander AAZ, Patel AA, Odland R. 2007. Paranasal sinus osteomas and Gardner's syndrome. *Ann Otol Rhinol Laryngol* 116:658–662.
- Aufderheide AC, Rodríguez. 2000. *The Cambridge encyclopedia of human paleopathology*.
- Barbieri G, Turchetti MA, Arcangeli L. 2012. *Il tesoro ritrovato, Sovana: la sezione archeologica nella Chiesa di San Mamiliano*. Laurum.
- Binder M, Roberts C, Spencer N, Antoine D, Cartwright C. 2014. On the antiquity of cancer: Evidence for metastatic carcinoma in a young man from ancient Nubia (c. 1200bc). *PLoS One* 9:1–11.
- de Boer HH, Maat GJR. 2018. Dry bone histology of bone tumours. *Int J Paleopathol*.
- De Boer HH, Van der Merwe AE, Maat GJR. 2013. The diagnostic value of microscopy in dry bone palaeopathology: A review. *Int J Paleopathol* 3:113–121.
- Brothwell DR. 1981. *Digging up bones : the excavation, treatment, and study of human skeletal remains*. Cornell University Press.
- Buikstra JE, Roberts CA. 2012. *The global history of paleopathology : pioneers and prospects*. Oxford University Press.
- Burattini V. 1997. *La Santa Chiesa Sovanese*. Pitigliano.
- Capasso L. 2005. Antiquity of cancer. *Int J Cancer* 113:2–13.
- Cheng KJ, Wang SQ, Lin L. 2013. Giant osteomas of the ethmoid and frontal sinuses: Clinical characteristics and review of the literature. *Oncol Lett* 5:1724–1730.
- Citter C. 2002. *Guida agli edifici sacri della Maremma..* (Nuova Immagine, editor.). Siena.
- Crowder C, Stout S. 2012. *Bone Histology: An Anthropological Perspective*. CRC Press.
- David AR, Zimmerman MR. 2010a. Cancer: an old disease, a new disease or something in between? *Nat Rev Cancer* 10:728–733.
- David AR, Zimmerman MR. 2010b. Cancer: an old disease, a new disease or something in between? *Nat Rev Cancer* 10:728–733.
- Fornaciari G., Giuffra V. 2009. *Lezioni di paleopatologia*. (Ecig, editor.).
- Galliera E, Corsi Romanelli MM. 2018. Molecular Basis of Bone Diseases. *Mol Pathol*:627–649.

- Galliera E, Romanelli MMC. 2017. Molecular basis of bone diseases. *Mol Pathol Mol Basis Hum Dis*:627–649.
- Hagedorn H, Zink A, Of AN-AB, 2002 U. 2002. Endoscopic examinations of the paranasal sinuses and the middle ear in ancient Egyptian mummies. *Univ Coimbra Coimbra*.
- Hakim DN, Pelly T, Kulendran M, Caris JA. 2015. Benign tumours of the bone: A review. *J Bone Oncol* 4:37–41.
- Halperin EC. 2005. Paleo-Oncology: The Role of Ancient Remains in the Study of Cancer. *Perspect Biol Med* 47:1–14.
- Hershkovitz I, Rothschild BM, Latimer B, Dutour O, Léonetti G, Greenwald CM, Rothschild C, Jellema LM. 1997. Recognition of sickle cell anemia in skeletal remains of children. *Am J Phys Anthropol* 104:213–226.
- Kanazawa T, Inoue R, Ohta Y, Watanabe Y, Iino Y. 2009. Maxillary haemangioma successfully resected by endoscopic approach. *J Laryngol Otol* 123:793–795.
- Kindler, W. 1972. Stirnhöhlenosteom in einer fossilen menschlichen Kalotte aus der Diluvialzeit. :3526170.
- Kumar V, Abbas AK, Fausto N, Aster JC. 2011. Robbins e Cotran - Le basi patologiche delle malattie : Vol. 1 Patologia generale - Vol. 2 Malattie degli organi e degli apparati. Elsevier Health Sciences Italy.
- Lehmer LM, Kissel P, Ragsdale BD. 2012. Frontal Sinus Osteoma with Osteoblastoma-like Histology and Associated Intracranial Pneumatocele. *Head Neck Pathol* 6:384–388.
- Lieverse AR, Temple DH, Bazaliiskii VI. 2014. Paleopathological description and diagnosis of metastatic carcinoma in an early bronze age (4588±34 Cal. BP) forager from the cis-baikal region of eastern siberia. *PLoS One* 9:1–25.
- Mann RW, Hunt DR. 2015. PHOTOGRAPHIC REGIONAL ATLAS OF BONE DISEASE - A Guide to Pathologic and Normal Variation in the Human Skeleton.
- Marques C, Matos V, Costa T, Zink A, Cunha E. 2018. Absence of evidence or evidence of absence? A discussion on paleoepidemiology of neoplasms with contributions from two Portuguese human skeletal reference collections (19th–20th century). *Int J Paleopathol* 21:83–95.
- Ortner DJ. 2003. Identification of pathological conditions in human skeletal remains.
- Pilloud M. 2018. Review of Osteoarchaeology: A Guide to the Macroscopic Study of

Human Skeletal Remains.

- Pinhasi R, Mays S. 2008. *Advances in Human Palaeopathology*.
- Premužić Z, Rajić Šikanjić P, Mašić B. 2013. Frontal sinus osteoma in a 16th century skeleton from Zagreb, Croatia. *Int J Paleopathol* 3:54–58.
- Raboso E, Rosell A, Plaza G, Martinez-Vidal A. 1997. Haemangioma of the maxillary sinus. *J Laryngol Otol* 111:638–640.
- Ragsdale BD, Campbell RA, Kirkpatrick CL. 2018. Neoplasm or not? General principles of morphologic analysis of dry bone specimens. *Int J Paleopathol* 21:27–40.
- Riccomi G, Fornaciari G, Minozzi S, Aringhieri G, Giuffra V. 2018a. A rare case of osteoblastoma from medieval Tuscany. *Lancet Oncol* 19:26.
- Riccomi G, Minozzi S, Pantano W, Catalano P, Aringhieri G, Giuffra V. 2018b. Paleopathological evidence of paranasal lesions: Two cases of frontal sinus osteomata from Imperial Rome. *Int J Paleopathol* 20:60–64.
- Rinaldo N, Zedda N, Bramanti B, Rosa I, Gualdi-Russo E. 2019. How reliable is the assessment of Porotic Hyperostosis and Cribra Orbitalia in skeletal human remains? A methodological approach for quantitative verification by means of a new evaluation form. *Archaeol Anthropol Sci*.
- Rokade A, Sama A. 2012. Update on management of frontal sinus osteomas. *Curr Opin Otolaryngol Head Neck Surg*:1.
- Rothschild BM, Rothschild C. 1995. Comparison of radiologic and gross examination for detection of cancer in defleshed skeletons. *Am J Phys Anthropol* 96:357–363.
- Rühli FJ, Böni T, Henneberg M. 2004. Hyperostosis frontalis interna: Archaeological evidence of possible microevolution of human sex steroids? *HOMO- J Comp Hum Biol* 55:91–99.
- Sanchez Burgos R, González Martín-Moro J, Arias Gallo J, Carceller Benito F, Burgueño García M. 2013. Giant osteoma of the ethmoid sinus with orbital extension: craniofacial approach and orbital reconstruction. *Acta Otorhinolaryngol Ital* 33:431–4.
- Schajowicz F. 1981. *Tumors and Tumorlike Lesions of Bone and Joints*. Springer US.
- Schmidt-Schultz TH, Schultz M. 2004. Bone Protects Proteins over Thousands of Years: Extraction, Analysis, and Interpretation of Extracellular Matrix Proteins in Archeological Skeletal Remains. *Am J Phys Anthropol* 123:30–39.

- Schultz M. 1986. Die microscopische untersuchung prähistorischer skelettfunde. Anwendung und Aussagemöglichkeiten der differentialdiagnostischen. In: Archäologie und Museum. Liestal: Kanton Baseland.
- Schultz M. 1987a. Der Gesundheitszustand der frühmittelalterlichen Bevölkerung von Bogazkale/Hattusa. *Arastirma Sonuc Toplancisc* 4:401–409.
- Schultz M. 1987b. Spuren unspezifischer Entzündungen an prähistorischen und historischen Schädeln.
- Schultz M. 1988. Paläopathologische Diagnostik. In: Knußmann R, editor. *Anthropologie. Handbuch der vergleichenden Biologie des Menschen I*, 1. Stuttgart. p 480–496.
- Schultz M. 1993. Light Microscopic Analysis of Macerated Pathologically Changed Bones. :253–296.
- Schultz M. 1993. Initial stages of systemic bone disease. In: Gruppe G GA, editor. *Histology of ancient human bone: Methods and diagnosis*. Berlin: Springer Verlag. p 185–203.
- Schultz M. 1994. Krankheit und Tod im Kindesalter bei bronzezeitlichen Populationen Disease and death in infancy in Bronze Age populations.
- Schultz M. 1997a. Microscopic structure of bone. In: Haglund W, Sorg M, editors. *Forensic taphonomy. The postmortem fate of human remains*. Boca Raton, FL: CRC Press. p 187–199.
- Schultz M. 1997b. Microscopic investigation of excavated skeletal remains A contribution to paleopathology and forensic medicine. In: Haglund W, Sorg M, editors. *Forensic taphonomy. The postmortem fate of human remains*. Boca Raton, FL: CRC Press. p 201–222.
- Schultz M. 2001. Paleohistopathology of bone: A new approach to the study of ancient diseases. *Am J Phys Anthropol* 116:106–147.
- Schultz M. 2003. Light microscopic analysis in skeletal paleopathology. In: Ortner DJ, editor. *Identification of pathological conditions in human skeletal remains*. Amsterdam: Academic Press/Elsevier Science. p 73–108.
- Schultz M, Brandt M. 1987. Neue Methoden zur Einbettung von Knochengewebe und zur Herstellung von Knochendünnschliffen. In: Kußmann R, editor. *Anthropologie. Handbuch der vergleichenden Biologie des Menschen I*. Stuttgart: Stuttgart: G. Fischer. p 698–730.

- Schultz M, Drommer R. 1983. Möglichkeiten der Präparateherstellung aus dem Gesichtsschädelbereich für die makroskopische und mikroskopische Untersuchung unter Verwendung neuer Kunststofftechniken. In: Hoppe W, editor. Experimentelle Mund-Kiefer-Gesichts-Chirurgie. Mikrochirurgische Eingriffe. Stuttgart: G. Thieme. p 95–97.
- Schultz M, Schmidt-Schultz TH. 2015. Microscopic Research on Fossil Human Bone. In: Handbook of Paleoanthropology. Berlin, Heidelberg: Springer Berlin Heidelberg. p 983–998.
- Seiler R, Öhrström LM, Eppenberger P, Gascho D, Rühli FJ, Galassi FM. 2019. The earliest known case of frontal sinus osteoma in man. *Clin Anat* 32:105–109.
- Stuart-Macadam P. 1987. Porotic hyperostosis: New evidence to support the anemia theory. *Am J Phys Anthropol* 74:521–526.
- Stuart-Macadam P. 1987. A radiographic study of porotic hyperostosis. *Am J Phys Anthropol* 74:511–520.
- Suzuki T. 1987. Paleopathological study on a case of osteosarcoma. *Am J Phys Anthropol* 74:309–318.
- Tondo L, Pellegrini E, Nanni M, Rafanelli S, Benicchi S. 2004. Indagini archeologiche a Sovana nel biennio 1998-1999. In: *Archeologica Pisana. Scritti per Orlanda Pancrazzi*.
- Tuci DBGMG. 2008. Scavi nella chiesa di San Mamiliano a Sovana. Scavi nella chiesa di San Mamiliano a Sovana:9–42.
- Walker PL, Bathurst RR, Richman R, Gjerdrum T, Andrushko VA. 2009. The causes of porotic hyperostosis and cribra orbitalia: A reappraisal of the iron-deficiency-anemia hypothesis. *Am J Phys Anthropol* 139:109–125.
- Wapler U, Schultz M. 1996. Une méthode de recherche histologique appliquée au matériel osseux archéologique : l'exemple des cribra orbitalia. *Bull Mem Soc Anthropol Paris* 8:421–431.
- Weidner N. 2009. *Modern surgical pathology*. Saunders/Elsevier.
- Wood JW, Milner GR, Harpending HC, Weiss KM, Cohen MN, Eisenberg LE, Hutchinson DL, Jankauskas R, Cesnys G, Katzenberg MA, Lukacs JR, McGrath JW, Roth EA, Ubelaker DH, Wilkinson RG. 2002. The Osteological Paradox: Problems of Inferring Prehistoric Health from Skeletal Samples. *Curr Anthropol* 33:343–370.

Wright LE, Yoder CJ. 2003. Recent Progress in Bioarchaeology: Approaches to the Osteological Paradox. *J Archaeol Res* 11:43–70.

CHAPTER 4

HOW TO ASSESS INJURIES IN BIOLOGICAL ANTHROPOLOGY: A NEW INVESTIGATIVE STRATEGY FOR THE ANALYSIS OF TRAUMATIC LESIONS

Defining lesion types and timing are of fundamental relevance in the anthropological context, independently of the age of the criminal scene. In this work, we discuss two cases of inflicted lesions, found in two skeletons from the cemetery of the St. Biagio Church, Ravenna (Northern Italy; 17th-19th century).

We explored the historical and archaeological context to unveil the living conditions of the individuals. We traced the individual biological profiles of both cases and their lesions were carefully examined with macroscopic, radiologic and microscopic techniques.

A new evaluation form was developed to handle the two cases, which is here proposed as a general tool to facilitate trauma recognition and interpretation, as well as timing of the injuries.

4.1 – Introduction

When dealing with inflicted injuries, one of the most critical aspects is to determine whether the injury occurred long before death (*ante mortem*), at death or near death (*peri mortem*), or long after death (*post mortem*). Moreover, it is necessary to distinguish the type of trauma and the weapon used, as well as the time elapsed from trauma before death. In case of *ante mortem* trauma, it is also important to detect eventual correlated pathologies, and the resulting conditions of health and well-being until death.

Skeletal traumas are described by Dirkmaat et al., 2008 as «a moment frozen in time which consistently contributes to understanding what had happened to the deceased individual» and their detailed analysis and careful interpretation can be decisive to solve forensic cases.

As proposed by Galloway et al., 1999, two main aspects must be taken into account during the analysis of trauma on dry bones. First: the trauma must be distinguishable from pathological conditions as well as from normal biovariability. Second: the number and sequence of skeletal injuries must be determined and the lesions distinguished according to the time of death.

For this latter purpose, it is of particular importance to distinguish among possibly different lesions retrieved on the skeleton and identify the kind of trauma as defined by the weapon used (Jerković et al., 2016). Skeletal injury is mostly described according to the mechanism of inference and ballistic investigation, i.e. the way weapon and/or force were applied to the bone (Christensen et al., 2014). By doing so, we can classify trauma in cutting wounds, blunt force traumas, sharp force traumas, chop wounds, stab wounds, high-velocity projectile (ballistic wounds), low-velocity projectile and several others (Lovell, 1997; Christensen et al., 2014; Blau and Ubelaker, 2016). Usually, the analyses of the lesions are based on morphological features detectable macroscopically. Radiological, microscopic and chemical techniques can also be useful (Cattaneo and Cappella, 2017). Lesions occurred during life are usually characterized by bone remodelling due to the ability of the bone tissue to regenerate, whereas injuries produced on the skeleton, i.e. on the dry bone (dry fracture), are identifiable on the basis of characteristic patterns due to the loss of elasticity of the dry bone, i.e. irregular fracture margin with several bone fragments (Reichs and Bass, 1998; Cappella et al., 2014).

Although it can be difficult to recognize which are the traumas that caused an individual's death in case of multiple or simultaneous lesions, the number and distribution of traumas

per person and per bone should be collected. In addition to the severity of the injury, the localization of skeletal traumas is crucial for establishing the cause of death. With regard to the head injuries examined in the following case studies, for example, the trauma inflicted to the vital organ (i.e. brain) have to be considered severe and may have resulted in a very limited survival time.

Aims of this study were: (i) to outline a new investigation strategy for the preliminary study of traumatic injuries, (ii) to present a new user-friendly diagnostic form (Figure 4.1) for the identification of traumas on human skeletal remains, which resumes the observations of several scholars (Barber, 1929, 1930, 1934; Lovell, 1997; Reichs and Bass, 1998; Moraitis and Spiliopoulou, 2006a; Maat, 2008; Symes et al., 2012; Kranioti, 2015; Ubelaker, 2015; Pasini et al., 2019), and (iii) to analyse and interpret two case-studies using the new form.

4.2 – Timing and interpretation of skeletal injuries

In a skeleton, we can identify injuries occurred during the life of the individual (*ante mortem*), as well as lesions occurred after his/her death (*post mortem*). The first type of lesion is usually characterized by a reaction of the bone tissue due to its elasticity and an event of bone remodelling due to its ability to regenerate (Blau, 2017). Conversely, lesions that occurred on dry bones, both intentionally inflicted or due to taphonomic processes, can be easily established through irregular fragmentation with sharp margins and different colour of the edge surfaces (Blau, 2017).

Considering this, the hardest work for an anthropologist is to distinguish between lesions occurred shortly before or shortly after the death (Cappella et al., 2014; Cattaneo and Cappella, 2017) while the individual was still alive, i.e. on fresh bone, or long dead, i.e. on the dry bone (Reichs and Bass, 1998; Cattaneo and Grandi, 2004; Dirkmaat et al., 2008; Dirkmaat, 2012; Spencer, 2012; Symes et al., 2012; Bunch, 2014; Mann and Hunt, 2015; Ubelaker, 2015). In fact, the injuries occurred along with the death (*peri mortem*) show patterns that depend on the elasticity and plasticity of the tissue with smooth edges of the same colour as the nearby bone.

Taking into account the considerable literature that has been devoted to this topic in forensic anthropology (Lovell, 1997; Reichs and Bass, 1998; Moraitis and Spiliopoulou, 2006b; Dirkmaat et al., 2008; Dirkmaat, 2012; Ubelaker, 2015), we observed that the term '*peri mortem*' assumes different meanings for forensic pathologists and forensic

anthropologists. For the first ones, *peri mortem* is an event associated with the death and has a narrow time focus (Dirkmaat et al., 2008; Dirkmaat, 2012; Spencer, 2012; Symes et al., 2012; Bunch, 2014; Mann and Hunt, 2015). Forensic anthropologists, instead, cannot determine the precise moment of death and can only assess what has happened when the bones were injured (Kranioti, 2015; Licata and Armocida, 2015; Miller, 2018). Nevertheless, this information can be of great help to forensic pathologists in reaching their conclusions (Blau and Ubelaker, 2016).

Moreover, anthropologists may provide detailed information about skeletal variations, pathological lesions and skeletal injuries thanks to their ability to discern congenital skeletal anomalies (e.g. supernumerary bone, non-fusion anomalies, congenital foramen and musculoskeletal stress markers) from trauma (Byers, 2016).

We have summarized the features lesions should present in the three main moments of occurrence in a specific evaluation form (Figure 4.1). We used synthetic descriptions and drawings to facilitate recognition and interpretation of traumas, also useful for a preliminary approach, e.g. during an archaeological excavation.

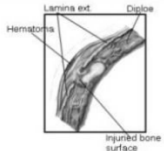
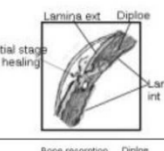
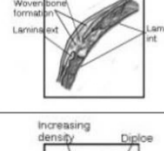
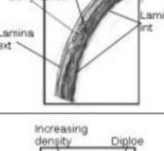
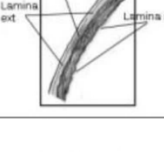
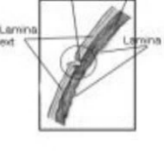

Archaeological site _____		Individual _____			
Date _____		Evaluator _____			
Time of trauma	Healing process	Duration	Bony responses	Presence	
<i>Ante mortem</i>	1. Formation of hematoma. Injured bone starts to regenerate due to the arrest of the hemorrhage	Within 24 hours	End of bleeding. Formation of hematoma histologically determinable.		<input type="checkbox"/>
	2. Cellular proliferation with deposition of osteoid tissue around each fragment by osteoblasts of periosteum and endosteum. Fracture is joined and visible on dry bones	Within 3 weeks	Osseous reaction. Presence of periostitis. Initial stage of healing		<input type="checkbox"/>
	3. Mineralization of osteoid that works such as a split for the periosteal and endosteal surfaces. Visible also radiologically	From 3 up to 9 weeks	Bone resorption and consequent formation of the callus made of woven bone (<i>soft callus</i>)		<input type="checkbox"/>
	4. Consolidation of the woven bone from callus precursor that results in a solidly united fracture area.	From few weeks to few months	Lamellar bone formation (<i>hard callus</i>)		<input type="checkbox"/>
	5. Gradual remodeling of bone to its original form.	From 6 to 9 years	Increase of density and strengthening along lines of mechanical stress radiologically determinable		<input type="checkbox"/>
<i>Peri mortem</i>	Occurring at or near the moment of death	Absence of bony response or healing	<ul style="list-style-type: none"> • Edges of injuries irregular and shaped; hinging bone fragments; • Cortical bone flakes along fracture margins; • Internal or/and external smoothed margins; • Radiating and concentric fractures; Staining maintained along fracture margins; • Plastic deformation. 		<input type="checkbox"/>
<i>Post mortem</i>	After death	Absence of bony response or healing	<ul style="list-style-type: none"> • Fracture margins colored of bright white, or lighter; • Bone shatters into regular fragments; • Possible taphonomic evidence (e.g. gnawing or carnivore puncture marks). 		<input type="checkbox"/>

Figure 4.1 - Trauma evaluation form with illustration and description of the features of different lesions and healing processes (Scianò et al., 2020).

4.3 – Materials and Methods

We isolated two interesting cases of trauma among 122 skeletons dating back to the 17th-19th centuries from the cemetery of the San Biagio church (Ravenna, Italy). Sex (Acsadi and Nemeskeri, 1970; Workshop of European Anthropologists, 1980; Krogman and Iscan, 1986; Gualdi-Russo, 2007), age at death (Acsadi and Nemeskeri, 1970; Workshop of European Anthropologists, 1980; Brothwell, 1981; Lovejoy, 1985; Meindl and Lovejoy, 1985; Işcan and Loth, 1986; Brooks and Suchey, 1990; Albert and Maples, 1995; Buckberry and Chamberlain, 2002; Hens and Belcastro, 2012; Belcastro et al., 2017), and stature (Trotter and Gleser, 1951, 1958; Manouvriere, 1982) were determined using standard anthropological methods and proper instruments (Figure 4.2a ,b, c).

The macroscopic evidence of injuries were examined with a magnifying glass and a light microscope (Optika Microscope – B-380) (Figure 4.2 d). Radiographic and multiplanar inquiries via Cone Beam (CBCT) was employed as well, in collaboration with the Department of Clinical Radiology of the Casa di Cura S. Maria Maddalena, (RO), and resulted in a digital volume render composed of a three-dimensional “picture” of the interested area; the 3D object was visualized and treated with the OsiriX DICOM Viewer software. To refine the analysis, histologic techniques were employed, using standard protocols for generating slides (An and Martin, 2003) and a stereomicroscope (Leica S8AP0 + Camera Leica DC500) (Figure 4.2 e) to analyze the microstructure of the bone and take pictures.

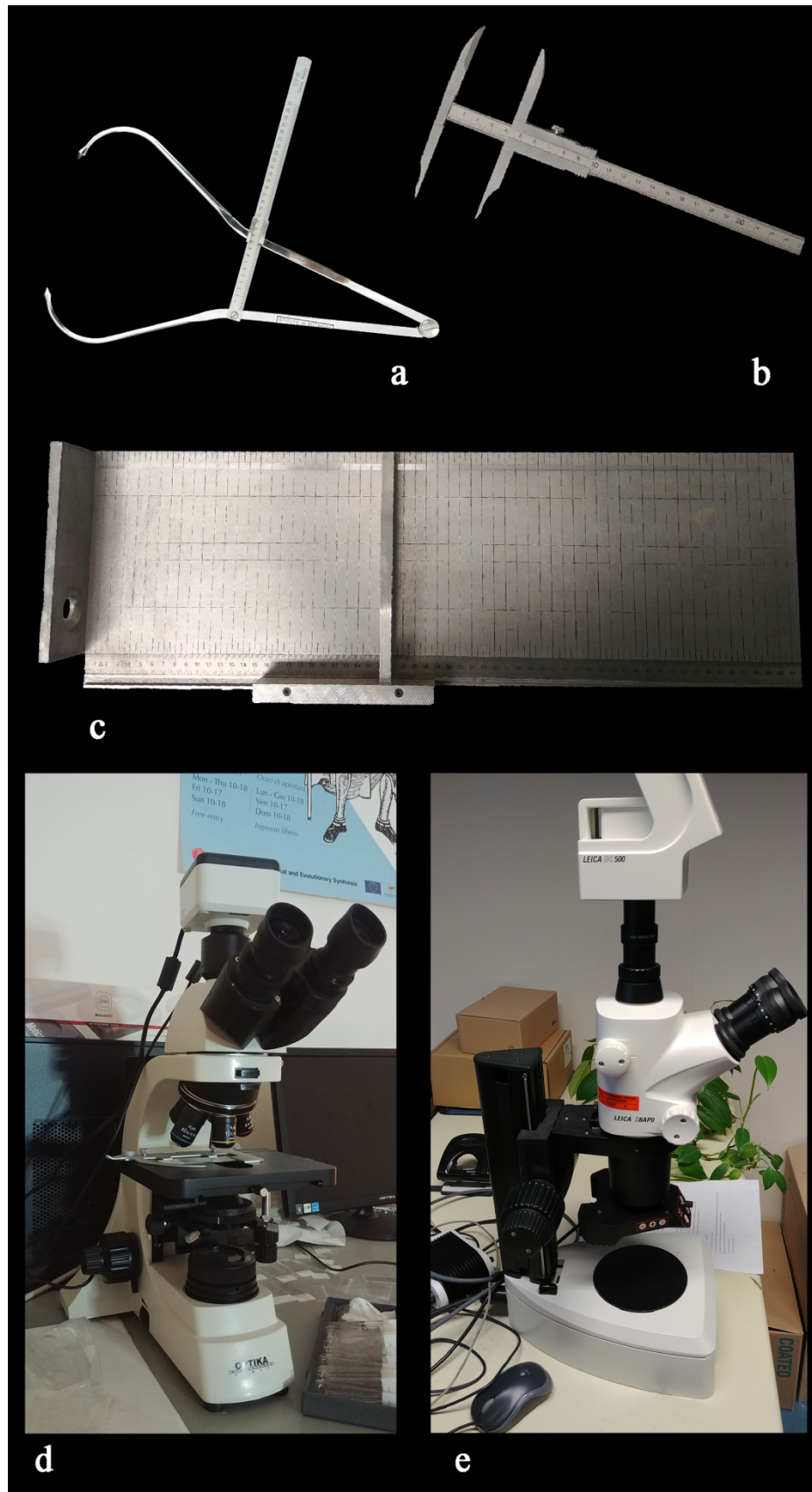


Figure 4.2 – Instruments used for the macroscopic and microscopic analyses: **a)** spreading caliper; **b)** sliding caliper; **c)** osteometric table; **d)** microscope Optika Microscope – B-380; **e)** microscope Leica S8AP0 with Leica Camera DC500 (Photo: Filippo Scianò).

4.4 – Results

Anthropological analysis has shown traumatic lesions of different aetiology on the skull of both individuals examined.

Analysis and interpretation of each injury were carried out with the new evaluation form (Figure 4.1) and reported in Table 4.1. Thus, , location, features of the lesion, timing of the injury, and measurements were recorded for each lesion and resumed in Table 4.2.

Table 4.1 - Assessment of the time of trauma occurrence in the examined case-studies

	Healing process	Bony responses	Ind. No. 114	Ind. No. 118
<i>Ante mortem</i>	1. Formation of the hematoma.	End of bleeding	✓	-
	2. Cellular proliferation. Fracture is joined and visible on dry bone	Pathological reaction (periostitis). Sub-periosteal bone formation	✓	-
	3. Mineralization of osteoid. Visible radiologically.	Formation of the (osseous) callus made of woven bone	✓	-
	4. Consolidation of the woven bone	Primary and secondary lamellar bone formation.	✓	-
	5. Gradual remodeling of bone	Increase of density and strengthening along lines of mechanical stress	✓	-
<i>Peri mortem</i>	Absence of healing processes	Edges of injuries irregular and shaped; hinging bone fragments. Cortical bone flakes along fracture margins. Plastic deformation.	-	-
<i>Post mortem</i>	Absence of bony response or healing	Fracture margins colored of bright white, or lighter. Bone shatters into regular fragments.	-	✓

Table 4.2 - Lesions characteristics

Ind. No.	Trauma number - per person	Trauma number - per bone	Location (side)	Shape	Size (cm)	Timing	Possible Aetiology
114	1	1, skull	Frontal bone, supraorbital margin (R)	Semilunar, irregular	3.8 x 1.3	<i>Ante mortem</i>	Heavy sharp weapon
118	4*	1, skull	Mastoid process (R)	Straight, regular	1.3 x 1.1	<i>Post mortem</i>	Accidental, unknown

* Other 3 lesions of traumatic traumatic entity have interested the vertebral column.

The individual No. 114 was a 45-55 years old man, 169.5 ± 4.3 cm tall. A deep injury was detected on the right supraorbital margin of the frontal bone (Figure 4.3a). The lesion appears fairly large with irregular edges and shape. The surface interested by the direct kerf is smooth with some parallel striations that form a 90° angle with the transverse plane. All around the hit area, there is evidence of bone resorption and remodeling (bone spicules and osteolytic reactions) (Lovell, 1997; Kimmerle and Baraybar, 2008; Licata and Vecchio, 2014; Licata and Armocida, 2015) (Figure 4.3 b,c), an observation, which suggests that it is an *ante mortem* lesion. In support of this hypothesis, we observed evidence of a periosteal reaction (*osteoperiostitis*) on the outer surface of the lesion, while traces of a nonspecific infection (*osteitis*) are visible on the inner surface.

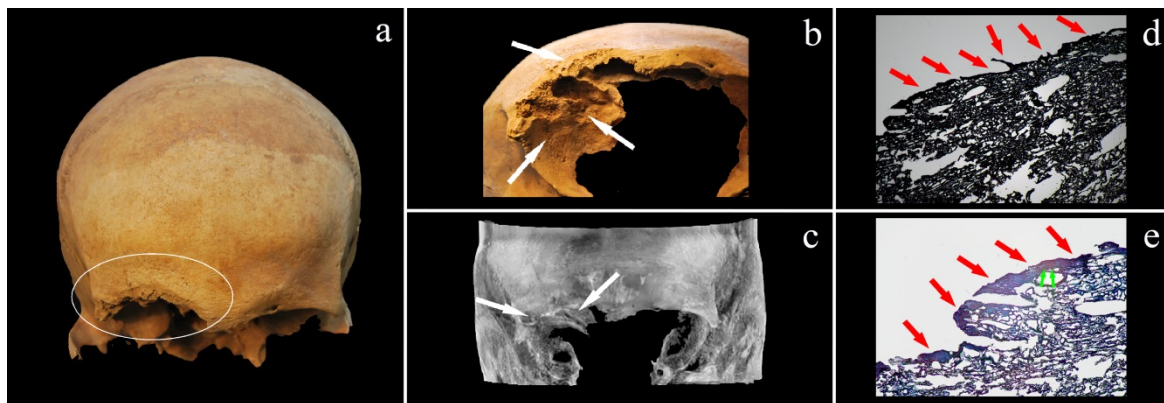


Figure 4.3 – Ind No. 114: **a)** Chop wound on the right supraorbital margin; **b)** Right orbital roof surface, with inflammatory process of the bone (white arrows); **c)** CT scan of the traumatized area, with different density districts (white arrows); **d)** Histologic section: view through the light microscope (15 µm section in Masson's trichrome stain, Magnification 40x) of the right supraorbital margin, with cortical bone, remodeled after the lesion (osteoblastic activity) on the entire surface (red arrows); **e)** Histologic section of the right supraorbital margin: view through the light microscope (15 µm section in Masson's trichrome stain, Magnification 200x) of the traumatized area with inflammatory reaction on the outer surface (red arrows) and signs of osteoclastic activity (Howship's lacunae – green arrows.; (Scianò et al., 2020)).

Histological analyses confirmed this interpretation showing osteoblastic and osteoclastic activities (e.g. *Howships lacunae*) and allowed us to identify the injury as an *ante mortem* lesion (Figure 4.3 d,e).

Both bony response might be the consequence of the same injury. Radiological analysis and densitometric data provided by OsiriX DICOM Viewer (Figure 4.4) show an increase of bone mineral density (BMD) in the healed surface of the injured area, feature usually observed for up 8-10 weeks after the traumatic event (Yochum and Rowe 2013). (Lovell, 1997; Resnick and Kransdorf, 2005). Besides, there are no traces of artifacts, created during radiographic and multiplanar scanning operations, that could invalidate the diagnosis (Schulze et al., 2011).

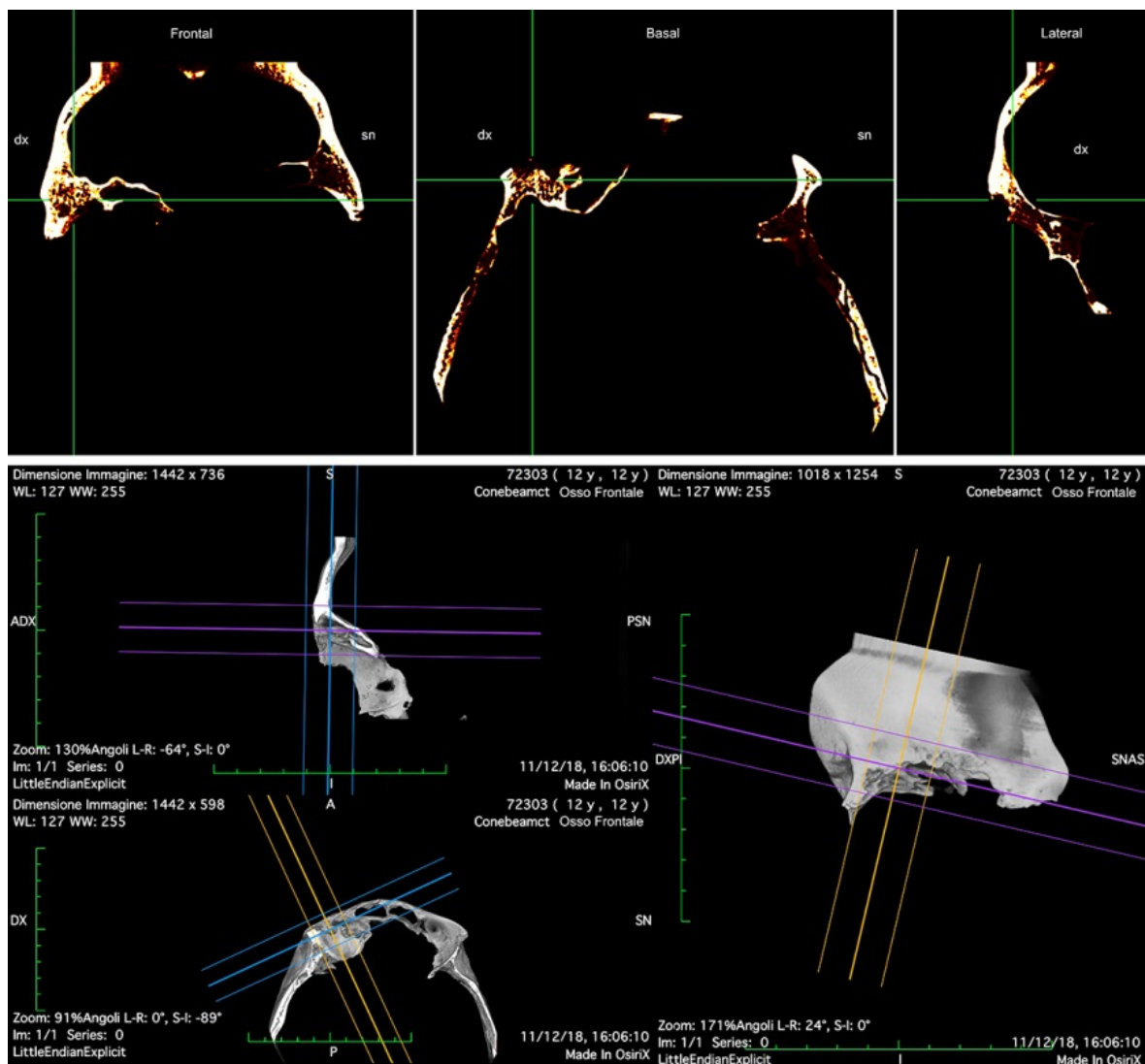


Figure 4.4 – Ind No. 114; Cone-Beam of the traumatized area on the right supraorbital margin; **a)** MPR scan in frontal, basal and lateral view and **b)** 3D-CT treated picture for in deep analyses of the injury (Picture: Filippo Scianò).

Hypothetically, a consequence of this traumatic event may have been the severe displacement of the mandible, with the right condyle shifted from its natural joint to the zygomatic arch where it formed a new articulation (Figure 4.5).

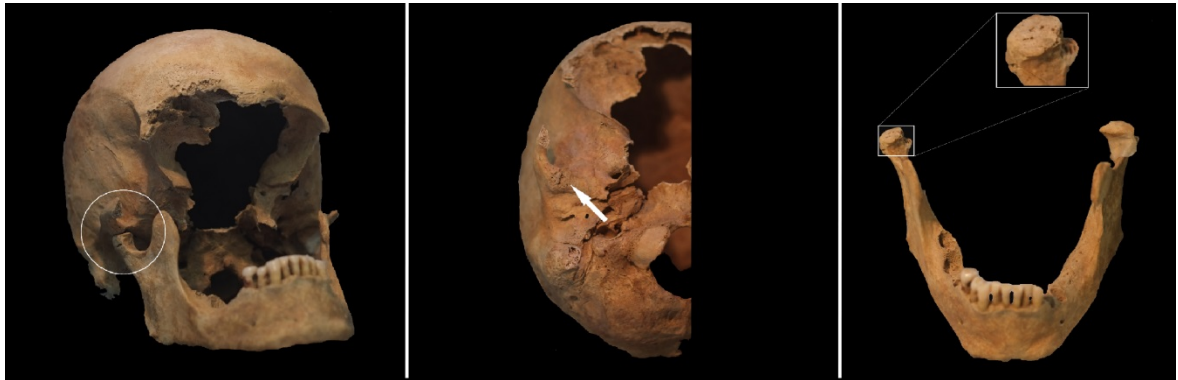


Figure 4.5 – Ind No. 114: Mandibular malocclusion due to **a)** dislocation of the temporo-mandibular joint; **b)** creation of new articular facet on the inferior inner surface of the zygomatic arch (white arrow); **c)** Erosion and adaptation of the right mandibular condyle (Photo: Filippo Scianò).

The individual No. 118 was a 30-39 years old male, 162.6 ± 3.3 cm tall. Multiple traumas of the skull and spine are detectable on his skeleton (Figure 4.6). The first is a small shape and deep cut-mark on the right mastoid process (Figure 4.6). Macroscopic and microscopic analyses have shown that the edges of the walls were perfectly clean and clear, and there was no presence of porosity around the cut mark; the color of the kerf was brighter than the rest of the mastoid surface, indicating a *post mortem* lesion.



Figure 4.6 – Ind No. 118: Post mortem cut mark of the right mastoid process (Photo: Filippo Scianò).

4.5 – Discussion and Conclusion

As was established in the published study (Scianò et al., 2020), the two case-studies represent a good example to pin-point differences among lesions of the dry bone tissue by employing anthropological methods. Radiographic and histological analyses may be of great help for defining timing and/or dynamics of the events occurred. The new evaluation form was demonstrated to be an indispensable tool for collecting useful elements for the diagnosis of *ante mortem* vs *peri mortem* or *post mortem* lesions (Scianò et al., 2020).

For Ind. No. 114, we concluded that likely the sharp force trauma on the orbit was a chop wound inflicted by a heavy and cutting instrument (axe, machete, adze or swords (Christensen et al., 2014)). Taking in account the historical period, we tended to consider a sword or a lumberjack/farmer axe (Lewis, 2008) as the most likely weapon used (Scianò et al., 2020). In all probability, the individual survived the trauma at least three months and this was not directly the cause of his death. We came to this conclusion after observing periosteal inflammation and bone remodeling in the specimen by means of macroscopic analyses (Lovell, 1997) along with other evidence of healing such as the lamellar bone formation visible through microscopic examination and the density increasing along lines of mechanical stress, visible through radiological analyses.

For Ind. No. 118, we proposed that the cut mark on the mastoid process was probably inflicted with a sharp-edged tool during the archaeological phase of excavation. The absence of osteogenic reactions excludes that the lesion occurred during the individual's lifetime. The features of the cut-surface, the shape and the color of the lesion exclude the occurrence of the trauma on occasion of his individual's death.

Anthropological methods enable to obtain relevant information on injuries found on skeletons from bioarchaeological or forensic contexts. The attention to skeletal patterns, the determination of biological parameters such as age-at-death and sex, the detection of variables that can be traced back to physical and sociocultural environments, all this information improves the accuracy of the diagnosis.

Nevertheless, bone injuries which date back to a period immediately after the death of the individual, still represent a challenge. In this case, the lesions could be defined as "*peri mortem*" because they show features similar to living bone tissue (green bone) with responses indicating high elasticity and plasticity. Therefore, particular caution is required in the interpretation of this type of lesions. Keeping this limitation in mind, the new

evaluation form represent a valuable tool to optimize the applicability of the current methods of detection.

We strongly encourage collaboration between different practitioners in anthropological and forensic sciences and we hope in a large use of the evaluation form also on skeletal trauma whose cause and timing are known. This would provide additional information and help in reaching new perspectives both, in forensic anthropology and pathology.

4.6 – References

- Acsadi G, Nemeskeri J. 1970. History of Human Life Span and Mortality. Budapest: Akadémiai Kiadó.
- Albert AM, Maples WR. 1995. Stages of epiphyseal union for thoracic and lumbar vertebral centra as a method of age determination for teenage and young adult skeletons. *J Forensic Sci* 40:623–33.
- An YH, Martin KL. 2003. Handbook of Histology Methods for Bone and Cartilage.
- Barber CG. 1929. Immediate and eventual features of healing in amputated bones. *Ann Surg* 90:985–92.
- Barber CG. 1930. The detailed changes characteristic of healing bone in amputation. *J Bone Jt Surg* 12:353–359.
- Barber CG. 1934. Ultimate anatomical modification in amputation stumps. *J Bone Jt Surg* 16:394–400.
- Belcastro MG, Bonfiglioli B, Pedrosi ME, Zuppello M, Tanganelli V, Mariotti V. 2017. The History and Composition of the Identified Human Skeletal Collection of the Certosa Cemetery (Bologna, Italy, 19th–20th Century). *Int J Osteoarchaeol* 27:912–925.
- Blau S. 2017. How traumatic: a review of the role of the forensic anthropologist in the examination and interpretation of skeletal trauma. *Aust J Forensic Sci* 49:261–280.
- Blau S, Ubelaker DH. 2016. Handbook of Forensic Anthropology and Archaeology. (Blau S, Ubelaker DH, editors.). Routledge.
- Brooks S, Suchey JM. 1990. Skeletal age determination based on the os pubis: A comparison of the Acsádi-Nemeskéri and Suchey-Brooks methods. *Hum Evol* 5:227–238.
- Brothwell DR. 1981. Digging up bones : the excavation, treatment, and study of human skeletal remains. Cornell University Press.
- Buckberry JL, Chamberlain AT. 2002. Age estimation from the auricular surface of the ilium: A revised method. *Am J Phys Anthropol* 119:231–239.
- Bunch AW. 2014. National academy of sciences “Standardization”: On what terms? *J Forensic Sci* 59:1041–1045.

- Byers S. 2016. Introduction to forensic anthropology.
- Cappella A, Amadasi A, Castoldi E, Mazzarelli D, Gaudio D, Cattaneo C. 2014. The difficult task of assessing perimortem and postmortem fractures on the skeleton: A blind test on 210 fractures of known origin. *J Forensic Sci* 59:1598–1601.
- Cattaneo C, Cappella A. 2017. Distinguishing between Peri- and Post-Mortem Trauma on Bone. In: *Taphonomy of Human Remains: Forensic Analysis of the Dead and the Depositional Environment*. Chichester, UK: John Wiley & Sons, Ltd. p 352–368.
- Cattaneo C, Grandi M. 2004. *Antropologia e odontologia forense : guida allo studio dei resti umani : testo atlante*. Monduzzi.
- Christensen AM, Passalacqua N V., Bartelink EJ. 2014. *Forensic anthropology : current methods and practice*. Elsevier Academic Press.
- Dirkmaat DC. 2012. *A Companion to Forensic Anthropology*.
- Dirkmaat DC, Cabo LL, Ousley SD, Symes SA. 2008. New perspectives in forensic anthropology. *Am J Phys Anthropol* 137:33–52.
- Gualdi-Russo E. 2007. Sex determination from the talus and calcaneus measurements. *Forensic Sci Int* 171:151–156.
- Hens SM, Belcastro MG. 2012. Auricular surface aging: A blind test of the revised method on historic Italians from Sardinia. *Forensic Sci Int* 214:209.e1-209.e5.
- Işcan MY, Loth SR. 1986. Determination of age from the sternal rib in white males: a test of the phase method. *J Forensic Sci* 31:122–32.
- Jerković I, Bašić Ž, Bečić K, Jambrešić G, Grujić I, Alujević A, Kružić I. 2016. Anthropological analysis of the Second World War skeletal remains from three karst sinkholes located in southern Croatia. *J Forensic Leg Med* 44:63–67.
- Kimmerle EH, Baraybar JP. 2008. *Skeletal Trauma: Identification of Injuries Resulting from Human Rights Abuse and Armed Conflict*. CRC Press.
- Kranioti E. 2015. Forensic investigation of cranial injuries due to blunt force trauma: current best practice. *Res Reports Forensic Med Sci* 5:25–37.
- Krogman WM, Iscan M. 1986. *The human skeleton in forensic medicine*. Springfield: Charles C Thomas Publisher.
- Lewis JE. 2008. Identifying sword marks on bone: criteria for distinguishing between cut marks made by different classes of bladed weapons. *Int J Osteoarchaeol* 35:2001–

2008.

- Licata M, Armocida G. 2015. Trauma lubanje: Analiza ozljeda na drevnim kosturima s arheoloških nalazišta u sjeverozapadnoj lombardiji. *AMHA - Acta Medico-Historica Adriat* 13:251–264.
- Licata M, Vecchio I. 2014. Analysis of ante-mortem injuries in medieval skeletons from the necropolis of caravate (Varese) Italy. *Acta Medica Mediterr.*
- Lovejoy CO. 1985. Dental wear in the Libben population: Its functional pattern and role in the determination of adult skeletal age at death. *Am J Phys Anthropol* 68:47–56.
- Lovell NC. 1997. Trauma Analysis in Paleopathology. *Yrbk Phys Anthr* 40:139–170.
- Maat GJR (George. 2008. Case Study 5.3: Dating of fractures in human dry bone tissue - the Berisha case. In: Erin H. Kimmerle JPB, editor. *Skeletal Trauma Identification of Injuries Resulting from Human Rights Abuse and Armed Conflict.* . p 245–254.
- Mann RW, Hunt DR. 2015. *PHOTOGRAPHIC REGIONAL ATLAS OF BONE DISEASE - A Guide to Pathologic and Normal Variation in the Human Skeleton.*
- Manouvriere L. 1982. Détermination de la taille d'après les gran os de membres. *Rev L'Ecole Antropol* 2:227–233.
- Meindl RS, Lovejoy CO. 1985. Ectocranial suture closure: A revised method for the determination of skeletal age at death based on the lateral-anterior sutures. *Am J Phys Anthropol* 68:57–66.
- Miller E. 2018. Forensic Anthropology. *Multidiscip Medico-Legal Death Investig*:215–225.
- Moraitis K, Spiliopoulou C. 2006a. Identification and Differential Diagnosis of Perimortem Blunt Force Trauma in Tubular Long Bones. *Forensic Sci Med Pathol* 2:221–230.
- Moraitis K, Spiliopoulou C. 2006b. Identification and Differential Diagnosis of Perimortem Blunt Force Trauma in Tubular Long Bones.
- Pasini A, Gualdi-Russo E, Scianò F, Thun Hohenstein U. 2019. Violence in the Early Bronze Age. Diagnosis of skull lesions using anthropological, taphonomic and scanning electron microscopy techniques. *Forensic Sci Med Pathol* 15:324–328.
- Reichs K, Bass WM. 1998. Forensic osteology : advances in the identification of human remains. Charles C Thomas.

- Resnick D, Kransdorf MJ. 2005. Bone and joint imaging. Elsevier Saunders.
- Schulze R, Heil U, Groß D, Bruellmann DD, Dranischnikow E, Schwanecke U, Schoemer E. 2011. Artefacts in CBCT: A review. *Dentomaxillofacial Radiol* 40:265–273.
- Scianò F, Bramanti B, Manzon VS, Gualdi-Russo E. 2020. An investigative strategy for assessment of injuries in forensic anthropology. *Leg Med* 42:101632.
- Spencer SD. 2012. Detecting violence in the archaeological record: Clarifying the timing of trauma and manner of death in cases of cranial blunt force trauma among pre-Columbian Amerindians of West-Central Illinois. *Int J Paleopathol* 2:112–122.
- Symes SA, L'Abbé EN, Chapman EN, Wolff I, Dirkmaat DC. 2012. Interpreting Traumatic Injury to Bone in Medicolegal Investigations. In: *A Companion to Forensic Anthropology*. Chichester, UK: John Wiley & Sons, Ltd. p 340–389.
- Trotter M, Gleser G. 1951. The effect of ageing on stature. *Am J Phys Anthropol* 9:311–324.
- Trotter M, Gleser GC. 1958. A re-evaluation of estimation of stature based on measurements of stature taken during life and of long bones after death. *Am J Phys Anthropol* 16:79–123.
- Ubelaker D. 2015. *The Concept of Perimortem in Forensic Science*.
- Workshop of European Anthropologists. 1980. Recommendations for Age and Sex Diagnosis of Skeletons. *J Hum Evol* 9:517–549.

CHAPTER 5

COLD CASES IN ANCIENT TIME: INVESTIGATION OF CRANIAL LESIONS OF EARLY BRONZE AGE AND RENAISSANCE

Two other interesting cases of injuries linked to the individual's cause of death regard two skulls dating back to the Early Bronze Age and Renaissance, respectively. The determination of their biological profile displayed that both skeletal remains belonged to adult individuals with no particular evidence of deep pathological changes.

Both crania showed multiple *peri mortem* lesions on the left frontal and left parietal bones. In addition, one of them showed the signs of a surgical activity carried out possibly *post mortem*.

Using the trauma evaluation form previously developed (see Chapter 4), and combining anthropological, forensic, taphonomic and microscopic investigation (through light microscopy and ESEM), we tried to establish the timing of the lesions and evaluate if some of the traumatic injuries might have been due to interpersonal violence.

All the analyses seem to confirm that the death of both individuals was a direct consequence of the injuries inflicted on the head.

5.1 – Introduction

The scientific interest in traumatology, and in particular in traumatic evidences related to interpersonal violence, is increasing in the fields of anthropology, as supported by the growing amount of literature (Boylston, 2000; Brickley et al., 2004; Parker Pearson and Thorpe, 2005; Otto et al., 2006; Lewis, 2008; Facchini et al., 2008; Jiménez-Brobeil et al., 2009; Black and Ferguson, 2011; Manzon et al., 2012; Spencer, 2012; Fleming-Farrell et al., 2013; Schwitalla et al., 2014; Wedel and Galloway, 2014; Cappella et al., 2014; Boldsen et al., 2015; Kranioti, 2015; Licata and Armocida, 2015; Martin and Harrod, 2015; Smith et al., 2015; Geber, 2015; Scheirs et al., 2017a; Downing and Fibiger, 2017; Kranioti et al., 2019; Pasini et al., 2019; Scianò et al., 2020).

The analytical study of traumas provides essential indications on the biomechanical stresses to which a bone may be subjected. On the other hand, the study of injuries also informs about the degree of violence within a society or a human group of the past.

In addition to the determination of the biological profile, anthropologists are often called upon to assess traumatic evidences as well as the time since death, especially in the forensic context. Although most deaths from natural causes and many accidental or violent events leave no traces on the skeleton (Cattaneo and Porta, 2009), in some particular cases, it is possible to determine the cause of death from human skeletal remains and their traumatic evidences, whether these were accidental or intentional.

Traumatic injuries caused by interpersonal violence are usually classified according to the weapon used to inflict them (see Chapter 4), as well as on the basis of the different nature of the fractures (Aufderheide and Rodríguez, 2000; Pinhasi and Mays, 2008). The timing of the lesion, as already explained in detail in the previous chapter, is another important part of the puzzle.

Extensive studies have shown that the overlying soft tissue thickness, the bone shape, the cortical density and the plasticity of the bone are related to the fracture pattern. In addition, the investigation of bone healing processes and decomposition, as well as the taphonomic variations, provide us with more information about the timing of infliction (Sauer, 1998; Pechníková et al., 2011; Manzon et al., 2012; Spencer, 2012; Licata and Armocida, 2015; Cattaneo and Cappella, 2017a; Kranioti et al., 2019; Pasini et al., 2019).

The aim of this study was to evaluate (*peri mortem* and *post mortem*) lesions found on two skulls from different periods to determine the probable causes of death of the two

individuals. Further, we needed to interpret an evidence of surgical practice found on the Renaissance skeletal remains.

5.2 – Materials and Methods

The human remains of two individuals were examined. The first individual, Ind. D (Figure 5.1), consisted of a skull in secondary deposition – the mandible was not present –, retrieved far from the main deposition site in the necropolis of Ballabio, Prato della Valle, Lecco (Italy) (Figure 5.2) (Manzon et al., 2012; Masotti et al., 2017). The Archaeological site was dated by ^{14}C to 3230 ± 90 years BP, which correspond to the Early Bronze Age/Middle Bronze Age (Lorenzi et al., 2010; Masotti et al., 2017).



Figure 5.1 – Ind. D from Ballabio: Frontal, lateral and posterior view, respectively (Photo: Filippo Scianò).



Figure 5.2 – The Archaeological site of Ballabio (Lecco) (Lorenzi, Corti and Gaetani, 2010)

The second individual, Ind. US 217 (Figure 5.3), consisted of a complete skeleton excavated in 2013 in the cemetery of the St. Biagio Church (Ravenna, Italy). The skeleton was found in a large necropolis with more than 200 individuals. It was in primary deposition and dated back from the 16th to the 18th century. The examined skeleton dates

back, presumably, to the early phase of the cemetery considering archaeological and stratigraphic details.



Figure 5.3 – Ind. US 217 from Ravenna: Skeleton during archaeological excavation procedures (Courtesy of the ‘Soprintendenza Archeologia, Belle Arti e Paesaggio per la città metropolitana di Bologna e le province di Modena, Ferrara e Reggio Emilia’).

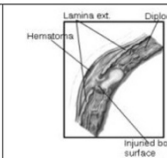
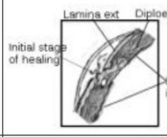
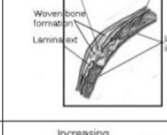
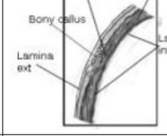
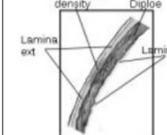
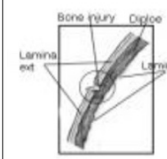
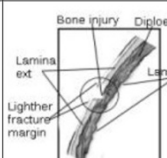
For both individuals, we determined the biological profile with the application of multiple morphometric anthropological methods for the estimation of age at death (Acsadi and Nemeskeri, 1970; Workshop of European Anthropologists, 1980; Brothwell, 1981; Lovejoy, 1985; Meindl and Lovejoy, 1985; Işcan and Loth, 1986; Brooks and Suchey, 1990; Albert and Maples, 1995; Buckberry and Chamberlain, 2002; Hens and Belcastro, 2012; Belcastro et al., 2017), sex (Acsadi and Nemeskeri, 1970; Workshop of European Anthropologists, 1980; Krogman and Işcan, 1986; Gualdi-Russo, 2007) and stature in life (Trotter and Gleser, 1951, 1958; Manouvriere, 1982). Osteometric traits were measured for the estimation of cranial capacity (Pearson, 1926; Sangeetha and Sathya Murthy, 2018).

Palaeopathological investigation and analysis of trauma were carried out *via* morphologic and microscopic approaches following indications found in the scientific literature (for morphologic analysis Pechníková, Porta, and Cattaneo 2011; Cristina Cattaneo and Cappella 2017; Cappella et al. 2014; Pickering and Bachman 2009a, Rose 1983b; Shipman 1993; Pasini et al. 2019; for microscopic analysis Schultz and Schmidt-Schultz 2015; Pechníková, Porta, and Cattaneo 2011; Pickering and Bachman 2009a; Orschiedt et al. 2003b). The description and evaluation of the traumas were carried out using the

trauma evaluation form (Figure 5.4), already described in Chapter 4 (Scianò et al., 2020) Microscopic analysis was performed on both skulls through Transmitted Light Microscope and Environmental Scanning Electronic Microscope (ESEM) at the Center of Electronic Microscopy, University of Ferrara.

To perform the microscopic analysis with ESEM, we generated a mould of the injured area. This method avoids the metallization (otherwise necessary for ESEM's analyses) of the original specimen. The cast was prepared with silicone elastomer and epoxy resin (Rose, 1983b; Orschiedt et al., 2003b), which retain any possible micro traumatic sign, ensuring a high degree of representation of micro (less than 1 μm) traces left on the surface.

Figure 5.4 – Trauma Evaluation Form (reported from Chapter 4).

Archaeological site _____ Individual _____		Date _____ Evaluator _____			
Time of trauma	Healing process	Duration	Bony responses	Presence	
<i>Ante mortem</i>	1. Formation of hematoma. Injured bone starts to regenerate due to the arrest of the hemorrhage	Within 24 hours	End of bleeding. Formation of hematoma histologically determinable.		<input type="checkbox"/>
	2. Cellular proliferation with deposition of osteoid tissue around each fragment by osteoblasts of periosteum and endosteum. Fracture is joined and visible on dry bones	Within 3 weeks	Osseous reaction. Presence of periostitis. Initial stage of healing		<input type="checkbox"/>
	3. Mineralization of osteoid that works such as a split for the periosteal and endosteal surfaces. Visible also radiologically	From 3 up to 9 weeks	Bone resorption and consequent formation of the callus made of woven bone (<i>soft callus</i>)		<input type="checkbox"/>
	4. Consolidation of the woven bone from callus precursor that results in a solidly united fracture area.	From few weeks to few months	Lamellar bone formation (<i>hard callus</i>)		<input type="checkbox"/>
	5. Gradual remodeling of bone to its original form.	From 6 to 9 years	Increase of density and strengthening along lines of mechanical stress radiologically determinable		<input type="checkbox"/>
<i>Peri mortem</i>	Occurring at or near the moment of death	Absence of bony response or healing	<ul style="list-style-type: none"> • Edges of injuries irregular and shaped; hinging bone fragments; • Cortical bone flakes along fracture margins; • Internal or/and external smoothed margins; • Radiating and concentric fractures; Staining maintained along fracture margins; • Plastic deformation. 		<input type="checkbox"/>
<i>Post mortem</i>	After death	Absence of bony response or healing	<ul style="list-style-type: none"> • Fracture margins colored of bright white, or lighter; • Bone shatters into regular fragments; • Possible taphonomic evidence (e.g. gnawing or carnivore puncture marks). 		<input type="checkbox"/>

5.3 – Results

5.3.1 - Ind. D from Ballabio (Early Bronze Age).

The skull from Ballabio was in a good condition of preservation and no severe diagenetic changes affected its integrity. According to the anthropological analysis, the skull belonged to a 25–35 years old male. Osteometric measures and indices (Table 5.1) described the form of the skull as broad (brachycranial) and high (ipsycranial), whereas the cranial capacity (obtained from the other cranial measurements) was in the male average, if compared with data from modern populations (Sangeetha and Sathya Murthy, 2018).

The paleopathological examination did not show signs of either active, nor residual pathologic features, and this both, on the internal and on the external surface of the skull. The same investigation led to the discovery of several traumatic lesions on the left parietal bone and on the frontal bone.

Table 5.1 –Measurements of the neurocranium

Ind. D (Ballabio)	Maximum Length (L) <i>(g-op)</i>	181 mm	Cephalic Index $(B \div L) * 100 = 81.2$ Brachycranial
	Maximum Width (B) <i>(eu-eu)</i>	147 mm	
	Height (H) <i>(ba-br)</i>	136 mm	Height Index $(H \div L) * 100 = 75.1$ Ipsycranial
	Cranial Capacity <i>Male:</i> $524.6 + (0.000266 * L * B * H)$	$524.6 + (0.000266 * 181 * 147 * 136) = 1487 \text{cm}^3$ Metrioccephaly	
Ind. 217 (Ravenna)	Maximum Length (L) <i>(g-op)</i>	159 mm	Cephalic Index $(B \div L) * 100 = 95$ Ultrabrachycranial
	Maximum Width (B) <i>(eu-eu)</i>	151 mm	
	Height (H) <i>(ba-br)</i>	140 mm	Height Index $(H \div L) * 100 = 88$ Ipsycranial
	Cranial Capacity <i>Female:</i> $812 + (0.000156 * L * B * H)$	$812 + (0.000156 * 159 * 151 * 140) = 1336 \text{cm}^3$ Metrioccephaly	

(Mallegni and Lippi, 2009; Minozzi and Canci, 2015; Sangeetha and Sathya Murthy, 2018)

The skull presented a particular injury on the frontal (Figure 5.5a) bone and an extended lesion on the left parietal bone (Figure 5.5b)



Figure 5.5 – Ind. D from Ballabio: **a)** Lesion on frontal bone (red arrow) and **b)** lesions on left parietal bone (Photo: Filippo Scianò).

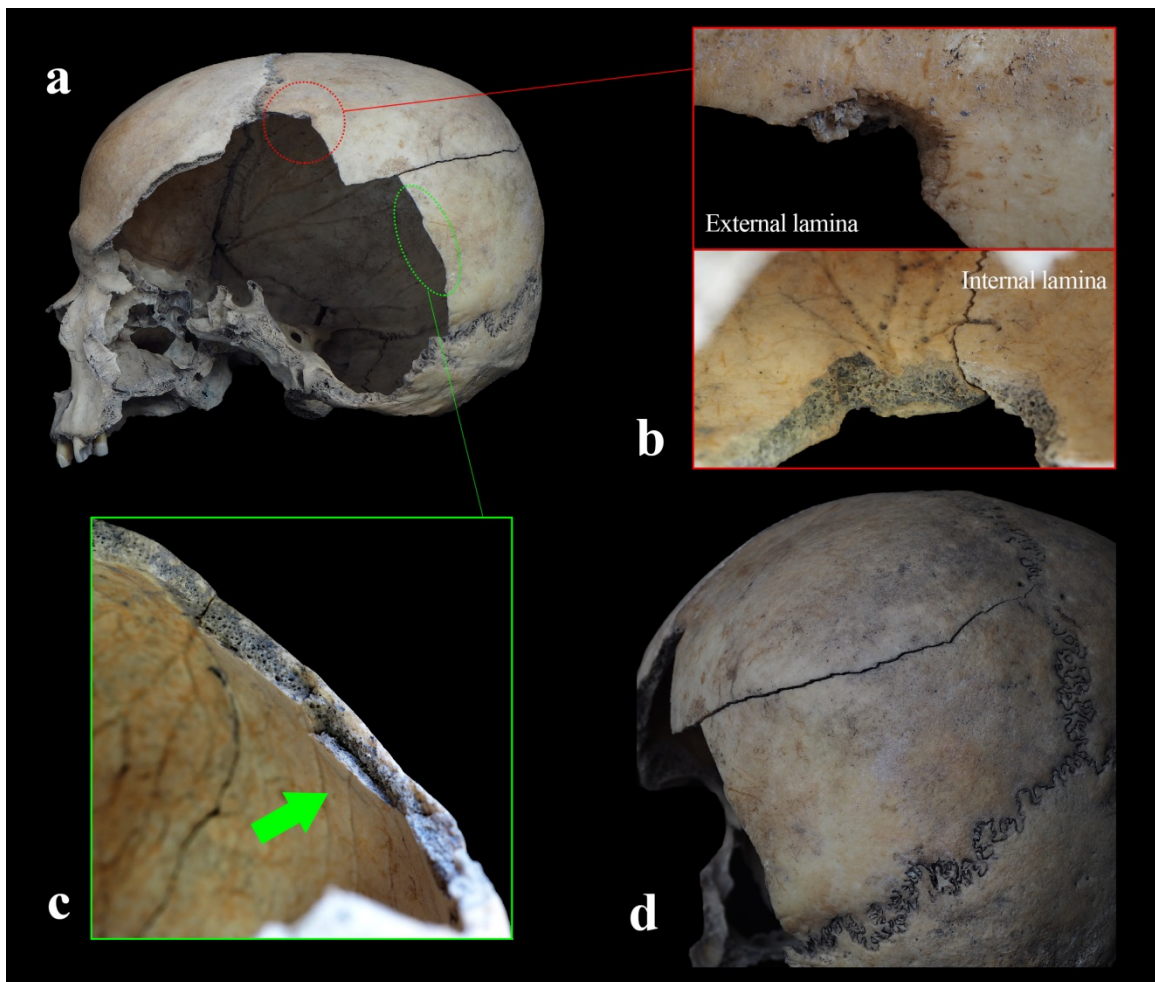


Figure 5.6 – Ind. D from Ballabio: **a)** Injuries on the parietal bone; **b)** magnified view of the injury; **c)** sharp borders and presence of bone flint (green arrow) **d)** radiating fracture (Photo: Filippo Scianò).

Two twin lesions of traumatic nature were detected on the left parietal bone (Figure 5.6a) both presented the typical features of blunt force trauma. In particular, the regular margins of the wound, the bevelling of the endocranial diplöe and the flaking of the internal lamina were diagnostic (Figure 5.6b,c). Moreover, a distinctive elastic fracture, probably a radiating fracture (Reichs and Bass, 1998; Kranioti, 2015; Kranioti et al., 2019; Pasini et al., 2019) crossed the parietal bone starting from a breakage point and ended up on the coronal suture (Figure 5.6d).

On the frontal bone, we detected a singular lesion of undetermined shape measuring 27×9 mm (Figure 5.7a). Three of the injury's margins appeared regular and sharp, forming a 90° angle to the bone surface; however, the right edge of the lesion had a sub circular enlargement (Figure 5.7a, red arrow).

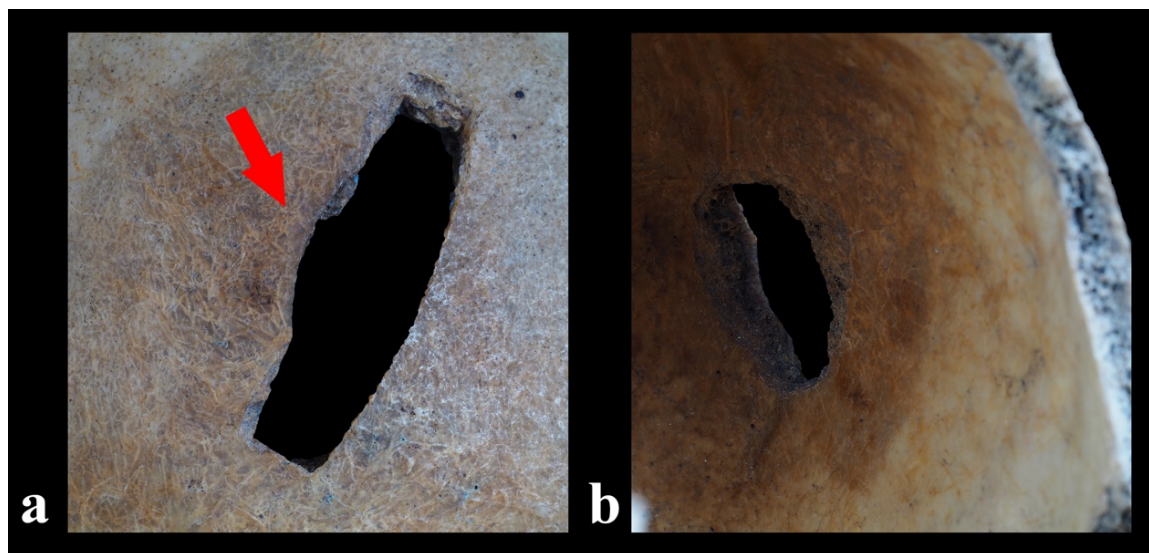


Figure 5.7 – Ind. D from Ballabio: **a)** External details of the frontal injury with a sub circular enlargement (red arrow); **b)** Internal details of the frontal injury (Photo: Filippo Scianò).

The inner wall of the latter margin was slightly inclined toward the cranial vault. All around the edges of the lesion, micro-fractures were visible on both, the inner and the outer surfaces. The internal lamina showed also a marked bevelling and partial exposure of the diplöe (Figure 5.7b). No radiating or further fractures were observed around this injury.

The analysis of the lesion's edges of the frontal bone by ESEM showed the presence of traumatic breakthrough attested by the regular notched morphology of the internal edges and the presence of micro-fractures (Figure 5.8).

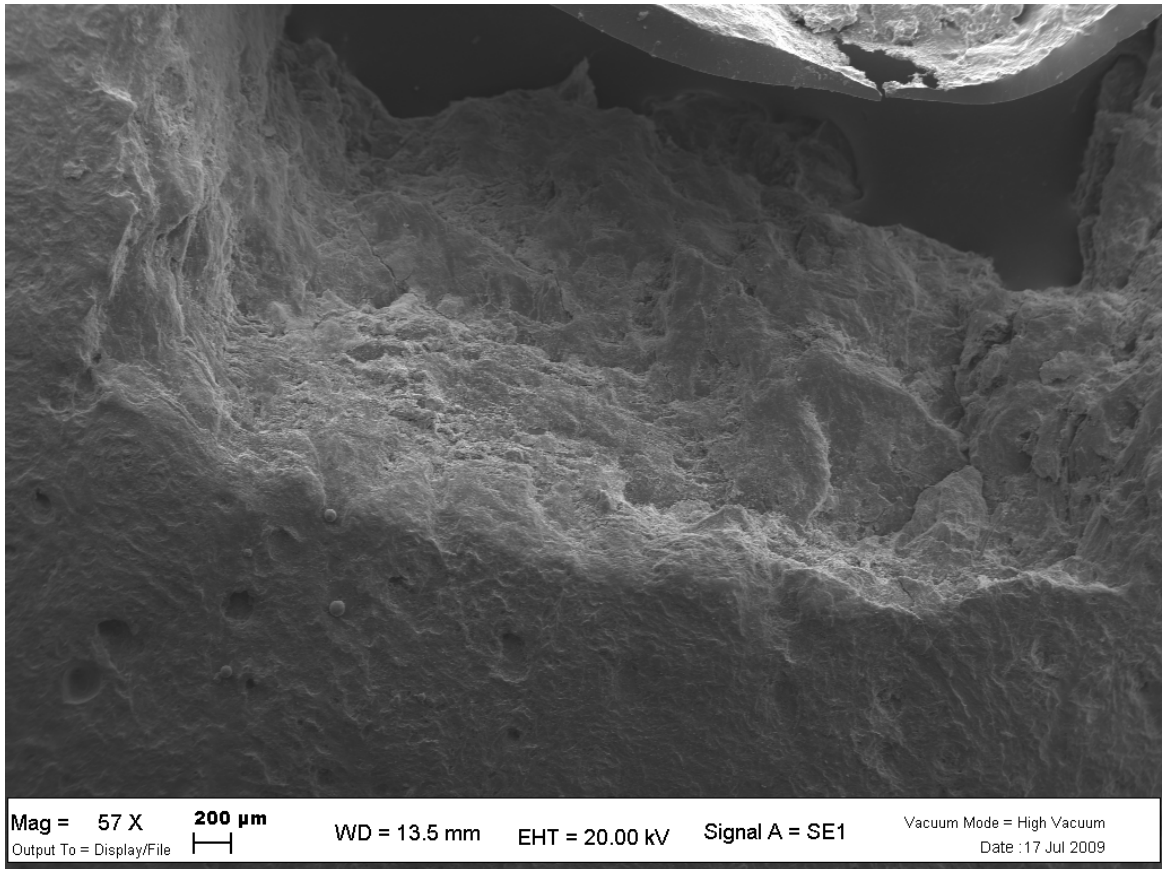


Figure 5.8 - Ind. D from Ballabio: Picture from the 'Environmental Scanning Electron Microscope', analysis of the internal rim of the frontal injury (Pasini et al., 2019).

5.3.2 - Individual US 217 from Ravenna (17th - 18th century).

The skeleton of the individual US 217 (Figure 5.3) was found in primary deposition and belonged to an adult woman with an age at death between 35 and 50 years, and an estimated stature in life of 156.4 ± 4.2 cm.

The osteometric analysis of the skull (Table 5.1) identified the individual as Ultra-brachycranial and Ipsyranic, with a cranial capacity in the female average, if compared with data from modern populations (Minozzi and Canci, 2015; Sangeetha and Sathya Murthy, 2018).

The paleopathological investigation showed the presence of an active cribra orbitalia on the left orbital roof (Figure 5.9), whose degree of severity was 3, while the degree of healing was 1, when calculated with a form previously developed by our group (Rivera and Mirazón Lahr, 2017; Rinaldo et al., 2019).

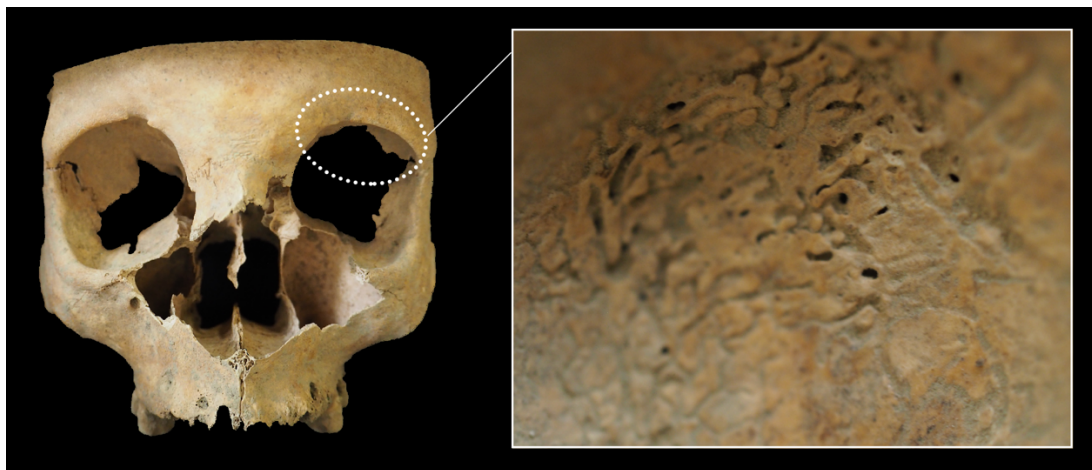


Figure 5.9 – Ind. US 217 from Ravenna: severe cribra orbitalia of the left orbital roof (Photo: Filippo Scianò).

On the left side of the endocranial surface of the frontal bone, we detected a singular and well identifiable osteolytic lesion of **14 mm** in diameter, closely connected to the deep blood vessels (*artery sulci prefrontali and venae superiores cerebri*) (Figure 5.10).

Yet, the most significant traumatic evidence of the calvaria was a deep sawing cut mark along the transversal plane, passing through the *Ophryon - Lambda landmarks* (Figure 5.11). On both, superior and inferior, sides of the sawed skull there were traces left by the tool used for the cut, likely a rip saw, as previously described (Kirkup, 1995; Reichs and Bass, 1998; Saville et al., 2007a).

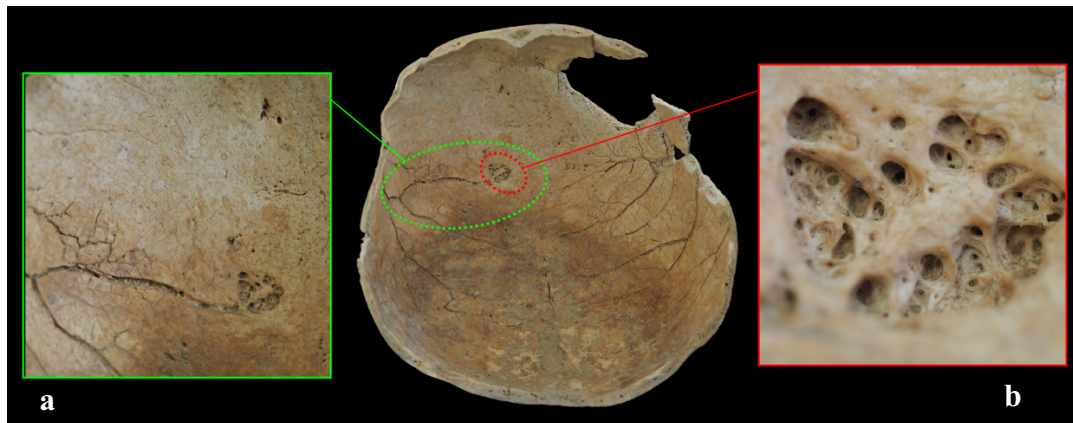


Figure 5.10 – Ind. US 217 from Ravenna: **a)** Deep vascular impression alongside the osteolytic lesion and **b)** macro view of osteolytic lesion of the right frontal bone (Photo: Filippo Scianò).



Figure 5.11 – Ind. US 217 from Ravenna: **a)** Frontal and **b)** left lateral view of the skull with the traumatic evidence on the left side of frontal bone; **c)** posterior and **d)** right lateral view with the extensive evidence of decalotting practice (Photo: Filippo Scianò).

Microscopically, it was possible to recognize all the distinctive traits of a complete craniotomy including: *a)* the **false start kerf** (Figure 5.12a) that indicates a possible point of departure or of resumption of the cutting action; *b)* the **kerf floor** (Figure 5.12b) with **parallel striae** left by the teeth of the saw (Figure 5.12c); *c)* the area of the fracture, when

the cut was ending, with the peculiar *break-away spurs* (positive) and *notch spurs* (negative) (Figure 5.12b, red arrow); *d*) the *kerf walls* with exit chipping (Figure 5.12d).

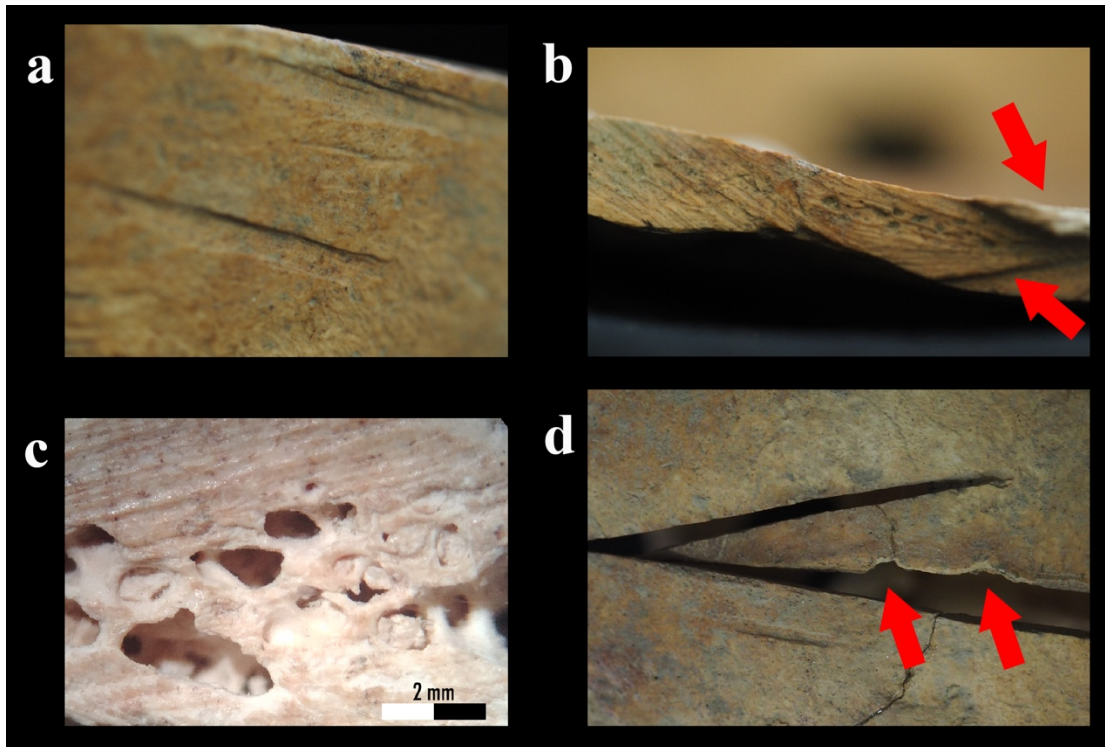


Figure 5.12 – Ind. US 217 from Ravenna: **a**) Macro view, double false-start kerf; **b**) Microscopic view of saw marks pattern (40x magnification); **c**) Macro view of saw marks on the kerf floor and convex break away spur (red arrow); **d**) Macro view of touch point between the two side of sawing lines, presence spine, false-start kerf and exit chipping (red arrows) (Photo: Filippo Scianò).

The saw marks left on the cut floor are compatible with rip saw blade made of 4/5 teeth for inch (TPI) (5/6 point for inch (PPI))¹ (cfr. Figure 5.13) (Symes, 1992; Reichs and Bass, 1998; Symes et al., 2014).

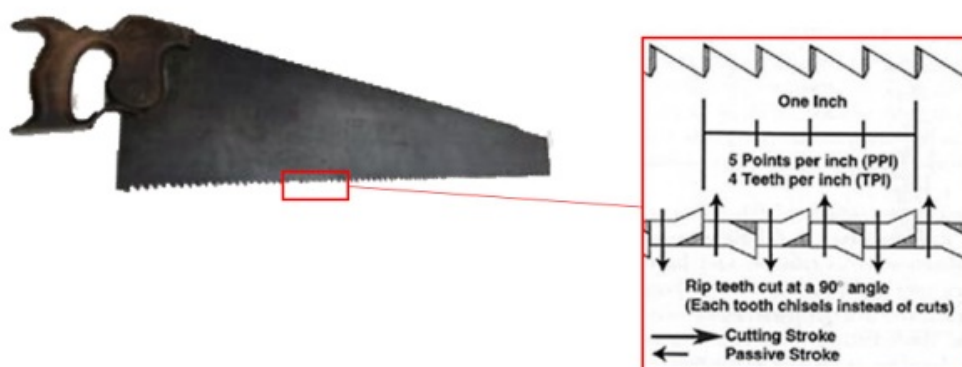


Figure 5.13 - Example of typical rip saw with number of TPI and PPI and verses of cut (cfr. Symes et al., 2014).

¹ 1 inch = 2,54 cm

Another injury, different in its features from the previous one, was observed on the left side of the frontal bone (Figure 5.14a). The lesion has an elliptical shape with a maximum diameter of 42.1 mm. Around the edges of this lesion, the external lamina is not affected by residual traces left by the “weapon”; neither there are signs of bone reaction (periostitis) or pathologic reaction (osteitis). The margins of this lesion were sharp and well defined, with no traces of bone remodelling (osteoblastic activity). There were no signs of *discoloration* and no *diagenetic changes* were visible on the area around the fracture. Vestiges of radial fractures were visible (Figure 5.14a, red arrows). On the endocranial surface, the edges of the lesion were irregular, the *diplöe* was exposed and the margins of the fracture intro-flexed (Figure 5.14b). In addition, the surface along the lesion was characterized by a typical detachment of small bone flakes (Figure 5.14b red arrows) and internal *beveling* along the periphery, as previously described in other cases (Lovell, 1997; Reichs and Bass, 1998).

The postcranial skeleton did not show any pathological or traumatic evidence, unlike the skull that was affected by different pathological changes as well as by a wide deformation due to diagenetic processes.

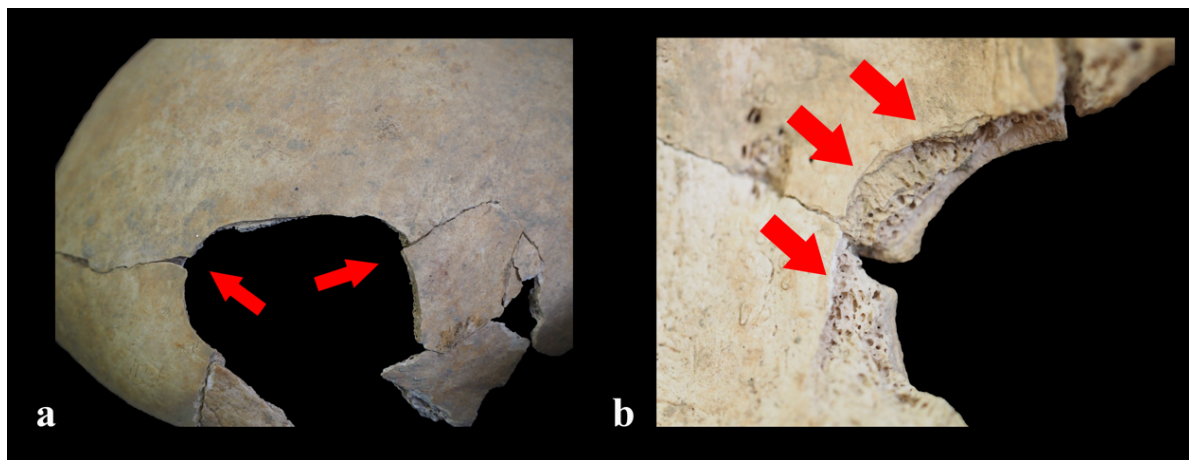
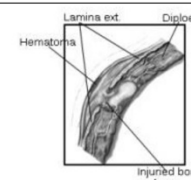
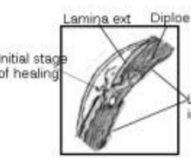
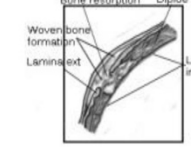
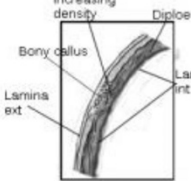
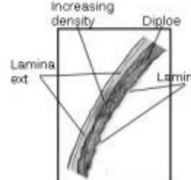
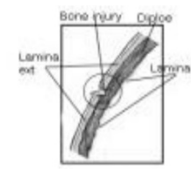
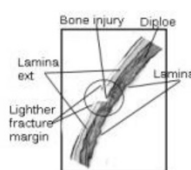


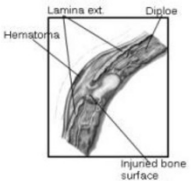
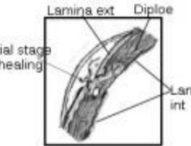
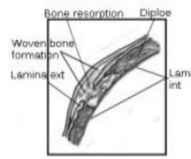
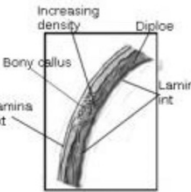
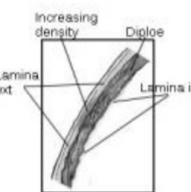

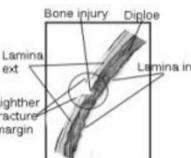
Figure 5.14 – Ind. US 217 from Ravenna: **a**) Area of traumatic lesion of the left frontal bone, probable radial fractures (red arrows) and **b**) macro view of the margin of the lesion – flakes’ detachment (red arrows) and beveling (Photo: Filippo Scianò).

All traumatic lesions present on both individual’s skull – Ind. D and Ind. US 217 – did not show any trace of healing processes. The comparison with other similar cases in the scientific literature (Symes et al., 2012; Bunch, 2014; Blau and Ubelaker, 2016; Blau, 2017) (Rose, 1983b; Shipman, 1993; Orschiedt et al., 2003b; Pickering and Bachman, 2009; Pechníková et al., 2011; Cappella et al., 2014; Schultz and Schmidt-Schultz, 2015; Cattaneo and Cappella, 2017a; Pasini et al., 2019) and the preliminary diagnosis through

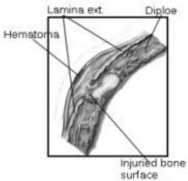
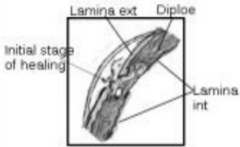
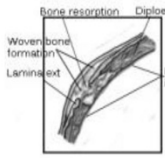
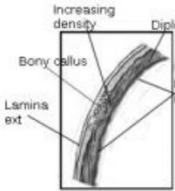
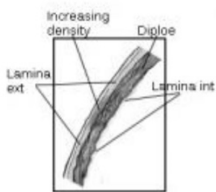

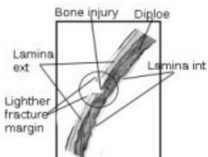
the *trauma evaluation form* (Figures. 5.15 & 5.16) suggest that the traumas occurred at or around the time of death in both subjects (Pasini et al., 2019; Scianò et al., 2020).

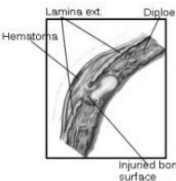
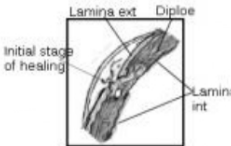
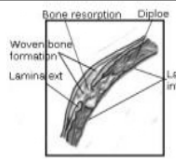
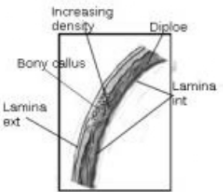
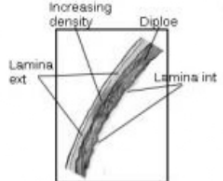


Figures 5.15 – Trauma Evaluation Forms of the Individual D from Ballabio.

Archaeological site: Ballabio		Individual: D (Frontal Lesion)			
Date 14/05/2019 /Ferrara		Evaluator: Filippo Scianò			
Time of trauma	Healing process	Duration	Bony responses	Presence	
<i>Ante mortem</i>	1. Formation of hematoma. Injured bone starts to regenerate due to the arrest of the hemorrhage	Within 24 hours	End of bleeding. Formation of hematoma histologically determinable.		<input type="checkbox"/>
	2. Cellular proliferation with deposition of osteoid tissue around each fragment by osteoblasts of periosteum and endosteum. Fracture is joined and visible on dry bones	Within 3 weeks	Osseous reaction. Presence of periostitis. Initial stage of healing		<input type="checkbox"/>
	3. Mineralization of osteoid that works such as a split for the periosteal and endosteal surfaces. Visible also radiologically	From 3 up to 9 weeks	Bone resorption and consequent formation of the callus made of woven bone (<i>soft callus</i>)		<input type="checkbox"/>
	4. Consolidation of the woven bone from callus precursor that results in a solidly united fracture area.	From few weeks to few months	Lamellar bone formation (<i>hard callus</i>)		<input type="checkbox"/>
	5. Gradual remodeling of bone to its original form.	From 6 to 9 years	Increase of density and strengthening along lines of mechanical stress radiologically determinable		<input type="checkbox"/>
<i>Peri mortem</i>	Occurring at or near the moment of death	Absence of bony response or healing	<ul style="list-style-type: none"> • Edges of injuries irregular and shaped; hinging bone fragments; • Cortical bone flakes along fracture margins; • Internal or/and external smoothed margins; • Radiating and concentric fractures; Staining maintained along fracture margins; • Plastic deformation. 		X X X X X
<i>Post mortem</i>	After death	Absence of bony response or healing	<ul style="list-style-type: none"> • Fracture margins colored of bright white, or lighter; • Bone shatters into regular fragments; • Possible taphonomic evidence (e.g. gnawing or carnivore puncture marks). 		<input type="checkbox"/> <input type="checkbox"/> <input type="checkbox"/>

Archaeological site: Ballabio		Individual: D (Parietal Lesion)			
Date 14/05/2019 /Ferrara		Evaluator: Filippo Scianò			
Time of trauma	Healing process	Duration	Bony responses	Presence	
<i>Ante mortem</i>	1. Formation of hematoma. Injured bone starts to regenerate due to the arrest of the hemorrhage	Within 24 hours	End of bleeding. Formation of hematoma histologically determinable.		<input type="checkbox"/>
	2. Cellular proliferation with deposition of osteoid tissue around each fragment by osteoblasts of periosteum and endosteum. Fracture is joined and visible on dry bones	Within 3 weeks	Osseous reaction. Presence of periostitis. Initial stage of healing		<input type="checkbox"/>
	3. Mineralization of osteoid that works such as a split for the periosteal and endosteal surfaces. Visible also radiologically	From 3 up to 9 weeks	Bone resorption and consequent formation of the callus made of woven bone (<i>soft callus</i>)		<input type="checkbox"/>
	4. Consolidation of the woven bone from callus precursor that results in a solidly united fracture area.	From few weeks to few months	Lamellar bone formation (<i>hard callus</i>)		<input type="checkbox"/>
	5. Gradual remodeling of bone to its original form.	From 6 to 9 years	Increase of density and strengthening along lines of mechanical stress radiologically determinable		<input type="checkbox"/>
<i>Peri mortem</i>	Occurring at or near the moment of death	Absence of bony response or healing	<ul style="list-style-type: none"> • Edges of injuries irregular and shaped; hinging bone fragments; • Cortical bone flakes along fracture margins; • Internal or/and external smoothed margins; • Radiating and concentric fractures; Staining maintained along fracture margins; • Plastic deformation. 		X X X X
<i>Post mortem</i>	After death	Absence of bony response or healing	<ul style="list-style-type: none"> • Fracture margins colored of bright white, or lighter; • Bone shatters into regular fragments; • Possible taphonomic evidence (e.g. gnawing or carnivore puncture marks). 		<input type="checkbox"/> <input type="checkbox"/> <input type="checkbox"/>

Figures 5.16 – Trauma Evaluation Forms of the Individual US 217 from Ravenna.

Archaeological site: Ravenna (Church of S. Biagio)		Individual: US 217 (Frontal Lesion)			
Date 14/05/2019 /Ferrara		Evaluator: Filippo Scianò			
Time of trauma	Healing process	Duration	Bony responses		Presence
<i>Ante mortem</i>	1. Formation of hematoma. Injured bone starts to regenerate due to the arrest of the hemorrhage	Within 24 hours	End of bleeding. Formation of hematoma histologically determinable.		<input type="checkbox"/>
	2. Cellular proliferation with deposition of osteoid tissue around each fragment by osteoblasts of periosteum and endosteum. Fracture is joined and visible on dry bones	Within 3 weeks	Osseous reaction. Presence of periostitis. Initial stage of healing		<input type="checkbox"/>
	3. Mineralization of osteoid that works such as a split for the periosteal and endosteal surfaces. Visible also radiologically	From 3 up to 9 weeks	Bone resorption and consequent formation of the callus made of woven bone (<i>soft callus</i>)		<input type="checkbox"/>
	4. Consolidation of the woven bone from callus precursor that results in a solidly united fracture area.	From few weeks to few months	Lamellar bone formation (<i>hard callus</i>)		<input type="checkbox"/>
	5. Gradual remodeling of bone to its original form.	From 6 to 9 years	Increase of density and strengthening along lines of mechanical stress radiologically determinable		<input type="checkbox"/>
<i>Peri mortem</i>	Occurring at or near the moment of death	Absence of bony response or healing	<ul style="list-style-type: none"> • Edges of injuries irregular and shaped; hinging bone fragments; • Cortical bone flakes along fracture margins; • Internal or/and external smoothed margins; • Radiating and concentric fractures; Staining maintained along fracture margins; • Plastic deformation. 		<input checked="" type="checkbox"/> <input checked="" type="checkbox"/> <input checked="" type="checkbox"/> <input checked="" type="checkbox"/> <input checked="" type="checkbox"/>
<i>Post mortem</i>	After death	Absence of bony response or healing	<ul style="list-style-type: none"> • Fracture margins colored of bright white, or lighter; • Bone shatters into regular fragments; • Possible taphonomic evidence (e.g. gnawing or carnivore puncture marks). 		<input type="checkbox"/> <input type="checkbox"/> <input type="checkbox"/>

Archaeological site: Ravenna (Church of S. Biagio)		Individual: US 217 (Surgical Scalping)			
Date 14/05/2019 /Ferrara		Evaluator: Filippo Scianò			
Time of trauma	Healing process	Duration	Bony responses	Presence	
<i>Ante mortem</i>	1. Formation of hematoma. Injured bone starts to regenerate due to the arrest of the hemorrhage	Within 24 hours	End of bleeding. Formation of hematoma histologically determinable.		<input type="checkbox"/>
	2. Cellular proliferation with deposition of osteoid tissue around each fragment by osteoblasts of periosteum and endosteum. Fracture is joined and visible on dry bones	Within 3 weeks	Osseous reaction. Presence of periostitis. Initial stage of healing		<input type="checkbox"/>
	3. Mineralization of osteoid that works such as a split for the periosteal and endosteal surfaces. Visible also radiologically	From 3 up to 9 weeks	Bone resorption and consequent formation of the callus made of woven bone (<i>soft callus</i>)		<input type="checkbox"/>
	4. Consolidation of the woven bone from callus precursor that results in a solidly united fracture area.	From few weeks to few months	Lamellar bone formation (<i>hard callus</i>)		<input type="checkbox"/>
	5. Gradual remodeling of bone to its original form.	From 6 to 9 years	Increase of density and strengthening along lines of mechanical stress radiologically determinable		<input type="checkbox"/>
<i>Peri mortem</i>	Occurring at or near the moment of death	Absence of bony response or healing	<ul style="list-style-type: none"> • Edges of injuries irregular and shaped; hinging bone fragments; • Cortical bone flakes along fracture margins; • Internal or/and external smoothed margins; • Radiating and concentric fractures; Staining maintained along fracture margins; • Plastic deformation. 		X X X X
<i>Post mortem</i>	After death	Absence of bony response or healing	<ul style="list-style-type: none"> • Fracture margins colored of bright white, or lighter; • Bone shatters into regular fragments; • Possible taphonomic evidence (e.g. gnawing or carnivore puncture marks). 		<input type="checkbox"/> <input type="checkbox"/> <input type="checkbox"/>

5.4 – Discussion and Conclusion

The biological profiles of the two individuals indicate that both died at an adult age and probably both suffered a violent death inflicted by another person. In the following, we propose a plausible reconstruction of the events occurred.

5.4.1 – *Ind. D from Ballabio (Early Bronze Age)*

Considering the frontal lesions of Ind. D (Ballabio, Early Bronze Age), the ESEM scanning provided important information on the microstructure of the lesion, although it was not possible to trace back which raw material the weapon was made of stone, metal, antler or bone were all plausible possibilities. Nevertheless, we were able to exclude stone tools due to the absence of typical multiple striae and micro-fragments present on the surface of the bone (Greenfield, 1999; Smith et al., 2007; Bertolini and Thun Hohenstein, 2017).

The features of the injuries on the left side of the skull were consistent with blunt force traumas (BFT) (Reichs and Bass, 1998; Galloway et al., 1999; Passalacqua and Fenton, 2012; Sulaiman et al., 2014; Wedel and Galloway, 2014; Scheirs et al., 2017a). The two partially conserved parietal wounds present features similar to the frontal lesion showing endocranial bevelling and a clear external margin. The fracture crossing the parietal bone shows typical traits of linear radiating fractures (Sulaiman et al., 2014; Wedel and Galloway, 2014; Miller, 2018; Pasini et al., 2019) such as elastic deformation, sharp edges, and the absence of discoloration. This traumatic evidence was probably generated by a high-energy force propagating from the impact site (Figure 5.6c) along a path of low resistance up to the coronal suture (Figure 5.6d) (Spencer, 2012; Schwitalla et al., 2014; Smith et al., 2015; Kranioti et al., 2019).

As many scholars suggest (Sauer, 1984; Bartelink et al., 2001; Cattaneo and Grandi, 2004; Brickley and Ferllini, 2007; Kimmerle and Baraybar, 2008; Lewis, 2008; Black and Ferguson, 2011; Pasini et al., 2019), sharp and blunt forces (axes or heavy swords – see also Chapter 4) yield chop-wounds marks similar to sharp-force injury marks but with fractured edges, impression fractures and often with scattering of fragments (Kimmerle and Baraybar, 2008; Lewis, 2008). Yet, on the other side, typical sharp force trauma (SFT) provide different evidences (Table 5.2), which were not observed in the Ballabio's skull.

Table 5.2 - Trauma breakdown patterns between Sharp Force Trauma (SFT) and Blunt Force Trauma (BFT) in the skull

<i>Sharp Force Trauma (SFT) Description</i>	<i>Blunt Force Trauma (BFT) Description</i>
<ul style="list-style-type: none"> • A narrow V-shaped groove with a distinct apex at the bottom. <p style="text-align: center;">or</p> <ul style="list-style-type: none"> • A broader U-shaped groove with a flat bottom. • Uniform patterns on the bones edges. • Clean and more even slicing margins (except for scalloped edge knives and saw-like blades). 	<ul style="list-style-type: none"> • Forces travel from the outside inwards. • Depressed fractures. • Internal bevelling on the concentric and linear fractures. • Plastic deformation of the injured bone. • Slow load applied to the bone (often blows by a heavy object).
<p>(Reichs and Bass, 1998; Pickering and Bachman, 2009; Dirkmaat, 2012; Symes et al., 2012; Wedel and Galloway, 2014; Miller, 2018)</p>	

After the determination of the lesion’s patterns, we considered the possibility that all the injuries were caused by the same weapon class in the same temporal event.

This is proven also by the absence of healing processes in both injuries (see Barbian and Sledzik 2008; Cappella et al. 2014; Geber 2015; Sauer 1998; Facchini, Rastelli, and Belcastro 2008). This occurrence led us to conclude that all the injuries were inflicted *perimortem*, probably during the same traumatic event.

Since soft tissues were not present, it was not possible to determine the exact sequence of the bumps, although, by comparison with other cases (Geserick et al., 2016; Pasini et al., 2019), we propose that this individual was probably struck by a right handedness offender, starting from his upper-left side and then laterally.

With particular regard to the singular shape of the frontal injury, we also tried to point out the probable class/type of the weapon involved in this traumatic occurrence. Light and sharp weapons such as the short swords usually used in Early Bronze Age produce cut-marks of incision with a narrow cross-section and V-shaped forms, the presence of scattering in these cases is minimal (Lovell, 1997; JiméNez-Brobeil et al., 2014a; Giuffra et al., 2015; Downing and Fibiger, 2017).

Heavy and sharp weapons such as the typical Early Bronze Age axes cause large breakthrough damage due to the impact propagation, with consequent concentric and depressed fractures that characterize cranial lesions (Lovell, 1997; Rodríguez-Martín, 2006; Kimmerle and Baraybar, 2008; Lewis, 2008; Martin and Harrod, 2015).

Considering the presence of small differentiated traumatic centres with well recognizable shapes, we excluded axes as the possible weapon used.

The typical projectile lesions leave on the bone ‘grazing grooves’ (Sauer 1984) with complete, linear, radiant and multi-fragmented fractures; the shape of the lesion is usually geometric and reflects the shape of the projectile itself (Sauer, 1984; Byers, 2005; Kimmerle and Baraybar, 2008; Manzon et al., 2012; Schwitalla et al., 2014). Often, a ‘mold fenestration’² (Cattaneo e Grandi 2004) occurs with at least one sharp edge, due to the widening action of the blade (Lovell, 1997; Reichs and Bass, 1998; Ortner, 2003; Cattaneo and Grandi, 2004).

The outcomes of this differential diagnose led us to hypothesize that the traumatic lesions were inflicted by a sharpened weapon or by an object similar to a weapon with sharp edges and a specific weight intermediate between that of a heavy weapon and that of a light one, as previously described in literature (Giuffra et al., 2015). The weapon pierced the bone mirroring the shape of that part involved in the blow (Anderson, 1996; Boylston, 2000; Lewis, 2008).

All traumatic evidences (compare Sulaiman et al. 2014; Flieger et al. 2016b; A. Pasini et al. 2019; Scheirs et al. 2017a; Jiménez-Brobeil et al. 2014a) reflect a quickly assault, probably the result of an explosion of violence resulted in the murder of Ind. D.

5.4.2 - Individual US 217 from Ravenna (17th - 18th century).

Focusing our attention on the other case, the anthropological analyses showed a premature obliteration of the cranial sutures, determining an age-at-death older if compared with other, more diagnostic, methods (Işcan and Loth, 1986; Brooks and Suchey, 1990). Having also observed the “small” size of the skull (Figure 5.11), we decided to measure the skull’s capacity to detect any developmental abnormality.

The cranial measurements showed that the endocranial capacity was within the normal range of **1100 - 1400 cm³** (Table 5.1) and the reduced size of the skull (in comparison to the postcranial skeleton) was not attributable to any form of abnormality.

On the endocranial surface, we identified traces of a pre-existing pathological condition. The lytic lesion showed no traces of inflammation and/or presence of osteoblastic activity, when observed microscopically. This lesion was initially attributed to a *fovea granularis*, as described in literature (Aufderheide and Rodríguez, 2000; Ortner, 2003). However,

² Negative area, left on a surface (fresh bone in our case ed), that usually corresponds to the shape of the object.

after more careful analyses, this diagnosis was reconsidered on the basis of the shape of the lesion, the microscopic modification and its connection with the upper blood vessels. In particular, due to microscopic analyses (Figure 5.10c), we considered more reliable the diagnosis of a benign neoplasm compatible with a meningioma or a granuloma (for similar cases, see Ortner 2003; Aufderheide and Rodríguez 2000; D. Brothwell 2012; Schajowicz 1981).

The lesion circumscribed on the left side of the frontal bone is similar to an injury, probably inflicted, as well as for the Ind. D, with high level of force. The features of the injury are compatible (Reichs and Bass, 1998; Galloway et al., 1999; Kimmerle and Baraybar, 2008; Passalacqua and Fenton, 2012; Sulaiman et al., 2014; Wedel and Galloway, 2014; Scheirs et al., 2017b) with a killing probably produced by a blunt force trauma (BFT) (Table 5.2). All around the periphery of the lesion, there were no signs of inflammation or bone remodelling indicating healing processes; thus, an *ante mortem trauma* (Pechníková et al., 2011; Fleming-Farrell et al., 2013; Licata and Vecchio, 2014) could be excluded.

The absence of bone wastage and discoloration of the edges and margins of the lesion together with the presence of the elastic deformation of the bone and the internal bevelling (Moraitis and Spiliopoulou, 2006; Barbian and Sledzik, 2008; Facchini et al., 2008; Pechníková et al., 2011; Cappella et al., 2014; Cattaneo and Cappella, 2017b), led us to exclude a *post mortem modification* and confirmed the *peri mortem* timing of the traumatic event.

The absence of any tool marks along the margin of the lesion does not allow us to recognize with precision the weapon used. Moreover, considering the breakthrough damage due to the impact propagation and the presence of linear and concentric fractures that characterize the lesion (Reichs and Bass, 1998; Passalacqua and Fenton, 2012; Symes et al., 2012), we can assume that the injury was inflicted by a hand weapon, or by a weapon-like object, with rounded edges and made of a material with a heavy specific weight. This severe traumatic injury, given the extent of the damage and the characteristics of the hole, has presumably caused the death of the Ind. US 217.

The larger lesion which divided the skull across the *Ophryon - Lambda* (Figure 5.11) led us immediately recognize a scalping procedure (given the precision, most likely of surgical nature). The blade left several coarse striae (90° angle of cut) on both sides of the sawed bone. Thanks to the number, the orientation and the progress of the striae, it was possible to argue with a high level of confidence that the cut was made with a surgical

hand medical saw with 4-5 teeth for inch, as described in literature (Symes et al. 2012; Kathy Reichs and Bass 1998; Sauer 1998; Symes et al. 2014; Symes 1992), together with other surgical complementary tools (e. g. chisels and/or surgical blades).

The dissection of human bodies for medical purposes made its first appearance in Northern and Central Italy in the second half of the 13th century: «where it was rapidly accepted and institutionalized as a technique for understanding the nature and structure of human bodies. In 1300 it was used in a variety of contexts, including not only public health and criminal justice, but also medical research and teaching» (Hirt and Kovác, 2005).

With the Renaissance, the interest in the study of the human body increased significantly. Pioneers were Leonardo Da Vinci and Michelangelo, who began to dissect the human body for their anatomical studies. Autopsies were not carried out regularly before the 18th century. In this period, one of the first significant contributions was made in 1761 by Giovanni Battista Morgagni, who published "*De sedibus et causis morborum per anatomen indagatis*", a book for the application of a new autoptic system based on a rigorous experimental method (King and Meehan, 1973). This book laid the foundations for the routine application of autopsy in the investigation of human pathology.

We can assume with high level of confidence that individual US 217 has undergone a surgical autopsy of the cranial vault, similar to those previously described in literature (Kirkup, 1995; Reichs and Bass, 1998; Saville et al., 2007b; Nystrom, 2014; Blau, 2017; Zanatta and Zampieri, 2017), while no other surgical evidences, such as sternotomy or traces of limb disarticulation, were found in his postcranial skeleton.

The reason because only the craniotomy was carried out might be two-sided: a) either it was carried out after the fatal trauma or b) after a surgical practice to treat the endocranial lesion which went wrong. Considering the pathologic and traumatic evidences, the first explanation seems to be the most suitable.

After the determination of the timing of lesions, we assessed that the injuries were the probable cause of death. Another aim of the current analysis was to evaluate whether the traumatic lesions present on both skulls were intentional or accidental. In this respect, since the lesions located on the cranial bones are usually linked to assault with the intent to kill the victim (Walker, 1989; Jiménez-Brobeil et al., 2009; Passalacqua and Fenton, 2012; Lefèvre et al., 2015; Pasini et al., 2019), we assessed that the action was intentional and violent in both cases.

In the case of the individual of Ballabio, the presence of multiple traumas (probably contemporary) provides further confirmation of a case of interpersonal violence that has resulted in the murder of this Bronze Age individual (Kimmerle and Baraybar, 2008; Pinhasi and Mays, 2008; Flieger et al., 2016b).

Whilst in the case of Ravenna, the presence of a singular traumatic lesion suggests that the inflicted lesion was the cause of the individual death and the body was then subjected to the surgical analysis for medical purposes.

In conclusion, the confidence in distinguishing between different types of injuries (sharp, blunt, etc.), their timing (*ante mortem*, *peri mortem* and *post mortem*) and their correct etiology (violence or accident, sacrifice, punishment or mass murder, etc.) still represents a major challenge in paleopathological studies. Today, thanks to modern techniques the resolution of ancient “cold cases” is possible and represents a concrete possibility to increase the knowledge in the field of trauma analysis and in forensic anthropology.

5.5 – References

- Acsadi G, Nemeskeri J. 1970. *History of Human Life Span and Mortality*. Budapest: Akadémiai Kiadó.
- Albert AM, Maples WR. 1995. Stages of epiphyseal union for thoracic and lumbar vertebral centra as a method of age determination for teenage and young adult skeletons. *J Forensic Sci* 40:623–33.
- Anderson T. 1996. Cranial weapon injuries from Anglo-Saxon Dover. *Int J Osteoarchaeol* 6:10–14.
- Aufderheide AC, Rodríguez. 2000. *The Cambridge encyclopedia of human paleopathology*.
- Barbian LT, Sledzik PS. 2008. Healing following cranial trauma. *J Forensic Sci* 53:263–268.
- Bartelink EJ, Wiersema JM, Demaree RS. 2001. Quantitative Analysis of Sharp-Force Trauma: An Application of Scanning Electron Microscopy in Forensic Anthropology. *J Forensic Sci* 46.
- Belcastro MG, Bonfiglioli B, Pedrosi ME, Zuppello M, Tanganelli V, Mariotti V. 2017. The History and Composition of the Identified Human Skeletal Collection of the Certosa Cemetery (Bologna, Italy, 19th–20th Century). *Int J Osteoarchaeol* 27:912–925.
- Bertolini M, Thun Hohenstein U. 2017. Bevel-ended tools on large ungulate ribs during the Bronze Age in northern Italy: Preliminary result of functional and experimental analyses. *Quat Int* 427:253–267.
- Black SM, Ferguson E. 2011. *Forensic anthropology : 2000 to 2010*. CRC Press.
- Blau S. 2017. How traumatic: a review of the role of the forensic anthropologist in the examination and interpretation of skeletal trauma. *Aust J Forensic Sci* 49:261–280.
- Blau S, Ubelaker DH. 2016. *Handbook of Forensic Anthropology and Archaeology*. (Blau S, Ubelaker DH, editors.). Routledge.
- Boldsen JL, Milner GR, Weise S. 2015. Cranial vault trauma and selective mortality in medieval to early modern Denmark. *Proc Natl Acad Sci* 112:1721–1726.
- Boylston A. 2000. Evidence for weapon-related trauma in British archaeological samples. In: Cox M, Mays S, editors. *Human Osteology in Archaeology and Forensic Science*.

- London; Greenwich Medical Media. p 357–380.
- Brickley M, Ferllini R. 2007. Forensic anthropology : case studies from Europe. Charles C Thomas.
- Brickley M, Mckinley JI, Boylston A, Brothwell D, Connell B, Mays S, O’connell L, Richards M, Roberts C, Zakrzewski S. 2004. Guidelines to the Standards for Recording Human Remains.
- Brooks S, Suchey JM. 1990. Skeletal age determination based on the os pubis: A comparison of the Acsádi-Nemeskéri and Suchey-Brooks methods. *Hum Evol* 5:227–238.
- Brothwell D. 2012. Tumors: Problems of Differential Diagnosis in Paleopathology. In: *A Companion to Paleopathology*. Oxford, UK: Wiley-Blackwell. p 420–433.
- Brothwell DR. 1981. *Digging up bones : the excavation, treatment, and study of human skeletal remains*. Cornell University Press.
- Buckberry JL, Chamberlain AT. 2002. Age estimation from the auricular surface of the ilium: A revised method. *Am J Phys Anthropol* 119:231–239.
- Bunch AW. 2014. National academy of sciences “Standardization”: On what terms? *J Forensic Sci* 59:1041–1045.
- Byers SN. 2005. *Introduction to forensic anthropology : a textbook*. Pearson/Allyn and Bacon.
- Cappella A, Amadasi A, Castoldi E, Mazzarelli D, Gaudio D, Cattaneo C. 2014. The difficult task of assessing perimortem and postmortem fractures on the skeleton: A blind text on 210 fractures of known origin. *J Forensic Sci* 59:1598–1601.
- Cattaneo C, Cappella A. 2017a. Distinguishing between Peri- and Post-Mortem Trauma on Bone. In: *Taphonomy of Human Remains: Forensic Analysis of the Dead and the Depositional Environment*. Chichester, UK: John Wiley & Sons, Ltd. p 352–368.
- Cattaneo C, Cappella A. 2017b. Post mortem anthropology and trauma analysis. In: Davide FS, editor. *P5 medicine and justice: Innovation, Unitariness and Evidences*. Springer International Publishing. p 167–179.
- Cattaneo C, Grandi M. 2004. *Antropologia e odontologia forense : guida allo studio dei resti umani : testo atlante*. Monduzzi.
- Cattaneo C, Porta D. 2009. Trauma Analysis of Skeletal Remains. In: *Wiley Encyclopedia*

of Forensic Science. John Wiley & Sons, Ltd.

Dirkmaat DC. 2012. *A Companion to Forensic Anthropology*.

Downing M, Fibiger L. 2017. An experimental investigation of sharp force skeletal trauma with replica Bronze Age weapons. *J Archaeol Sci Reports* 11:546–554.

Facchini F, Rastelli E, Belcastro MG. 2008. Peri mortem cranial injuries from a medieval grave in Saint Peter's Cathedral, Bologna, Italy. *Int J Osteoarchaeol* 18:421–430.

Fleming-Farrell D, Michailidis K, Karantanas A, Roberts N, Kranioti EF. 2013. Virtual assessment of perimortem and postmortem blunt force cranial trauma. *Forensic Sci Int*.

Flieger A, Kölzer SC, Plenzig S, Heinbuch S, Kettner M, Ramsthaler F, Verhoff MA. 2016a. Bony injuries in homicide cases (1994–2014). A retrospective study. *Int J Legal Med* 130:1401–1408.

Flieger A, Kölzer SC, Plenzig S, Heinbuch S, Kettner M, Ramsthaler F, Verhoff MA. 2016b. Bony injuries in homicide cases (1994–2014). A retrospective study. *Int J Legal Med* 130:1401–1408.

Galloway A, Symes SA, Haglund WD, France DL. 1999. The role of the forensic anthropologist in trauma analysis. In: *Broken bones: Anthropological analysis of blunt force trauma*. . p 5–31.

Geber J. 2015. Comparative Study of Perimortem Weapon Trauma in Two Early Medieval Skeletal Populations (AD 400-1200) from Ireland. *Int J Osteoarchaeol* 25:253–264.

Geserick G, Krockner K, Schmeling T. 2016. On manual laterality (handedness) in humans and its forensic significance - a literature review. *Arch Kriminol* 239:145–166.

Giuffra V, Pejrani Baricco L, Subbrizio M, Fornaciari G. 2015. Weapon-related Cranial Lesions from Medieval and Renaissance Turin, Italy. *Int J Osteoarchaeol*.

Greenfield HJ. 1999. The origins of metallurgy: Distinguishing stone from metal cut-marks on bones from archaeological sites. *J Archaeol Sci* 26:797–808.

Gualdi-Russo E. 2007. Sex determination from the talus and calcaneus measurements. *Forensic Sci Int* 171:151–156.

Hens SM, Belcastro MG. 2012. Auricular surface aging: A blind test of the revised method on historic Italians from Sardinia. *Forensic Sci Int* 214:209.e1-209.e5.

- Hirt M, Kovác P. 2005. History of forensic medicine-the second part. The autopsy in the Middle Age and the Renaissance. *Soud Lek* 50:32–7.
- Işcan MY, Loth SR. 1986. Determination of age from the sternal rib in white males: a test of the phase method. *J Forensic Sci* 31:122–32.
- Jiménez-Brobeil SA, Roca MG, Laffranchi Z, Nájera T, Molina F. 2014a. Violence in the Central Iberian Peninsula during the Bronze Age: A Possible Prehistoric Homicide. *Int J Osteoarchaeol* 24:649–659.
- Jiménez-Brobeil SA, Roca MG, Laffranchi Z, Nájera T, Molina F. 2014b. Violence in the Central Iberian Peninsula during the Bronze Age: A Possible Prehistoric Homicide. *Int J Osteoarchaeol* 24:649–659.
- Jiménez-Brobeil SA, Du Souich P, Al Oumaoui I. 2009. Possible relationship of cranial traumatic injuries with violence in the South-East Iberian Peninsula from the Neolithic to the Bronze Age. *Am J Phys Anthropol* 140:465–475.
- Kimmerle EH, Baraybar JP. 2008. *Skeletal Trauma: Identification of Injuries Resulting from Human Rights Abuse and Armed Conflict*. CRC Press.
- King LS, Meehan MC. 1973. A history of the autopsy. A review. *Am J Pathol* 73:514–44.
- Kirkup J. 1995. The history and evolution of surgical instruments. VI. The surgical blade: from finger nail to ultrasound. *Ann R Coll Surg Engl* 77:380–8.
- Kranioti E. 2015. Forensic investigation of cranial injuries due to blunt force trauma: current best practice. *Res Reports Forensic Med Sci* 5:25–37.
- Kranioti EF, Grigorescu D, Id KH. 2019. State of the art forensic techniques reveal evidence of interpersonal violence ca. 30,000 years ago.
- Krogman WM, Iscan M. 1986. *The human skeleton in forensic medicine*. Springfield: Charles C Thomas Publisher.
- Lefèvre T, Alvarez JC, Lorin de la Grandmaison G. 2015. Discriminating factors in fatal blunt trauma from low level falls and homicide. *Forensic Sci Med Pathol* 11:152–161.
- Lewis JE. 2008. Identifying sword marks on bone: criteria for distinguishing between cut marks made by different classes of bladed weapons. *Int J Osteoarchaeol* 35:2001–2008.
- Licata M, Armocida G. 2015. Trauma lubanje: Analiza ozljeda na drevnim kosturima s

- arheoloških nalazišta u sjeverozapadnoj lombardiji. *AMHA - Acta Medico-Historica Adriat* 13:251–264.
- Licata M, Vecchio I. 2014. Analysis of ante-mortem injuries in medieval skeletons from the necropolis of caravate (Varese) Italy. *Acta Medica Mediterr.*
- Lorenzi J, Corti P, Gaetani M. 2010. Un sito sepolcrale dell'età del Bronzo a Ballabio. In: Ruffa M, editor. *Carta archeologica della Provincia di Lecco. Aggiornamento. Musei Civici di Lecco.*
- Lovejoy CO. 1985. Dental wear in the Libben population: Its functional pattern and role in the determination of adult skeletal age at death. *Am J Phys Anthropol* 68:47–56.
- Lovell NC. 1997. Trauma Analysis in Paleopathology. *Yrbk Phys Anthr* 40:139–170.
- Mallegni F, Lippi B. 2009. *Non omnis moriar : manuale di antropologia : dar voce ai resti umani del passato.* CISU.
- Manouvriere L. 1982. Détermination de la taille d'après les gran os de membres. *Rev L'Ecole Antropol* 2:227–233.
- Manzon VS, Thun Hohenstein U, Gualdi-Russo E. 2012. Injuries on a skull from the Ancient Bronze Age (Ballabio, Lecco, Italy): A natural or an anthropic origin? *J Archaeol Sci* 39:3428–3435.
- Martin DL, Harrod RP. 2015. Bioarchaeological contributions to the study of violence. *Am J Phys Anthropol* 156:116–145.
- Masotti S, Varalli A, Goude G, Moggi-ecchi J, Gualdi-russo E. 2017. A combined analysis of dietary habits in the Bronze Age site of Ballabio A combined analysis of dietary habits in the Bronze Age site of Ballabio (northern Italy).
- Meindl RS, Lovejoy CO. 1985. Ectocranial suture closure: A revised method for the determination of skeletal age at death based on the lateral-anterior sutures. *Am J Phys Anthropol* 68:57–66.
- Miller E. 2018. Forensic Anthropology. *Multidiscip Medico-Legal Death Investig*:215–225.
- Minozzi S, Canci A. 2015. *Archeologia dei resti umani : dallo scavo al laboratorio.* Carocci.
- Moraitis K, Spiliopoulou C. 2006. Identification and Differential Diagnosis of Perimortem Blunt Force Trauma in Tubular Long Bones.

- Nystrom KC. 2014. The Bioarchaeology of Structural Violence and Dissection in the 19th-Century United States. *Am Anthropol* 116:765–779.
- Orschiedt J, Häußler A, Haidle MN, Alt KW, Buitrago-Téllez CH. 2003a. Survival of a multiple skull trauma: the case of an early neolithic individual from the LBK enclosure at Herxheim (Southwest Germany). *Int J Osteoarchaeol* 13:375–383.
- Orschiedt J, Häußler A, Haidle MN, Alt KW, Buitrago-Téllez CH. 2003b. Survival of a multiple skull trauma: the case of an early neolithic individual from the LBK enclosure at Herxheim (Southwest Germany). *Int J Osteoarchaeol* 13:375–383.
- Ortner DJ. 2003. Identification of pathological conditions in human skeletal remains.
- Otto T, Thrane H, Vandkilde H. 2006. Warfare and society : archaeological and social anthropological perspectives. Aarhus University Press.
- Parker Pearson M, Thorpe IJ. 2005. Warfare, violence and slavery in prehistory : proceedings of a Prehistoric Society conference at Sheffield University. London: Archaeopress.
- Pasini A, Gualdi-Russo E, Scianò F, Thun Hohenstein U. 2019. Violence in the Early Bronze Age. Diagnosis of skull lesions using anthropological, taphonomic and scanning electron microscopy techniques. *Forensic Sci Med Pathol* 15:324–328.
- Passalacqua N V., Fenton TW. 2012. Developments in Skeletal Trauma: Blunt-Force Trauma. *A Companion to Forensic Anthropol*:400–411.
- Pearson K. 1926. On the Reconstruction of Cranial Capacity from External Measurements. :46-50.
- Pechníková M, Porta D, Cattaneo C. 2011. Distinguishing between perimortem and postmortem fractures: are osteons of any help? *Int J Legal Med* 125:591–595.
- Pickering RB, Bachman DC (David C. 2009. The use of forensic anthropology. CRC Press.
- Pinhasi R, Mays S. 2008. *Advances in Human Palaeopathology*.
- Reichs K, Bass WM. 1998. *Forensic osteology : advances in the identification of human remains*. Charles C Thomas.
- Rinaldo N, Zedda N, Bramanti B, Rosa I, Gualdi-Russo E. 2019. How reliable is the assessment of Porotic Hyperostosis and Cribra Orbitalia in skeletal human remains? A methodological approach for quantitative verification by means of a new

evaluation form. *Archaeol Anthropol Sci*.

Rivera F, Mirazón Lahr M. 2017. New evidence suggesting a dissociated etiology for cribra orbitalia and porotic hyperostosis. *Am J Phys Anthropol* 164:76–96.

Rodríguez-Martín C. 2006. Identification and Differential Diagnosis of Traumatic Lesions of the Skeleton. In: *Forensic Anthropology and Medicine*. Totowa, NJ: Humana Press. p 197–221.

Rose JJ. 1983a. A replication technique for scanning electron microscopy: Applications for anthropologists. *Am J Phys Anthropol* 62:255–261.

Rose JJ. 1983b. A replication technique for scanning electron microscopy: Applications for anthropologists. *Am J Phys Anthropol* 62:255–261.

Sangeetha K, Sathya Murthy B. 2018. Estimation of the cranial capacity in dry human skull bones. *6:5181–5185*.

Sauer N. 1984. Manner of death: skeletal evidence of blunt and sharp instrument wounds. In: Rathbun T, Buikstra J, editors. *Human identification: case studies in forensic anthropology*. Springfield: Charles C Thomas Publisher. p 177–84.

Sauer N. 1998. The timing of injuries and manner of death: distinguishing among antemortem, perimortem and postmortem trauma. In: Reichs K, editor. *Forensic osteology: advances in the identification of human remains*. Springfield: Charles C Thomas Publisher. p 321–32.

Saville PA, Hainsworth S V., Rutty GN. 2007a. Cutting crime: the analysis of the “uniqueness” of saw marks on bone. *Int J Legal Med* 121:349–357.

Saville PA, Hainsworth S V., Rutty GN. 2007b. Cutting crime: the analysis of the “uniqueness” of saw marks on bone. *Int J Legal Med* 121:349–357.

Schajowicz F. 1981. *Tumors and Tumorlike Lesions of Bone and Joints*. Springer US.

Scheirs S, Malgosa A, Sanchez-Molina D, Ortega-Sánchez M, Velázquez-Ameijide J, Arregui-Dalmases C, Medallo-Muñiz J, Galtés I. 2017a. New insights in the analysis of blunt force trauma in human bones. Preliminary results. *Int J Legal Med* 131:867–875.

Scheirs S, Malgosa A, Sanchez-Molina D, Ortega-Sánchez M, Velázquez-Ameijide J, Arregui-Dalmases C, Medallo-Muñiz J, Galtés I. 2017b. New insights in the analysis of blunt force trauma in human bones. Preliminary results. *Int J Legal Med* 131:867–

875.

- Schultz M, Schmidt-Schultz TH. 2015. Paleopathology: Vestiges of Pathological Conditions in Fossil Human Bone. In: Handbook of Paleoanthropology.
- Schwitalla AW, Jones TL, Pilloud MA, Coddling BF, Wiberg RS. 2014. Violence among foragers: The bioarchaeological record from central California. *J Anthropol Archaeol* 33:66–83.
- Scianò F, Bramanti B, Manzon VS, Gualdi-Russo E. 2020. An investigative strategy for assessment of injuries in forensic anthropology. *Leg Med* 42:101632.
- Shipman P. 1993. Life history of a fossil: an introduction to taphonomy and paleoecology. Harvard University Press.
- Smith MJ, Brickley MB, Leach SL. 2007. Experimental evidence for lithic projectile injuries: improving identification of an under-recognised phenomenon. *J Archaeol Sci* 34:540–553.
- Smith MJ, James S, Pover T, Ball N, Barnetson V, Foster B, Guy C, Rickman J, Walton V. 2015. Fantastic plastic? Experimental evaluation of polyurethane bone substitutes as proxies for human bone in trauma simulations. *Leg Med* 17:427–435.
- Spencer SD. 2012. Detecting violence in the archaeological record: Clarifying the timing of trauma and manner of death in cases of cranial blunt force trauma among pre-Columbian Amerindians of West-Central Illinois. *Int J Paleopathol* 2:112–122.
- Sulaiman NA, Osman K, Hamzah NH, Amir Hamzah SPA. 2014. Blunt force trauma to skull with various instruments. *Malays J Pathol*.
- Symes SA. 1992. Morphology of Saw Marks in Human Bone: Identification of Class Characteristics.
- Symes SA, L'Abbé EN, Chapman EN, Wolff I, Dirkmaat DC. 2012. Interpreting Traumatic Injury to Bone in Medicolegal Investigations. In: *A Companion to Forensic Anthropology*. Chichester, UK: John Wiley & Sons, Ltd. p 340–389.
- Symes SA, Ph D, Chapman EN, Rainwater CW, Cabo LL, Myster SMT, Ph D. 2014. Knife and Saw Toolmark Analysis in Bone: A Manual Designed for the Examination of Criminal Mutilation and Dismemberment.
- Trotter M, Gleser G. 1951. The effect of ageing on stature. *Am J Phys Anthropol* 9:311–324.

- Trotter M, Gleser GC. 1958. A re-evaluation of estimation of stature based on measurements of stature taken during life and of long bones after death. *Am J Phys Anthropol* 16:79–123.
- Walker PL. 1989. Cranial injuries as evidence of violence in prehistoric southern California. *Am J Phys Anthropol* 80:313–23.
- Wedel VL, Galloway A. 2014. Broken bones : anthropological analysis of blunt force trauma.
- Workshop of European Anthropologists. 1980. Recommendations for Age and Sex Diagnosis of Skeletons. *J Hum Evol* 9:517–549.
- Zanatta A, Zampieri F. 2017. Gli scalottati di Vicenza. Analisi antropologica dei resti rinvenuti a Palazzo San Michele. *Antrocom Online J Anthropol* 13:99–108.

CHAPTER 6

CONCLUSION

This dissertation aimed to illustrate the investigate work carried out during my PhD research training, in order to simplify the diagnosis of some lesions that are difficult to interpret in ancient human remains.

We observed early, during this research, that in the majority of the cases, an accurate diagnosis of the lesions found on ancient skeletons cannot be obtained only with the morphological observation, even though this is the fundamental starting point. Here we proposed alternative strategies for the study of the skeletal lesions and for their differential diagnosis. The development of new strategies was possible thanks to recent biomedical advances and clinical studies that have provided more insights applicable to the study of ancient diseases.

We developed and successfully applied to osteological samples of different archaeological periods a workflow consistent of progressive analyses. This approach has been demonstrated to provide a precise and accurate identification of all modifications of the bone, even if not visible at the macroscopic level.

For the diagnosis of β -thalassemia on dry human bones, we identified several indicators and classified them as ‘nonspecific’, ‘specific not-diagnostic’ and ‘diagnostic’. On this basis, we developed a new evaluation form for the preliminary detection of β -thalassemia from osteological materials. The application of the evaluation form to 71 samples, enabled us to find several potentially (homozygote or heterozygote) β -thalassemic individuals at Sovana. For many centuries, the presence of large marshlands in Maremma, has been an ideal boost for the development of malaria and, consequently, a favourable condition for the presence of thalassemia syndrome in the genetic pool of the population of this region. On the other hand, the evaluation form denied the presence of the β -thalassemia in the three individuals from Spina, despite the presence of several nonspecific indicators on the skull, and their provenience from a similar environment.

A further development of the study on β -thalassemia might consider the analysis of hemozoin, a molecule released in malaria patients, which is also detectable in archaeological samples, and the study of ancient DNA, to confirm the results obtained with our analyses.

The same work-strategy has permitted us also to shed a light on other pathological lesions of difficult detection and interpretation, like the tumours (i.e., osteoblastoma) of the frontal sinus. We highlighted the importance of this finding, which has been only once reported previously in the scientific literature (see Chapter 3). Curiously, the previous reported case was originated from a locality not far away from Sovana, where our affected individuals came from, and was almost coeval. This aspect should be analysed more in-deep, if there was some carcinogen substance or habit in the region, which may have constituted a concomitant cause of the neoplastic formations.

Chapters fourth and fifth dealt with the lively debate on the difficulty of the assessment of the lesion's timing in anthropology. Considering the high incidence of traumatic lesions in ancient time, to ascertain if the lesion was caused before, around or after the death is mandatory. We thought that distinguishing between different types of injuries with confidence, and establishing their timing and their correct aetiology represented the main challenge in paleopathological studies.

In this regard, the development of a new evaluation form to assess the lesion' timing, in order to facilitate the detection of traumas and interpret them as *ante mortem*, *peri mortem* and *post mortem* injuries, was an additional significant result. The outcomes of this study are now published in a peer-reviewed journal.

In conclusion, we are confident that the multidisciplinary and progressive approach we have developed for the preliminary diagnosis of bone lesions, and successfully applied, may be of great help in physical anthropology, especially for the identification of those diseases difficult to be diagnosed, such as hematopoietic disorders, tumours, and unclear traumatic lesions. We wish that the strategies developed will be used also by other scholars, a necessary condition for a further confirmation or an improvement of our studies on skeletal lesions.

LIST OF TABLES

Chapter 2

- Table 2.1** - Characteristics of β -Thalassemia Syndromes (from Kumar et al. 2011, modified). pag. 24
- Table 2.2** - Lesions of β -thalassaemia syndrome on archaeological human remains. pag. 32
- Table 2.3** – Evaluation Form Score Results (Accuracy Range). pag. 33
- Table 2.4** – Application of the Evaluation Form on specimens from published studies. pag. 36
- Table 2.5** – Kind of analyses performed and results obtained with the application of the Evaluation Form on Spina Valle Pega human remains. pag. 38
- Table 2.6** – Kind of analyses performed and Results obtained with the application of the Evaluation Form on the Sovana, Chiesa di San Mamiliano human remains. pag. 38

Chapter 3

- Table 3.1:** Differential diagnosis carried out considering the most probable tumors affecting the skull pag. 112
- Table 3.2:** Paleopathological scientific literature reporting cases of osteoma and osteoblastomas in ancient human remains. pag. 117

Chapter 4

- Table 4.1** - Assessment of the time of trauma occurrence in the examined case-studies. pag. 132
- Table 4.2** - Lesions characteristics. pag. 133

Chapter 5

- Table 5.1** – Measurements of the neurocranium. pag. 149
- Table 5.2** - Trauma breakdown patterns between Sharp Force Trauma (SFT) and Blunt Force Trauma (BFT) in the skull. pag. 162

LIST OF FIGURES

Chapter 1

Figure 1.1 – Example of a) severe porotic hyperostosis on the right parietal and b) severe cribra orbitalia on the orbital roof (Photo: Filippo Scianò). pag. 4

Figure 1.2 – The Molecular basis of β -thalassemia. **a)** Human β -globin gene in chromosome 11. The grey areas are that region transcribed but not translated. The red areas are the exons. The numbers represent the β -globin amino-acids residues encoded by the three exons. **b)** Type and distribution of the mutations in the β -thalassaemia syndrome (Original picture taken from Origa, 2017)[©]. pag. 5

Figure 1.3 – Methodological approach and progressive analysis carried out in our study (Picture: Filippo Scianò). pag 12

Chapter 2

Figure 2.1 – Red Blood Cell abnormalities in Eurasia. pag. 22

Figure 2.2 – Distribution of Malaria in Italy, illustrated by Luigi Torelli - Firenze: G. Pellas, 1882, Firenze. pag. 28

Figure 2.3 – Work-flow for the detection of probable β -thalassemia individuals in skeletal populations. pag. 31

Figure 2.4 – Evaluation Form for the investigation of β -thalassemia in skeletons. pag. 34

Figure 2.5 – Distribution of presence/absence of β -thalassemia syndrome in the Sovana San Mamiliano specimens. pag. 40

Figure 2.6 – Frontal, superior and basal view of the neurocranium of Individual 4IIa (Photo: Filippo Scianò). pag. 41

Figure 2.7 – X-ray view of the frontal bone of Individual 4IIa (Photo: Filippo Scianò). pag. 41

Figure 2.8 –Endoscopic views of: **a)** vascular impression due to an emorragic process and **b)** Porotic Hyperostosis of the frontal bone; The TGSs show: **c)** compression of the cortical bone tissue by blood vessels (70 μ , polarized light microscope with quartz as compensator, 100x magnification); **d)** sclerosis of the diploe which appears irregular and enlarged (70 μ , polarized light microscope with quartz as compensator, 25x magnification) (Photo: Filippo Scianò). pag. 42

Figure 2.9 – Endoscopic **(a)** and microscopic **(b)** view of the severe cribra orbitalia of the right orbital roof. The TGSs show: **c)** sclerotic changes with a lateralization of the trabeculae (70 μ , polarized light microscope with quartz as pag. 43

compensator, 25x magnification), and **d**) a severe brush-like trabeculae with thinning process of the external lamina (50 μ , polarized light microscope with quartz as compensator, 16x magnification) (Photo: Filippo Scianò).

Chapter 3

Figure 3.1 – Sovana (GR), Italy, and the complex of the Church of San Mamiliano (Ph®). pag. 103

Figure 3.2 – Plan of the Church of San Mamiliano (Sovana, Italy). The floor is entirely occupied by burials. Underneath, the ruins of a Roman building (red) and of late antique structures (green) are visible. pag. 103

Figure 3.3 – Skull of Individual SSM 81: a) Posterior view: signs of inflammation of the cortical bone are present on both parietals. The red square shows the area where a sample was taken; b) Frontal view: the red square shows the area where the first sample was taken, the green one shows the place where the second sample was taken; c) Right lateral view: *post-mortem* abrasion on the right parietal (red arrow) (Photo: Filippo Scianò). pag 106

Figure 3.4 - Skull of Individual SSM 81: The Radiography (b) in left lateral view (a), shows the presence of the small teardrop-shaped new bone formation on the edge of the left frontal sinus (red circle) (Photo: Filippo Scianò). pag. 106

Figure 3.5 –TGSs of the right parietal from the skull of Individual SSM 81: **a**¹) microscopy of the cortical bone, which appears enlarged and irregular, and shows presence of periosteal inflammation (16x Magnification, 50 μ m and 70 μ m, transmitted light); **a**²) vision in polarized light; **a**³) vision in transmitted light and polarizing filter with quartz as compensator; **b**¹) microscopy of the cortical and trabecular bone. The external lamina appears thick with traces of blood vessel canals. The trabeculae are irregular but normal for the range of age-at-death of the individual; **b**²) vision in polarized light; **b**³) vision in transmitted light and polarizing filter with quartz as compensator (16x Magnification, 50 μ m and 70 μ m, transmitted light and polarizing filter with quartz as compensator) (Photo: Filippo Scianò). pag. 107

Figure 3.6 –TGS of the frontal bone from the skull of Individual SSM 81: **a**) microscopy of the cortical bone, which appears thickened due an osteolytic reaction of the bone. Some traces of diagenetic changes are present; **b**) vision in polarized light, post production in B&W; **c**) vision in transmitted light and polarizing filter with quartz as compensator (16x Magnification, 70 μ m) (Photo: Filippo Scianò). pag. 108

Figure 3.7 - Skull vault of Individual SSM 92: **a**) Area (white square), where a sample of the frontal bone was taken from; **a**¹) endoscopy of the frontal right sinus with the neoplastic lesion on the internal surface of the pag. 109

bone. Two level of magnification (10x & 20x) (white circles). Green arrows show the *fovea granulares*; The white narrow indicates the localization of the lesion in the frontal sinus; **b**) Norma superioris of the right parietal with the lesioned area, where the sample was taken (white square); **b¹**) magnified view (10x & 20x) of the area with the lesion which affects the lamina interna (white circle) (Photo: Filippo Scianò).

Figure 3.8 - Skull vault of Individual SSM 92: **a**) Sampling area of the right supraorbital margin taken for TGSs preparation (white square); **a¹**) microscopy of the cortical bone, which appears enlarged, sclerotic and ipervascularized (50µm, transmitted light and polarizing filter with quartz as compensator); **b**) TGS of the neoplastic lesion (white arrow); **b¹**) Partially globular new bone formation which involved the diploe (70µm, transmitted light and polarizing filter with quartz as compensator); **c**) TGS of the right parietal bone (white circle & white square); **c¹**) irregular and confused trabecular growth; **c²**) Slight osteolytic slow-growing lesion with multiple layers of new bone apposition which became mature bone (Haversian systems are present) (50µm and 70µm, polarizing filter with quartz as compensator) (Photo: Filippo Scianò).

pag. 111

Chapter 4

Figure 4.1 - Trauma evaluation form with illustration and description of the features of different lesions and healing processes (Scianò et al, 2020).

pag. 129

Figure 4.2 – Instruments used for the macroscopic and microscopic analyses: **a**) spreading caliper; **b**) sliding caliper; **c**) osteometric table; **d**) microscope Optika Microscope – B-380; **e**) microscope Leica S8AP0 with Leica Camera DC500 (Photo: Filippo Scianò).

pag. 131

Figure 4.3 – Ind No. 114: **a**) Chop wound on the right supraorbital margin; **b**) Right orbital roof surface, with inflammatory process of the bone (white arrows); **c**) CT scan of the traumatized area, with different density districts (white arrows); **d**) Histologic section: view through the light microscope (15 µm section in Masson's trichrome stain, Magnification 40x) of the right supraorbital margin, with cortical bone, remodeled after the lesion (osteoblastic activity) on the entire surface (red arrows); **e**) Histologic section of the right supraorbital margin: view through the light microscope (15 µm section in Masson's trichrome stain, Magnification 200x) of the traumatized area with inflammatory reaction on the outer surface (red arrows) and signs of osteoclastic activity (Howship's lacunae – green arrows.; (Scianò et al, 2020).

pag 133

Figure 4.4 – Ind No. 114; Cone-Beam of the traumatized area on the right supraorbital margin; **a**) MPR scan in frontal, basal and lateral view and **b**)

pag. 134

3D-CT treated picture for in deep analyses of the injury (Picture: Filippo Scianò).

Figure 4.5 – Ind No. 114: Mandibular malocclusion due to **a)** dislocation of the temporo-mandibular joint; **b)** creation of new articular facet on the inferior inner surface of the zygomatic arch (white arrow); **c)** Erosion and adaptation of the right mandibular condyle (Photo: Filippo Scianò). pag. 135

Figure 4.6 – Ind No. 118: Post mortem cut mark of the right mastoid process (Photo: Filippo Scianò). pag. 135

Chapter 5

Figure 5.1 – Ind. D from Ballabio: Frontal, lateral and posterior view, respectively (Photo: Filippo Scianò). pag. 145

Figure 5.2 – The Archaeological site of Ballabio (Lecco) (Lorenzi, Corti and Gaetani, 2010). pag. 145

Figure 5.3 – Ind. US 217 from Ravenna: Skeleton during archaeological excavation procedures (Courtesy of the ‘Soprintendenza Archeologia, Belle Arti e Paesaggio per la città metropolitana di Bologna e le province di Modena, Ferrara e Reggio Emilia’). pag. 146

Figure 5.4 – Trauma Evaluation Form (reported from Chapter 4). pag. 148

Figure 5.5 – Ind. D from Ballabio: **a)** Lesion on frontal bone (red arrow) and **b)** lesions on left parietal bone (Photo: Filippo Scianò). pag. 150

Figure 5.6 – Ind. D from Ballabio: **a)** Injuries on the parietal bone; **b)** magnified view of the injury; **c)** sharp borders and presence of bone flint (green arrow) **d)** radiating fracture (Photo: Filippo Scianò). pag. 150

Figure 5.7 – Ind. D from Ballabio: **a)** External details of the frontal injury with a sub circular enlargement (red arrow); **b)** Internal details of the frontal injury (Photo: Filippo Scianò). pag. 151

Figure 5.8 - Ind. D from Ballabio: Picture from the ‘Environmental Scanning Electron Microscope’, analysis of the internal rim of the frontal injury (Pasini et al., 2019). pag. 152

Figure 5.9 – Ind. US 217 from Ravenna: severe cribra orbitalia of the left orbital roof (Photo: Filippo Scianò). pag. 153

Figure 5.10 – Ind. US 217 from Ravenna: **a)** Deep vascular impression alongside the osteolytic lesion and **b)** macro view of osteolytic lesion of the right frontal bone (Photo: Filippo Scianò). pag. 154

Figure 5.11 – Ind. US 217 from Ravenna: **a)** Frontal and **b)** left lateral view of the skull with the traumatic evidence on the left side of frontal bone; **c)** pag. 154

posterior and **d**) right lateral view with the extensive evidence of decalotting practice (Photo: Filippo Scianò).

Figure 5.12 – Ind. US 217 from Ravenna: **a**) Macro view, double false-start kerf; **b**) Microscopic view of saw marks pattern (40x magnification); **c**) Macro view of saw marks on the kerf floor and convex break away spur (red arrow); **d**) Macro view of touch point between the two side of sawing lines, presence spine, false-start kerf and exit chipping (red arrows) (Photo: Filippo Scianò). pag. 155

Figure 5.13 - Example of typical rip saw with number of TPI and PPI and verses of cut (cfr. Symes et al., 2014). pag. 155

Figure 5.14 – Ind. US 217 from Ravenna: **a**) Area of traumatic lesion of the left frontal bone, probable radial fractures (red arrows) and **b**) macro view of the margin of the lesion – flakes' detachment (red arrows) and bevelling (Photo: Filippo Scianò). pag. 156

Figures 5.15 – Trauma Evaluation Forms of the Individual D from Ballabio. pag. 157

Figures 5.16 – Trauma Evaluation Forms of the Individual US 217 from Ravenna. pag. 159